SURVIVING UNDER WATER

PHYSIOLOGICAL LIMITATIONS AND TECHNICAL POSSIBILITIES

Mårten Silvanius

Blekinge Institute of Technology
Doctoral Dissertation Series No. 2023:10

Department of Mathematics and Natural Sciences

ABSTRACT

The survival of humans in underwater environments necessitates a comprehensive understanding of both physiological factors and advanced technologies. Diving with self-contained underwater breathing apparatuses (SCUBA) remains one of the most common ways for human underwater activities. This thesis explores the challenges of surviving underwater by investigating diving equipment performance and human physiological modeling from both a deterministic and statistical perspective.

The research examines the change of gas composition when storing nitrox gas in a composite gas cylinder over extended periods, up to one year. This analysis aims to better understand the implications of long-term storage on gas properties and safety.

The efficacy of a signal analysis software algorithm designed to ascertain the accuracy of electronic rebreather oxygen sensors is evaluated. The algorithm's purpose is to provide enhanced safety measures for oxygen sensors integrated into various closed-circuit rebreathers, pursuing reliable data.

The reliability of temperature monitoring of carbon dioxide scrubbers is investigated as a method to predict remaining carbon dioxide absorption capacity. This temperature monitoring acts as a crucial "fuel gauge," contributing to diver safety by preventing potential risks associated with scrubber material depletion.

The research seeks to explore the principles and methodologies that can be employed to optimize the decompression algorithm, with the purpose of enhancing diver safety during decompression procedures. By employing probabilistic modeling techniques, the research aims to propose innovative solutions to minimize the risk of decompression sickness, contributing to advancements in underwater safety practices.

Additionally, the thesis explores the possibilities of altering the oxygen breathing regimen for the Inside Attendant during long-duration hyperbaric oxygen therapy (HBOT) to facilitate rapid decompression without compromising safety.

BLEKINGE TEKNISKA HÖGSKOLA · BTH ·

ISSN 1653-2090

2023:10

ISBN 978-91-7295-461-8

Surviving under water

Physiological limitations and technical possibilities

Mårten Silvanius

Blekinge Institute of Technology Doctoral Dissertation Series
No 2023:10

Surviving under water

Physiological limitations and technical possibilities

Mårten Silvanius

Doctoral Dissertation in Systems Engineering

Department of Mathematics and Natural Sciences
Blekinge Institute of Technology
SWEDEN

Department of Mathematics and Natural Sciences
Publisher: Blekinge Institute of Technology
SE-371 79 Karlskrona, Sweden
Printed by Media-Tryck, Lund, Sweden, 2023
ISBN: 978-91-7295-461-8
ISSN: 1653-2090
urn:nbn:se:bth-24811

Media-Tryck is a Nordic Swan Ecolabel certified provider of printed material. Read more about our environmental work at www.mediatryck.lu.se
MADE IN SWEDEN

Abstract

The survival of humans in underwater environments necessitates a comprehensive understanding of both physiological factors and advanced technologies. Diving with self-contained underwater breathing apparatuses (SCUBA) remains one of the most common ways for human underwater activities. This thesis explores the challenges of surviving underwater by investigating diving equipment performance and human physiological modeling from both a deterministic and statistical perspective.

The research examines the change of gas composition when storing nitrox gas in a composite gas cylinder over extended periods, up to one year. This analysis aims to better understand the implications of long-term storage on gas properties and safety.

The efficacy of a signal analysis software algorithm designed to ascertain the accuracy of electronic rebreather oxygen sensors is evaluated. The algorithm's purpose is to provide enhanced safety measures for oxygen sensors integrated into various closed-circuit rebreathers, pursuing reliable data.

The reliability of temperature monitoring of carbon dioxide scrubbers is investigated as a method to predict remaining carbon dioxide absorption capacity. This temperature monitoring acts as a crucial "fuel gauge," contributing to diver safety by preventing potential risks associated with scrubber material depletion.

The research seeks to explore the principles and methodologies that can be employed to optimize the decompression algorithm, with the purpose of enhancing diver safety during decompression procedures. By employing probabilistic modeling techniques, the research aims to propose innovative solutions to minimize the risk of decompression sickness, contributing to advancements in underwater safety practices.

Additionally, the thesis explores the possibilities of altering the oxygen breathing regimen for the Inside Attendant during long-duration hyperbaric oxygen therapy (HBOT) to facilitate rapid decompression without compromising safety.

Keywords

Diving, diving apparatus, unmanned testing, hyperbaric, scuba, oxygen sensor, composite gas cylinder, carbon dioxide monitoring, decompression, hyperbaric oxygen therapy

Acknowledgements

The progress in my work could not have been possible without the support of my colleagues in the Swedish Armed Forces. Your contribution has been fundamental.

My supervisor Associate Professor Oskar Frånberg, who has shared knowledge and energy in every aspect of this work and contributes with a story for every occasion,

Commander Mathias Jansson for believing in my capabilities and trusting the importance of this work to increase the safety for humans in the underwater domain,

Dr. Hans Rullgård for your patient and tireless support in the world of mathematical analyzes,

The dedicated, loyal and wise men and women at Swedish Armed Forces Diving and Naval Medicine Centre for their prominent work to realize the practical parts of this research.

A word of respect and humbleness goes to all divers contributing to this research by carrying out their day-to-day military duties accepting the risks involved in safeguarding our country. This work is my attempt to contribute to their efforts.

To all sparring partners within the national and international industry, military and academia.

This thesis would never exist without the support and love of my amazing family Henrietta, Gabriella, Edvard, Lucky and Jane.

In memory of my father Björn *(the B in SWEN21B)*

List of appended papers

The thesis is based on the following patent and papers, which are referred to by their Roman numerals:

Patent I

SILVANIUS M, Frånberg O. (2017) PPO2 Sensor authentication for electronic closed circuit rebreathers. *Patent filed - International Application number PCT/IB2017/054822*

Paper I

SILVANIUS M, Mitchell S J, Pollock N W, Frånberg O, Gennser M, Lindén J, Mesley P, Gant N. (2019) The performance of 'temperature stick' carbon dioxide absorbent monitors in diving rebreathers. *Diving and Hyperbaric Medicine Volume 49 No. 1*

Paper II

SILVANIUS M, Frånberg O. (2020) Permeability properties of a pressure induced compacted polymer liner in gas cylinder. *Journal of Applied Polymer Science. 2021;138(18):50335*

Paper III

SILVANIUS M, Rullgård H, Frånberg O, (2023) Proposed Thalmann algorithm air diving decompression table for the Swedish Armed Forces. *Undersea and Hyperbaric Medicine Volume 50 No. 2:67-83*

Paper IV

SILVANIUS M, Plogmark O, Frånberg O, (2023) Early nitrogen wash-out for inside attendants during hyperbaric oxygen therapy – a novel oxygen distribution regimen. *Submitted to Diving and Hyperbaric Medicine 2023-03-18*

Appendix A

Air decompression table - SWEN21 *(Limited to total 60 min decompression time on air, oxygen and surface decompression included)*

Author's contribution to the papers

Patent I

Conceived and designed the analysis. Performed the computer simulations. Wrote the technical parts of the patent.

Paper I

Conceived and designed the analysis for the hyperbaric tests. Collected the data for the hyperbaric tests. Contributed with data. Performed the analysis of the data from the hyperbaric tests. Wrote specific parts of the paper related to background, method, analysis, results and conclusions from the hyperbaric tests.

Paper II

Conceived and designed the analysis for the gas cylinder measurements. Collected the data. Performed the analysis of the data. Performed the computer simulations. Wrote the paper.

Paper III

Conceived and designed the analysis for the deterministic model and the validation dives. Collected the data from the validation dives. Performed the analysis of the data from the validation dives. Wrote specific parts of the paper related to background, method, analysis, results and conclusions related to the the deterministic modelling and validation dives.

Paper IV

Conceived and designed the analysis. Performed the computer simulations. Wrote the paper.

Table of contents

Nomenclature

AGE: Arterial gas emboli

ADivP: Allied Division Publication

Barrer: unit for permeability – cc(STP) cm/cm²s cm Hgx10^{-10}

CCR: closed circuit rebreather

CO_2: carbon dioxide

CNS-DCS: Central nervous system decompression sickness

DCMRI: demand constant mass ratio injection

DCS: Decompression sickness

eCCR: electronic closed-circuit rebreathing apparatus

Ke: ventilatory equivalent $RMV/V\,O2$

EL-DCM: Exponential Linear Decompression Computer Model

$FO2$: oxygen fraction in a defined volume

FOI: Swedish defence research agency

HBO: hyperbaric oxygen

NEDU: Navy Experimental Diving Unit

O2: oxygen

OC: open circuit (diving apparatus)

OCS: oxygen control system

P: pressure in ATA

PO_2/PPO_2: partial pressure of oxygen

PCO_2/$PPCO_2$: partial pressure of carbon dioxide

PPE: Personal Protective Equipment Directive

PFO: Patent foramen ovale

RB: Rebreather (diving apparatus)

ROS: Ratio of supersaturation in the compartment

RMV minute ventilation in liter/min

R_Q: respiratory quotient, the amount of produced CO2 per consumed O2

SCUBA: self-contained underwater breathing apparatus

SCR: Semi closed rebreather

SS: Steady state, the state where balance of metabolized oxygen and dosage of oxygen is at equilibrium.

STANAG:	Standardization Agreement
Std:	Standard devitation
STP:	Standard Temperature Pressure
SwAF DNC:	Swedish Armed Forces Diving and Naval Medicine Centre
SWEN88:	SWEdish Navy decompression table developed in 1988
SWEN21:	SWEdish Navy decompression table developed in 2021
SWEN21B:	maximum permissible tissue tension parameters used to develop SWEN21
t:	time in minutes
TPE:	thermoplastic elastomer
TT6:	hyperbaric oxygen treatment table 6
Vd:	dead space volume in liters
VGE:	Venous gas emboli
$VO2$:	oxygen consumption in liter/min STPD
wv	Wet volume in liter

"The more I learn, the more I realize how much I don't know." – Albert Einstein

Surviving under water –

Physiological limitations and technical possibilities

1. Introduction

Despite advancements in technology and equipment, the underwater arena remains a formidable challenge for even the most experienced divers and underwater professionals. Surviving under water comprises understanding of both physiology and technology. This understanding is still relevant to develop as we see still see accidents some 150 years after the Brooklyn bridge was built and caisson sickness or the bends was revealed as a mortal ailment.

Underwater work is a highly specialized and a challenging occupation that require divers to work in a hostile aquatic environment. The profession is mainly undertaken by commercial or military divers who work with construction, oil and gas, marine engineering, transportation, and military operations. These divers, contractors and authorities follow strict regulations to ensure safety. Sometimes with own capabilities to provide treatment or care. Recreational diving is also a popular activity where safety is provided by themselves, a dive center or possible governmental rescue service.

1.1 Hazards and risks

The main hazards in the underwater arena is the surrounding media, the water. This dense Materia is well known to be unbreathable for humans. The pressure variations, which the diver experience when changing depth, must be considered. To mitigate these hazards, divers use specialized equipment such as gas cylinders, regulators, mouthpieces, buoyancy control devices, thermoregulatory suits etc., as well as decompression methods and awareness of depth narcosis. The most common breathing device is the open circuit OC. Umbilical diving, where the diver is connected to surface supply hoses, is common within commercial diving where helmets or hard-hats are used. Rebreathers, where gas is exhaled into and rebreathed from a counter lung, are mainly used within military diving where the signature and endurance are of highest importance. Some specially trained recreational divers also use rebreathers in the search for greater depths and endurance.

Any equipment failure underwater can be life-threatening to a diver, as it can cause inability to breathe and control buoyancy. With rebreathers, additional risks are present, such as flooding the loop, erroneous gas sensors or depleted carbon dioxide scrubber. The most common triggering event in civilian open-circuit diving accidents are however related to insufficient gas and only 15% are related to equipment failure. [1] Ranking risk factors amongst civilian diving accidents reveal that human factors are dominant. [2] Divers must nonetheless regularly maintain and check their equipment, both during and between dives, to prevent malfunctions and have backup equipment in case of emergencies.

An inevitable hazard when decreasing ambient pressure is arterial gas emboli AGE which could occur from pulmonary barotrauma. Venous gas emboli VGE could also occur from dissolved inert gas which then is referred to as decompression sickness DCS. If shunts are present in the circulatory system this venous gas emboli could transfer to the arterial side. [3] This condition origins from when inert gas dissolves into the body tissues while the diver breathes compressed gas with diluent at depth. When the diver ascends the inert gas, dissolved in the tissues, can

form bubbles and if the ascend is too rapid cause pain, nausea, numbness and even death. To prevent this, divers must follow decompression schedules that allow their bodies to slowly release the excess gas and return to normal atmospheric pressure. [4]

The risk of hypothermia is present for most human underwater work. The temperature of water could decrease rapidly as depth increases, and cold water can cause hypothermia, even in relatively warm water. Divers must wear appropriate thermal protection to prevent this, such as wetsuits, drysuits with undergarments or hot water suits.

Limited visibility is also a hazard of underwater work, which can be caused by factors such as murky water, silt, or low light conditions. This can make it difficult for divers to orient and detect hazards or communicate with other divers. To prevent accidents and be able to orient, divers must sometimes use underwater lights and communication devices, such as radios or hand signals, to communicate with each other or the surface and navigate through the underwater environment.

These risks put the diver, supervisor, employer, manufacturer, authorities, regulations and researchers in an important interdependence just to avoid any accidents. This research is focused on surviving under water and stretches from both technology, methodology to modelled physiology. These challenges are illustrated but only a mere fraction of all the perils are studied herein.

1.2 Diving apparatuses

If the self-contained underwater breathing apparatus SCUBA is of open circuit OC type, where the exhaled gas is released to the surroundings, the main strategy is to breathe pressure regulated gas through a mouthpiece from a high-pressure gas cylinder. The divers breathing gas is strictly depending on what the gas cylinder contains. The main advantage is the simplicity. However, there are some disadvantages as the gas consumption increases with deeper depths and the desired operational time could be too short. Additionally, the gas composition might not be appropriate for the desired depth range. In military applications it can also be disadvantageous to release bubbles into the surrounding as this can be observed from surface or detected by acoustic sensors. When breathing on a rebreather RB the gas consumption generally does not increase with depth. Further, the gas composition can be optimized for the current depth. A rebreather is described as a closed circuit CCR where all exhaled gas is reclaimed or semi-closed circuit SCR where some of the excessive gas injected from a dosage system triggers loop gas to be released to the surroundings and the rest is reclaimed in a counter lung. This requires some additional functions compared to OC. The preferable compact format normally includes a fresh gas supply and dosage to compensate for the body´s consumed oxygen and a scrubber to cleanse the exhaled gas from carbon dioxide. Many modern rebreathers are electronically controlled eCCR and include some sort of monitoring sensors to verify the validity of the gas composition, and solenoid valve to inject oxygen. [5, 6, 7]

1.3 Standards

The function of diving equipment can be tested and evaluated according to standards. The European standards EN-250 and EN-14143 are regulating safety and function of open circuit and rebreather diving apparatuses respectively. A diving system consists of many components which can be tested separately or as a complete system. Both regimes are present in the standards and represents different stages of the safety approval. Even if certain components are working correctly, they need to be verified to work and interact as a complete system.

Relevant tests in the European standards for this thesis are of the following:

- Oxygen regulation system, which shall keep the partial pressure of oxygen at 0.20-1.60 bar at all time according to EN-14143:2013 5.7. Deviations close to the upper region of PO_2 may be allowed during the descent phase and one minute at the bottom if PO_2 is held below 2.0 bar. The inspired partial pressure of oxygen shall be held within ± 0.10 bar from the actual setpoint during constant depth and at a respiratory minute volume *RMV* of 40 l/min. During the ascent phase the PO_2 should not pass below 0.5 bar. The display should have an accuracy of ±0.03 to 0.06 bar.
    - Monitor for inspired gases
        - 5.9.3.1 - Monitor for inspired PPO2 shall have a response time of 15s to reach 90% of the step change for PO_2. The system must be designed according to FMECA analysis.
        - 5.9.4 Warning must be activated if levels are outside the range of 0.27-1.6 bar.
- Soda-lime testing according to 5.6.6 in EN-14143:2013 where the stated endurance of the soda-lime scrubber shall keep the inspired partial pressure of carbon dioxide at a level below 5 mbar and below 10 mbar within 10 minutes thereafter.
    - 5.9.3.2 - Monitor for inspired partial pressure of carbon dioxide shall have a range of 0-25.0 mbar and an accuracy of ±3mbar at all conditions. A warning must be announced if levels increase above 5 mbar.
- Gas cylinder leakage according to
    - EN 12245:2009+A1:2011 Transportable gas cylinders – Fully wrapped composite cylinders
        - 5.2.14 Test 14 – Permeability test of cylinders with non-metallic or without liners: No more than 0.25 ml/h/l (water capacity). Gas cylinders shall be charged to 2/3 of working pressure. Measures are taken up to 28 days after test is initiated.
    - ISO 11119-3:2013 Refillable composite gas cylinders and tubes – Design, construction and testing - Part 3: Fully wrapped fibre reinforced composite gas cylinders and tubes up to 450L with non-load-sharing metallic or non-metallic liners
        - 8.5.12 Permeability test shall be performed with air, nitrogen (*or natural gas*) if the application is valid and the leakage shall be less than X=0.25 ml/h/l (water capacity). Other specialized applications where the cylinder contains other gases, the value of X can be different. Gas cylinders shall be charged to working pressure. Measures are taken 500h after start of storage.

1.4 Testing facilities

The different testing regimes for diving equipment almost always demand some sort of testing facility and preferably a breathing simulator to be able to perform all tests appropriately. When all systems are thoroughly tested and approved by a certified test house, a notified body can certify the breathing apparatus function or gas cylinder. Since there are many parameters such as ventilation, temperature, depth, oxygen consumption and ventilatory equivalent included in the testing parameters there are a few chosen to represent the whole spectrum of combinations.[8] This means that some conditions remain untested and could occur during the breathing apparatus life-time since it is not plausible to test every failure mode. In addition to this, the testing does not include any long-term testing which could reveal unexpected failure

modes in the long run. An example of this is gas-diffusion through gas cylinder wall, where initial problems cannot be detected from more than analysis of the gas cylinders properties or from long duration testing, which is not comprised in the testing standards for breathing apparatuses. The longest storing time described in the European diving apparatus standards are 3 hours. [8] There are rebreathers on the market however that check if the oxygen and diluent gas is appropriate and of the correct fraction, and warns the diver if outside of specifications. [2]

If a standard does not exist, for the specific system, a manufacturer in cooperation with the notified body can create a Technical File to test according to. This should then harmonize with the demands of the directive. In the case of breathing apparatuses this would be the Personal Protective Equipment Directive, PPE. [9]

1.5 Physiological aspects

There are no standards for the human being and a diver is no exception. Each of us are individuals and more or less prone to diseases, physical and psychological challenges. Determining certain rules for the human as one identical object cannot be done. This creates some difficulties when trying to determine general properties and demands for the human in the underwater environment. These problems are well known within the medical community and statistics are common to overcome the issue with describing a potential remedy for a population. [10]

The challenges for a diver and the individual differences are not always that obvious. The differences are of course less if we analyze a certain population, such as military divers but differences in sex, age, body composition and fitness are always present. Decompression tables does not incorporate any differences between divers, and this might get you to believe that each dive and diver are identical. The actual environment such as temperature, sea-state and currents (workload for the diver) matters as well as the actual status of the diver. Is the diver fully rested and fit for the job or is the diver exhausted? Parameters like these are often up to the dive supervisor to consider when planning the dive. An experienced dive supervisor knows what risk factors that might affect and also knows his/her divers and compensates with less time in the water or something else to make the dive more conservative. Some dive manuals also support the dive planning to add extra safety if workload is high, temperature is low and individual factors of diver such as age and BMI. [11]

Dive computer algorithms are common to incorporate so called gradient factors. These are used to add conservatism by adjusting the controlling parameters in the algorithm. Some dive computers are also equipped with heart rate monitors and skin temperature sensors to know if the diver is experiencing high workload or coldness and therefore compensate for that with more conservatism. [12]

However, the human can experience other dangerous implications during the dive, additionally to the decompression sickness. The most serious implication would unarguably be drowning. Other examples of fatal implication could be lung barotrauma, heart attack or unconsciousness from for example diabetes. These risks can only be mitigated by physical and medical fitness and training.

2. Research Methodology

During my almost ten years of performing manned and unmanned tests of diving equipment in the ISO 17025 accredited laboratory at the Swedish Armed Forces Diving and Naval Medicine Centre SwAF DNC I've encountered several issues with both test procedures and equipment being investigated, but also methodological issues related to dive profiles with overrepresented outcome of decompression sickness. I have performed accident investigations as well as test of equipment that are planned, but not yet released on the market. My guide during these investigations have been well written procedures such as the European standards, as well as diving physiology literature. I've used the standards to verify the relevance and accuracy of the data collected, but also to apprehend the requirements. The diving physiology and methods to develop decompression algorithms have been used to understand the underlying theories of the suggested profiles. The laboratories yearly revisions from SWEDAC have verified the correctness of the testing facility and the competence of the laboratory.

When analyzing diving equipment failures in the SwAF DNC laboratory, primarily during accident investigations, it has come down to three main components being overrepresented. Carbon dioxide scrubbers, oxygen analysis/dosage systems and gas storage. Human factors are however overrepresented for civilian divers. [4] Military divers generally have longer training and are more exposed to aggressive dive procedures and potential equipment failures rarely end up with injuries due to high training level and good readiness level of the diving organization. Human factors are not further evolved herein.

The research plan includes experience and investigate some of the topics encountered. While gathering data in my general work I've been able to build up enough information and knowledge to write patents and peer reviewed papers covering both mechanics and modelling of the human.

2.1 Objectives and research questions

As can be recognized by the design of the two types of autonomous diving apparatuses OC and RB there are some vital components and requirement that must not fail. Identifying and investigating these components and requirement have been the objective of this thesis.

Table 1, minimum requirements for conducting a dive with breathing apparatus. Thermal protection, gauges and buoyancy control devices are deliberately excluded.

Component/ requirement	OC	CCR (oxygen RB)	SCR	eCCR
Gas cylinder	X	X	X	X
Pressure regulator	X	X	X	X
Mouthpiece/mask	X	X	X	X
Gas dosage system		X	X	X
Breathing loop		X	X	X
CO_2 scrubber		X	X	X
Loop gas monitoring system and sensors			(X)*	X
Decompression procedures	X		X	X
Main limitation	Gas volume	Depth	Gas volume	Decompression

*there are Semi closed rebreathers SCR that pneumatically controls the presence of fresh gas dosage, however not monitoring the actual gas content in the loop (ex. ISMIX Interspiro Täby). There are also SCR that have integrated PO_2 sensors but generally the idea with an SCR is that the gas is controlled mechanically without the need for electronics.

From table 1 it can be understood that the complexity increases with rebreathing diving apparatuses. These complexities underlying risks have been focused on in this thesis. The schematics of an OC, CCR, SCR and electronic CCR is shown in figure 1-4.

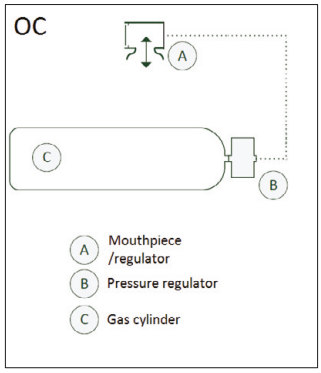

Figure 1, schematic picture of an open circuit breathing apparatus, OC.

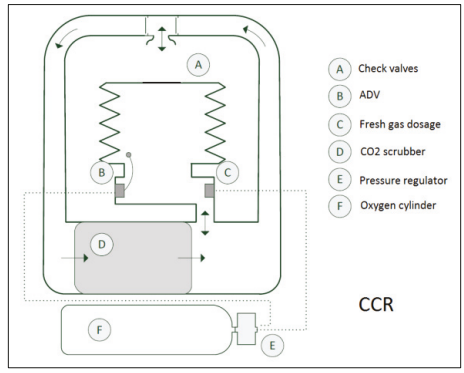

Figure 3, schematic picture of a closed-circuit rebreather CCR (oxygen rebreather).

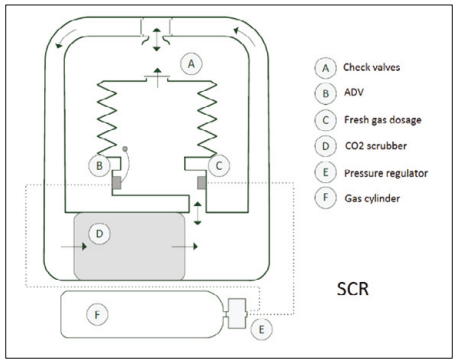

Figure 2, schematic picture of a semi closed rebreather, SCR.

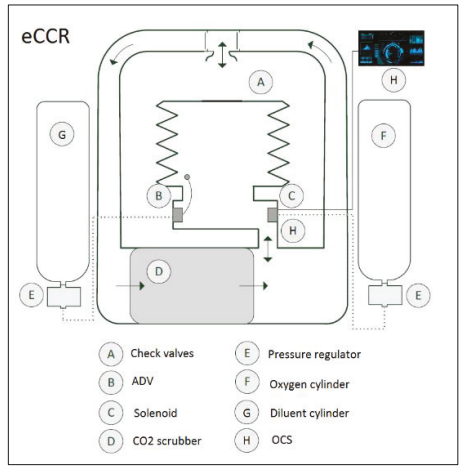

Figure 4, schematic picture of an electronic closed-circuit rebreather, eCCR.

Improving safety can be done by encouraging manufacturers to provide reliable diving equipment, for procuring organizations to verify and validate function and for customers to put up relevant demands. There is also an aim in this thesis to encourage diving organizations to provide reliable and well understood decompression schedules. These issues and solutions could be applicable in the general diving community; however, some specific equipment or risk elevated methods are more common within military diving where risks are mitigated with routines, medical readiness and availability of oxygen or hyperbaric treatment within certain criteria. The regulations for Swedish military diving are described in the current version of RMS-Dyk. [13]

Knowing the capabilities, possibilities and limitations of the equipment and the human in the underwater arena are crucial to fulfil safety requirements as an employer in the underwater domain. The objective of this study is therefore also strongly related to the Swedish Armed Forces responsibility for each dive and each diver to be performed safe and under controlled conditions. An equally important responsibility lies on the Material Commands verification and validation process when procuring equipment. General requirements for underwater work are described in the Swedish Work Environment Authority AFS 2010:16 and AFS 2019:4. [14, 15] The equipment also undergoes testing and can fulfill agreements in certain performance standards to achieve CE-marking and thereby be considered appropriate.

The thesis focuses on surviving under water and comprise both equipment performance and physiological modelling to examine human performance from a deterministic and statistical perspective. The research questions are as follows:

RQ1: How will the gas composition change when storing nitrox gas in a composite gas cylinder over extended periods up to one year?

RQ2: Can a signal analysis software algorithm, without additional hardware, determine if an electronic rebreather oxygen sensor provides correct or incorrect information?

RQ3: Is temperature monitoring of the carbon dioxide scrubber a reliable method to avoid depletion of soda-lime?

RQ4: How can the design of a decompression algorithm be developed to provide a risk of decompression sickness less than 1%, and/or less than 0.1% for neurological decompression sickness?

RQ5: Can the oxygen breathing regimen for the Inside Attendant be changed during hyperbaric oxygen HBO (TT6) to allow rapid decompression?

The papers included in this thesis tries to answer these research questions. In chronological order of publication, I initially in the form of a patent, suggest an algorithm for determining erroneous oxygen sensor signals. The purpose of the algorithm is to provide an increased safety feature for oxygen sensors incorporated in many closed-circuit rebreathers. Secondly the reliability of so called 'temperature sticks' in carbon dioxide scrubbers are investigated. The function of the temperature monitoring could be described as a fuel gauge for the active material soda-lime used in rebreathers. Thirdly the permeability properties of a composite gas cylinder used in diving is examined. This aims to avoid leaking gas cylinders to alter the anticipated gas content during storage. Fourthly a probabilistic model for decompression sickness is evolved with the aim for less than 1% risk of DCS. Validation trials are also reported therein. Fifthly the possibilities to abort a hyperbaric oxygen therapy without exposing the inside attendant to unnecessary risk is described and suggested. A general overview of the work is provided here and in the following chapters. Detailed analyses are attached herein as journal articles, submitted manuscript and a patent.

3. Background

The object of this thesis is related to the diving apparatus ability to deliver a safe, appropriate and breathable gas to the diver, and the aspects of safe decompression from a dive. Focus has been put into investigating commonly used decompression algorithms and modelling the anticipated gas transportation in the human body, as well as examining possible weaknesses in the gas monitoring, control and storage components of the self-contained breathing apparatus, SCUBA. Some methods and experiments previously not published are presented and discussed.

3.1 Decompression algorithms

When the obstacle of breathing underwater was solved by ancient explorers, fishermen and salvagers another obstacle occurred; how to decompress safely? Descriptions of decompression sickness was made public during the construction of the Brooklyn Bridge were the workers, so called sandhogs, were put in caissons to be protected from the surrounding water and able to dig deeper.[1] The caissons were pressurized, and several deaths occurred from decompression, as well as regular decompression sickness, 'the bends', including the engineer leading the work.[2]

Paul Bert is described as the first to identify decompression sickness in the 1870's from observing dogs after decompression. [16] Ernest Moir was the first engineer to decompress his workers in a hyperbaric chamber when they were to return to surface building the Hudson River tunnel in the 1890's. He lowered the death rates from 25% to near zero. [17] John Scott Haldane was a British physiologist and was together with Edwin Arthur Boycott the first to describe the theories of decompression with mathematical modelling. [18] These theories were later evolved by Robert Workman at the US Navy in the 1960's where specific values of acceptable over pressures in fictive tissues or compartments were determined. These so called maximum permissible tissue tensions were also believed to change with depth, where a higher tension was allowed at depth and linearly regressed to the allowed tissue tension at surface. [19] In the 1970's a Swiss physiologist Albert Bühlmann described Workman's theories with additional compartments and also allowed for altitude diving by setting the lower ambient pressure at 0 bar instead of the previous ~1 bar, atmospheric pressure, meaning that it was possible to perform calculations at ambient pressures below atmospheric pressure, such as in a mountain lake. [20] During the 1970-80's a US Navy physiologist, Edward Thalmann evolved the current US Navy decompression theories, by suggesting that the decompression should be a linear process and applied during decompression when the modelled tissue pressure exceeds ambient pressure by a given amount called cross-over pressure PXO. However if the sum of tissue pressure and PXO is lower than ambient nitrogen pressure, exponential kinetics are applied. [21]

The work with decompression theories herein originates from the ideas of Thalmann, mainly because it is the strategy used by the Swedish Navy's previous tables sprung from the US Navy Diving Manuals.

[1] The SANDHOG-criteria describing severeness of DCS was derived from the acronym for San Diego Diving and Hyperbaric Organizations for the group that helped to develop the criteria, and it is also a colloquial term used for caisson workers. [22]

[2] Decompression sickness was initially called 'the bends' as the forward leaning posture of the affected individuals resembled the Grecian Bend which was a chic Victorian posture. [23]

3.2 Oxygen sensors and control systems

In electronically controlled rebreathers the mechanisms of upholding correct partial pressure of oxygen, PO_2 are nowadays mainly performed by some sort of electronically controlled solenoid and a sensor system which continuously analyzes the oxygen levels of the breathing gas. The analysis of the breathing gas is done by a galvanic oxygen sensor or through optical analysis with a so called optode or optical solid-state oxygen sensor, which is a more recent technology. These sensors are in most applications of a rebreather only a distributor of signal varying on the partial pressure of oxygen. However, there are exceptions of rebreathers that perform analysis of the sensor reliability before allocating it to the dive computer and the user. [24] These tests are however not performed at the operating setpoint of PO_2, but rather analyzes the sensor response. If the gas analysis/injection system of a diving rebreather fails or gives incorrect information to either the analyzing system or the diver, this could result in serious injuries or death; examples are presented by Frånberg and Silvanius (2012) [25]

3.2.1 Galvanic oxygen sensors

Galvanic oxygen sensors operate similar to a metal air battery. [26] The original design was designated to applications at atmospheric pressures; however, in a rebreather it is not uncommon to have a PO_2-setpoint at 1.3 bar and thus partial pressures above those possible at surface. In addition to this there could be issues with moisture blocking the sensor or disrupting the galvanic process. Despite this, the sensors generally work correctly with help from additional features like hydrophobic filter and temperature compensation.

The chemical reaction producing the current from the sensor can be described as follows. [27]

Cathode reaction: $O_2 + 2H_2O + 4e^- \rightarrow 4OH$

Anode reaction: $2Pb + 4OH^- \rightarrow 2PbO + 2H_2O + 4e^-$

Overall reaction: $O2 + 2Pb \rightarrow 2PbO$

Oxygen will diffuse and separate from diluent gases through a limiting barrier and reach an electrolyte, normally potassium hydroxide (KOH). This will oxidize the metal anode, usually lead. A noble metal, usually platinum or gold, is used as a cathode which completes the electrochemical reaction and produces a current over a resistor where the voltage can be measured. [27, 28] Figure 5 shows a cross section of a galvanic sensor.

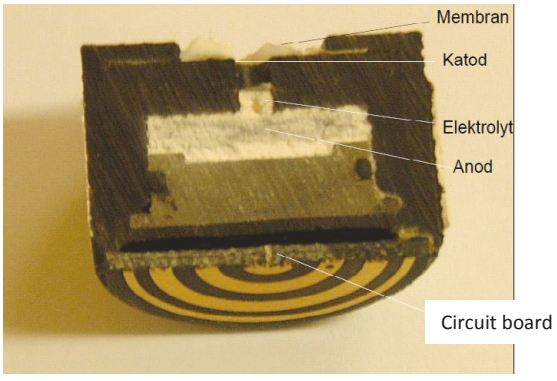

Figure 5, the cross section of a galvanic oxygen sensor. Reprinted from Frånberg (2005).

When the sensor is depleted all the lead is converted to lead oxide whereas the sensor cannot produce any current. The higher PO_2 the more oxygen is available for the electrochemical reaction causing a higher current and voltage output.

These types of sensors include a temperature sensitive element, as the hydrophobic membrane diffusion is limiting the diffusion depending on temperature and the signal will be temperature compensated which is fundamental to reach a reliable signal. The response time is also dependent on the temperature and can be as slow as t^{90}=25s at 2°C ambient temperature. [29]

Sensors issues are also related to lifetime, where the sensors can become "current-limited". Like batteries, they run out of anode and change impedance over time which causes a deviation from the expected linear behavior. Manufacturers recommended that these sensors are changed every 12-18 months. Recommendations are independent on whether the sensors are stored in air or nitrogen. Nitrogen could be used to stop the depletion of the sensor; however, this is not recommended as it might lead to a passivation of the electrodes and cause other issues. [29]

3.2.2 Optical oxygen sensors

The technology of optodes has for a long time been investigated for use in diving rebreathers and PO_2 higher than 1 bar. [30] The technology relies on a light source that illuminates a chemical layer which starts to fluoresce differently depending on the amount of present oxygen or rather the PO_2. Through optical filters the fluorescence and illumination are separated. When measuring the fluorescence, the output signal drops when oxygen partial pressures increase. The primary development has been with the fluorescence material.

Sieber (2012) presented results from laboratory tests where they have tested optodes to a PO_2 up to 2.0 bar. They also claimed an accuracy of 2-3 percent for partial pressures of oxygen from 0.2 to 1.6 bar. Response time was measured to 100 ms. [31] Today optical solid-state oxygen sensors are ready for customer.

3.2.3 Failure modes

Human errors represent most factors for diving accidents, although equipment does fail. [5, 25, 32, 33] When a galvanic oxygen sensor fails it is primarily one of the following [34]

- Current limitation due to depleted anode,
- Badly performed calibration done in an erroneous manner or with unknown gas previous to the dive,
- Blocked sensor by water or humidity so that the gas doesn't reach the electrolyte,
- Non-linearity which becomes a problem since the sensor will normally be used at PO_2 levels of 1.1-1.3 which is above where it was calibrated at.

3.3 Testing and evaluation methods

To test and evaluate the performance of an oxygen sensor or the complete PO_2-control system some reference documents can be used. In Europe the main documents are the standards, preferably EN-14143 for diving rebreathers. In the United States of America another test regime is defined by the Navy Experimental Diving Unit, NEDU and its laboratory. This is all thoroughly described in a public technical manual NEDU TM NO.15-01. [35] In the document it is possible to follow how to test oxygen sensors and its control system for PO_2.

The general idea for testing the oxygen control system is to simulate an oxygen metabolism. This is performed by some sort of artificial metabolism, extracting the oxygen from the loop

gas in an amount equal to what should be consume. However, the loop-gas is normally not 100% oxygen, which otherwise would have made the simulated oxygen consumption simple, since one could extract the loop gas in the same amount as the desired oxygen consumption. 1 liter/min extracted gas of 100% oxygen would be equal to 1 l/min metabolized oxygen, or oxygen consumption $\dot{V_{O^2}}$=1 l/min. If the gas in the loop is 50% oxygen and 50% diluent, one would need to extract 2 l/min of loop gas to reach $\dot{V_{O^2}}$=1 l/min. This however means that 1 l/min of diluent was extracted simultaneously. To compensate for that undesired loss, 1 l/min of diluent must be reinjected to the breathing loop. This can be done manually with flow meters or mass flow controllers. However, it gets harder to do this if the oxygen fraction changes over time or with depth as can be expected to occur while the rebreather loop reaches steady state of oxygen. At the SwAF DNC a computer-controlled metabolism simulator with this gas-exchange method was developed in 2012.

The Swedish Defense Research Agency, FOI, have also been using a metabolic simulator where in catalytic combustion of propylene described by Loncar (1991) and used in experiments by Frånberg (2015). [36, 37] This method combusts the oxygen and imitates the human metabolism in a more physiological manner than the gas exchange method described above. The equipment needed and the method proposed is however more complex and involves high temperatures combined with high pressures and combustible gases.

3.3.1 U.S. Navy unmanned test methods and performance limits for underwater breathing apparatus

How the underwater breathing apparatus UBA oxygen dosage principle is evaluated at NEDU is described, as previously mentioned, in detail in their technical manual. [35] Historically this type of test was performed by manually adjusting the valves and flow meters to reach desired values which proved to be daunting. Nowadays NEDU use a computer, controlling the flow rates with signals to the mass flow controllers, continuously adjusting depending on analyzed oxygen levels. The test can also incorporate a carbon dioxide scrubber test if CO_2 is injected simultaneously. [35]

3.3.2 Swedish Navy unmanned test regimen with oxygen consumption

SwAF DNC has, as previously mentioned, a similar computer-controlled system. Personal experiences with a gas exchange method reveals that it can be troublesome with low levels of oxygen, as very large amount of gas needs to be exchanged. At shallow depths there can be issues with removing enough gas as the background pressure is too low to operate the mass flow controllers properly. What also must be carefully observed during this test is the balance between extraction of loop gas and injection of diluent, primarily if the diving apparatus is of Demand Constant Mass Ratio Injection DCMRI type, like the ISMIX® Interspiro, Täby Sweden.[3] If the gas exchange proves to be slightly favoring the diluent injection, due to delays or measurement errors, a negative spiral will occur continue the increase of diluent replenishment and eventually cause the loop gas to reach unexpected low oxygen levels due to the laboratory setup and possible weaknesses in the laboratory control system. The diving apparatus can be perfectly working but suspected not to be so due to faulty testing.

[3] See explanation of oxygen dosage principle in Morrison, Reimers (1982), Nuckols et. al. (1999) and Frånberg (2015). [37, 38, 39]

3.3.3 EN14143 Respiratory equipment – Self-contained rebreathing diving apparatus

The European standard for diving rebreathers is more specific, than the NEDU Technical manual 15-01, regarding the demands of the oxygen control system, but less thorough in the testing procedure. It states that the system must, under conditions specified by the manufacturer, maintain an inspired partial pressure of oxygen greater than 0.20 bar and less than 1.6 bar, in steady state. If the partial pressure is not maintained automatically the system must provide 0.5 l/min of oxygen at a constant flow rate otherwise it must also comprise some sort of monitoring system with a display of the actual inspired partial pressure of oxygen. In addition to this there must be some sort of warning device for low and high PO_2.

An automatic PO_2-sensor controlled oxygen control system must also be able to keep the setpoint of PO_2 at desired levels, within ±0.10 bar at constant depth and an oxygen metabolization $\dot{V}_{O^2}$ of 1.78 l/min at a respiratory minute volume *RMV* of 40 l/min, resulting in a ventilatory equivalent, $K_e = RMV/V_{O2}$ used in the standard test to be 22.5. These demands are expanded when the diving apparatus oxygen control system is purely depending on the diver's ventilation. The tests are then also performed at *RMV* of 22.5 l/min and 62.5 l/min with an $\dot{V}_{O^2}$ of 0.75 l/min and 3.47 l/min respectively, revealing a K_e of 30 and 18. However, this factor is also expected to change with depth. [40] Deviations in the PO_2 levels are permitted during ascent.

3.4 Carbon dioxide scrubbing in rebreathers

High levels of PCO_2, causing hypercapnia, could lead to anxiety, panic and respiratory malfunctions and be described as unsafe or even lethal. [41, 42] These consequences are evident results of the importance of the CO_2 scrubbing system. In the European rebreather standard, the accepted maximum level of inhaled PCO_2 is 20 mbar, including CO_2 rebreathed from the dead space V_d in the mouthpiece as well as CO_2 expelled from the depleting canister. The canister duration is measured and defined to CO_2-levels between 5 and 10 mbar, measured in the inhale hose before the mushroom valve in the mouthpiece. [8] According to the NATO-standard ADivP-03 the capacity of the scrubber material is determined rather than the capacity for the actual rebreather. The US Navy test center NEDU have combined these two tests to determine the abilities of CO_2-absorption, however the injection rate when testing the rebreather is normally less than in the European standard, 0.9 l CO_2/min or 1.35 l CO_2/min. The breakthrough of a canister is usually exponential as the molecules breaking through adds up with the newly exhaled CO_2, adding to the overall CO_2 volume in the loop. [35]

Normally the carbon dioxide scrubber cleans the expired gas from carbon dioxide so that it can be inhaled and rebreathed. The scrubber usually consists of granules of carbon dioxide reactive material such as soda lime, containing of a mixture of calcium hydroxide (slaked lime, $Ca(OH)_2$) and sodium hydroxide (caustic soda, NaOH). The chemical reactions during CO_2-absorption are described in three stages [43]:

(i) Reaction at aqueous layer

$$CO_{2\,(gas)} + H_2O \rightarrow CO_{2\,(aqua)}$$

(ii) Bicarbonate formation

$$CO_{2\,(aqua)} + NaOH \rightarrow NaHCO_3$$

(iii) Decomposition/regeneration of NaOH catalyst

$NaHCO_3 + Ca(OH)_2 \rightarrow CaCO_3 + NaOH + H_2O$

The overall balanced equation being

$CO_{2(gas)} + Ca(OH)_{2(solid)} \rightarrow (H_2O/NaOH) \rightarrow CaCO_{3(solid)} + H_2O_{(liquid)}$

The scrubber endurance is affected by the workload of the diver, as it only can bind a certain amount of carbon dioxide. Specifications from manufacturers reveal an uptake capacity of approximately 110-150 l CO_2/kg. [43]

According to the NATO-standard ADivP-03 from 2013, previously called STANAG 1411, a test-procedure where a fully humidified, 5% CO2-mixture in nitrogen is flushed over a sample tube of 105 ml scrubber material. Batches of soda lime present at the time of testing in the Swedish Armed Forces originating from Molecular Products, Harlow Essex U.K., Sofnolime® S-grade, where shown by factory acceptance test, to provide a capacity of 85 l CO_2/kg. [44] Similar tests of the same batch performed by an external independent accredited lab showed a capacity of 105 l CO_2/kg. The same batch was tested at SwAF DNC, accredited according to EN-14143:2013, in a closed (JJ-CCR® eCCR, JJ-CCR, Presto Denmark), and semi closed rebreather (ISMIX® Interspiro, Täby Sweden). Previously unpublished test-results from SwAF DNC showed less capacity than the theoretical performance when used in a rebreathing diving apparatus. 70-80 l CO_2/kg for the closed circuit and 45-65 l CO_2/kg for the semi-closed rebreather, at these specific standardized test-conditions and for these specific batches of soda lime. The degradation compared to ADivP-03 could be dependent on the 4°C cold water surrounding the apparatus. These results and an alternative test method are further described under the chapter Discussion.

3.5 Permeability of a gas composite cylinder

The general function of a gas cylinder for diving purposes is to withhold gas to be used for breathing. This gas must reach the standards of certain quality to avoid being harmful for the human. The content of a gas cylinder must normally be kept within EN 12021 which regulates the cleanliness and accuracy of concentrations, among other parameters. Oxygen and nitrogen mixtures are declared to have an oxygen level to be kept within 0.5-1.0% of the total mixture, depending on the oxygen concentration. [45] This is similar to the demands in the Swedish Armed Forces regulations. [13] Other contaminants such as carbon dioxide, carbon monoxide, oil etc. are also strictly regulated. In addition to this, the gas cylinder permeability properties are regulated by ISO 11119-3:2013 and/or EN 12245:2009+A1:2011. These regulations comprise storage of gas which is measured by weight periodically up to 21 or 28 days. The demands are presented in ml of gas leaked / hour /l water capacity of the cylinder or wet volume *wv* and shall not exceed 0.25 ml/h/l *wv*.

The tested gas cylinders in paper II are designed by Interspiro and consist of a glass-/carbon fibre outer shell to take pressure load, which is gas porous, and an inner bellow of co-poly ether ester named Arnitel® EB460 to contain the gas. Three different designs are presented in this thesis, where two of them called type 1 and 2, has a wet volume of 10 and 5 liter respectively, where type 1 is 2x5 liter. The third cylinder, called type 3, is similar of the first two types but has a wet volume of 6.7 l and inner bellow of Arnitel® EB463.

Polymer materials are due to its denseness prone to separate oxygen in favor of nitrogen as the two molecules differ in kinetic diameter, oxygen being smaller. Applications are described where oxygen/nitrogen generators are built upon this technique. [46]

4. Results

4.1 PPO2 Sensor authentication for electronic closed-circuit rebreathers – Patent I

The sensor authentication in the suggested patent is described as improving the reliability without adding any extra hardware. The main theory is that the PO_2-sensor should react in a predestined manner if exposed to an injection or consumption of oxygen or ambient pressure alternation. If the system volume in the rebreather is predesignated to a certain maximum/minimum level and the current oxygen levels are known, as well as the amount of injected oxygen, the onboard dive computer could analyze the expected PO_2 level after the injection. This could then be fine-tuned by adding additional information such as breathing frequency, the diver's lung volume etc. Another expected result, which should correlate, is the increased PO_2 in relationship to increased ambient pressure. The increase of oxygen fraction or increase in ambient pressure results in a higher PO_2, these events are then recorded and analyzed by the PO_2-monitoring system.

4.2 The performance of 'temperature stick' carbon dioxide absorbent monitors in diving rebreathers – Paper I

The chemical reaction involved in CO_2-scrubbing is exothermic, the heat release is 16.4 Kcal/mol CO_2, and this creates an opportunity to monitor the heat of the soda-lime present in the scrubber. [47] An obvious heat-front can be observed in the canister as the reaction moves from depleted to active material. Canisters are usually of radial or axial design and from a design perspective it becomes easier to monitor an axial scrubber as the area of heat is more concentrated.

Currently there are two carbon dioxide scrubbers with heat monitoring available. One is designed and patented by Dan Warkander and manufactured by rEvo rebreathers, Bruges Belgium, whereas the other one is designed, patented and manufactured by AP Diving, Water-Ma-Trout U.K. Both these are evaluated in paper I. It is shown that surface testing could cause the CO_2-exothermic heat monitor prediction of scrubber lifetime to be deceiving; however at depth they become more reliable.

4.3 Permeability properties of a pressure induced compacted polymer – Paper II

The gas cylinders leakage presented in Paper II are described in the unit *barrer* which is different from the one suggested in the standard. Converted results (from *barrer* to ml/h) are presented in table 2, with additional data from previously unpublished measurements. These additional cylinders are called type 3 and are similarly manufactured as type 1 and 2 but have a wet volume of 6.7 liter.

Table 2, The actual measures of leakage from the experiments performed in paper II. The leak requirement from the standard X=0,25 ml/h/l wv is presented for each wet volume of gas cylinder, where a larger volume accepts a bigger leakage. It is apparent that type 1 manages the requirements, with some exceptions, type 2 does not meet the requirements. Type 3 does not meet the requirements in this test setup.

Type	S.nr.	Design pressure [bar]	Design gas FO2 [%]	Wet Volume [l]	Avg. storage pressure [bar]	Avg. FO2 [%]	Leak [ml/h]	Leak requirement according to standard [ml/h]
1	4307	*300*	21	*10*	59,9	*12,1*	**2,1**	***2,5***
1	4170	*300*	21	*10*	10,0	*27,3*	**1,2**	***2,5***
1	4145	*300*	21	*10*	48,9	*20,5*	**2,8**	***2,5***
1	4018	*300*	21	*10*	6,9	*30,2*	**0,8**	***2,5***
1	4793	*300*	21	*10*	44,5	*20,5*	**2,2**	***2,5***
1	4200	*300*	21	*10*	252,3	*19,3*	**3,5**	***2,5***
1	4199	*300*	21	*10*	240,7	*43,7*	**5,9**	***2,5***
1	4234	*300*	21	*10*	243,2	*43,9*	**3,8**	***2,5***
1	4306	*300*	21	*10*	94,0	*12,7*	**2,5**	***2,5***
1	4370	*300*	21	*10*	86,5	*16,5*	**2,3**	***2,5***
2a	40459	*300*	28	*5*	200,9	*27,5*	**16,3**	***1,3***
2a	40483	*300*	28	*5*	197,1	*27,3*	**12,3**	***1,3***
2a	40548	*300*	28	*5*	202,1	*27,6*	**15,5**	***1,3***
2a	40840	*300*	46	*5*	198,4	*45,1*	**16,2**	***1,3***
2b	40450	*200*	28	*5*	179,1	*26,4*	**5,2**	***1,3***
2b	40617	*200*	28	*5*	73,6	*28,3*	**4,4**	***1,3***
2b	40665	*200*	46	*5*	50,2	*36,8*	**3,1**	***1,3***
3	744	*300*	21	*6,7*	50,8	*20,1*	**5,3**	***1,7***
3	779	*300*	21	*6,7*	50,9	*20,2*	**5,0**	***1,7***

The permeability properties of the gas cylinders have a permselectivity favoring oxygen versus nitrogen, related to higher pressure. At lower pressures the permeability is higher but permselectivity lower. This is presumed to occur as the plastic inner-liner is compacted when the cylinder is pressurized to the harder outer-shell of glass-/carbon-fibre composite. The so called 'torturous path' becomes compacted and more obstructed at higher pressures and decreases the general permeability but allows the smaller oxygen molecule to diffuse more rapidly compared to the nitrogen molecules, hence the higher permselectivity. This delicate correlation is described in detail in paper II.

Cracks in the inner liner of type 2a have caused an unexpected decrease of oxygen fraction in the contained gas, which might cause decompression injuries of divers, as the decompression schedules are altered if the diver is breathing a different gas than anticipated. Picture of the cracks are shown in figure 6. The cracks are not penetrating the liner completely, hence diffusion and not effusion.

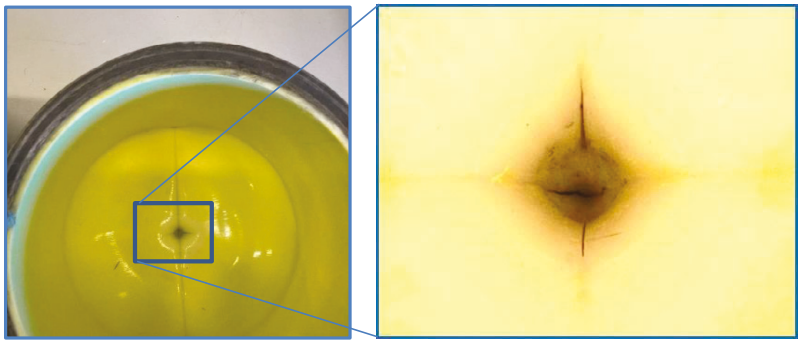

Figure 6, left shows the gas composite cylinder split in half, right shows an enlarged picture of the cracks discovered in the crease at the bottom of the cylinder. The cracks where not penetrating the liner.

4.4 Proposed Thalmann algorithm air diving decompression table for the Swedish Armed Forces – Paper III

The results from the analysis, calculations and validations of the suggested decompression table SWEN21 is presented in paper III. This work was initialized after the conclusions from a workshop held at SwAF DNC in November 2019, where participants from authorities, academia and industry met to discuss the desired properties of a decompression algorithm. [48] The properties that were taken into consideration when choosing path are summarized as:

- Safety / Risk appetite
- Cost
- Fulfill operational demands
- Interoperability
- Time to delivery
- Partners during development
- Acquiring of knowledge
- Flexibility

There were three proposed alternatives for the path ahead.

1. Follow the US Navy and switch to the tables presented in US Navy Diving Manual rev. 7 (EL-DCM Thalmann with VVAL-79 parameters), [49]
2. re-engaging with the SWEN88 table that was originally developed at the SwAF Marine Diving Centre (MDC) in the 1980s, with the assistance of Bill Hamilton, [50]
3. engage in a development of new table calculations that would match the SwAF risk appetite for DCS.

The first alternative was tempting as it was developed by a trustworthy organization and comprise a suggested DCS risk-level for each profile. This is a highly sought-after property when discussing these questions with decision-makers. However, the SwAF adopted the tables from the US Navy DM rev. 6 in 2009 with the aim to use oxygen decompression on the longer decompression dives. This was never implemented for the SwAF divers and not until the late 2010's for tethered divers at the dive support ship HMS Belos. Oxygen decompression,

calculated with EL-DCM Thalmann, is generally more conservative as only 80% is accounted for even though 100% oxygen is breathed. Additionally the so called Saturation Desaturation Ratio (SDR) is set to 0.7 during oxygen breathing which practically means that the decompression algorithm calculates with only 70% of the actual pressure differential between the loaded compartment and the ambient pressure making the off-gassing slower than if SDR is not used. [51] These interventions could of course be suggested as a safety factor depending on the diver's possibility to have a good seal between mask/mouthpiece and mouth or if the gas is not completely perfectly distributed for other reasons. It could also be considered as a factor that addresses the human body's ability to vasoconstrict when exposed to high fractions of oxygen, which is relevant to the discussion. [52] Despite the potential conservative benefits of oxygen decompression, the SwAF has not yet fully utilized it and continue to mainly rely on air decompression, which hence is comparatively more liberal than oxygen decompression. The air decompression will continue within the SwAF whereas it is important to have a table without unnecessary high risk of DCS, similar to the US Navy. The SwAF has identified a maximum risk-level for DCS 1% and CNS-DCS 0.1%, whereas the USN DM rev.7 states a risk-level of 2.3% for direct-ascent dives although not uniformly distributed. [48, 53] The Swedish Navy experience of the USN DM rev.6 air dive table was that some profiles, where also manual adaptations have been implemented, were prone to cause decompression sickness, for example 40msw/20min (deco 6msw/4min) and 24msw/39min direct-ascent. [54]

Suggestion no.2 was interesting as this would use previously done work within the SwAF. This table has been used in Finland since the 1990's and was also used to develop TRIMIX tables for the Swedish and Danish Navy in the early 2010's, where several validation dives already have been performed. [55] This work was never adopted by the SwAF due to several different aspects where equipment issues were one, as well as issues with calculating repetitive dives and limitations in the old software developed in the 1980's. During the analysis phase of this work we replicated the so called DCAP software algorithm which is identical to a Workman (Bühlmann) exponential/exponential algorithm with 11 compartments with 5 to 670 min half-time, certain acceptable maximum permissible tissue tensions with slope change (delta) at depth, and with an additional feature of decreasing the maximum permissible tissue tensions for dives deeper than 50 meter. As it was possible to replicate the DCAP this was no obstacle to continue the work due to old software. However, it turned out after interviews with representatives from the Finnish Navy that the tables were not exactly followed, and additional safety was added on a regular basis. This was interpreted to cause a deviation from the tables towards conservatism and the operational experience of very few DCS could be a result of this manually added safety. [56]

The most appealing alternative from the previously mentioned workshop considerations would be no.3 with the perfect understanding that this would require thorough work. This option would aim for the 1% DCS/0.1% CNS-DCS risk goal. [57] A deliberate choice was the EL-DCM Thalmann as this is a well-proven model by the US Navy and the strategy would be to only modify the maximum permissible tissue tensions, MPPT, and keep number of compartments, half-times, descent and ascent speed, alveolar pressure, cross-over pressure PXO and saturation-desaturation ratio, SDR.

The chosen method was to approach the problem with probabilistic models and implement a maximum likelihood model with logistic regression on scientifically well described direct ascent dives. The idea was to let bottom-time and depth be the two controlling parameters. Some variance in these dives were expected but the idea was to embrace as many dives as

possible as long as they fulfilled the criteria of being direct ascent on air. Ascent/descent time, wet or dry, thermal-protection or breathing equipment would not constitute any excluding criteria but rather incorporated in a sufficient amount to be concealed by the mere amount of dives. The result from the probabilistic model would be certain acceptable direct ascent times which in the next step would be transferred to the MPTT's. The transfer was done by starting with determining the MPTT for fastest compartment by correlating the time provided by the decompression algorithm at the greatest depth, 60 msw. As long as the MPTT correlated with the maximum allowed bottom time that MPTT will continue to control the next shallower direct ascent profile. If the shallower depth calculations suggest too long bottom time the next compartment will start controlling that profile and depth until the same occurs for a shallower depth. This will naturally be dependent on the ascent speed for deep dives as the asend time is even longer than the suggested direct ascend bottom time for a dive to 60 msw with 9msw/min ascend speed. The average of all included dives ascent speed was chosen and performed these analyses with an ascent speed of 10.5 msw/min. The complete analysis is found in paper III.

The main work with the decompression algorithm was performed during late 2020 and the 163 validation dives where performed in the SwAF DNC hyperbaric laboratory during the first and second quarter of 2021. The report to the SwAF was finished in late 2021 where it was suggested that the SwAF should implement these tables as they could not be falsified to be outside of the desired 1% decompression sickness risk and 0.1% for neurological, even though there where a total of three cases of DCS treated with hyperbaric oxygen. [57] The SwAF plan to implement the SWEN21 dive table during 2023. The table is attached in Appendix A.

4.5 Early nitrogen wash-out for inside attendants during hyperbaric oxygen therapy – a novel oxygen distribution regimen – Paper IV

Paper IV comprise a new strategy or regimen for oxygen distribution for the inside attendant during hyperbaric therapy. The purpose of the new strategy is to allow for emergency decompression during a larger period of time of the therapy, without any major risk of DCS for the inside attendant. The oxygen regimen and decompression strategy are based on EL-DCM Thalmann algorithm with SWEN21B parameters. The so-called lock in time have decreased, where the inside attendant has a mandatory decompression stop, with 147 min for a standard treatment table 6. To compare hyperbaric treatment tables decompression stress for the inside attendant a comparison of the fraction of maximum permissible tissue tension is introduced. This can be expressed for each compartment but also as an average for all compartments. This could be applicable on any dive profile comparison.

5. Discussion

5.1 Sensors in rebreathers

The presented work is describing some of the issues related to sensor controlled electronic rebreathers for diving. The vital functions of maintaining the oxygen partial pressure and keeping the carbon dioxide levels to a minimum are depending on the functions of the components. The monitoring systems can reveal if something is not working correctly, however a rigorous testing procedure during standardized tests can and already have given the diving community safer equipment. Sensors for analyzing inhaled gas are common and widely used. There could be an increased interest in analyzing the exhaled gas to understand the wellness of the diver and further understand hypoventilation and avoid CO_2 retaining. Additional

reasons to motivate this is described by Deng et. al. (2015) who showed that several divers where completely unaware of a non-present CO_2-scrubber in a breathing loop and where completely unaffected by high end-tidal CO_2 levels. [58]

5.2 Gas diffusion in polymers

From the analysis of the gas diffusion of the composite gas cylinders it is also rudimentary to understand if anything is changed during storage of these types of gas cylinders. This is expected to occur if the liner is of plastics, but with different pace depending on the permeability properties, thickness, pressure and contained gas. Previous experience within the Swedish Navy was that these gas cylinders did not emerge any issues with gas diffusion over time as they originally where made of non-magnetic metal material, which is less diffusive. Later these gas cylinders where made of composite, with a known diffusive property, however unanticipated liner cracks hypothetically occurred when raising pressure from 200 to 300 bar as previously described herein and in paper II. Unfortunately, there have been accidents involved with divers using gas expected to be unaltered after storage. Swedish Navy divers were informed that when switching from metal cylinders and then further to composite gas cylinders they did not need to analyze the actual gas cylinder. The only analysis that needed to be conducted was from the metal cylinder bank from which they were filled. This caused a false belief that every refilled small composite cylinder contained the same gas as from the bank, which turned out to be incorrect since oxygen diffused from the small composite gas cylinders and long term storage gas was still acceptable in them. A specification of the requirements during procurement of the equipment related to gas leakage, referring to the standards, could have avoided this. It is also important that this could be verified according to appropriate standards by the manufacturer at time of delivery and/or by the Material Administration verification and validation process, especially if the system is modified.

5.3 Developing decompression algorithms

It is questionable whether we fully understand the physiological mechanisms of decompression sickness. Most decompression theorists would probably answer no, but still emphasize the importance of the algorithms we use. We need something to describe our safe return from overpressure environments and from empirics and theories we've been able to design models and algorithms.

5.4 Treatment of decompression sickness

When the decompression has failed, in a sense where the diver suffers from decompression sickness, the general treatment is hyperbaric oxygen, HBO. [59] The standard treatment is performed at 18 msw with 100% oxygen for selected periods of time (US Navy TT6), to provide as high oxygen partial pressure that is possible without severe consequences. Treatment is also performed at shallower depth, for example 10 msw. These treatment tables are mostly derived from empirics with some background theory where bubble size compression, discarding any diluent gas and high oxygen partial pressure is fundamental. Possible negative consequences of high oxygen fractions related to for example vasoconstriction are rarely discussed. [60] Potential negative consequences of breathing a dense gas could also be subject for future work and possible benefits of shallower recompression investigated.

5.5 Patent and papers

5.5.1 PPO2 sensor authentication for electronic closed-circuit rebreathers – Patent I

The difficulties of measuring oxygen in a rebreather diving apparatus are related to high partial pressures of oxygen, humidity, power supply, ambient environment and pressure and a potential malfunction or depletion of the actual sensor, mainly if galvanic. [61] The galvanic sensor also has a slow response time, especially if encountering cold environment. [29] This is normally not an issue since the decrease of oxygen-level is not fast, dependent of the oxygen metabolism of the diver. Higher oxygen metabolism, which occurs with higher workload, causes a more rapid decrease of oxygen in the loop. This decrease is, as previously described, predicted by the suggested algorithm in patent I by analyzing the decrease of PO_2 with possible combinations of oxygen amount available and oxygen consumption. Hence it is possible to determine whether the sensor is reading within its specifications, however in a quite rough accuracy. With additional sensors to determine *RMV* or pressure drop in oxygen cylinder it is possible to do a more accurate analysis. In the application of our proposed sensor analysis algorithm both optical and galvanic sensors can be used, however the galvanic sensor appears to have more failure modes than the optical.

5.5.1.1 Further on O2-sensing in rebreathers

Difficulties with interpreting the oxygen sensor information could occur when analyzing the loop gas in a semi-closed rebreather, as the oxygen dosage system is different from an electronically closed-circuit rebreather. The two main differences are the injection principle and the actual gas injected. In a mechanical semi-closed rebreather, a rather large amount of fresh gas is injected, and is usually a nitrox, heliox or trimix blend. An electronically closed-circuit rebreather eCCR has an electronically controlled solenoid that injects pure oxygen in small doses to compensate for the oxygen metabolized. Small amounts of gas with high level of oxygen will increase the FO_2/PO_2 in the loop consecutively in a controlled manner. The loop gas however will be affected as a unity. In a semi-closed rebreather as the ISMIX®, which is ventilatory keyed, the effects on the loop gas will be rapid breath by breath. Other types of semi-closed rebreathers with super-sonic orifices, that continuously injects gas at a pre-determined rate, are also expected to have a slow rate of changes in FO_2/PO_2. Examples of these types of apparatuses are the CUMA®/SIVA®/VIPER® apparatuses from Cobham Limited, Dorset UK.

An example, examined more thoroughly here, is the semi-closed demand controlled mine clearance rebreather ISMIX® where the fresh gas dosage is keyed to the ventilation and injects gas from the gas supply at each exhalation. Depending on the placing of an external oxygen sensor, as there are none in the original design, the output will differentiate. Figure 7 shows an example of how a fast optical oxygen sensor, placed in the inhalation hose, can reveal the breath by breath analysis of the loop gas.

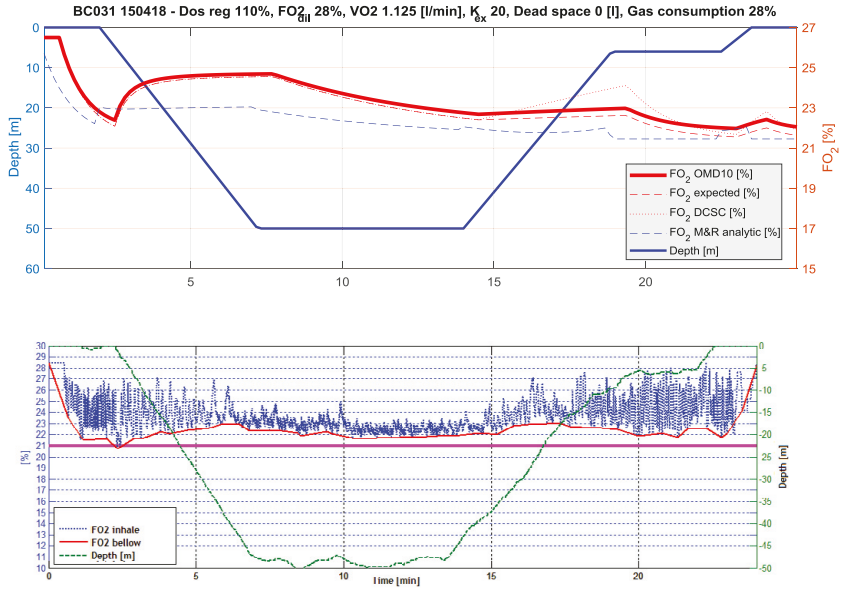

Figure 7, top figure shows the analytical solution according to Frånberg 2015 for the two types of semi-closed rebreathers OMD10/ISMIX® and DCSC, its predecessor. *FO_2 expected* is what to expect with a normally configured apparatus and is slightly lower than the others since the dosage is set to 110% for them. *FO_2 M&R* is the predicted oxygen level according to Morrison and Reimers 1982. Bottom figure shows a human dive with registered fraction of oxygen from an optical oxygen sensor. Because of its rapid reaction it is possible to register both fresh gas dosage peaks from *Fo_2 inhale* and lowest FO_2 loop gas, from the same sensor located in the inhale hose. See correlation between *FO_2 OMD10* in top figure and *FO_2 inhale* in bottom figure.

The high peaks of the FO_2-signal are close to the gas supply of 28% oxygen whereas the low signals represent the loop gas. The highest peaks are dwelled in the loop gas during the bottom phase. The inhaled oxygen level is close to average of the signal; however, the sensor will experience the time-weighted average of the loop gas in the inhalation hose and the diver's lung will experience the volume-weighted average of the inhaled loop gas. The analysis of the actual inhaled gas must be done carefully. The fresh gas dosage at depth is a small amount in relative volume, but big enough for the sensor to detect.

With reference to the results in figure 7, a galvanic sensor would not show the gas dosage peaks, as the response time is slower for such sensor. Compare with figure 8, where a similar dive is performed in a wet chamber with minimum workload. Data is collected from a galvanic oxygen sensor with a sample rate of 1 Hz in the inhale hose, and similar loop setup and breathing apparatus as for the optical oxygen sensor. The galvanic sensor cannot fully follow the fluctuations in the loop and does not always detect the peaks, especially during descend. At depth it is specifically hard to notice any fresh gas dosage as the injected gas is compressed with ambient pressure and becomes relatively smaller at depth. [37] It is likely to believe that the steady state of the inhaled gas is 24.5% of oxygen, see red dots between 8 and 12 minutes. The actual inhaled gas is thought to be lower. A higher registered time averaged FO_2 should occur as the diver pause each breath on the exhale, not the inhale, and fresh gas is buffered in the inhale hose. [18] However, the actual steady state of the breathing loop cannot be determined by this sensor, but is believed to be represented by the average, see black line in bottom figure 8.

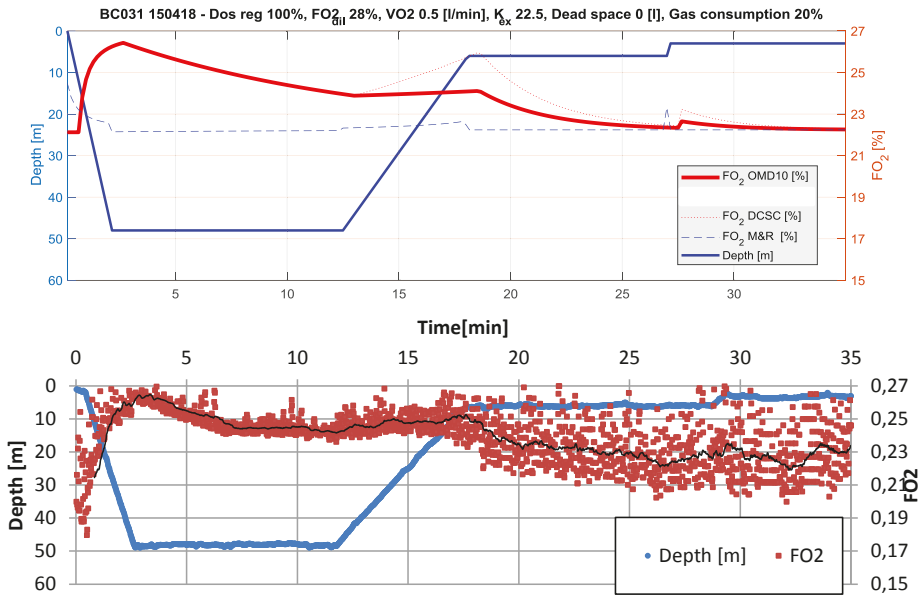

Figure 8, top figure shows the analytical solution according to Frånberg (2015) for two types of semi-closed rebreathers OMD10/ISMIX® and DCSC, its predecessor. *FO_2 M&R* is the predicted oxygen level according to Morrison and Reimers (1982). Bottom figure shows a human dive with registered fraction of oxygen from a galvanic oxygen sensor. See correlation between *FO_2 OMD10* in top figure and the averaged value represented by the black line in bottom figure. At 5 and 10 minutes a flush of 28% nitrox is performed with only slight response.

An oxygen sensor can only measure the partial pressure; hence the results presented in figure 7 and 8 have been converted into FO_2. The results are interesting since it shows the difference in response time between optical and galvanic sensor in an ISMIX® and the correlation between theory and empery, even though the interpretation of the sensor readings must be done carefully.

5.5.2 The performance of 'temperature stick' carbon dioxide absorbent monitors in diving rebreathers - Paper I

The different methods for testing soda-lime are separated into testing the actual material, soda-lime, or the full rebreather application. Both tests give important data on the performance and to get a more complete understanding one should use both. However, assigning a specific performance of the soda-lime CO_2 absorption capability could result in false safety, believing that the rebreather CO_2-scrubber endurance is similar to the amount of soda-lime put into it. By calculating the weight and expected capacity of the soda-lime and anticipate the expected workload during the dive, it is possible to estimate the endurance, which is a method that is deceiving. Other factors like ambient temperature or scrubber design are not taken into consideration for example.

As CO_2-production correlates to the oxygen metabolism, the standard EN-14143 prescribes a respiratory quotient R_Q of 90%, meaning a production of CO_2 in relationship to oxygen consumption, the CO_2-production can be calculated from the oxygen consumption. [8] Some

apparatuses oxygen supply is designed to be consumed before the soda-lime is depleted. If the fresh gas supply is filled up at the start of the dive, it is stipulated to change the soda-lime when oxygen, or other fresh gas, is ready to be refilled.

It is possible to do a short dive, leave the soda-lime as it is, and then return days or weeks later to find the soda-lime to still be operational and can continue to scrub carbon dioxide. [62] It is important that the soda-lime is not dried out however, why it is recommended to store in a closed loop or in plastic bags. [63] Pollock et. al. (2018) discuss that it is not the CO_2 in the ambient air that causes degradation of the soda-lime, however any loss of humidity in the soda-lime should be compensated by the humidity in the exhaled gas, at least if the apparatus is of closed circuit type. This correlates with unpublished tests from the SwAF DNC laboratory where a 25-year-old soda-lime batch, stored in a dried rock shelter, were tested under EN14143:2013 conditions. It was shown that the capacity was within approved range but the amount of dust, suggested to be the result of the soda-lime being dried out, was unacceptable and could have caused problem if inhaled. Dust amount is not specified in the standard.

5.5.2.1 Further on soda-lime performance

Another aspect of scrubber performance was brought up for investigation in the hyperbaric laboratory at SwAF DNC; the inability for the ADivP-03 test to actually detect poor performing batches for the application submarine and semi-closed rebreather. The issue was brought up after communicating with submarine personnel describing this. The difference in performance was significant and this caught our interest. After contact with the manufacturer they described that the test procedure STANAG 1411/ADivP-03 was performed for every batch and nothing left the facility without passing this test. They saved all test-protocols and could show us that the actual batches, that were identified as poor performing, had passed the test. We moved on by taking an actual submarine scrubber to the test-lab and commenced testing but realized quite quickly that it was necessary to downscale the test as the scrubber-time would provide a too time-consuming test. Additionally, the different batches were tested according to EN-14143:2013 in the semi-closed rebreather ISMIX® with obvious performance differences, see figure 9.

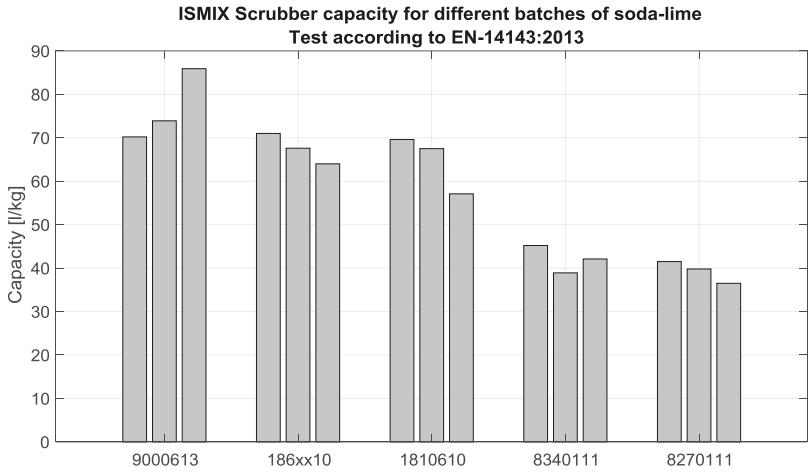

Figure 9, EN-14143 tests with different batches of soda-lime from the same manufacturer and type.

Parallel to this, the various performing batches were sent to a STANAG 1411/ADivP-03 accredited laboratory to verify the manufacturers results and also investigate whether the batches might have been affected during storage or handling. The different performing batches could not be separated by this third-party laboratory and were all performing well, similar to what the manufacturer stated.

By suggesting alternative test-methods it was iteratively investigated if a suitable test could be found. The conclusion was to keep the same Reynolds number as the ADivP-03-test (Re<10), upscale the tube sample size to 6 cm of diameter and 200 gr of soda-lime. The final adjustment was to decrease the CO_2-fraction for the injected gas to 1% but increase the flow to 30 lpm. This was initially tested with dry gas to resemble a submarine environment, but it was not until we also humidified the gas that we could separate a poor performing batch from a good performing batch, see table 3 and figure 10.

Table 3, data from tests with soda-lime capacity. The EN-14143 tests were performed with the ISMIX SCR. The batches starting with nr 90 and 18 (green) are performing well whereas batches starting with nr. 83, 82 and 78 (yellow) performs poor. This is valid for both test methods, as desired. Be advised that only three batches are repeated for both tests as the crates where eventually emptied. Batches 8270111 and 781113 were identified as poor performing in a submarine application.

Test type	Batch	Capacity [l CO_2/kg] Test number			Mean	Std
		1	2	3		
EN-14143	9000613	70	74	86	77	6,7
	186xx10	71	68	64	68	2,9
	181610	70	68	57	65	5,5
	8340111	45	39	42	42	2,6
	8270111	42	40	37	39	2,1
Alternative test method	9000613	69	72	86	76	7,2
	186xx10	69	75	93	79	10,2
	8340111	44	47	46	45	1,3
	781113	47	48	49	48	1,0

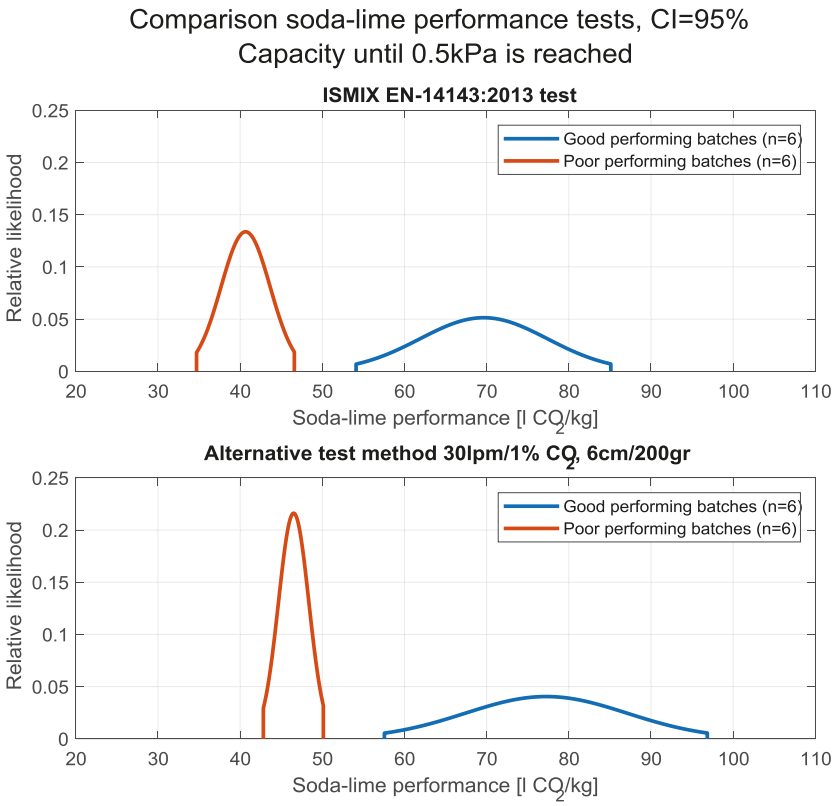

Figure 10, Comparison of results from full scale tests with the semiclosed rebreather ISMIX (upper) and the alternative test method (lower), until 0.5kPa is reached with 95% confidence interval. These results can be found in table 2 but presented as a normal distributed graphical plot.

An interesting observation is that the breathing apparatus ISMIX loses about 10% of the overall soda-lime performance at 40 msw in 4 °C cold water. This could be related to the apparatus design, scrubber design or ambient pressure/temperature.

A poor performing batch in an environment where it is possible to exchange the soda-lime is generally not lethal as one can switch, however in a rebreather during a long decompression it is not possible to take such measures. It is not even sure that the diver will notice it. [58] Note that the difference in batches where only present in the semi-closed rebreather ISMIX. The closed-circuit rebreathers JJ-CCR and KISS which were also tested did not show any noticeable difference between batches. This is arguably a matter of dwell-time and humidity levels where an increase in both is preferable.

There are technologies on the market to reveal a high CO_2-level in the loop by analyzing the loop gas. This can be performed by a traditional IR-sensor as in the Inspiration by AP Diving, Water-Ma-Trout U.K or illuminated reaction patches as in the MCM100 by AVON Protection, Wiltshire U.K. This could be considered as an important safety device if reliable.

5.5.3 Permeability properties of a pressure induced compacted polymer - Paper II

The results from the gas leakage experiments in paper II shows that type 2 and 3 composite gas cylinders do not meet the demands of the standards. However, it is important to bear in mind that the tests in paper II are not designed according to the standardization tests in ISO 11119-3:2013 and/or EN 12245:2009+A1:2011. Results should therefore only be interpreted as an indication to what a standard test would reveal.

The main differences between the test regimes are the measure of gas volume lost, the gas composition and the prescribed cylinder pressure. The standard test prescribes that the cylinders should be weighed before and after storage, whereas we measured pressure drop between measures simultaneously as FO_2, since we were mostly interested in the drop of oxygen fraction being more critical for the diver application. The gas composition of the stored gas is important as it is determined in paper 2 that oxygen diffuses faster than nitrogen through the cylinder wall. This means that an oxygen richer gas composition will lose gas quicker than one with less oxygen. This can be observed for cylinder 4199 and 4234 in table 2. The pressure prescribed in the testing regimes is determined to be either working pressure or 2/3 of maximum design pressure, which is not always the case in the presented experiments from table 2. The result that can be expected if higher storage pressure where prepared, is a greater leakage, even if the permeability coefficient would decrease as shown in paper II.

Type 1 composite gas cylinders are performing well and reach acceptable levels to contain gas. Type 2a has cracks in the inner liner, which was determined after cutting the cylinders in two halves and can also be noticeable from the deviating results of leakage. From a manufacturer perspective it must be of relevance to conclude why these cracks have appeared. Type 3 was never published in paper II because of uncertainties regarding the specifications of its inner liner. Type 3 is however a gas-cylinder that is marked with EN 12245:2009. This reveals that there has been testing involved during its development and production. Why our results are much higher than allowed could depend on thinner liner than during the standardized tests or that other gases were used during the standardized tests. What also can be observed, correlating with the theories of diffusion, is that drive pressure increases the leakage. What is less intuitive and not brought up in the standards is that the fraction of oxygen is a relevant parameter. Higher fraction of oxygen results in more leakage. In the paper II study it is determined that oxygen diffuses more rapidly than nitrogen. This correlates with the material properties of a thermoplastic elastomer, TPE. If other gases than those analyzed here are used, it is necessary to perform additional diffusion analysis of the combination of gas and gas cylinder.

5.5.4 Proposed Thalmann algorithm air diving decompression table for the Swedish Armed Forces - Paper III

The SWEN21 table is developed from experience of scientifically published dives and put into a statistical database. All dives where not performed identically when it comes to workload, thermal protection, ambient temperature, submersed or not, ascend and descent temperature or for the presence of PFO. Naturally different diving organizations have different operative conditions, and this must of course be considered during the actual diving operation. The SWEN21 could therefore only be described as a general table with mean times for safe direct ascent dives. If the conditions are determined to be unprofitable the dive supervisor could add extra safety such as picking a deeper depth in the table or shorten the time. [11]

Germonpré et al. (2021) argue that divers with PFO should dive more conservatively. [64] Bove (1998) describe that there is an increased risk of CNS-DCS for divers with PFO, but since that risk is only slightly increased from already low levels it is not necessary take measures. [65]

For decompression dives our research group still consider not having found an appropriate method to statistically determine the risk but expect this to be part of future work. Other authors have published statistical risk analyses for decompression dives. [66, 67, 68]

Other articles related to the validation dives have been published or are to be published, mainly by the authors MD O. Plogmark who investigated correlation between ultrasound detectable venous gas emboli VGE and the O'Dive™ that scores and detects vein bubbles and MD C. Hjelte[4] who compared our measured VGE during validation dives with previous data on the subject, and the risk of DCS. [69]. Experience from the work with SWEN21 will help improve future models.

Figure 11, divers during validation dives in the hyperbaric chamber wet pot at SwAF DNC.

5.5.4.1 Further on the relationship to dive computer algorithms

An algorithm with suitable parameters for dive computers should have margins to the risk of DCS since each dive could be performed to the limits i.e. a dive computer, constantly knowing the ambient pressure, calculates remaining time more accurately than if a prescribed time and depth combination from a table would have been used. In the latter case the maximum depth could be set to the maximum depth at that position, and a bottom-time is decided, however the actual dive will probably not be spent at that maximum depth but shallower. The maximum dive time is not increased due to this because that was decided before the dive, however with a dive-computer the diver would have gotten more bottom time if the dive partially is spent shallower. Hence a dive-table planning is more conservative than the continuous calculation performed by a dive computer, something that must be considered when going from tables to dive computers.

5.5.5 Early nitrogen wash-out for inside attendants during hyperbaric oxygen therapy – a novel oxygen distribution regimen - Paper IV

A method to be able to perform an emergency decompression based on the experience from the table development, decompression algorithm and the SWEN21B-parameters controlling the decompression strategies is suggested. If an emergency decompression is necessary today,

[4] *Submitted to Diving and Hyperbaric Medicine 2023-02-24*

very little guidance is provided by the Swedish Regulations RMS-Dyk 2013 but somewhat more detailed in US Navy Diving Manual rev.7.

5.6 Density and work of breathing

Due to the fluid dynamics in the airway and the human respiratory design, the ability to perform high ventilation and thus high workload is limited with increased density. If we also apply an external work of breathing from a breathing apparatus this will be additionally difficult and could imply hypoventilation and cause CO_2 retention which is difficult to revert at depth. [22] The standard EN-14143 prescribes testing ventilation between 15-75 l/min, the standard EN-250 suggests a ventilation of 62.5 l/min and the US Navy tests at ventilation rates between 22.5-90 l/min. These ventilations correlates with expected workload and resulting ventilation, but there doesn't seem to be any consensus on which maximum ventilation that is physiologically possible or relevant. A human's ventilation rate is mainly governed by the PCO_2 in the blood. [70] In the NOAA diving manual the following correlation for a diver is presented, see table 4. [71]

Table 4, ventilatory response for different swimming speeds

Workload	RMV [l/min]	Swimming speed[knots]
Rest	10	*0*
Light	20	*0.5*
Moderate	30	*0.85*
Heavy	40	*1*
Severe	60	*1.2*

The discussion in chapter 5.6 will focus on the relationship between the standard demands for work of breathing in a diving apparatus, i.e. the external work of breathing, the internal breathing resistance from the airway and gas density.

5.6.1 Turbulent or laminar flow

The fluid mechanics involved, controlling the resistance in the airways and breathing apparatuses, will be individual. It is important to understand that depending on the type of flow different parameters will control the airway resistance. Clarke and Flook in The Lung at Depth discuss this extensively. [72] They refer to Olson et. al. and Weibel, which uses mathematical modelling, and determined that the airways will keep a laminar flow at an RMV below 30 l/min and generally expect a laminar flow in the airway tree. [73, 74] This reveals a density independent flow resistance which rely more on viscosity. For higher ventilations transitional or turbulent flow is expected, at least in the mouth and the trachea. Clarke and Flook concludes that the exact nature of the flow velocity profile is difficult to describe. [72]

The importance of the flow rates can be described as depending on what factor that controls the resistance. It is of importance to introduce the Reynolds number Re which is a dimensionless ratio describing a flow's inertial forces to its vicious forces.

$$Re = \frac{v \cdot D \cdot \rho}{\mu} \qquad \text{eq. 1}$$

Where v is the fluids velocity

D is the diameter

ρ is the density

μ is the viscosity

A Reynolds number below 2000 can be described as laminar and flow resistance is independent on flow velocity, from 2000 to 10.000 a transitional flow between laminar and turbulent is evolved. Above 10.000 a fully evolved turbulent flow is present. At this stage the flow resistance is proportional to flow velocity $\dot{V}$ to the power of 0.75. [72]

Olsen et. al. and Weibel theorizes that the trachea achieves the highest Reynolds number thus being the most restricted path through the airways. *Re* of 2000 at an RMV of 30 l/min and 3500 at RMV of 60 l/min is theorized. At 120 l/min fully turbulent flow of *Re* 10000 is achieved. [72, 73, 74]

For tests involving fluid dynamic resistance, for example a standardized rebreather WOB test according to EN-14143:2013, it is reasonable to involve the *Re* as a governing parameter as it could reveal weather viscosity or density is the dominating parameter. Determining WOB by interpolation of WOB for different gases with different density and viscosity could be deceiving as there are complexities to determine what parts of the human airway or breathing apparatus that provides laminar, transitional or turbulent flow. However, if the ventilation is high it could be argued that the flow is turbulent and therefore density dependent, but a laminar or transitional flow is the most relevant for a divers ventilation.

5.6.2 Substitution of depth with dense gas when testing equipment

Standardized tests of work of breathing is related to the breathing performance in the breathing apparatus. For untethered breathing apparatuses the applicable standards are EN-250 and EN-14143. These standards set the demands for work of breathing to a depth of 50 msw for open circuit and 40 msw for rebreathers. To facilitate such a test, a very expensive test equipment is necessary.

An idea is whether it would be possible to get trustworthy results if one changed the gas density in a rebreather loop, rather than increasing the depth. If this would be the case it would be possible to perform tests with work of breathing at a simulated depth but at surface. Gavin Anthony, previously employed at Qinetiq U.K., has shown the correlation between density and work of breathing and discussed whether depth could be substituted with a denser gas. [75] The benefits would be to work with testing equipment and breathing simulators at surface without the necessity of a pressure vessel. The density difference between helium (1.78E-4 g/cm^3) and nitrogen (1.3E-3 g/cm^3) at 20°C at atmospheric pressure is seven-fold. Compare this to the density difference between air at surface and at 40 msw and it is less difference, only five-fold. Would this mean that we could substitute a test at 60 msw with a test with pure helium compared to a test with pure nitrogen at surface? Companies that wish to perform indicative tests before CE-certification would in this case have a cheaper test setup and could extrapolate to a higher density to understand WOB at depth. Note that this can only be applicable in a rebreather since open circuit involves other regulator flow situations and volume distributions at deeper depths which cannot be simulated with denser gas. Also consider any viscosity issues which of course might be mitigated with selecting high flow rates, see previous discussion on Reynolds number. Sulfur hexafloride (6.5E-3 g/cm^3) is a very dense gas that might be applicable and used by Maio and Farhi (1967) on humans. [76] Be advised that this an extremely potent greenhouse gas and should not be released into the atmosphere.

5.6.3 Physiological limitations of respiratory minute volume at depth

Serious ventilatory failures due to dense gas has been described by Mitchell (2007). [41] A diver conducting a dive to 264 mfw experienced respiratory failure at depth, presumably due to high density and inability to expel sufficient carbon dioxide due to hypoventilation and excessive work. The density was calculated to be 10.2 g/l at depth. Clarke (2015) describes that divers during the deepest dives performed at NEDU, at a gas density of 9.3 g/l, were sent to their bunks due to respiratory difficulties. [77]

A denser gas creates a larger internal and external work of breathing and the actual work able to be performed by the lung is limited. Warkander (1994) determined that the total work possible for the human to sustain during a longer time is 4.29 kPa (or J/l, in the NEDU terminology kPa is preferred rather than J/l). [78] It is affected by training level, muscle strength and surface maximum respiratory minute volume. Additionally, Moon and Longphre (2006) describes in the book Encyclopedia of Respiratory Medicine under the chapter '*Diving'* that the effect of immersion decreases the maximum voluntary ventilation (MVV) to 90% when immersed. [79] Further Moon and Longphre suggests a decrease of MVV to 70% at a depth of 10 meters with air. Data summarized and interpolated by Camporesi and Bosco (2003) suggests a decrease to 50% of MVV at 30 msw with air. [80] A k-value can be applied according to equation 2 where a compensation of immersion effect (0.9) on MVV is included. A k-value of 0.5 would correlate with the square root relationship suggested by Miller (1989). [81]

$$MVV_{amb_{im}} = MVV_{surf_{dry}} \cdot 0.9 \cdot \sigma^{-k} \qquad \text{eq.2}$$

Where $MVV_{anb_{im}}$ is the maximum voluntary ventilation at depth immersed,

$MVV_{surf_{dry}}$ is the maximum voluntary ventilation at surface non-immersed,

σ is the density at ambient pressure,

k is the value for which the decreased MVV is controlled.

Figure 12 shows a power regression of data from Wood et. al. (1962) and Eves (2003) suggesting a density relationship to the power of -0.48, k=0.48. [82, 83] To include the standard deviation in the data an interpolation method including Monte Carlo simulation in Matlab was used. Both heliox and nitrox as breathing gas is included in the plot as comparison, relating to previous discussion on viscosity being of little relevance at high ventilation, but the interpolation is only done on the nitrox dives.

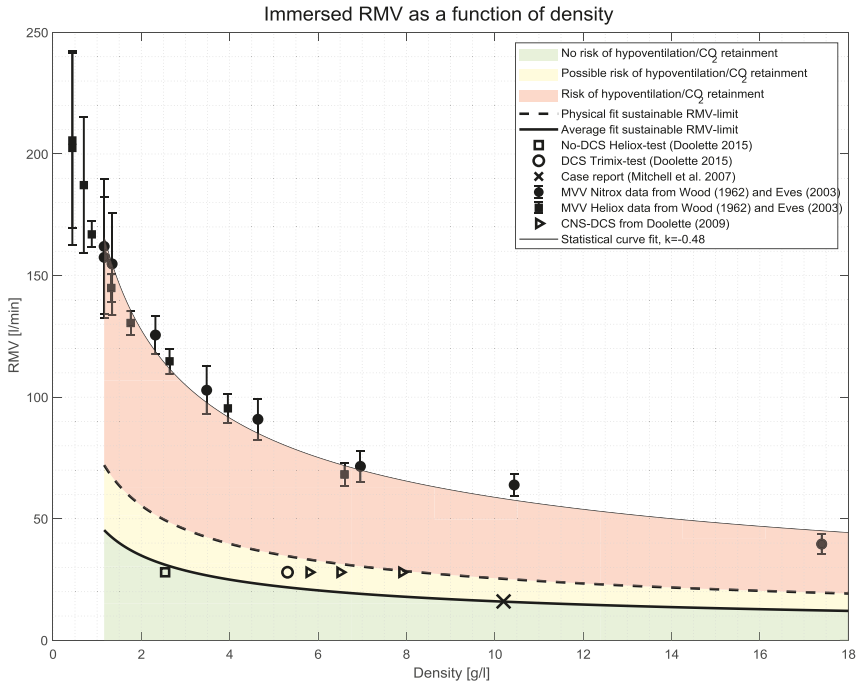

Figure 12, datapoints of MVV from Wood (1962) and Eves (2003) with a power curve fit based on a Monte Carlo simulation to include the data points standard deviation which correlates to the density to the power of -0.48 times RMV. The dashed and solid lines are derived from RMV=80 l/min for very fit divers and RMV=50 l/min for average fit divers, with immersion effect of 90% included. Some cases of DCS and respiratory failure cases are included (circle Trimix test Doolette (2015), triangle Doolette (2009) and cross Mitchell (2007)). In comparison, an uneventful heliox profile identical of the trimix-test is shown as a square, in the green area. RMV for the Doolette examples are derived from the published statement of average workload corresponding to an oxygen consumption of 1.3 l/min, resulting in a ventilation of about 28 l/min. [84, 85, 86] RMV for the Mitchell example is only shown as where the maximum is achieved staying in the green area. As a reference of required RMV NOAA states a ventilation of 18 l/min for swimming at 0.5 knots. [71] Areas in where there is an anticipated risk of CO_2 retention, yellow for average fit divers and red for very fit divers in immersion.

The figure also includes additional hypothetical analyses such as where hypoventilation or CO_2 retention could be expected. A fit human would be able to hold a ventilation of <80 l/min (72 l/min immersed) during a long period of time at surface. [87] From this maximum allowed or sustainable ventilation an assumption is introduced that the decrease in sustainable ventilation correlates to equation 2 and the k-value previously determined for MVV, 0.48. The yellow area is potentially where a fit diver still would be able to avoid CO_2 retainment. An average fit diver should be able to ventilate <50 l/min (<45 l/min immersed) and should as suggested stay in the green zone to avoid suffering from CO_2 retainment due to hypoventilation. [88] From the validation dives performed during the development of SWEN21 it is possible that divers performed work corresponding to ventilations above 20 l/min as divers were instructed to swim calmly hooked in a rubber band. It is also possible to consider that long duration dives, like the 18 msw for 59 minutes induces a thermal regulation corresponding to an increased $\dot{V}_{O_2}$ and CO_2 production. [89, 90] Jauchem (1988) discuss the correlation between exercise, CO_2 and DCS incidence and suggest a potential correlation. [91]

A time factor is necessary to address. If the diver exceeds the recommended ventilation for a short time, which is possible to do as there is margin to MVV, it will take time to restore from the carbon dioxide retainment that might have occurred. Warkander et. al. (1990) showed the implications of CO_2 retention with measuring end-tidal CO_2 >8.5 kPa over five consecutive breaths and associated with incapacitation for the diver. [92] Note that no external work of breathing is added yet, this will be discussed later.

A physiological explanation of the increased resistance is that of dynamic airway compression at high densities mentioned by other authors like Mitchell (2009). [93] This will not be further evolved here.

The physical description of the airway restriction is more related to the state of the flow being laminar or turbulent and related to studies by Olsen et al. and Weibel and believed to be a result of increasing turbulence in the airways as the density increases, i.e. a turbulent boundary layer is dominating. [73, 74] The turbulence and wide boundary layer causes a strict density dependent resistance whereas a laminar flow at lower flow rates are more viscosity dependent. This suggests that an ability to ventilate at high densities remains, although at very low RMV. At very low densities which could be a result of the diluent molecular weight and/or low ambient pressures, other restrictions are expected such as the lung musculature ability to frequently contract and relax. [94] A linear behavior would apply in this region of low densities, see correlation in figure 12 of this for helium which is also suggested by Eves et al. (2004). [83]

5.6.4 The effect of external work of breathing to respiratory failure

As previously mentioned the maximum WOB that can be sustained from respiratory muscles has empirically been determined to be 4.29 J/l. [78] Evolving this argument with the US Navy and NEDU limits for external work of breathing which is 2.99 J/l at surface with air, we expect the maximum acceptable internal work of breathing to be 1.3 J/l. [95] Since a divers respiratory muscles don't get stronger at depth, the density that causes an inevitable increased work of breathing internally must be compensated with a decrease in WOB externally to avoid respiratory failure.

The previous argument of limitations until CO_2 retaining occurred can be limited by external work of breathing such as from a breathing apparatus. Clarke (2015) summarized data from successful and unsuccessful dives, where the later was categorized as breathlessness (dyspnea), loss of consciousness, diaphragmatic or other respiratory muscle fatigue. [77] The data suggests that there is a linear relationship between density, external work of breathing and respiratory failure. Tests are performed at a fixed exercise protocol. In figure 13 data from Clarke (2015) and Warkander (2001) are extracted and plotted and curve fitted with 95% CI, represented as the yellow area. [77, 96] Note that the WOB is converted from peak to peak respiratory pressures ΔP to WOB by integrating a sinusoidal wave with ΔP values given in Clarke (2015). [77]

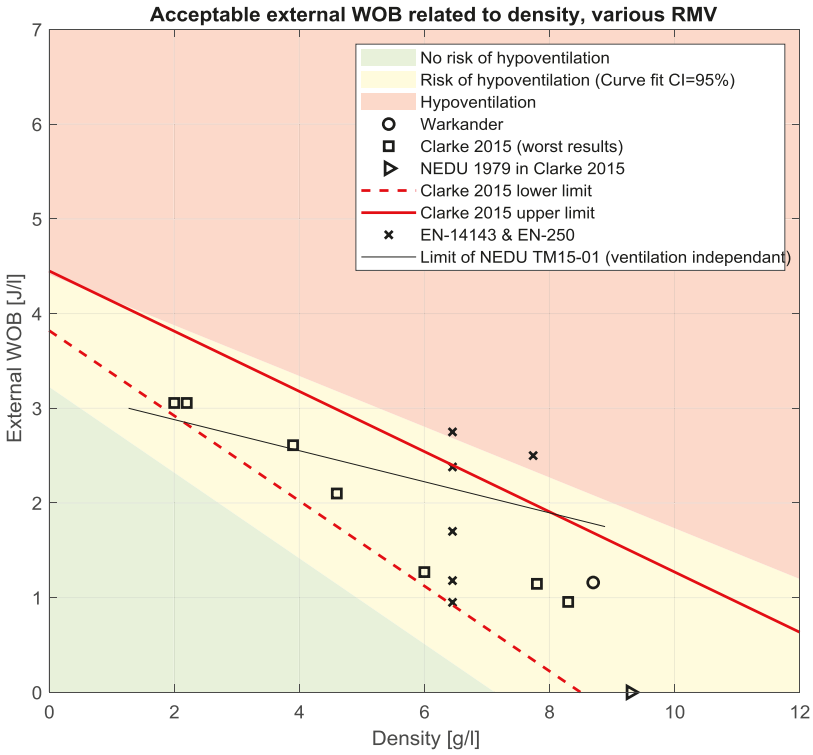

Figure 13, the figure shows data from Clarke (2015) worst cases and from Warkander et. al. (2001) where respiratory failure occured. There are also reports in Clarke (2015) of dives performed with a 9.3 g/l dense gas which did not allow any external work of breathing or high workload (triangle). The standard tests EN-14143 and EN-250 shows to be well out of safe limits. We could theorize that the fitted 95% confidence interval CI (yellow area) comprise acceptable WOB-levels for fit diver. The red area should induce respiratory failure and definite CO_2-retention during sustained work and correlates well with Clarke (2015) upper limit.

There are also limitations in how high additional external work of breathing the human can add while keeping acceptable levels of ventilation related to a sustained workload and avoid respiratory failure. Naturally there is a connection between physical fitness and MVV, but limitations apply, nonetheless. Data from Wood (1962) in figure 12 reveals that any differences between individuals decrease with depth. Standards prescribe limitations in a manner related to what ventilation is tested, with which gas, at which depth (density) and correlate this with a maximum allowed work of breathing. For the rebreather standard EN-14143:2013 the maximum external work of breathing is 2.75 J/l at a gas density of 6.45 g/l (STPD), clearly in the red area from figure 13. For the open circuit standard EN-250:2014 the maximum external work of breathing is 2.5 J/l at a gas density of 7.74 g/l (STPD), also in the red area. Clarke (2015) presented a suggested density limitation related to probabilistic theories of acceptable ventilatory load, derived from Clarke et al (1989a,b; 1992), Bentley (1973), and Mead (1955). [97-101] The probabilistic approach used a fix workload translated to a ventilation of about 60-75 l/min and set the density as a variable. A NEDU in-house developed software called *Predict* is used to give a statistical result for the risk of ventilatory failure related to WOB and density. [77]

Warkander suggest a lesser external work of breathing with increased depth, or density. [95] This is justifiable based on the analysis that is performed herein.

Anthony and Mitchell (2015) also observed an increase in respiratory failure with increased gas density and suggest a density limitation to 6 g/l which also is motivated with similar arguments; however, this does not specify the breathing apparatus WOB or the diver's workload. [102] Applying the Anthony and Mitchell results on the Clarke lower limit in figure 13 it is anticipated that the divers that failed were having an external WOB >1 J/l. To perform an analysis of the combined limitations it is necessary to include both the external and internal work of breathing limitations, which go beyond those stated in the standard but could determine the actual RMV or workload allowed to avoid hypoventilation.

5.6.5 Combining external and internal resistance and WOB

Imagine a diver on air at 50 msw; gas density is ~7.5 g/l depending on what temperature applicable. This would according to figure 12 allow an preferable workload correlating to a ventilation of a mere ~20 l/min to avoid hypoventilation and CO_2 retaining, whereas figure 13 provides information on the maximum allowed external WOB to about 1.7 J/l, for a fit diver (*using the average curve fit line from figure 13, not shown*). It could however be recommended that no external WOB should be added as we've entered the yellow zone. To evolve the discussion, we introduce a breathing apparatus with known WOB. By analysis of the combined data it is possible to predict if the Swedish Navy Mine Clearance Rebreather ISMIX® have an acceptable work of breathing for this dive. Data retrieved from SwAF DNC in-house testing reveals that this particular rebreather has a WOB of ~0.5 J/l at this ventilation, gas and depth. According to figure 14 we are unfortunately in the "double" yellow zone for this particular dive, so it is both limited by external WOB and RMV requirements. However, even if the external WOB would have been less at this depth and ventilation, it would still have been in the double yellow zone even without external WOB, i.e. without any apparatus.

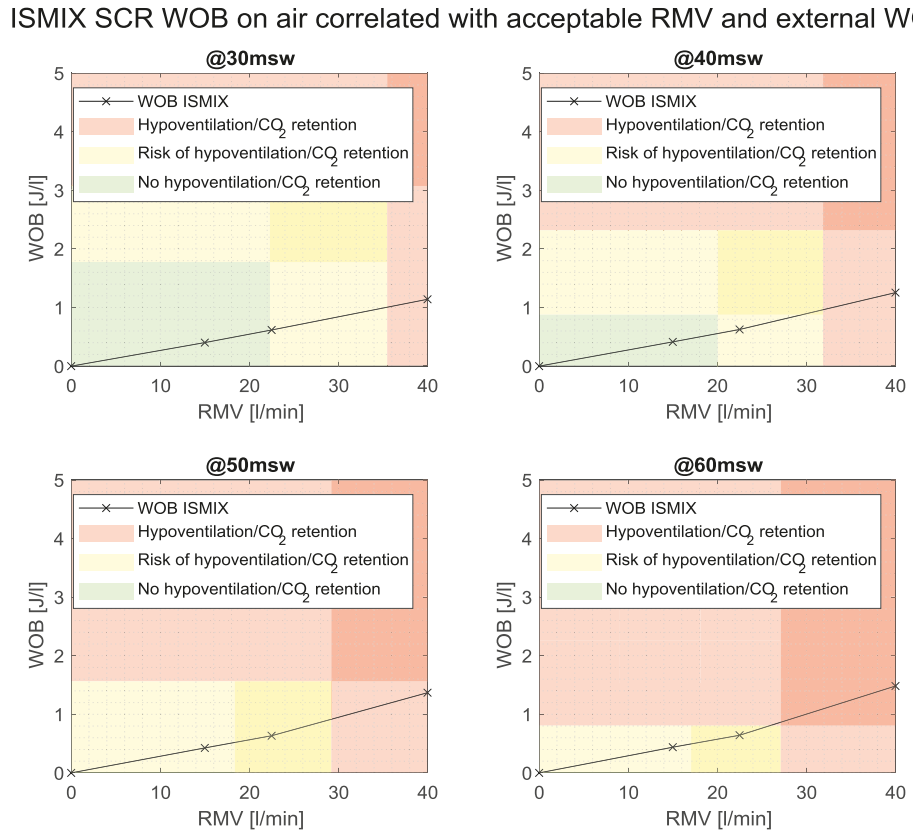

Figure 14, the semi closed rebreather ISMIX® is used to further describe the theory of maximum external WOB and necessary RMV for the diver depending on density. The green area is acceptable at any time and the ISMIX® is capable to provide a safe dive in ventilation from 22 (safe) to 36 (risk) l/min at 30 msw, 20 (safe) to 32 (risk) l/min at 40 msw. For dives to 50 msw there is an immediate risk up to 20 l/min but increased risk (both yellow areas interfere) up to 29 l/min of RMV. At 60 msw it is even less. Dives with ISMIX® and air deeper than 40 msw should hence be carefully considered.

It would according to this hypothesis and figure 14 require careful considerations to perform a dive deeper than 40 msw dive with this gas, air. For dive profile 50 and 60 msw it is the external WOB that is limiting meaning that no breathing apparatus would be applicable, whereas at 30 and 40 msw it is the required ventilation to avoid hypoventilation that is limiting and only a breathing apparatus with higher WOB could interfere this.

If the same dive would have been performed on heliox 80/20 the density would be ~2.7 g/l. From figure 13 we see that the external WOB would be acceptable up to ~3.6 J/l preferably <2.0 J/l, while at the same time the WOB from the diving apparatus will be significantly less due to the gas shift. We can also imply that the workload and ventilation could increase to ~30 l/min without the risk of CO_2 retaining by referring to figure 12. The work of breathing for ISMIX under these heliox conditions is ~1 J/l so there is no risk of excessive external WOB or hypoventilation/CO_2 retention if RMV is <30 l/min.

As a comparison the case report described by Mitchell et. al. (2007), where trimix was used and a gas density of 10.2 g/l was present, is shown in figure 15.

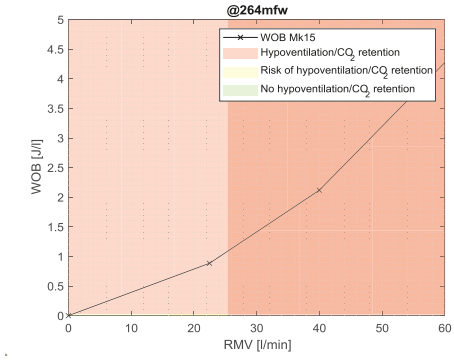

Figure 15, The WOB of an eCCR Biomarine Mk 16 at 264 mfw (the actual apparatus used was a Mk 15.5) with a trimix gas and PO_2 setpoint at 1.3 bar ending up with a density of 10.2 g/l. Neither a compliable ventilation nor external WOB is possible. Still this diver performed over 5 minutes of struggling bottom time, but then perished. WOB data for collected and extrapolated from Warkander (2010). [103]

Figure 15 reveals a hypothetical risk of hypoventilation and CO_2 retention during the extreme dive to 264 mfw. The conditions to perform sufficient ventilation would have been otherwise if heliox was used. As a comparison to the data presented in figure 15 the mk 16 rebreather in the US Navy configuration, i.e. using heliox, is analyzed in figure 16.

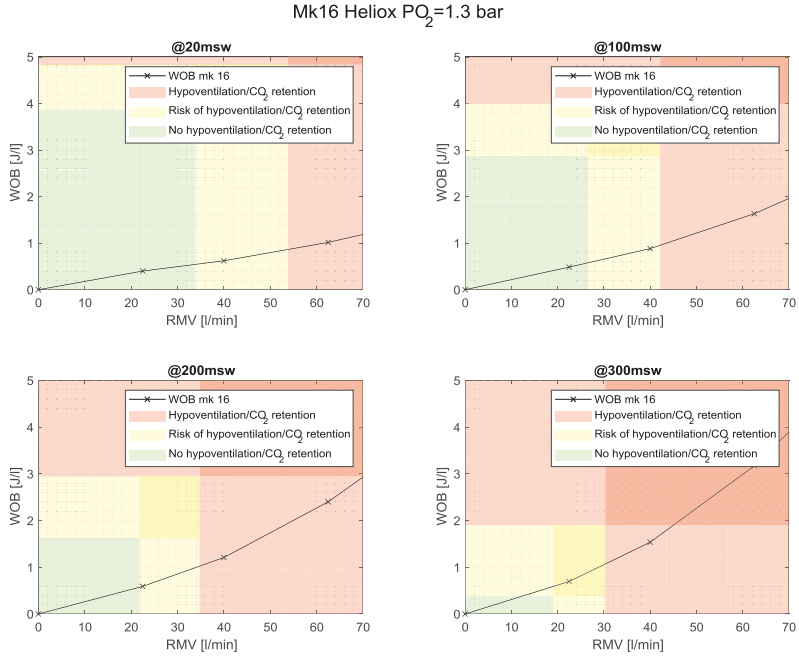

Figure 16, the WOB for a Mk 16 rebreather plotted in a chart where limits of respiratory capability and external WOB are represented by green (acceptable), yellow (risk) and red areas that correlate to acceptable sustainable ventilation rates. It is not until 300 msw as the apparatus WOB sets the limit for recommended ventilation represented by the black line entering the yellow area.

As a summary of these performance charts, figure 17 is compiled. It shows the hypothetical limits for two diving apparatuses with different gases to avoid hypoventilation by staying below a recommended (dashed line) and maximum (solid line) RMV.

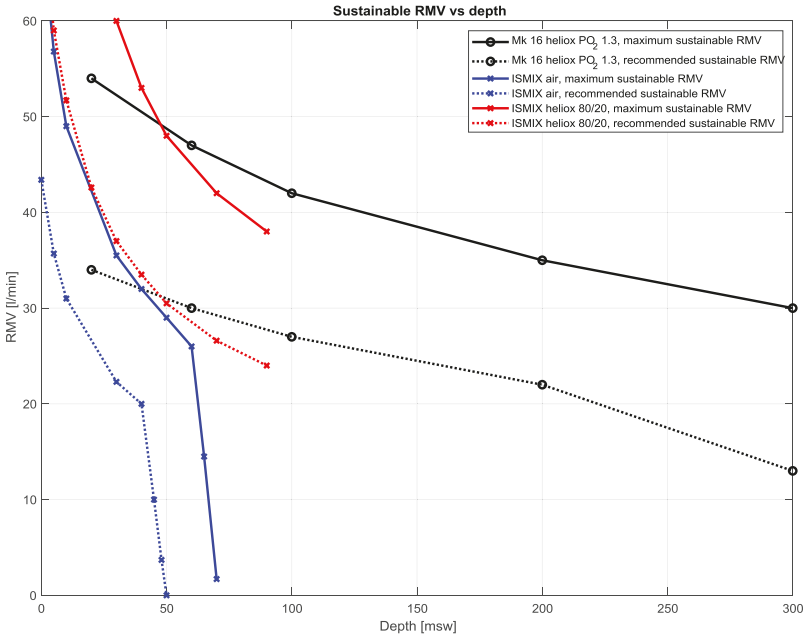

Figure 17, the figure is a summary of the information in figure 14 and 16 with additional heliox data for the ISMIX® down to 80 meters which is the maximum depth the Royal Netherlands Navy dive to. We see that the hypothetical limitations are well below the recommended standardized tests in EN-14143. Limits are mainly controlled by the diver's ability to avoid hypoventilation according to figure 12 but at some stage the external WOB becomes dominant and data from figure 13 becomes dominant. This is shown as a drop in *recommended* sustainable RMV for ISMIX® air past 40 msw and Mk 15.5 past 200 msw as well as deeper than 60 msw for *maximum* sustainable RMV for ISMIX® air.

From the hypothetical limits suggested herein one could suggest that the standards EN-250 and EN-14143 have focused on ventilation that might not even be relevant as CO_2 retention might occur at those ventilations.

5.6.6 The relevance of carbon dioxide, density and work of breathing for decompression sickness

Rebreathing carbon dioxide or inhaling fractions of CO_2 has been known to trigger DCS. In animals it was shown that CO_2 breathing prior to simulated submarine escape triggered CNS-DCS in one animal and none in the group with no CO_2. [104] Referring to Mano and Arrigo (1978) the most common site of affliction among caisson workers just prior to decompression was found to lie within the body region where the highest tissue tensions of CO_2 would be expected during decompression. The results could be questioned as the time exposed to CO_2 is not included and the dive profiles. [105] Ishiyama (1983) measured gas composition in bubbles produced from decompressing rabbits and found that CO_2 was to a high extent present and suggests that Haldanian decompression models should be modified to include other gases than nitrogen. [106] Instead of inhaling CO_2, which, according to Boycott et. al. (1908), was even believed to depress DCS as it increases circulation to the muscles, what if hypoventilation and CO_2 retention occurs leading to possible respiratory acidosis. Could this trigger DCS? Does this

mean that it could be CO_2 that triggers unexplained DCS? Does it suggest that a diver with capability to expel lactate and CO_2 more efficiently, has less risk of DCS? Could the design of the breathing apparatus have more influence of the outcome of decompression sickness than anticipated or is it more of a gas density question? It can be noticed that Wood et al. (1962) recommends that all nitrox scuba diving should be abandoned in favor of heliox diving motivated by the detoriating respiratory functions with increased density. Further recommendations from Wood also include national researchers at Experimental Diving Unit USA to develop heliox-tables, adequate breathing apparatuses and gases and the relevance of the narcotic properties, similar to the discussions we still have 60 years later.

5.7 Summary of discussion

If a standardized test is designed improperly this might cause a sense of false safety. An example of this could be the results that are presented in this text under paper I. Soda-lime are stated to endure at a much higher level in the ADivP-03 than what is actually achieved in EN-14143, possibly due to temperature differences in the testing regimes. However, it can be questionable if a diver can withhold a workload corresponding to a ventilation of 40l/min throughout a 2-3 hour long dive. This is emphasized by the test regime suggested by NEDU in TM 15-01, where a CO_2 injection of 0.9 l CO2/min or 1.35 l CO2/min is recommended at an *RMV* of 22.5 l/min or 34 l/min, with a ventilatory equivalent set to 22.5. When discussing carbon dioxide it is also of great relevance to understand the influence of the mouthpiece or full face mask regarding dead-space.

If a product is marked with a label to be approved according to a standard, this must be trusted. The results from gas leakage tests indicate that the requirements may be unfulfilled, but not definite, as the tests were not performed according to relevant standard. For standardized tests and labelling to be trustworthy it is fundamental that nothing is altered between production and laboratory testing. Even small changes of design could require new tests for verification of the label.

It should be reasonable to recommend that a diving apparatus should endorse a gas density and workload limitation instead of a certain WOB at a certain depth. For the ISMIX® table 5 and the Mk 16 table 6 could serve as an example with data derived from previous analysis method used in figure 14 and 16, data from figure 12 and 13 and the specific WOB for the breathing apparatus. Data correlation for workload, RMV and swimming speed is taken from the NOAA manual. [71]

Table 5, a suggested performance table for ISMIX®

Workload	RMV [l/min]	Swimming speed [knots]	Recommended maximum gas density [g/l]	Absolute maximum gas density [g/l]
Rest	10	*0*	6.5	9.7
Light	20	*0.5*	6.0	9.2
Moderate	30	*0.85*	2.8	7.0
Heavy	40	*1*	1.5	4.0
Severe	60	*1.2*	0.6	1.7

Table 6, a suggested performance table for Mk 16.

Workload	RMV [l/min]	Swimming speed [knots]	Recommended maximum gas density [g/l]	Absolute maximum gas density [g/l]
Rest	10	*0*	7.1	9.6
Light	20	*0.5*	6.6	9.0
Moderate	30	*0.85*	2.8	7.0
Heavy	40	*1*	1.5	4.0
Severe	60	*1.2*	0.6	1.7

Comparing table 5 and 6 we see that most of the density limits correlate, at least ≥30 l/min. This is due to identical limitation factor for most of the ventilations which is suggested to be the physiological limitations for the diver when breathing dense gas, i.e. limitations shown in figure 12. However, it is more probable that a calm diver would be in the RMV 20 l/min area and the difference between the apparatuses are then clear. This limitation is then related to the work of breathing of the apparatus. Note that for densities, below those of air at atmospheric pressure, are results of extrapolation from figure 12 and should possibly be linearly extrapolated as previously discussed.

6. Conclusion

A diving apparatus comprise of some more or less vital components. These components must nevertheless be reliable and robust during long term operations or storage. To verify a breathing apparatus, function a series of tests are described in the European standards. These tests are both unmanned and manned. The challenges of performing these tests are many, as small measurement errors can have a big effect on the outcome. For these reasons it can be recommended to use an accredited laboratory to perform these tests. If the product aims to be CE-certified the tests has to be performed by such a laboratory and verified by a notified body.

Products that are used over a long period of time can be aged and change its properties. Re-testing in intervals might be considered. It can be remembered that the standardization requirements where only fulfilled at the time the tests were performed and there is no demand for any follow up on the performance of the product.

The relevance of the standardized tests should be unarguable. How these tests are designed and performed and potentially updated could be, and already is debated in technical committees. Specific interest should be in the gas density and risk for unpredictable hypoventilation. The standard for composite gas cylinders EN-1119-3 and EN-12245 only recommend a measurement of the gas amount lost. However, it must be recommended to also analyze any gas fraction deviation. Carbon dioxide scrubbers duration time in a diving apparatus can only be determined by testing in the actual rebreather according to for example EN-14143, however there are also tests like the ADivP-03 that indicate the performance of the sole scrubber material. An alternative test procedure for soda-lime that would be more appropriate for submarine and semi-closed rebreather performance is suggested herein. In all

- Theoretical findings demonstrate that a software-based monitoring algorithm for a partial pressure oxygen sensor could effectively detect current limitations, erroneous calibrations, or blocked sensors without requiring any additional hardware. This algorithm identifies anomalies in the expected signal output from the sensor.

- Indications are presented that temperature monitoring of a carbon dioxide scrubber may be misleading under specific conditions, particularly on the surface. The accuracy of temperature monitoring is influenced significantly by even slight changes in ambient pressure. Moreover, tested scrubber temperature sensors exhibit variations in readings and calibration within controlled temperature environments, which can impact readings even at depth.
- Composite gas cylinder with co-poly ether ester inner-liner and a carbon-/glassfibre outer shell are prone to leak gas in favor of oxygen over nitrogen at different ratios depending on cylinder pressure which causes compaction of the liner. It is also shown that anomalies such as cracks in the inner liner, stimulates a faster progress of the leakage. The standards for this type of cylinder describe the acceptable leakage of gas but do not comprise any limits of gas composition change which can occur since different molecules have dissimilar permeability properties.
- An alternative soda-lime testing procedure is proposed.
- A new air and nitrox equivalent diving table, SWEN21, based on the El-DCM Thalmann algorithm but with adjusted parameters aiming for a maximum risk of decompression sickness of less than 1% and less than 0.1% for neurological symptoms, is suggested.
- An alternative oxygen strategy for the inside attendant during hyperbaric therapy on treatment table 6 is proposed, anticipating a reduced risk of decompression sickness during emergency decompression. Additionally, a method to compare the compartmental gas loads in the decompression model between different treatment tables is presented.
- A discussion is provided on the significance of considering CO_2, gas density, and hypoventilation when addressing, respiratory failures, and acceptable external work of breathing, and possibly even decompression strategies.

7. References

1. DENOBLE, P. J., Caruso, J. L., de L Dear, G., Pieper, C. F., & Vann, R. D. (2008). Common causes of open-circuit recreational diving fatalities. *Undersea & Hyperbaric Medicine*, *35(6), 393*.

2. BUZZACOTT, P., Rosenberg, M., & Pikora, T. (2009). Using a Delphi technique to rank potential causes of scuba diving incidents. *Diving and Hyperbaric Medicine*, *39(1), 29-32*.

3. VANN, R. D., Butler, F. K., Mitchell, S. J., & Moon, R. E. (2011). Decompression illness. *The Lancet*, *377(9760), 153-164*.

4. HAMILTON R.W, Thalmann E. (2003) Decompression practice. In. Brubakk AO, Neuman TS, eds. Bennett and Elliott's Physiology and Medicine of Diving, 5th ed. Edinburgh, UK. Saunders.

5. PARKER J.M. (2004) Self-contained breathing apparatus. *European patent specification EP1580116A1*

6. SJÖBLOM K, Stone W.C, Jones N. (2008) Oxygen control in breathing apparatus *European patent specification EP2205322A1*

7. GURR K, Bushnell N.K. (2010) (12) Rebreather control parameter system and dive resource management system. *United States Patent Application Publication No.. US 2017/0106954 A1*

8. EN 14143:2013 Respiratory equipment. Self-contained re-breathing diving apparatus. *European committee for standardization Brussels Belgium*

9. Regulation (EU) 2016/425 of the European parliament and of the council of 9 March 2016 on personal protective equipment and repealing Council Directive 89/686/EEC

10. CHINN, S. (1991). Statistics in respiratory medicine. 2. Repeatability and method comparison. *Thorax, 46(6), 454*.

11. RISBERG J, Møllerløkken A, Sande Eftedal O. (2019) Norwegian Diving- and Treatment Tables 5th edition ISBN 978-82-690699-6-9

12. HOFFMANN U, Dräger T. (2012) Heartrate measurement for better workload assessment. https.//scubapro.johnsonoutdoors.com/sites/default/files/2022-10/scp_productmanual_hrm_2012_en.pdf, accessed 2023-06-07

13. Regler för militär sjöfart RMS-Dyk. Vol. 2013. Stockholm, Sweden. Högkvarteret; 2013 *M7739-351116*.

14. AFS 2010.16 Dykeriarbete - Arbetsmiljöverkets föreskrifter om dykeriarbete samt allmänna råd om tillämpningen av föreskrifterna.

15. AFS 2019.4 Dykeriarbete - Arbetsmiljöverkets föreskrifter om ändring i Arbetsmiljöverkets föreskrifter (AFS 2010.16) om dykeriarbete.

16. BERT, P. (1878). La pression barométrique. recherches de physiologie expérimentale. G. Masson.

17. PHILLIPS, J. L. (1998). The bends. compressed air in the history of science, diving, and engineering. Yale University Press.

18. BOYCOTT, A. E., Damant, G. C. C., & Haldane, J. S. (1908). The prevention of compressed-air illness. *Epidemiology & Infection, 8(3), 342-443*.

19. WORKMAN, R. D. (1965). Calculation of decompression schedules for nitrogen-oxygen and helium-oxygen dives (p. 0040). Washington, DC: Navy Experimental Diving Unit.

20. BÜHLMANN, A. A., Völlm, E. B., & Nussberger, P. (2013). Tauchmedizin: Barotrauma Gasembolie· Dekompression Dekompressionskrankheit Dekompressionscomputer. Springer-Verlag.

21. PARKER, E. C., Survanshi, S. S., Weathersby, P. K., & Thalmann, E. D. (1992). Statistically based decompression tables. VIII. Linear-exponential kinetics. *NMRI Report, 92-73*.

22. GROVER, I., Reed, W., & Neuman, T. (2007). The SANDHOG criteria and its validation for the diagnosis of DCS arising from bounce diving. *Undersea and Hyperbaric Medicine, 34(3), 199*.

23. MOON, R. E., Vann, R. D., & Bennett, P. B. (1995). The physiology of decompression illness. *Scientific American, 273(2), 70-77*.

24. JONES N. (2012) PO2 sensor redundancy. *Proceedings Rebreather Forum 3*

25. FRÅNBERG O, Silvanius M. (2012) Post-incident investigations of rebreathers for underwater diving. *Proceedings Rebreather Forum 3*

26. LAMB J. S. (1999) The Practice Of Oxygen Management for Divers. *U.K., West Yorkshire Best Publishing Company; 1st Edition*

27. FRÅNBERG O, Örnhagen H. (2005) Oxygenceller i hyperbar miljö, *Totalförsvarets Forskningsinstitut FOI-R-1622-SE ISSN 1650-1942*

28. SIEBER A, Enoksson P, Krozer A. (2012) Smart Electrochemical Oxygen Sensor for Personal Protective Equipment. *IEEE Sensors Journal (Volume. 12, Issue. 6)*

29. SIEBER A. (2012) Oxygen sensor technology for rebreathers. *Proceedings Rebreather Forum 3*

30. BORISOV S, Nuss G, Klimant I. (2008) Red light-excitable oxygen sensing materials based on platinum(II) and palladium(II) benzopor-phyrins. *Anal. Chem. 9435-42*.

31. SIEBER A. (2011) Solid-state electrolyte sensors for rebreather applications. a preliminary investigation. *Diving and Hyperbaric Medicine Volume 41 No. 2*

32. VANN R.D, Pollock N.W, Denoble P.J. (2007) Rebreather fatality investigation. *Diving for science 2007*

33. FOCK A.W. (2013) Analysis of recreational closed-circuit rebreather deaths 1998-2010. *Diving Hyperb Med 43(2). 78-85*

34. SIEBER, A., L'Abbate, A., & Bedini, R. (2009). Oxygen sensor signal validation for the safety of the rebreather diver. *Diving and Hyperbaric Medicine*, 39(1), 38-45.

35. U.S. Navy unmanned test methods and performance limits for underwater breathing apparatus. (2015) *Navy experimental diving unit technical manual NO. 15-01*

36. LONCAR M. (1991) Simulation of the human metabolism by catalytic combustion of propylene. *Department of Naval Architecture and Ocean Engineering, Chalmers University of Technology, Report B 50144-5.1, ISSN 0281-0263, Gothenburg, Sweden*

37. FRÅNBERG, O. (2015). Oxygen content in semi-closed rebreathing apparatuses for underwater use: Measurements and modeling (*Doctoral dissertation, KTH Royal Institute of Technology*).

38. MORRISON, J. B., & Reimers, S. D. (1982). Design principles of underwater breathing apparatus. The physiology and medicine of diving. 3rd edn. London: Baillière Tindall.

39. NUCKOLS M.L, Clarke J.R, Marr W.J. (1999) Assessment of oxygen levels in alternative designs of semiclosed underwater breathing apparatus. *Life Support Biosph Sci 6(3).239-249*

40. KLOS R. (2019) Designing of diving technologies – process approach. *Polish hyperbaric research Vol. 66 Issue 1 pp. 7 - 2*

41. MITCHELL S.J, Cronje F, Meintjes W.A.J, Britz H.C. (2007) Fatal respiratory failure during a technical rebreather dive at extreme pressure. *Aviat Space Environ Med. 78.81*

42. WARKANDER D.E, Norfleet W T, Nagasawa G K, Lundgren C E. (1990) CO2 retention with minimal symptoms but severe dysfunction during wet simulated dives to 6.8 atm. *Undersea Biomed Res. 17(6).515-23*

43. Technical datasheet Carbon Dioxide Absorption, Sofnolime Military Diving and submarine grade. https.//www.molecularproducts.com/wp-content/uploads/2018/06/Sofnolime-D-L-S-TDS-v10.pdf , accessed 2020-09-07

44. Benchmark testing from factory acceptance test provided upon delivery, performed by Molecular Products.

45. EN 12021:2014 Respiratory equipment – Compressed gases for breathing apparatus. *European committee for standardization Brussels Belgium*

46. ROBESON L.M, (1999) Polymer membranes for gas separation. *Current Opinion in Solid State and Materials Science Volume 4, Issue 6, Pages 549-552*

47. W.R. Grace and Co. (1986) The Sodasorb manual of carbon dioxide absorption. Fifth printing. *W.R. Grace & Co., Dewey and Almy Chemical Division. Sectionp-1, Chemical and Physical Processes in Carbon Dioxide Absorption, Lexington, MA*

48. SILVANIUS M. (2019) Workshop FM framtida dekompressionsalgoritmer. Karlskrona. Försvarsmakten; FM2019-15019.4.

49. US Navy Diving Manual, Rev. 7. (2017) Washington DC, USA. Naval Sea Systems Command.

50. HAMILTON RW, Muren A, Röckert H, Örnhagen H. (1988) Proposed new Swedish air decompression tables. *In. Paper no 10. Aberdeen. EUBS.*

51. THALMANN, E. D. (1985). Development of a decompression algorithm for constant 0.7 ATA oxygen partial pressure in helium diving. *NEDU Report, 1-85.*

52. ARIYARATNAM, P., Loubani, M., Bennett, R., Griffin, S., Chaudhry, M. A., Cowen, M. E., Morice, A. H. (2013). Hyperoxic vasoconstriction of human pulmonary arteries: a novel insight into acute ventricular septal defects. *International Scholarly Research Notices*.

53. GERTH, W. A., & Doolette, D. J. (2007). VVal-18 and VVal-18M Thalmann algorithm air decompression tables and procedures. *NEDU TR 07-09*, Navy Experimental Diving Unit, Panama City, FL.

54. FRÅNBERG O, Silvanius M, Rullgård H, Plogmark O, Hjelte C. (2020) Delrapport. Framtagande av dekompressionstabell för luft och nitrox i öppna andningssystem. Karlskrona. Blekinge Tekniska Högskola TIMN; Report No. BTH-6.1.1-0107-2020.

55. GENNSER, M., Blogg, L. (2015) Effect of gas switch on decompression from trimix dives. *Presented at the EUBS 41st Scientific Conference, 2015.*

56. Personal communication with Tuomas Runola Finnish Navy (2020)

57. FRÅNBERG O, Silvanius M. (2020) Final Report. SWEN21B development of new decompression tables for air and nitrox Karlskrona. Blekinge Tekniska Högskola TIMN; Report No.. BTH-6.1.1-0107-2020

58. DENG, C., Pollock, N. W., Gant, N., Hannam, J. A., Dooley, A., Mesley, P., & Mitchell, S. J. (2015). The five-minute prebreathe in evaluating carbon dioxide absorption in a closed-circuit rebreather: a randomized single-blind study. *Diving Hyperb Med, 45(1), 16-24.*

59. MOON, R. E., & Mitchell, S. J. (2021). Hyperbaric oxygen for decompression sickness. *Undersea & hyperbaric medicine, 48(2), 195-203.*

60. ARIYARATNAM, P., Loubani, M., Bennett, R., Griffin, S., Chaudhry, M. A., Cowen, M. E., Morice, A. H. (2013). Hyperoxic vasoconstriction of human pulmonary arteries: a novel insight into acute ventricular septal defects. *International Scholarly Research Notices*.

61. SIEBER, A., L'Abbate, A., & Bedini, R. (2009). Oxygen sensor signal validation for the safety of the rebreather diver. *Diving and Hyperbaric Medicine, 39(1), 38-45.*

62. EATON DJ. (1995) Effects on scrubber endurance of storing soda lime in CF rebreathers. *Technical Report DCIEM No. 95–47.* Defense and Civil Institute of Environmental Medicine

63. POLLOCK N.W, Gant N, Harvey D, Mesley P, Hart J, Mitchell S.J. (2018) Storage of partly used closed-circuit rebreather carbon dioxide absorbent canisters. *Diving Hyperb Med.*; *48(2). 96–101*

64. GERMONPRÉ, P., Lafère, P., Portier, W., Germonpré, F. L., Marroni, A., & Balestra, C. (2021). Increased risk of decompression sickness when diving with a right-to-left shunt: results of a prospective single-blinded observational study (the "Carotid Doppler" study). *Frontiers in physiology, 12, 763408.*

65. BOVE, A. A. (1998). Risk of decompression sickness with patent foramen ovale. *Undersea & hyperbaric medicine, 25(3), 175.*

66. MURPHY, F. G., Swingler, A. J., Gerth, W. A., & Howle, L. E. (2018). Iso-risk air no decompression limits after scoring marginal decompression sickness cases as non-events. *Computers in Biology and Medicine, 92, 110-117.*

67. GERTH, W. A., & Vann, R. D. (1997). Probabilistic gas and bubble dynamics models of decompression sickness occurrence in air and nitrogen-oxygen diving. *Undersea & hyperbaric medicine, 24(4), 275-292.*

68. SOUTHERLAND, D. G. (1992). Logistic regression and decompression sickness (*Doctoral dissertation, Duke University*).

69. PLOGMARK, O., Hjelte, C., Ekström, M., Frånberg, O. (2022). Agreement between ultrasonic bubble grades using a handheld self-positioning Doppler product and 2D cardiac ultrasound. *Diving and Hyperbaric Medicine, 52(4), 281-285.*

70. GUYENET, P. G., & Bayliss, D. A. (2015). Neural control of breathing and CO2 homeostasis. *Neuron, 87(5), 946-961.*

71. NOAA Manual Diving for Science and Technology 4th edition (2001) Best Publishing Co., Flagstaff, AZ

72. LUNDGREN C, Miller JN. (1999) The Lung at Depth. Marcel Dekker Inc, New York, NY

73. OLSON, D. E., Dart, G. A., & Filley, G. F. (1970). Pressure drop and fluid flow regime of air inspired into the human lung. *Journal of applied physiology, 28(4), 482-494.*

74. WEIBEL, E. R., Cournand, A. F., & Richards, D. W. (1963). Morphometry of the human lung (Vol. 1). Berlin: Springer.

75. ANTHONY G. (2014) Gas density. A forgotten factor. Presented at. Eurotek; September 2014; Birmingham U.K.

76. MAIO, D. A., & Farhi, L. E. (1967). Effect of gas density on mechanics of breathing. *Journal of Applied Physiology, 23(5), 687-693.*

77. CLARKE, J. R. (2015). The History and Implications of Design Standards for Underwater Breathing Apparatus–1945 to 2015. *NEDU TR 15-03*, Panama City, FL

78. WARKANDER D.E (1994) Comprehensive Performance Limits for divers' Underwater Breathing gear. Consequences for Underwater Breathing Apparatus, *NEDU TM 01-94*, Panama City, FL

79. MOON RE, Longphre JP. (2006) Diving; Laurent, G. J., & Shapiro, S. D. (Eds.) Encyclopedia of respiratory medicine (Vol. 3). Academic Press Elsevier.

80. CAMPORESI EM, Bosco G. (2003) Ventilation, gas exchange, and exercise under pressure. In. Brubakk AO, Neuman TS, eds. Bennett and Elliott's Physiology and Medicine of Diving, 5th ed. Edinburgh, UK. Saunders. 77-114.

81. MILLER JN. (1989) Physiological limits to breathing dense gas. In. Lundgren CEG, Warkander DE, eds. Physiological and human engineering aspects of underwater breathing apparatus. *Proceedings of the fortieth Undersea and Hyperbaric Medical Society Workshop*. Bethesda, MD.

82. WOOD WB, Leve LH, Workman RD. (1962) Ventilatory Dynamics Under Hyperbaric States, *NEDU TR 01-62*. Panama City, FL

83. EVES N, Petersen S, Jones R. (2004) Effects of Helium and 40% O 2 on Graded Exercise With Self-Contained Breathing Apparatus. *Canadian journal of applied physiology = Revue canadienne de physiologie appliquée. 28.910–26.*

84 DOOLETTE, D. J., Gault, K. A., Gerth, W. A. (2015). Decompression from He-N 2-O 2 (trimix) bounce dives is not more efficient than from He-O 2 (heliox) bounce dives, *NEDU TR 15-04,* Panama City, FL.

85 SHYKOFF B. E., Oxygen Consumption As a Function of Ergometer Setting in Different Diver's Dress: Regression Equations, (2009), *NEDU TM 09-06,* Panama City, FL.

86 DOOLETTE D. J, Gerth W. A., Gault K. A. Addition of Work Rate and Temperature Information to the Augmented NMRI Standard (ANS) Data Files in the "NMRI98" Subset of the USN N2-O2 Primary Data Set (2011), *NEDU TR 11-02*, Panama City, FL.

87. MAHLER, D. A., & Loke, J. (1985). The physiology of marathon running. *The Physician and Sportsmedicine, 13(1), 84-97.*

88. BRUCE, R. M. (2017). The control of ventilation during exercise: a lesson in critical thinking. *Advances in physiology education, 41(4), 539-547.*

89. TIKUISIS, P., Gonzalez, R. R., Oster, R. A., & Pandolf, K. B. (1988). Role of body fat in the prediction of the metabolic response for immersion in cold water. *Undersea biomedical research, 15(2), 123-134.*

90. MEKJAVIC, I. B., Tipton, M. J., Gennser, M., & Eiken, O. (2001). Motion sickness potentiates core cooling during immersion in humans. *The Journal of physiology, 535(2), 619-623.*

91. JAUCHEM, J. R. (1988). Effects of exercise on the incidence of decompression sickness: a review of pertinent literature and current concepts. *International archives of occupational and environmental health, 60, 313-319.*

92. WARKANDER, D. E., Norfleet, W. T., Nagasawa, G. K., & Lundgren, C. E. (1990). CO2 retention with minimal symptoms but severe dysfunction during wet simulated dives to 6.8 atm abs. *Undersea biomedical research, 17(6), 515-523.*

93. MITCHELL S.J. (2009) Tales from the deep. The physiological challenges of deep diving. *Annual Queenstown update in Anaesthesia. p.67-73*

94. MAIO, D.A.; Farhi, L.E. (1970) Effect of Gas Density on Mechanics of Breathing. SAM-TR-70-5; USAF School of Aerospace Medicine. Dayton,OH, USA; pp. 15–21.

95. WARKANDER D.E, (2008) Recommended amendment to NEDU technical manual 01-94. U.S. Navy Unmanned Test Methods and Performance Goals for Underwater Breathing Apparatus, *NEDU TM 08-17*, Panama City FL

96. WARKANDER, D. E., Nagasawa, G. K., & Lundgren, C. E. G. (2001). Effects of inspiratory and expiratory resistance in divers' breathing apparatus. *Undersea & hyperbaric medicine, 28(2), 63.*

97. CLARKE, J. R., Vila, D., Cabeca, A., Thalmann, E. D., & Flynn, E. T. (1989). The testing of physiological design criteria for underwater breathing apparatus (UBA). *Diving and Hyperbaric Medicine, Proc 15th European Undersea Biomedical Society (EUBS), Israeli Navy Publications, 171-176.*

98. CLARKE, J. R., Survanshi, S., Thalmann, E., & Flynn, E. T. (1989). Limits for mouth pressure in underwater breathing apparatus (UBA). *Physiological and human engineering aspects of underwater breathing apparatus: proceedings of the fortieth Undersea and Hyperbaric Medical Society workshop*. Bethesda, MD: UHMS.

99. CLARKE, J. R. (1992). Diver tolerance to respiratory loading during wet and dry dives from 0 to 450m. *Lung Physiology and Diver's Breathing Apparatus, 33-44.*

100. BENTLEY, R. A., Griffin, O. G., Love, R. G., Muir, D. C., Sweetland, K. F. (1973). Acceptable levels for breathing resistance of respiratory apparatus. *Archives of Environmental Health: An International Journal, 27(4), 273-280.*

101. MEAD, J. (1955). Resistance to breathing at increased ambient pressures. *Natl. Acad. Sci.-Natl. Res. Council, Washington, 112-20.*

102. ANTHONY, G., & Mitchell, S. J. (2015). Respiratory physiology of rebreather diving. Rebreathers and Scientific Diving, *Proceedings of NPS/NOAA/DAN/AAUS June 16-19, 2015 Workshop*. Durham, NC.

103. WARKANDER D.E. (2010) Work of Breathing Limits for Heliox Breathing, *NEDU TR 10-14*, Panama City, FL.

104. GENNSER, M., & Blogg, S. L. (2008). Oxygen or carbogen breathing before simulated submarine escape. *Journal of applied physiology, 104(1), 50-56.*

105. MANO, Y., D'Arrigo, J. S. (1978). Relationship between CO2 levels and decompression sickness: implications for disease prevention. *Aviation, Space, and Environmental Medicine, 49(2), 349-355.*

106. ISHIYAMA, A. (1983). Analysis of gas composition of intravascular bubbles produced by decompression. *The Bulletin of Tokyo Medical and Dental University, 30(2), 25-35.*

Patent I

(12) INTERNATIONAL APPLICATION PUBLISHED UNDER THE PATENT COOPERATION TREATY (PCT)

(19) World Intellectual Property Organization
International Bureau

(43) International Publication Date
14 December 2017 (14.12.2017)

WIPO | PCT

(10) International Publication Number
WO 2017/212464 A1

(51) International Patent Classification:
B63C 11/24 (2006.01)

(21) International Application Number:
PCT/IB2017/054822

(22) International Filing Date:
07 August 2017 (07.08.2017)

(25) Filing Language: English

(26) Publication Language: English

(30) Priority Data:
1600186-9 08 June 2016 (08.06.2016) SE

(72) Inventors; and
(71) Applicants: **FRÅNBERG, Oskar** [SE/SE]; Idrottsvägen 13, 371 41 Karlskrona (SE). **SILVANIUS, Mårten** [SE/SE]; Skavkulla Backe 10, 373 33 Nättraby (SE).

(74) Agent: **ZACCO SWEDEN AB**; P.O. Box 5581, Valhallavägen 117N, 114 85 Stockholm (SE).

(81) Designated States *(unless otherwise indicated, for every kind of national protection available)*: AE, AG, AL, AM, AO, AT, AU, AZ, BA, BB, BG, BH, BN, BR, BW, BY, BZ, CA, CH, CL, CN, CO, CR, CU, CZ, DE, DJ, DK, DM, DO, DZ, EC, EE, EG, ES, FI, GB, GD, GE, GH, GM, GT, HN, HR, HU, ID, IL, IN, IR, IS, JO, JP, KE, KG, KH, KN, KP, KR, KW, KZ, LA, LC, LK, LR, LS, LU, LY, MA, MD, ME, MG, MK, MN, MW, MX, MY, MZ, NA, NG, NI, NO, NZ, OM, PA, PE, PG, PH, PL, PT, QA, RO, RS, RU, RW, SA, SC, SD, SE, SG, SK, SL, SM, ST, SV, SY, TH, TJ, TM, TN, TR, TT, TZ, UA, UG, US, UZ, VC, VN, ZA, ZM, ZW.

(84) Designated States *(unless otherwise indicated, for every kind of regional protection available)*: ARIPO (BW, GH, GM, KE, LR, LS, MW, MZ, NA, RW, SD, SL, ST, SZ, TZ, UG, ZM, ZW), Eurasian (AM, AZ, BY, KG, KZ, RU, TJ, TM), European (AL, AT, BE, BG, CH, CY, CZ, DE, DK, EE, ES, FI, FR, GB, GR, HR, HU, IE, IS, IT, LT, LU, LV, MC, MK, MT, NL, NO, PL, PT, RO, RS, SE, SI, SK, SM, TR), OAPI (BF, BJ, CF, CG, CI, CM, GA, GN, GQ, GW, KM, ML, MR, NE, SN, TD, TG).

(54) **Title:** PPO2 SENSOR AUTHENTICATION FOR ELECTRONIC CLOSED CIRCUIT REBREATHERS

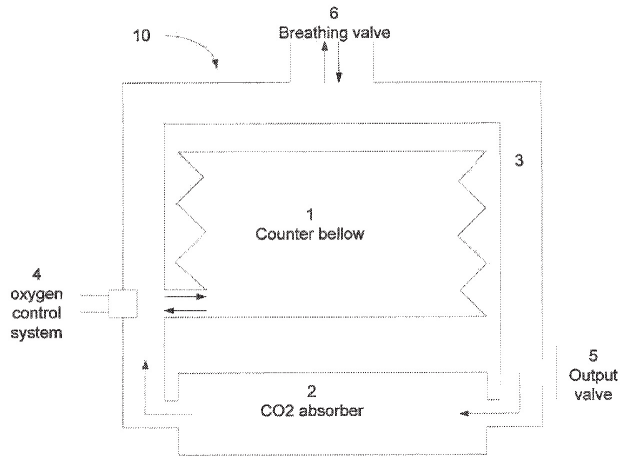

Fig 16

(57) **Abstract:** A method for determining the validity of an oxygen, O2, sensor, wherein the O2 sensor is comprised in a breathing apparatus used for diving purposes, the method comprises the steps of retrieving one or more partial pressure of oxygen, PPO2, signals from the O2-sensor, comparing the PPO2 signal to a calculated PPO2 signal, determining the validity of the retrieved PPO2 signal based on the comparison, determining the validity of the O2 sensor based on the validity of the PPO2 signal and wherein the current operation of the breathing apparatus is updated based on the validity of the O2 sensor.

WO 2017/212464 A1

[Continued on next page]

Published:

— *with international search report (Art. 21(3))*
— *before the expiration of the time limit for amending the claims and to be republished in the event of receipt of amendments (Rule 48.2(h))*
— *with information concerning request for restoration of the right of priority in respect of one or more priority claims; the decision of the receiving Office regarding the request for restoration is pending and will be published separately once available (Rules 26bis.3 and 48.2(j))*

PPO2 SENSOR AUTHENTICATION FOR ELECTRONIC CLOSED CIRCUIT REBREATHERS

TECHNICAL FIELD

The present invention relates in general to the field of diving and diving rebreathers, and more particularly, to the analyses of partial pressure of oxygen, PPO2, sensor signals in electronic closed circuit rebreathers, eCCR.

BACKGROUND

Electronically controlled rebreathing apparatuses have been on the market for a long time now, and available for a big enthusiastic audience mainly within diving. The purpose of a rebreathing system 10, as shown in fig 16, is to control the gas content of a typical breathing loop consisting of a counter bellow 1 that receives the exhaled gas. The exhaled gas needs to be cleaned from carbon dioxide, CO2, and this is usually performed by some sort of CO2-scrubbing mechanism 2. The exhaled gas also needs to be replenished to compensate for the consumed oxygen. This is usually done using a gas injection technique employing some sort of mechanically controlled valve or, if an electronic control system is present, by an electronically controlled solenoid or other means such as needle valve. The electronic control system is relying on the gas injection technique and a multitude of sensors to uphold life-supporting function for the diver.

Current control systems could incorporate:

- solenoid valve, or other means for gas injection, for controlling the gas levels in the loop;
- O2-sensors, or other means, to measure the oxygen content in the loop;

- loop/ambient pressure sensors to measure pressures;
- PCO2-sensors to measure pressure of carbon dioxide, PCO2, in the loop; and
- advanced microcomputers to calculate decompression algorithms etc.

However, the accuracy and reliability is sometimes weak, especially for the PPO2 monitoring, and often needs to include redundant sensors. Examples of semi-closed circuit and closed circuit rebreather are presented in, for example the patents US 5,503,145 and US 6,302,106.

The benefits compared to traditional self-contained breathing apparatuses with open circuit systems are many. Some examples are reduced gas-consumption and the ability to breathe an optimal oxygen/diluent blend at the current depth. However, there are some disadvantages of current electronic rebreathers where mainly the PPO2-sensors are described as a weak link. If they are abused, aged or blocked, the signal cannot be described as reliable. The user could in worst case result in that the diver is exposed to hyperoxia or hypoxia which is what the control-system primary is developed to avoid.

The design of such a control system must therefore be of such robustness that this never happen, because of the severeness of the outcome, which could be fatal for the diver. Hypoxia could lead to unconsciousness and is mostly spoken of in situations of hypobaric environments but can also occur if breathing from a closed circuit. In the case of being underwater, it could lead to drowning. Hyperoxia occurs when a user is exposed to an excessive level of oxygen pressure and is mainly present in hyperbaric environment. Hyperoxia could cause oxygen toxicity, which may lead to a fatal cause of events.

Acceptable levels of PPO2 are usually thought to be within 0.16-1.6 bar and are described as the product of oxygen fraction, FO2, and ambient pressure measured in bars. In water the pressure increases with 1 bar per 10 meters.

At surface the pressure absolute is 1 bar and altitude decreases the ambient pressure. An example is while at surface sea level and breathing air (assuming average sea-level pressure being 1 bar and FO2=21%) the PPO2=0.21bar, while at ten meters of water depth the pressure has increased to ~2 bar and the PPO2 has also increased by a factor 2 and is ~0.42 bar.

Even if the human body could manage these variations in PPO2, there are other factors that make it important to know the actual PPO2 at your actual depth. If one is heading for a higher ambient pressure than the current, it is necessary to be aware of the expected PPO2 related to what gas is brought. Unfortunately, the human body also picks up diluent (the gas that is not oxygen, normally nitrogen) during the pressure increase, which must be ventilated from the tissues before returning or going to lower pressure. Otherwise hyperbaric/decompression illness could occur. Another risk with changing to a lower ambient pressure is if the FO2 in the breathing loop is low and the ambient pressure drops, a hypoxic situation might occur. Benefits with having a high PPO2 i.e. a low partial pressure of diluent could make the decompression time shorter. If the sensor system or the signal system fails, the breathing loop might become hyperoxic or hypoxic.

With the above in mind it is essential to be aware of the breathing loops PPO2 and thus be able to trust the sensors in the diver´s life-support system.

There are currently several approaches to address the fact that PPO2-sensor reading in breathing circuits might be erroneous or unreliable due to

a) unlinearity;

b) current limitation: when the PPO2-sensor becomes nonlinear above a certain level of PPO2 since the output current of the sensor (or the output voltage) due to an error cannot rise over a certain level. This results in too low sensor signals for high levels of PPO2;

c) erroneous signal from one or more sensors respectively whichever the sensor signal is processing, where the sensors may be blocked by moisture, aging, system fault etc; and

d) erroneous calibration, where the user has calibrated the sensor-system with erroneous reference gas, loop gas or pressure.

Some manufacturers use redundancy with two or more sensors as shown in patent US 6,712,071. If the system incorporates three sensors it is also possible to use voting logic that excludes any sensor that doesn't agree with a majority of the others two. Another approach is to look at the reaction at the sensor after flushing it with a known gas and thereby validating the output.

The validation method is currently used and patented by Poseidon (US20110041848, US20070215157) and Arne Sieber (US20100313887) and described as follows. The PPO2-sensors are calibrated at surface using 100% oxygen, which can indicate a maximum partial pressure of oxygen, PPO2, to 1.0 bar. A normal set point is 1.2-1.3 bar and anticipated to measure up to 1.6 bar. A set point is the level of PPO2 which the OCS is regulating towards, by injecting oxygen to increase the set point or by letting the diver's metabolism consume the oxygen, alternatively purge with diluent gas to decrease the oxygen partial pressure. The set point is often above atmospheric pressure and thus the sensors are not calibrated at the set point before the dive. What set point to choose depends on several aspects but the higher the set point the shorter decompression stops the diver has to do before surfacing, but the higher the risk of oxygen toxicity. The set point can be chosen manually or automatically depending on which the user prefers and physiological limitations This means that the actual functioning pressure of oxygen, PO2, is never achieved during calibration and it cannot be determined whether the sensors are erroneous above PPO2 1.0 bar. To address this problem a solenoid injects gas at depth and at 6 meters it is possible to receive a PPO2 signal equivalent to 1.6 bar. This also determines whether a correct calibration has been done. This is only done in this depth

area and normally during descent and this is also the only time when the sensor is tested in the upper range PPO2>1 bar and this cannot be done at deeper depths.

During the dive a similar flush with diluent can be done to rinse humidity from the sensor and to determine the step answer and the linearity of the sensor, especially if the expected PPO2 from the diluent is lower than actual. The method used in Poseidon mkVI rebreather system is based on checking the response of the sensor with diluent flush, see the White Paper by Poseidon "A New Approach to Closed Circuit Rebreather Gas Monitoring: Why Two Oxygen Sensors can be Better than Three". However, since this method uses a gas with lower PPO2 than the setpoint it does not determine the validity of the sensor at that specific setpoint of PPO2.

Previous patent US6, 302,106 (entitled Rebreather system with optimal PPO2 determination) describes a method for injecting oxygen and diluent at a certain rate to achieve a perfect blend with optimal PPO2 for the particular ambient pressure using a digital signal-processing unit. This, however, has no bearing on sensor validation.

In patent US20030188744 (entitled Automatic control system for rebreather) it is shown that an automatic control system for a rebreather with improved life-supporting characteristics can be designed. However, the system analysis of the oxygen sensor signal is not significantly different from others and described by having a microcontroller that takes the median of the two closest signals as being the true oxygen value. The result is used to maintain an accurate PPO2 in the breathing circuit. The system of US20030188744 do not detect whether multiple sensors are presenting an incorrect signal.

The patent WO 2012025834 (entitled Rebreather control parameter system and dive resource management system) incorporate a method for controlling the PPO2-setpoint in the breathing loop of an underwater rebreathing apparatus related to ambient pressure. The user has the possibility to control the settings during the dive. In this method, the diver can specify some input

values for a control parameter like a minimum and maximum value of partial pressure of oxygen and a concentration of oxygen in a gas supply. The maximum operating value of partial pressure of oxygen is calculated as a function of ambient pressure and concentration of oxygen in the gas supply. However, this system does not integrate the characteristics of the PPO2-signal and cannot be said to increase accuracy of the control system or signal management.

Thus, a method and system that can validate the O2 sensor during the whole usage, at high PPO2 >1.0 bar is therefore highly sought after.

SUMMARY OF THE INVENTION

With the above description in mind, then, an aspect of some embodiments of the present invention is to provide a method and a system for determining the validity of an oxygen, O2, sensor, an oxygen control system, OCS, in rebreathers, which seeks to mitigate, alleviate or eliminate one or more of the above-identified deficiencies in the art and disadvantages singly or in any combination. With the suggested method, it is possible to address issues described above without increasing the mechanical complexity of the system, in the case where an electronically controlled system already is present.

According to some aspects the disclosure provides for a method for determining the validity of an oxygen, O2, sensor, wherein the O2 sensor is comprised in a breathing apparatus used for diving purposes

According to some aspects, the method comprises the steps of retrieving one or more partial pressure of oxygen, PPO2, signals from the O2-sensor, comparing the PPO2 signal to a calculated PPO2 signal, determining the validity of the retrieved PPO2 signal based on the comparison, determining the validity of the O2 sensor based on the validity of the PPO2 signal and wherein the current operation of the breathing apparatus is updated based on the validity of the O2 sensor. By performing these steps, a way to provide

validity control of each O2 sensor included in breathing apparatus separately is provided.

According to some aspects, the method comprises measuring the time interval to reach a determined set point of the PPO2 signal and wherein the validity of the PPO2 signal is based on the time to reach the determined set point.

According to some aspects, the step of comparing comprises determining whether the retrieved PPO2 signal is coherent and reasonable or if the PPO2 signal is deviating from the calculated PPO2 signal based on the comparison.

According to some aspects, wherein the PPO2 signal is deviating from the calculated PPO2 signal, the method comprises changing a first PPO2 set point to a second PPO2 set point, measuring the time interval to reach the second PPO2 set point by measuring at least one of a breathing volume of the breathing apparatus, an oxygen injection rate, an oxygen injection volume, an oxygen injection flow and an oxygen consumption, calculating an incline of a graph presenting the values of the PPO2 signal collected over the time interval for the PPO2 set point change and determining the validity of the PO2 signal based on the calculated incline of the graph.

According to some aspects, the method comprises detecting at least one of an oxygen injection rate, oxygen injection volume, oxygen injection flow, breathing loop volume or oxygen consumption of the breathing apparatus, comparing the current amplitude of the PPO2 signal to an amplitude of a calculated PPO2 signal related to at least one of the detected oxygen injection rate, oxygen injection volume, oxygen injection flow, breathing volume and oxygen consumption of the breathing apparatus and determining the validity of the PPO2 signal based on the comparison.

According to some aspects, the method comprises initiating a test cycle, which is performed by altering the current PPO2 set point to either a lower or higher value, when each value is reached the PPO2 set point is changed to

the opposite side of the current PPO2 set point, registering the time to perform the test cycle and determining the validity of the PPO2 signal based on the registered time.

According to some aspects, the breathing apparatus comprises an oxygen control system, OCS, wherein the method comprises loading the OCS with data related to the breathing apparatus and the dive to be performed, wherein the OCS is configured to predict expected characteristics of the PPO2 signal from an O2 sensor of the OCS, based on the loaded data, calculating S420, by OCS, characteristics of the PPO2 signal, both previous and actual, during the dive performed by the diver, comparing S430, by OCS during the dive, the calculated characteristics of the PPO2 signal with the expected characteristics of the PPO2 signal and determine whether previous and actual calculated characteristics of the PPO2 signal are valid or if the PPO2 signal has changed characteristics based on the comparison.

According to some aspects, a PPO2 set point is calculated for the OCS and the method comprises comparing at least one of the calculated PPO2 value, an amplitude of the PPO2 signal, a sawtooth pattern of a graph of the calculated PPO2 values and a speed of change of PPO2 set point with expected values of PPO2 values, amplitude of the PPO2 signal, sawtooth pattern of a graph of PPO2 values and speed of change of PPO2 set point and determining the validity of the PPO2 signal based on the comparison.

According to some aspects, the method comprises collecting volume information from a solenoid injection of O2, wherein the total breathing volume of the OCS is calculated by adding the collected volume information to the existing breathing volume.

Another aspect of the disclosure provides for an oxygen control system, OCS, comprised in a breathing apparatus used for diving purposes, for determining the validity of an oxygen, O2, sensor, comprised in the OCS.

According to some aspects the OCS is configured to perform the above discussed method.

The features of the above-mentioned embodiments can be combined in any combinations.

BRIEF DESCRIPTION OF THE DRAWINGS

Further objects, features and advantages of the present invention will appear from the following detailed description of the invention, wherein embodiments of the invention will be described in more detail with reference to the accompanying drawings, in which:

Fig 1a shows a graph of the actual PPO2 value, the OCS believed PPO2 value and a functioning OCS variation;

Fig 1b shows a graph of characteristics of a linear and an erroneous PPO2 sensor in the case of fig 1a;

Fig 2a show a graph of the actual PPO2 value, the OCS believed PPO2 value and a functioning OCS during a PPO2 increase during descent or set point change;

Fig 2b shows a graph of characteristics of a linear and an erroneous PPO2 sensor in the case of fig 2a;

Fig 3a shows a graph of how the amplitude will differs for a functioning sensor and an erroneous calibrated sensor that was calibrated with air for PPO2=0.21 bar and 80% oxygen at PPO2=1 bar;

Fig 3b shows a graph of characteristics of a linear and an erroneous PPO2 sensor in the case of fig 3a;

Fig 4a shows a graph of how the characteristics of the PPO2-reading will deviate between a functioning and an erroneous calibrated sensor;

Fig 4b shows a graph of characteristics of a linear and an erroneous PPO2 sensor in the case of fig 4a;

Fig 5a shows a graph of a sensor characteristic that presents a maximum output for a functioning and erroneous sensor;

Fig 5b shows a graph of characteristics of a linear and an erroneous PPO2 sensor in the case of fig 5a;

Fig 6a shows a graph of the deviation between an erroneous and functioning OCS when VO2 is 2-2.5 l/min;

Fig 6b shows a graph of characteristics of a linear and an erroneous PPO2 sensor in the case of fig 6a;

Fig 7 shows a graph of the amount of oxygen added in a functioning and erroneous OCS;

Fig 7b shows a graph of characteristics of a linear and an erroneous PPO2 sensor in the case of fig 7a;

Fig 8 shows a graph of the actual values of PPO2 for a functioning OCS;

Fig 9a shows a graph of any possible readings independent of VO2 for a specified system volume;

Fig 9b shows a graph of the depth in the case of fig 9a;

Fig 10a shows a graph of PPO2 values when performing a test-cycle with a PPO2 set point change;

Fig 10b shows a graph of characteristics of a linear and an erroneous PPO2 sensor in the case of fig 10a;

Fig 13 shows a graph of characteristics of the OCS sensor signal for oxygen consumption between 0.3-4 l/minute;

Fig 14 shows a graph of the saw tooth pattern of a functioning OCS and an erroneous OCS;

Fig 15 shows a graph of an erroneous and a functioning PPO2-sensor;

Fig 16 shows a rebreathing apparatus, rebreather, according to an embodiment of the present disclosure;

Fig 17 shows a flowchart illustrating the method according to an embodiment of the present disclosure;

Fig 18 shows a flowchart illustrating the method according to an embodiment of the present disclosure;

Fig 19 shows a flowchart illustrating the method according to an embodiment of the present disclosure;

Fig 20 shows a flowchart illustrating the method according to an embodiment of the present disclosure;

Fig 21 shows a flowchart illustrating the method according to an embodiment of the present disclosure.

DETAILED DESCRIPTION

Embodiments of the present invention relate, in general, to the field of diving equipment and particularly to the field of analyzing the output of PPO2 sensor signals in systems used for diving purposes. A preferred embodiment relates to rebreathers, such as a closed circuit rebreather. However, it should be appreciated that the invention is as such equally applicable to other similar diving systems such as semi-closed circuit rebreather and other diving and breathing applications where determining if an oxygen sensor reading is correct or not is important. However, for the sake of clarity and simplicity, most embodiments outlined in this specification are related to an electronic closed circuit rebreather, eCCR.

Embodiments of the present invention will be described more fully hereinafter with reference to the accompanying drawings, in which embodiments of the invention are shown. This invention may, however, be embodied in many different forms and should not be construed as limited to the embodiments set forth herein. Rather, these embodiments are provided so that this disclosure will be thorough and complete, and will fully convey the scope of the invention to those skilled in the art. Like reference signs refer to like elements throughout.

To address the problem of an erroneous PPO2 signal coming from a faulty O2-sensor of the eCCR there are currently multiple methods on the market as previously described in the background section. The method, according to an embodiment of the present invention, is depending on an oxygen control system, OCS, to collect and analyze one or multiple PPO2-sensor signals independent of type of O2-sensor. The method according to the present invention is based on analyzing the characteristics of the retrieved PPO2-signals. This is performed by analyzing the behavior of the PPO2-signal retrieved by the system and/or determining the validity of the PPO2 signal compared to any one or more of the ambient pressure change, solenoid injection volume, rate or flow, pressure decrease in an oxygen or diluent cylinder, gas injection from automatic diluent valve, breathing frequency of the diver, heart rate of the diver, flow rate in breathing loop etc. According to another aspect, the determination of the validity of the PPO2 signal compared to the expected output from the O2-sensor of the eCCR can be done by analyzing a change of a PPO2-setpoint.

While using the inputs as described above it is possible to determine whether the sensors are giving a coherent and reasonable signal or if they are deviating from what is expected. The deviations can be described as not following a predicted pattern of output, see figure 8. The graph presented in figure 8 shows possible PPO2 values for a fully functional eCCR, with PPO2 setpoint at 1.3/0.7 bar, FO2 diluent at 7%, total volume 18.6 L, maximum solenoid injection 8.4 L/m. In this case the expected PPO2-signal is

predetermined or calculated. The PPO2-sensor values are depending on the PPO2 setpoint which normally is set to 1.2-1.3 bar. The setpoint can be chosen manually or automatically depending on which the user prefers and physiological limitations. If the setpoint is changed, manually or automatically by the OCS (normally 0.7 bar at shallow depths <10 m), the time for the change will to a large degree be determined by the system volume and the oxygen injection rate, injection volume and injection flow and the oxygen consumption. The incline of the graph presenting the PPO2-values during setpoint change are expected to be linear, and steep with a functional oxygen control system (OCS) of the eCCR, whereas the graph presenting the PPO2 values of an erroneous OCS could fade in the upper region (>1 bar). The amplitude of the PPO2 signal at the current setpoint is related to the oxygen injection rate, volume, flow and the breathing volume of the eCCR. The amplitude of the PPO2 signal is also dependent on configuration of the OCS and on the oxygen consumption. By knowing these factors, it is possible to see that a correct OCS will provide different amplitude of the PPO2 signal than an erroneous OCS, if the predetermined settings are similar, see figure 1 a-b, 3 a-b and 5 a-b. Figure 1a-b graphically presents possible PPO2 values for a functional eCCR with PPO2 set point at 1.3/0.7 bar, FO2 diluent at 21%, total system volume of 10-18 L, maximum solenoid injection of 9.4 L/min. Figure 3a-b and figure 5a-b graphically presents possible PPO2 values for a functional eCCR with PPO2 set point at 1.3/0.7 bar, FO2 diluent at 21%, total system volume of 10-18 L, VO2 at 0.3-3.9 L, maximum solenoid injection of 9.4 L/min. If the OCS is unable to accept higher PPO2 signal than a certain current (i.e. current limitation), see figure 5 a-b, this is also revealed as a lower amplitude than expected. When the OCS is unable to follow expected PPO2 values during a pressure drop or an increase, see figure 2 a-b, 4 a-b and 6 a-b, the OCS will interpret this in a similar way as a setpoint change. Figure 2a-b and 4 a-b graphically presents possible PPO2 values for a functional eCCR with PPO2 set point at 1.3/0.7 bar, FO2 diluent at 21%, total system volume of 10-18 L, VO2 at 0.3-3.9 L, maximum solenoid injection of 9.4 L/min. Figure 6a-b graphically presents possible PPO2 values

for a functional eCCR with PPO2 set point at 1.3/0.7 bar, FO2 diluent at 21%, total system volume of 10-18 L, VO2 at 2-2.5 L, maximum solenoid injection of 9.4 L/min. The incline of the graph of PPO2-values during setpoint change are expected as correlated to the depth change and diluent compensation with functional OCS, whereas an erroneous system has a different time to reach the new setpoint and thereby also a different incline of the graph of PPO2 values. If the OCS is unable to find a definite reliable and trustworthy PPO2 signal it is possible to initiate a manual or automatic full or half test cycle. This is performed by altering the actual setpoint to either a lower or higher value. When this value is reached the setpoint is changed to the opposite side or level of the original setpoint. By registering the time it takes to perform this test-cycle it can be determined if the system is erroneous or not. A fully functional system will typically have a shorter duration and less oxygen injection than an erroneous for the test-cycle, see figure 10 a-b. Figure 10 a-b graphically presents possible PPO2 values for a functional eCCR with PPO2 set point at 1.3/0.7 bar, FO2 diluent at 21%, total system volume of 10-18 L, VO2 at 2-2.5 L, maximum solenoid injection of 9.4 L/min. As mentioned in the description of the test-cycle above it is also possible to retrieve information on the gas injection rate, the gas injection volume and gas injection amount. The characteristics of larger amount injected oxygen is graphically presented in figure 7a-b where it is shown how identical diver's profiles, oxygen consumption rates and setpoint changes lead to different amount of oxygen injected.

The intelligence of the OCS relies on the accuracy of the oxygen, O2, sensors. This includes more information than the actual sensor-reading. By looking at the dynamics of the signal it can be determined if the diver needs to be warned or if the system is correct. The work-flow, as shown in figure 21, for determining the dynamics of the signal from the O2 sensor can be described as follows:

In step S410 the OCS is loaded with data to predict the expected characteristics or values for a PPO2 sensor signal from an O2 sensor of the

OCS, i.e. the PPO2-levels, amplitudes, sawtooth pattern and PPO2-setpoint change speed, for example a linear sensor. This means that the behavior of the signal is known and pre-determined or calculated. The data is related to the breathing apparatus, i.e. total breathing volume and the dive to be performed, i.e. planed diving depth, time.

In step S420, the calculations of, both historically, actual and future PPO2-values of the PPO2 signal must be determined during the dive performed by a diver, since the OCS doesn't know the upcoming dive profile.

In one aspect, the OCS is also loaded data related to the oxygen fraction, FO2, in a gas-supply of the breathing apparatus.

In one aspect, additional information regarding max and min breathing loop volume is also of interest as optional input to increase accuracy of the expected O2 sensor signal output.

In step S430, depending on the set point for PPO2 that is chosen for the OCS at the actual depth, the PPO2-levels, amplitudes, sawtooth pattern and PPO2-setpoint change speed of the PPO2 signal will be compared to the expected the PPO2-levels, PPO2-amplitudes, PPO2-sawtooth pattern and PPO2-setpoint change speed.

In one aspect, additionally, the OCS also records data to compare whether previous and actual data values are valid or if the OCS related data has changed.

By collecting information from solenoid injection volume and rate as shown in figure 7, and from the saw tooth pattern of the PPO2 signal from the O2 sensors, as shown in figure 14, it is possible to approximate the system breathing volume. By determining the graphical area of possible PPO2 values it is possible to decide an optimal solenoid injection flow rate. It is important to determine the volume of the system in order to be able to predict the sensor-output. This can be done by assuming the total variation of the system volume, i.e. approximation of the volume of the lungs of the diver and

the rebreathers loop volume, and use it as a one compartment model. One method is to measure the flow in the breathing volume loop 3, as shown in figure 16. This flow, together with a time-value, can be used as an estimation of the system volume, as long as there is no oxygen consumption between the oxygen injection and the oxygen sensor. The amount of injected oxygen and the flow are in this case the main determinants of the oxygen variation. One method is to estimate the flow in the breathing loop 6 (i.e. divers ventilation) without a flow-sensor is to determine the oxygen consumption and the known relationship between the oxygen consumption and the user's ventilation.

In one example: The sensor is measuring a specific PPO2 value which can be translated to FO2 with an ambient pressure sensor. The volume between the O2-injection and the sensor is fixed (for example the volume of canister). This volume does not change during the dive. If a flow sensor is measuring x l/min over the area where it is mounted one can calculate the expected increase of one or more of PPO2 and FO2 when injecting a known amount of oxygen.

To determine the oxygen consumption, rate a number of methods can be employed. In one method the pressure drop in the oxygen cylinder related to temperature is measured. In another method the oxygen consumption from breathing frequency could be estimated. In yet another method the oxygen consumption is determined from the heart rate of the diver. In yet another method the oxygen consumption rate is determined from how much oxygen that is injected into the breathing loop 3 by the oxygen injection system. In yet another method the time it takes for the PPO2-value to return to the same level as previous of an oxygen injection is determined.

The results related to the proposed method and system will now be described referring to figures 1-15. As previously discussed, the disclosure provides a method 100 and system 10 for determining the validity of an

oxygen, O2, sensor, wherein the O2 sensor is comprised in a breathing apparatus used for diving purposes.

General valid values (predicting PPO2)

According to the present invention, it is possible to determine whether a signal is correct or erroneous depending on predetermined data given by the user, system/breathing apparatus specific data and sensor data. During current operation, it is possible to do a prediction of the PPO2 signal or PPO2-value. It is also possible to analyze the PPO2-data recorded during the actual dive. By recording the PPO2-data it can be determined whether the sensor presents any differences, that could be found from the historical PPO2-data and whether the OCS signal deviates.

General valid values (predicting PPO2)

According to the present invention, it is possible to determine whether a signal is correct or erroneous depending on predetermined data given by the user, system/breathing apparatus specific data and sensor data. During current operation, it is possible to predict the PPO2-signal or PPO2-value. It is also possible to analyze the PPO2-data recorded during the actual dive. By recording the PPO2-value it can be determined whether the sensor presents any differences, that could be found from the historical PPO2-data and whether the OCS signal deviates over time.

By picking or collecting a new value sample of a PPO2 signal with a pre-determined interval it can be determined whether the sensor reading is incorrect, by looking at the decrease of PPO2, related to ambient pressure. If the slope is flat the oxygen consumption is low, if the slope is steep the consumption is high. This gives a specific characteristic depending on how accurate the oxygen consumption is determined. The pattern is shown in figure 13 for oxygen consumption between 0.3-4 l/minute (with FO2 diluent of 7%). Figure 13 shows how new sample values of a PPO2 signal are collected every second minute (120 second), from this point the

characteristics of the OCS sensor signal should stay within the plotted area for consumptions between 0,3-4 l/min.

When predicting the PPO2 in the breathing loop it is thereby possible to find an optimal injection rate for the solenoid injection. An optimal solenoid injection is presented as a small area/amplitude of possible values when using the prediction method.

PPO2-signal characteristics

The variation in amplitude between a functioning and erroneous sensor is depending on system volume, oxygen consumption and solenoid or manual injection quantity of oxygen. The amplitude difference is different if the PPO2-sensor is functioning compared to if there is a nonlinear- or current limit-problem or has an erroneous calibration. If the sensor is static the amplitude change is obviously very low. The amplitude changes from low value to higher value correlates to the solenoid injection timing and opening time as well as maximum flowrate. It also correlates to ambient pressure increase where automatic diluent addition should be considered. The decrease of PPO2-sensor signal correlates to a pressure decrease or an oxygen consumption. These characteristics can be analyzed and separate a fully functioning sensor from an erroneous sensor.

Test-cycle

In one aspect, a potentially erroneous calibration, linearity problem, static behavior and maximum output limitation is determined by analyzing the behavior of the sensor when changing setpoint for a short period. All of the above described methods for finding erroneous sensor-reading will become more accurate if additional sensors are present, such as flow-rate in the breathing loop, pressure from cylinders, the heart rate of the diver etc.

If the OCS cannot detect any specific characteristics or if the signals are within a value where it can have multiple interpretations, it is possible to perform a test-cycle. The test-cycle is performed by changing the setpoint to

a different value from the current setpoint. When the preset level for high or low PPO2 test value is reached another setpoint is chosen on the opposite level from the origin. The time and characteristics for the signal to travel along this test-cycle is used to determine whether the signal is correct or erroneous as shown in figure 10. The method used is to compare how long time the test-cycle should take compared to the actual time for the test cycle. If the duration is longer than expected an error can be determined. The characteristics are unlinear for an erroneous sensor-signal as compared to a linear response for a functioning sensor.

Oxygen injection pattern and quantity

The injection of oxygen correlates to the consumption of oxygen and/or a setpoint change and ambient pressure change. When oxygen is injected by the control system it is possible to determine how much oxygen is added. The injection should give a corresponding signal from the PPO2-sensor and OCS similar to a sawtooth-pattern as shown in figure 14. Figure 14 shows the sawtooth pattern of possible PPO2 values for a fully functioning OCS (solid) and an erroneous OCS (dashed) where PPO2 setpoint is 1.3/0.7, FO2 diluent is 7%, the total system volume is 16-18 L, VO2 is 1.5 L and maximum solenoid injection is 9.4 L/m. The amplitude is clearly lower for the erroneous sensor. The PPO2-sensor characteristics are shown in figure 15. Figure 15 shows the characteristics of an unlinear sensor (dashed) and a functioning sensor (solid) which is linear.

The quantity of oxygen that is injected is also of interest. If the expected amount of oxygen to achieve a certain setpoint is different from the actual amount of oxygen, then there is an error that can be related to an erroneous PPO2-sensor signal. As is shown in figure 7a-b where the dotted area shows the amount of injected oxygen for and the solid area is less and is showing the injected amount of oxygen for a functioning system.

Method to adapt an erroneous signal to ensure accurate PPO2-control

If the signal is proven to be erroneous it is also possible to adjust and adapt the values through a signal processing unit that can determine a correction for the erroneous signal. If the correction is found adequate the user doesn't have to abort, but can continue the usage. The signal is adapted in accordance to how the sensor error is analyzed. An alternative action from the OCS is to decrease the setpoint to a level where it can be trusted and instruct the user to abort the usage. If it is suggested that the sensors are reliable new iterations to determine the validity of the readings should continue.

Unlinear Sensor

For an unlinear PPO2-sensor the amplitude for setpoints, in the range of inaccuracy, will differentiate from a correct sensor. In figure 1a-b it is shown how the amplitude will differ.

In figure 1a-b, top graph, fig 1a, shows the actual PPO2 value (dotted), the oxygen control system OCS believed PPO2 value (dotted fat) and a functioning OCS (solid) variation. By analyzing the max-min value of the PPO2 amplitude, the OCS can be analyzed to have an erroneous behavior. The bottom graph, fig 1b, shows the erroneous sensor (unlinear) characteristics. The system volume is allowed to vary between 10-18 liters and the oxygen consumption VO2 is set to 0.3-4 l/min. For this type of error, we expect a high level of OCS error identification.

During a PPO2-increase during descent or setpoint change the characteristics of the PPO2-reading will vary depending on whether you have a functioning OCS or not. In figure 2 a-b it is shown how the characteristics deviate, however only slightly for this error.

In figure 2 a-b an unlinear sensor is show, which will not necessarily be detected during setpoint change. The difference between the characteristics are shown in the figure where the actual PPO2 value (dotted), the oxygen

control system OCS believed PPO2 value (dotted fat) and a functioning OCS (solid) are presented. The predicted data is more or less overlapping.

Erroneous Calibrated Sensor

For an erroneous calibrated PPO2-sensor the amplitude for setpoints, in the range of inaccuracy, will differentiate from a correct sensor. In figure 3 a-b it is shown how the amplitude will differ for a sensor that was calibrated with air for PPO2=0.21 bar and 80% oxygen at PPO2=1 bar. As shown in figure 3 a-b, similar to a nonlinear sensor the characteristics will be different between a functioning sensor and an erroneous calibrated sensor.

A PPO2-increase during descent or setpoint change the characteristics of the PPO2-reading will vary depending on whether you have a functioning OCS or not. In figure 4 a-b it is shown how the characteristics deviate. As shown in figure 4, during PPO2-increase the characteristics of the reading will deviate between functioning and erroneous calibrated sensor.

Static Sensor

If the sensor is blocked by humidity or other reasons there will be little or no PPO2 sensor fluctuations in the sensor output. This means that there will be no PPO2-signal variations, which should occur as long as there is some sort of oxygen consumption. In figure 14 the dynamic is shown as a sawtooth pattern. If the signal doesn't have any dynamics an error can be expected. This type of error is not commonly analyzed in other systems as the normal OCS only reacts to a PPO2 below setpoint and then injects oxygen. This means that as long as the PPO2 is above setpoint OCS believes the system is ok, but the truth is that a system must have a variation in the PPO2 as long as the diver is consuming oxygen and oxygen is injected. The simplest method would be to take the interval between different oxygen injections. If the numbers of injections are fewer than expected, something is wrong with the PPO2 signal or OCS.

Output Limitation

If the PPO2-sensor has any limitation of the maximum output values this can be detected in similar way as previously described, i.e. low amplitude and little or no PPO2-sensor fluctuation, which is shown in figure 5 a-b.

Figure 5 a-b, with a sensor-characteristic that presents a maximum output for the sensor, the amplitude variation will be very small. This is shown with very small amplitude for erroneous sensor and relative large amplitude for functioning sensor. The rise in PPO2-setpoint will not affect this type of error.

Increase accuracy

If one can determine or at least approximate the OCS volume and the oxygen consumption it can be used to improve the accuracy of the OCS failure detection. In figure 6 a-b it is graphically shown that by determining the VO2 with +/- 0.25 bars the sensor failure is detected immediately during descent.

Figure 6 a-b graphically shows the deviation between erroneous and functioning OCS when VO2 is better approximated. VO2 is to 2-2.5 l/min in the case shown in figure 6 a-b.

Also factors like dive depth and FO2 in diluent will affect the accuracy or possibility to detect an erroneous OCS. It is also claimed that the O2-injection can be used to determine an erroneous sensor. In figure 7 a-b a method is used to analyze the amount of oxygen injected from the number of solenoid injection and from that notice the difference between a correctly calibrated sensor and not. With a method, as shown in Figure 7 a-b, to determine the amount of oxygen added (either by solenoid injection rate or gas cylinder pressure decrease) one can see an obvious difference. For the erroneous calibrated sensor, an abnormal amount of oxygen is needed to increase the PPO2. In this case diluent of FO2 21%, VO2 = 2-2.5 L/min, system volume 10-18 L is used.

In one method, the PPO2 value validity is determined by looking at the overall possible PPO2 for a functioning oxygen control system OCS. If the OCS is functioning correctly the signal should follow a determined profile for PPO2 related to the dive profile. In figure 8 it is shown how this profile could look. With the current described method, it is also possible to find an optimal maximum injection for the solenoid. The smaller area of possible values of PPO2 values, the better tuned solenoid injection volume and rate.

Figure 8 graphically shows the actual values of PPO2 for a functioning oxygen control system OCS. The PPO2 is held at near perfect settings and a value outside of this indicates a probable error in the overall system.

If the OCS retrieves a new PPO2-value at specific times it is possible to determine any possible future signal from that time, independent on oxygen consumption. The sooner a new value is retrieved and considered valid the better validity. If the PPO2 reading is outside of these determined levels, the OCS is erroneous and a warning is presented to the user. In figure 9 a-b any possible PPO2 values independent of VO2 for a specified system breathing volume is graphically presented. In the case presented in figure 9a-b, the OCS is expected to be fully functioning when a new reading of the PPO2 values, with VO2 = 0.3 – 4 L/min and FO2 Diluent of 7%, is performed each 2 minutes (120 seconds) and the OCS predicts any possible readings after that.

The prediction is defined by the PPO2 decrease from maximum (4L/min) and minimum (0.3 L/min) oxygen consumption. These boundaries create the area of valid PPO2 values, which is shown in figure 9 a-b.

Test-cycle

A test-cycle is performed whenever the user finds it necessary (manual) or if the OCS finds the PPO2-values unreliable. This is performed by changing the setpoint, let the system adjust and then make another setpoint change

opposite of the previous setpoint, see figure 10 a-b. The time it takes to perform this test cycle will reveal erroneous oxygen control systems.

By performing a test-cycle with a PPO2-setpoint change, as shown in figure 10 a-b, it is possible to determine the validity of the sensor signal. In this case the test-cycle is expected to take maximum 4 minutes but could in this case take up 10 minutes for an erroneous sensor.

Figure 11a-b shows an over-view of the different sensor signals for functioning and erroneous calibrated sensor for a fictive dive profile. Figure 11 a-b graphically presents possible PPO2 values for a fully functional eCCR with PPO2 set point at 1.3/0.7 bar, FO2 diluent at 21%, total system volume of 10-18 L, VO2 at 2-2.5 L, maximum solenoid injection of 9.4 L/min.

Figure 12 a-c presents PPO2 values collected from a live, simulated oxygen consumption in a breathing simulator type ANSTI at the depth of 30 m with O2 consumption of 1.78 L/m. The OCS is an electronic rebreather with PPO2-control system running on full automatic. The other data presented are from calculated predictions from the algorithm, with knowledge of the oxygen injection flow rate, in this case approximated to 7.5 l/min. With this information, the oxygen consumption, total loop volume, ventilation, O2-cylinder pressure drop and total injected oxygen can be approximated and compared.

The oxygen control system OCS described here is used to determine erroneous PPO2-signals that could occur while using a rebreathing device. By analyzing the characteristics of the signals it is possible to separate a a characteristic of a fully functioning O2 sensor from an erroneous O2 sensor. Not only by looking at the actual PPO2-signal, but also at the amount of oxygen injected, related to oxygen consumption. The system is able to determine the error and both give the diver a warning and/or adjust the OCS so that a correct PPO2 in the breathing loop can be achieved.

The proposed method will now be described referring to figures 16 - 21. As previously discussed, the disclosure provides a method 100 and system 10 for determining the validity of an oxygen, O2, sensor, wherein the O2 sensor is comprised in a breathing apparatus used for diving purposes.

Figure 16 shows a breathing apparatus according to some aspect of the disclosure. The figure illustrates a rebreathing apparatus 10, eCCR, comprising a counter bellow 1, a CO2 absorber 2, a breathing volume 3, an oxygen control system 4, OCS, an output valve 5 and a breathing valve 6.

Figure 17 – 21 are flow diagrams depicting example operations which may be taken by the system 10 of figure 16. The operations of the flow diagram will be described together with the device of figure 16.

The method comprises retrieving S110 one or more partial pressure of oxygen, PPO2, signals from the O2-sensor and comparing S120 the retrieved PPO2 signal to a calculated PPO2 signal. In one aspect, the step of comparing S120 comprises determining S121 whether the retrieved PPO2 signal is coherent and reasonable or if the PPO2 signal is deviating from the calculated PPO2 signal based on the comparison. In one aspect, wherein the PPO2 signal is deviating from the calculated PPO2 signal, the method comprises changing S1211 a first PPO2 set point a second PPO2 set point; measuring S1212 the time interval to reach the second PPO2 set point by measuring at least one of a breathing volume of the breathing apparatus, an oxygen injection rate, an oxygen injection volume, an oxygen injection flow and an oxygen consumption; calculating S1213 an incline of a graph presenting the values of the PPO2 signal collected over the time interval for the PPO2 set point change; and determining S1214 the validity of the PO2 signal based on the calculated incline of the graph.

According to some aspects, the method comprises determining S130 the validity of the retrieved PPO2 signal based on the comparison. In one aspect, the method comprises measuring the time interval to reach a determined set

point of the PPO2 signal and wherein the validity of the PPO2 signal is based on the time to reach the determined set point.

According to some aspects, the method comprises determining S140 the validity of the O2 sensor based on the determined validity of the PPO2 signal and wherein the current operation of the breathing apparatus is updated S150 based on the validity of the O2 sensor.

According to some aspects, the method comprises detecting S210 at least one of an oxygen injection rate, oxygen injection volume, oxygen injection flow, breathing loop volume or oxygen consumption of the breathing apparatus, comparing S220 the current amplitude of the PPO2 signal to an amplitude of a calculated PPO2 signal related to at least one of the detected oxygen injection rate, oxygen injection volume, oxygen injection flow, breathing volume and oxygen consumption of the breathing apparatus and determining S130 the validity of the PPO2 signal based on the comparison.

According to some aspects, the method comprises initiating S310 a test cycle, which is performed by altering the current PPO2 set point to either a lower or higher value, when each value is reached the PPO2 set point is changed to the opposite side of the current PPO2 set point, registering S320 the time to perform the test cycle and determining S130 the validity of the PPO2 signal based on the registered time.

According to some aspects, wherein the breathing apparatus comprises an oxygen control system, OCS, the method comprises loading S410 the OCS with data related to the breathing apparatus and the dive to be performed, The data is related to the breathing apparatus, i.e. total breathing volume and the dive to be performed, i.e. planed diving depth, time. The OCS is configured to predict expected characteristics for the PPO2 signal from an O2 sensor of the OCS, based on the loaded data. Examples of characteristics are the levels, amplitudes, sawtooth pattern and setpoint change speed. The method comprises calculating S420, by OCS, characteristics of the PPO2 signal, both previous and actual, during the dive

performed by the diver, comparing (S430), by OCS during the dive, the calculated characteristics of the PPO2 signal with the expected characteristics of the PPO2 signal and determine whether previous and actual calculated characteristics of the PPO2 signal are valid or if the PPO2 signal has changed characteristics based on the comparison.

According to one aspect, wherein a PPO2 set point is calculated for the OCS, the method comprises comparing at least one of the calculated characteristics of the O2 sensor, PPO2 value, amplitude of the PPO2 signal, saw tooth pattern of a graph of the calculated PPO2 values and speed of change of PPO2 set point with the corresponding expected characteristics of the O2 sensor and determining S130 the validity of the PPO2 signal based on the comparison.

According to one aspect, the method comprises collecting volume information from a solenoid injection of O2 wherein the total breathing loop volume of the OCS is calculated by adding the collected O2 injection volume information to the existing breathing loop volume. According to one aspect, the method comprises determining maximum and minimum loop volume of a breathing loop volume of the breathing apparatus.

According to one aspect, the method comprises measuring one or more of the pressure drop in an oxygen cylinder of the OCS related to temperature, a breathing frequency of the user, breathing minute ventilation of the user, heart rate of the user, the oxygen injection volume or the time it takes for the PPO2 value to return to the same level as before an oxygen injection to determine the oxygen consumption.

According to one aspect, an oxygen control system, OCS, comprised in a breathing apparatus used for diving purposes, for determining the validity of an oxygen, O2, sensor, comprised in the OCS, is configured to perform the above discussed method is provided.

Embodiments and aspects are disclosed in the following items:

Item 1. A method for determining the validity of an oxygen, O2, sensor reading, wherein the sensor is comprised in a breathing apparatus used for diving purposes, the method comprises the steps of analyzing the behavior of the retrieved PPO2-signal and/or determining the validity of the signal compared to an ambient pressure change, solenoid injection, pressure decrease in oxygen or diluent cylinder, gas injection from automatic diluent valve, breathing frequency, heart rate and flow rate in a breathing loop wherein it is determined, while using the retrieved PPO2-signal, whether the PPO2-sensors are giving a coherent and reasonable PPO2-signal or if they are deviating from what is expected based on the behavior and validity.

Item 2. The method according to item 1, wherein the step of analyzing further comprises analyzing the change of a PPO2-setpoint to determine the PPO2 validity compared to a sensor output.

Item 3. The method according to item 1, wherein the deviations can be described as not following a predicted pattern of output, the expected PPO2-signal is predetermined and the PPO2-sensor values are depending on a PPO2 set point wherein if the set point is changed, a time for the change will to a large degree be determined by a system volume, an oxygen injection rate, injection volume, injection flow and an oxygen consumption, wherein the method comprises determining an incline of the graph presenting the PPO2-values during set point change.

Item 4. The method according to item 3, wherein the amplitude of the PPO2-signal at a current set point is related to an injection rate, injection volume, injection flow and a system volume and dependent on configuration, also on the oxygen consumption, wherein the method comprises knowing these factors, to see that a correct system will have a different amplitude than an erroneous, if the predetermined settings are similar.

Item 5. The method according to any of item 1-4, wherein if the OCS is unable to find a definite reliable and trustworthy PPO2 signal it is possible to initiate a manual or automatic full or half test cycle, which is performed by altering the actual set point to either a lower or higher value, when this value is reached the set point is changed to the opposite side or level of original set point, wherein the method comprises registering the time it takes to perform this cycle it can be determined if the system is erroneous or not.

Item 6. The method according to item 1, wherein the breathing apparatus comprises an oxygen control system, wherein the method comprises loading the OCS with data to predict the expected characteristics for the PPO2 signal; and calculating, both historically, actual and future, PPO2 values during the dive performed by a diver, wherein the OCS is analyzing the data during the dive and comparing whether previous and actual data values are valid or if the OCS has changed characteristics.

Item 7. A oxygen control system, comprised in a breathing apparatus used for diving purposes, for determining the validity of an oxygen, O2, sensor reading, wherein the OCS comprises sensors for measuring pressure of oxygen, PPO2, and the OCS is configured to perform the steps of analyzing the behavior of the retrieved PPO2-signal and/or determining the validity of the signal compared to an ambient pressure change, solenoid injection, pressure decrease in oxygen or diluent cylinder, gas injection from automatic diluent valve, breathing frequency, heart rate and flow rate in a breathing loop, wherein it is determined, while using the retrieved PPO2-signal, whether the PPO2-sensors are giving a coherent and reasonable PPO2-signal or if they are deviating from what is expected based on the behavior and validity.

Item 8. The system, according to item 7, wherein the system is configured to perform the step of analyzing further comprises analyzing the change of a PPO2-setpoint to determine the PPO2 validity compared to a sensor output.

Item 9. The system according to item 7, wherein the deviations can be described as not following a predicted pattern of output, the expected PPO2-signal is predetermined and the PPO2-sensor values are depending on a PPO2 set point wherein if the set point is changed, a time for the change will to a large degree be determined by a system volume, an oxygen injection rate, injection volume, injection flow and an oxygen consumption, wherein the system is configured to perform the step of determining an incline of the graph presenting the PPO2-values during set point change.

Item 10. The system according to item 7, wherein the amplitude of the PPO2-signal at a current set point is related to an injection rate, injection volume, injection flow and a system volume and dependent on configuration, also on the oxygen consumption, wherein the system is configured to perform the step of knowing these factors, to see that a correct system will have different amplitude than an erroneous, if the predetermined settings are similar.

Item 11. The system according to any of item 7-10, wherein if the OCS is unable to find a definite reliable and trustworthy PPO2 signal it is possible to initiate a manual or automatic full or half test cycle, which is performed by altering the actual set point to either a lower or higher value, when this value is reached the set point is changed to the opposite side or level of original set point, wherein the system is configured to perform the step of registering the time it takes to perform this cycle it can be determined if the system is erroneous or not.

Item 12. The system according to item 7, wherein the system is configured to perform the step of loading the OCS with data to predict the expected characteristics for the PPO2 signal and calculating, both historically, actual and future, PPO2 values during the dive performed by a diver, wherein the OCS is analyzing the data during the dive and comparing whether previous and actual data values are valid or if the OCS has changed characteristics.

Item 13. The system according item 7, wherein, depending on the set point for PPO2 that is chosen for the OCS at the actual depth, the system is

configured to perform the step of comparing the PPO2-levels, PPO2-amplitudes, PPO2-sawtooth pattern and PPO2-setpoint change speed to the expected values.

Item 14. The system according to item 7, wherein the system is configured to perform the step of collecting information from solenoid injection volume and rate and a saw tooth pattern of a graph of PPO2 values collected from the O2 sensors and wherein the total volume of the OCS is approximated.

The terminology used herein is for the purpose of describing particular embodiments only and is not intended to be limiting of the invention. As used herein, the singular forms "a", "an" and "the" are intended to include the plural forms as well, unless the context clearly indicates otherwise. It will be further understood that the terms "comprises" "comprising," "includes" and/or "including" when used herein, specify the presence of stated features, integers, steps, operations, elements, and/or components, but do not preclude the presence or addition of one or more other features, integers, steps, operations, elements, components, and/or groups thereof.

Unless otherwise defined, all terms (including technical and scientific terms) used herein have the same meaning as commonly understood by one of ordinary skill in the art to which this invention belongs. It will be further understood that terms used herein should be interpreted as having a meaning that is consistent with their meaning in the context of this specification and the relevant art and will not be interpreted in an idealized or overly formal sense unless expressly so defined herein.

The foregoing has described the principles, preferred embodiments and modes of operation of the present invention. However, the invention should be regarded as illustrative rather than restrictive, and not as being limited to the particular embodiments discussed above. The different features of the various embodiments of the invention can be combined in other combinations than those explicitly described. It should therefore be appreciated that variations may be made in those embodiments by those skilled in the art

without departing from the scope of the present invention as defined by the following claims.

CLAIMS

1. A method (100) for determining the validity of an oxygen, O2, sensor, wherein the O2 sensor is comprised in a breathing apparatus used for diving purposes, the method comprises the steps of:

   - retrieving (S110) one or more partial pressure of oxygen, PPO2, signals from the O2-sensor;

   - comparing (S120) the PPO2 signal to a calculated PPO2 signal;

   - determining (S130) the validity of the retrieved PPO2 signal based on the comparison;

   - determining (S140) the validity of the O2 sensor based on the validity of the PPO2 signal; and

   wherein the current operation of the breathing apparatus is updated (S150) based on the validity of the O2 sensor.

2. The method according to claim 1, wherein the method comprises:

   - measuring the time interval to reach a determined set point of the PPO2 signal and wherein the validity of the PPO2 signal is based on the time to reach the determined set point.

3. The method according to claim 1, wherein step of comparing (S120) comprises:

   - determining (S121) whether the retrieved PPO2 signal is coherent and reasonable or if the PPO2 signal is deviating from the calculated PPO2 signal based on the comparison.

4. The method according to claim 3, wherein the PPO2 signal is deviating from the calculated PPO2 signal, wherein the method comprises:

- changing (S1211) a first PPO2 set point a second PPO2 set point;

- measuring (S1212) the time interval to reach the second PPO2 set point by measuring at least one of a breathing volume of the breathing apparatus, an oxygen injection rate, an oxygen injection volume, an oxygen injection flow and an oxygen consumption;

- calculating (S1213) an incline of a graph presenting the values of the PPO2 signal collected over the time interval for the PPO2 set point change; and

- determining (S1214) the validity of the PO2 signal based on the calculated incline of the graph.

5. The method according to claim 1, wherein the method comprises:

- detecting (S210) at least one of an oxygen injection rate, oxygen injection volume, oxygen injection flow, breathing loop volume or oxygen consumption of the breathing apparatus;

- comparing (S220) the current amplitude of the PPO2 signal to an amplitude of a calculated PPO2 signal related to at least one of the detected oxygen injection rate, oxygen injection volume, oxygen injection flow, breathing volume and oxygen consumption of the breathing apparatus; and

- determining (S130) the validity of the PPO2 signal based on the comparison.

6. The method according to claim any of claim 2-5, the method comprises:

- Initiating (S310) a test cycle, which is performed by altering the current PPO2 set point to either a lower or higher value, when each value is reached the PPO2 set point is changed to the opposite side of the current PPO2 set point;

- registering (S320) the time to perform the test cycle; and

- determining (S130) the validity of the PPO2 signal based on the registered time.

7. The method according to claim 1, wherein the breathing apparatus comprises an oxygen control system, OCS, wherein the method comprises:

- loading (S410) the OCS with data related to the breathing apparatus and the dive to be performed, wherein the OCS is configured to predict expected characteristics of the PPO2 signal from an O2 sensor of the OCS, based on the loaded data;

- calculating (S420), by OCS, characteristics of the PPO2 signal, both previous and actual, during the dive performed by the diver;

- comparing (S430), by OCS during the dive, the calculated characteristics of the PPO2 signal with the expected characteristics of the PPO2 signal; and

- determine whether previous and actual calculated characteristics of the PPO2 signal are valid or if the PPO2 signal has changed characteristics based on the comparison.

8. The method according claim 7, wherein a PPO2 set point is calculated for the OCS, the method comprises:

- comparing at least one of the calculated characteristics of the O2 sensor, PPO2 value, amplitude of the PPO2 signal, saw tooth pattern of a graph of the calculated PPO2 values and speed of change of PPO2 set point with the corresponding expected characteristics of the O2 sensor; and

- determining S130 the validity of the PPO2 signal based on the comparison.

9. The method according to claim 7, wherein the method comprises:

- collecting volume information from a solenoid injection of O2; and

wherein the total breathing loop volume of the OCS is calculated by adding the collected O2 injection volume information to the existing breathing loop volume.

10. An oxygen control system, OCS, comprised in a breathing apparatus used for diving purposes, for determining the validity of an oxygen, O2, sensor, comprised in the OCS and wherein the OCS is configured to perform the steps of:

- retrieving (S110) one or more partial pressure of oxygen, PPO2, signals from the O2-sensor;

- comparing (S120) the PPO2 signal to a calculated PPO2 signal;

- determining (S130) the validity of the retrieved PPO2 signal based on the comparison;

- determining (S140) the validity of the O2 sensor based on the validity of the PPO2 signal; and

wherein the current operation of the breathing apparatus is updated (S150) based on the validity of the O2 sensor.

11. The system according to claim 10, wherein the system is configured to perform the step of:

- measuring the time interval to reach a determined set point of the PPO2 signal and wherein the validity of the PPO2 signal is based on the time to reach set point.

12. The system according to claim 10, wherein the system is configured to perform the step of:

- determining (S121) whether the retrieved PPO2 signal is coherent and reasonable or if the PPO2 signal is deviating from the calculated PPO2 signal based on the comparison.

13. The system according to claim 11, wherein the PPO2 signal is deviating from the predetermined PPO2 signal, wherein the system is configured to perform the step of:

- changing (S1211) a PPO2 set point from a first set point to a second set point;

- measuring (S1212) the time interval to reach the second PPO2 set point by measuring at least one of a breathing volume of the breathing apparatus, an oxygen injection rate, an oxygen injection volume, an oxygen injection flow and an oxygen consumption,

- calculating (S1213) an incline of a graph presenting the values of the PPO2 signal over the time interval for the PPO2 set point change; and

- determining (S1214) the validity of the PO2 signal based on the calculated incline of the graph.

14. The system according to claim 11, wherein the system is configured to perform the step of:

- detecting at least one of an oxygen injection rate, oxygen injection volume, oxygen injection flow, breathing loop volume or oxygen consumption of the breathing apparatus;

- comparing the current amplitude of the PPO2 signal to an amplitude of a predetermined PPO2 signal related to at least one of the detected oxygen injection rate, oxygen injection volume, oxygen injection flow, breathing volume and oxygen consumption of the breathing apparatus; and

- determining the validity of the PPO2 signal based on the comparison.

15. The system according to claim any of claim 11-14, wherein the system is configured to perform the step of:

- Initiating (S310) a test cycle, which is performed by altering the current PPO2 set point value to either a lower or higher value, when each value is reached the PPO2 set point is changed to the opposite side of the current PPO2 set point;

- registering (S320) the time it takes to perform the test cycle; and

- determining (S130) the validity of the PPO2 signal based on the registered time.

16. The system according to claim 10, wherein the OCS is configured to perform the steps of:

- loading (S410) the OCS with data related to the breathing apparatus and the dive to be performed, wherein the OCS is configured to predict expected characteristics of the PPO2

signal from an O2 sensor of the OCS, based on the loaded data;

- calculating (S420), by OCS, characteristics of the PPO2 signal, both previous and actual, during the dive performed by the diver;

- comparing (S430), by OCS during the dive, the calculated characteristics of the PPO2 signal with the expected characteristics of the PPO2 signal; and

- determine whether previous and actual calculated characteristics of the PPO2 signal are valid or if the PPO2 signal has changed characteristics based on the comparison.

17. The system according claim 10, wherein a PPO2 set point is calculated for the OCS, the OCS is configured to perform the steps of:

- comparing at least one of the calculated characteristics of the O2 sensor, PPO2 value, amplitude of the PPO2 signal, saw tooth pattern of a graph of the calculated PPO2 values and speed of change of PPO2 set point with the corresponding expected characteristics of the O2 sensor; and

- determining S130 the validity of the PPO2 signal based on the comparison.

18. The system according to claim 10, wherein the OCS is configured to perform the steps of:

- collecting volume information from a solenoid injection of O2;

- wherein the total breathing volume of the OCS is calculated by adding the collected volume information to the existing breathing volume.

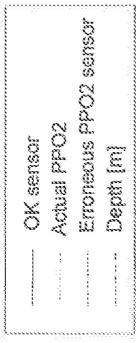
OK sensor
Actual PPO2
Erroneous PPO2 sensor
Depth [m]

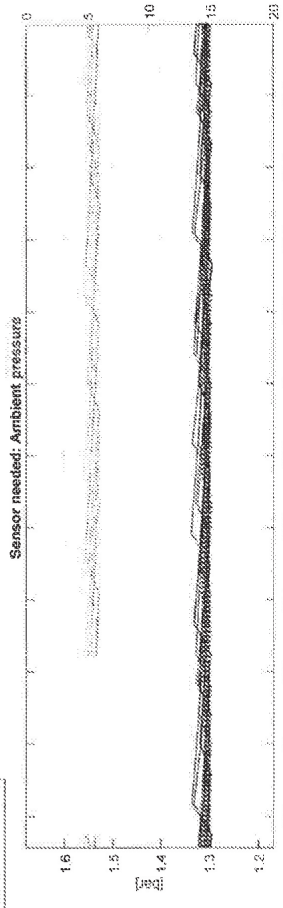
Sensor needed: Ambient pressure
Time [min]
[m]
[bar]

Fig 1a

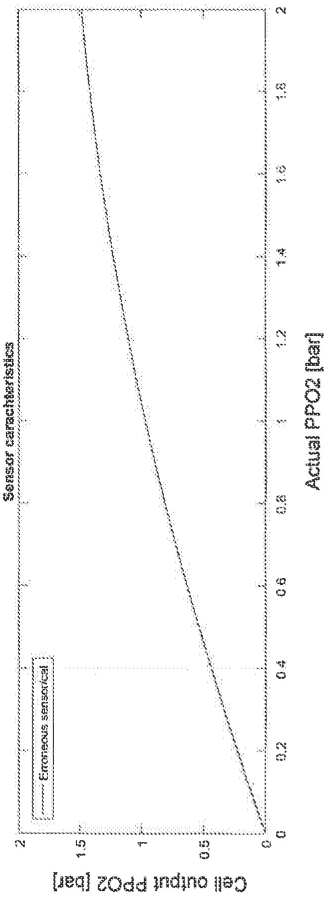
Sensor caracheristics
Erroneous sensor/cal
Actual PPO2 [bar]
Cell output PPO2 [bar]

Fig 1b

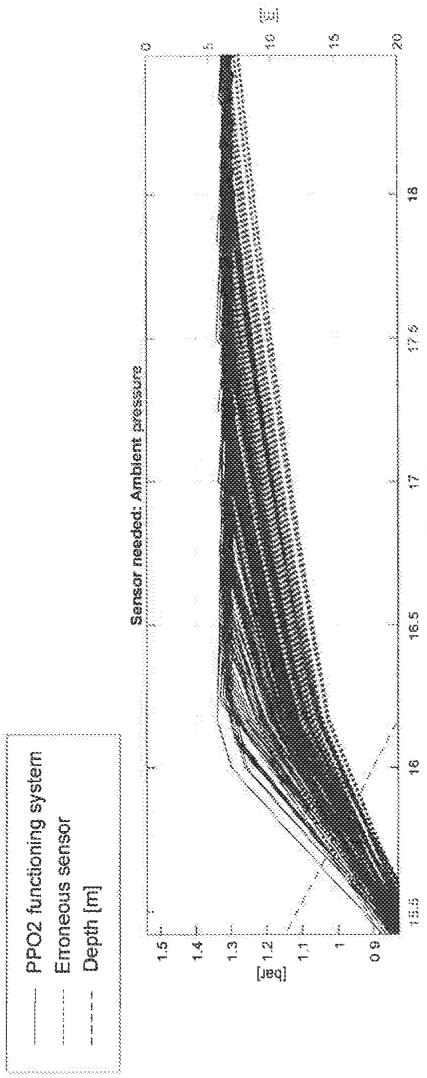
PPO2 functioning system
Erroneous sensor
Depth [m]
Sensor needed: Ambient pressure
[bar]
Time [min]
m

Fig 2a

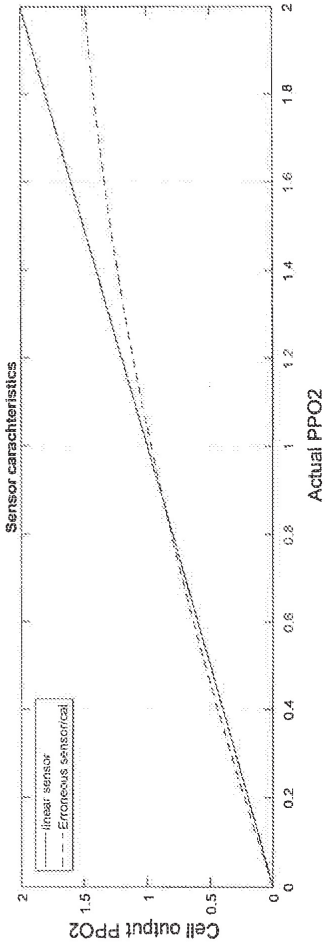
Sensor carachteristics
linear sensor
Erroneous sensorical
Cell output PPO2
Actual PPO2

Fig 2b

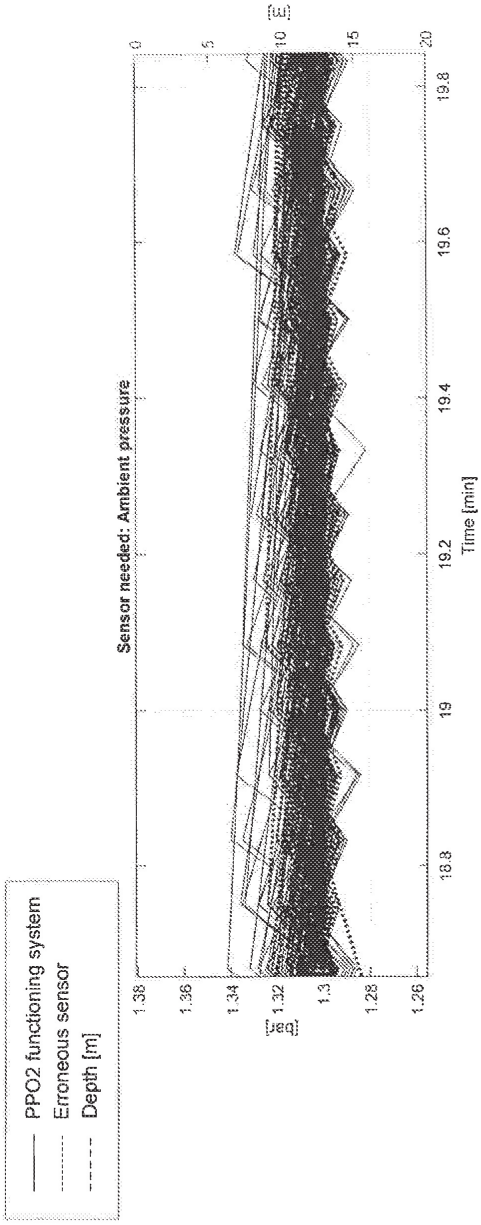
PPO2 functioning system
Erroneous sensor
Depth [m]
Sensor needed: Ambient pressure
[bar]
[m]
Time [min]

Fig 3a

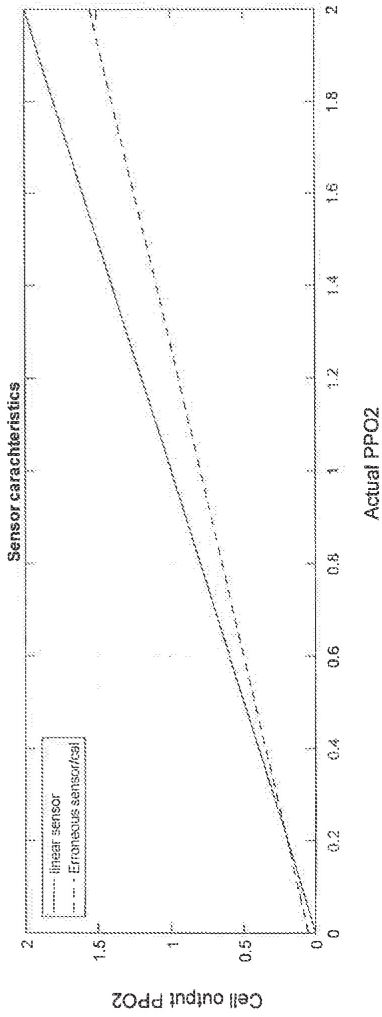
Sensor carachteristics
linear sensor
Erroneous sensor/real
Cell output PPO2
Actual PPO2

Fig 3b

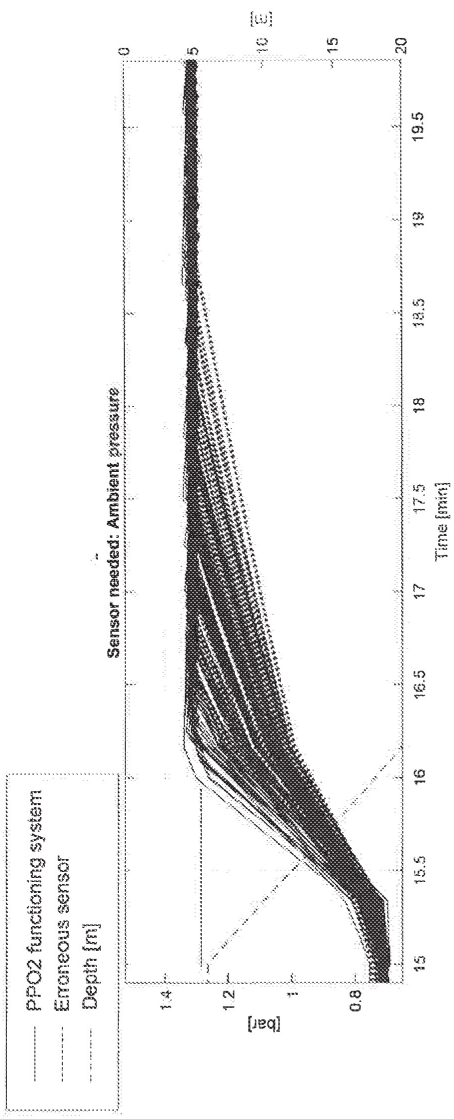
PPO2 functioning system
Erroneous sensor
Depth [m]
Sensor needed: Ambient pressure
[bar]
Time [min]

Fig 4a

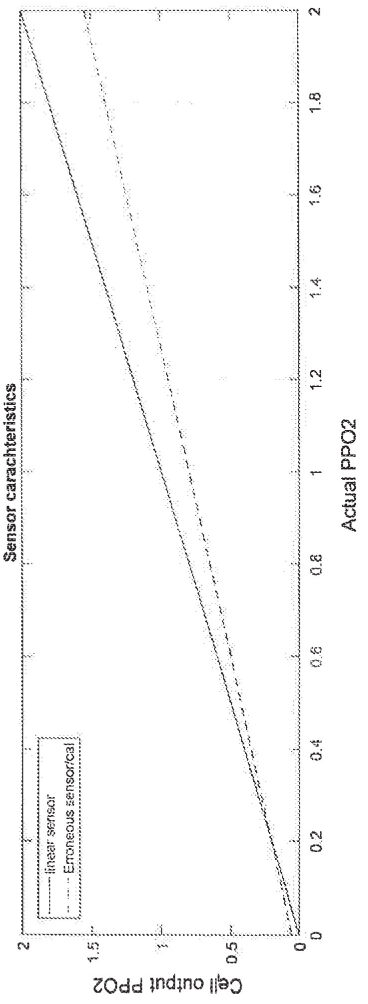
Sensor carachteristics
linear sensor
Erroneous sensorical
Cell output PPO2
Actual PPO2

Fig 4b

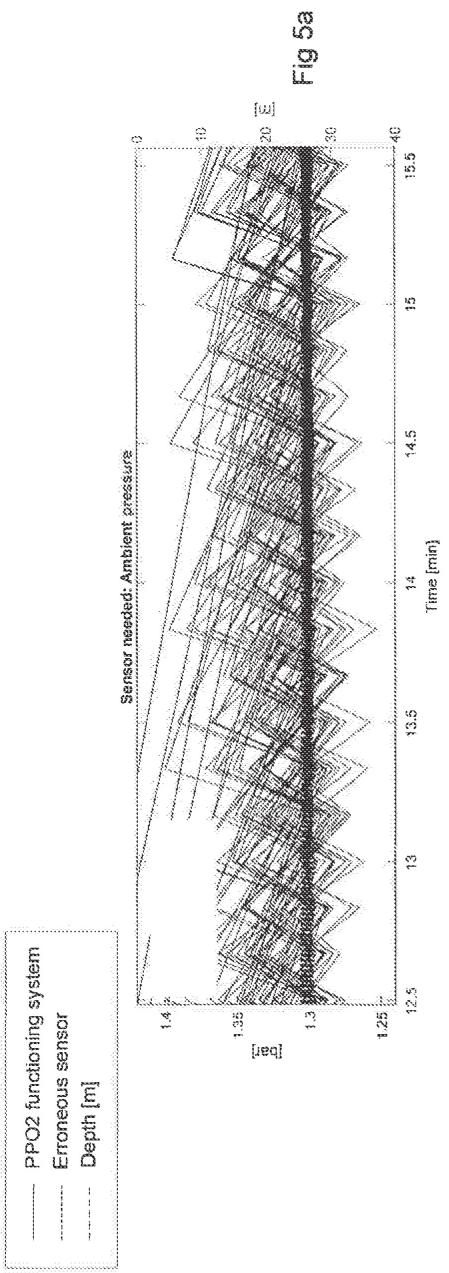
PPO2 functioning system
Erroneous sensor
Depth [m]
Sensor needed: Ambient pressure
[bar]
Time [min]
[m]

Fig 5a

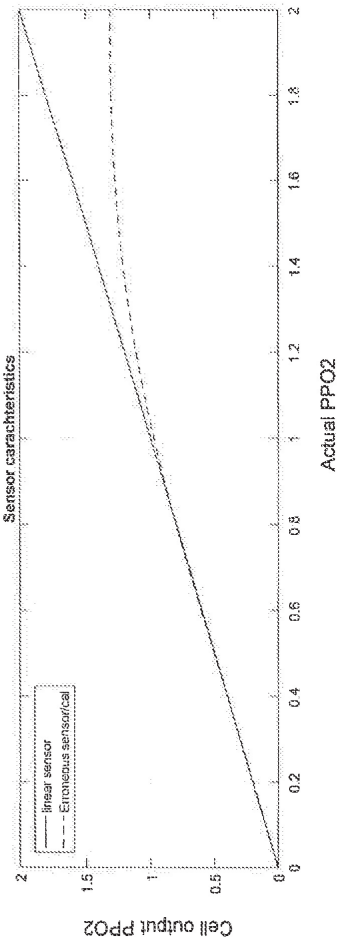
Sensor carachteristics
linear sensor
Erroneous sensor/cal
Cell output PPO2
Actual PPO2

Fig 5b

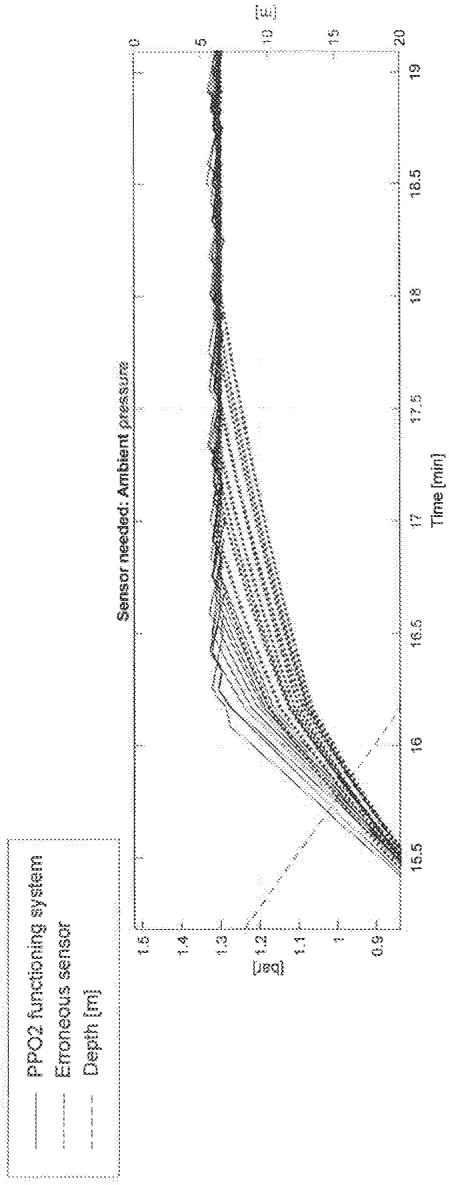
PPO2 functioning system
Erroneous sensor
Depth [m]
Sensor needed: Ambient pressure
[bar]
[m]
Time [min]

Fig 6a

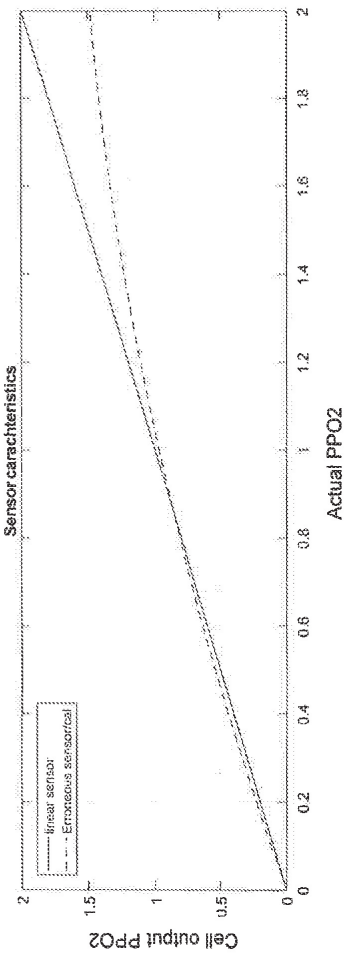
Sensor carachteristics
linear sensor
Erroneous sensor
Cell output PPO2
Actual PPO2

Fig 6b

Fig 7a

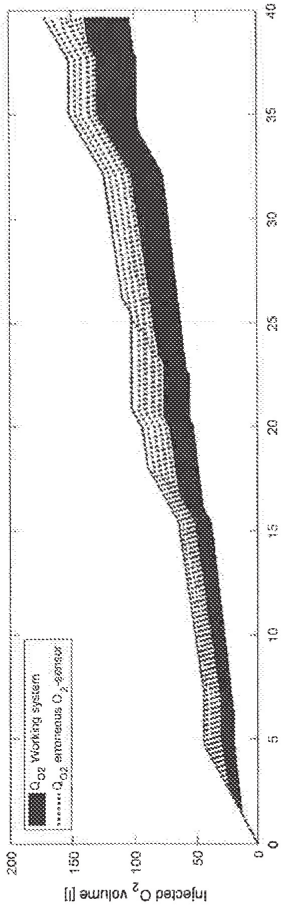
Injected O2 volume [l]
Time [min]
Q02 Working system
Q02 erroneous O2-sensor
0
50
100
150
200
0
5
10
15
20
25
30
35
40

Fig 7b

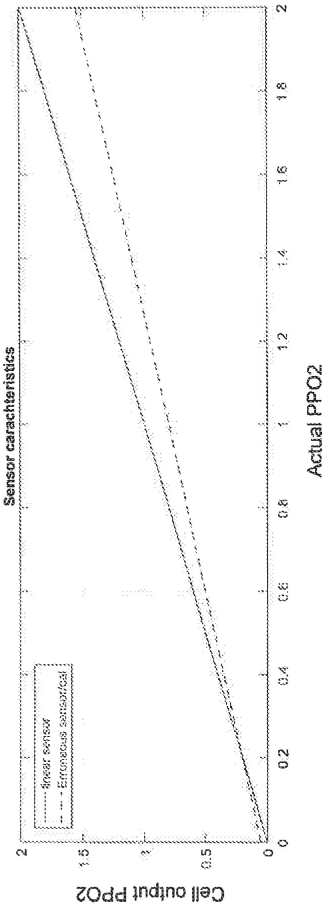
Sensor carachteristics
Cell output PPO2
Actual PPO2
Ideal sensor
Erroneous sensorcal
0
0.5
1
1.5
2
0
0.2
0.4
0.6
0.8
1
1.2
1.4
1.6
1.8
2

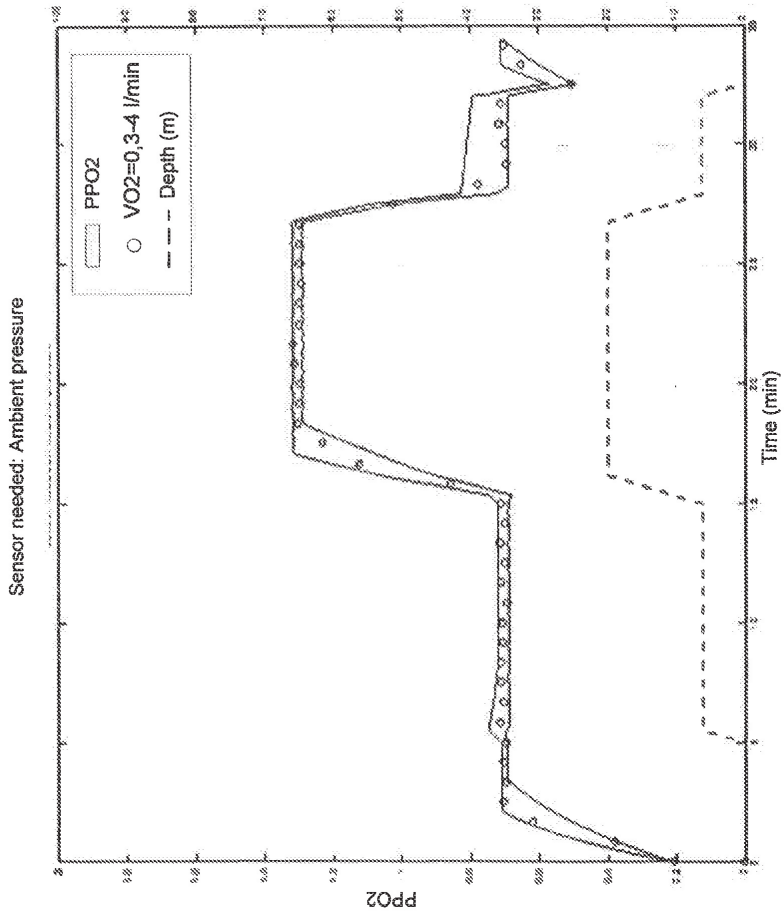
Sensor needed: Ambient pressure
PPO2
VO2=0,3-4 l/min
Depth (m)
ppO2
Time (min)

Fig 8

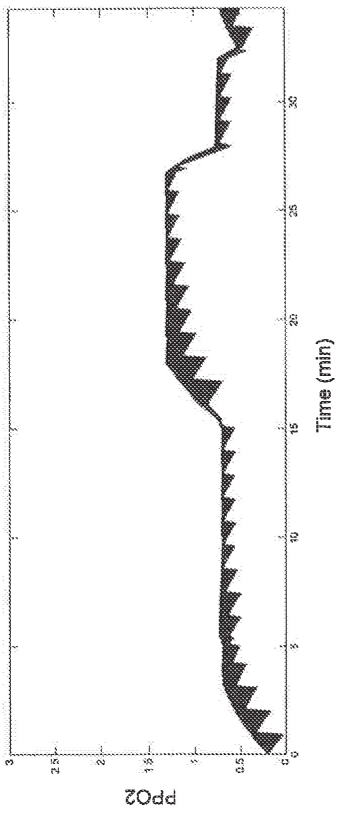

Fig 9a

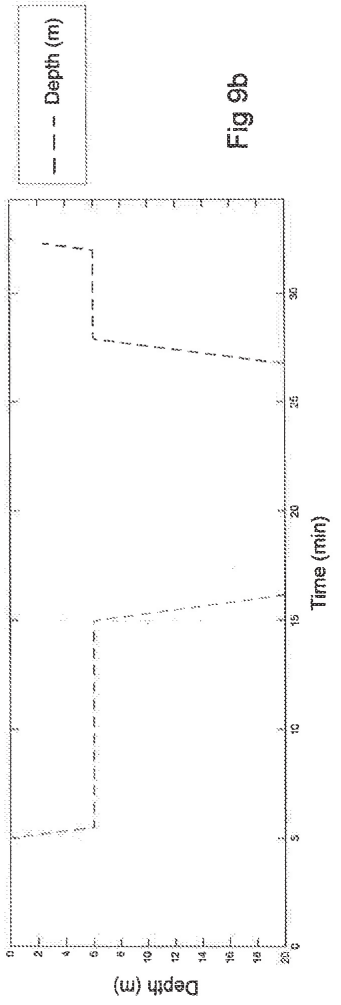

Fig 9b

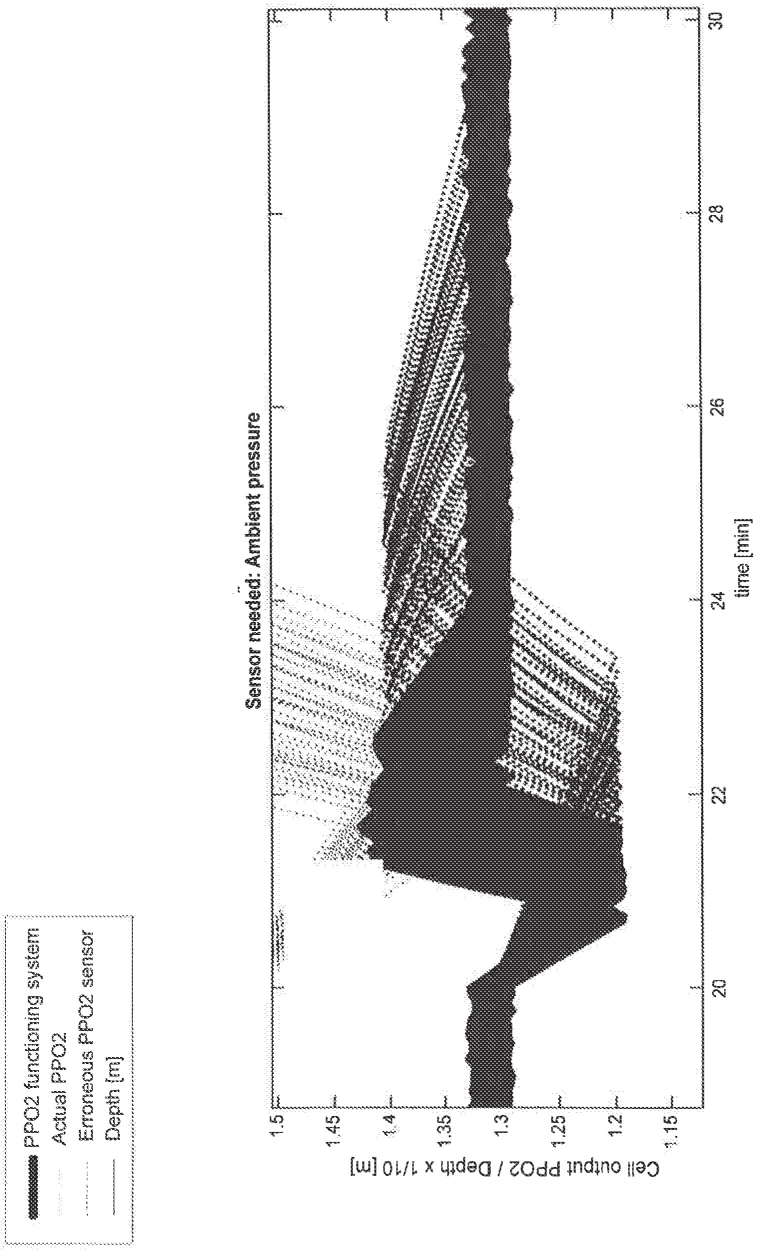
PPO2 functioning system
Actual PPO2
Erroneous PPO2 sensor
Depth [m]
Sensor needed: Ambient pressure
Cell output PPO2 / Depth x 1/10 [m]
time [min]
1.5
1.45
1.4
1.35
1.3
1.25
1.2
1.15
20
22
24
26
28
30

Fig 10a

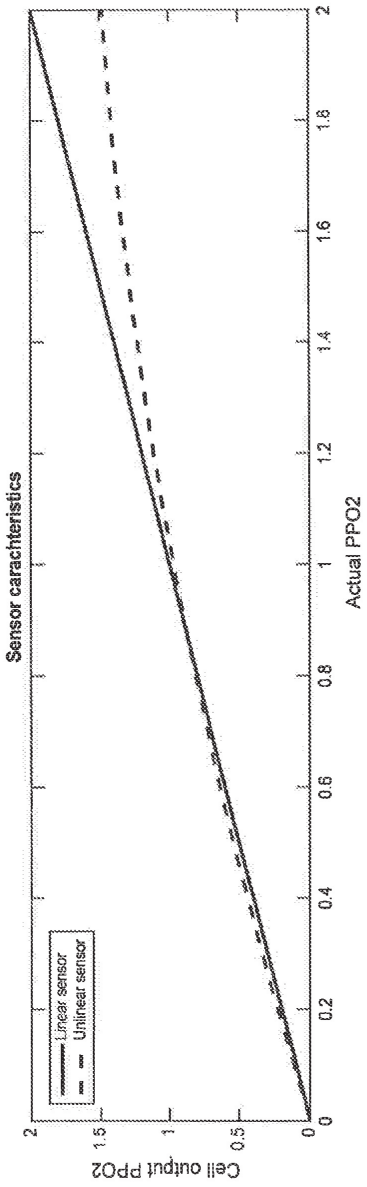
Sensor carachteristics
Linear sensor
Unlinear sensor
Cell output PPO2
Actual PPO2
0
0.2
0.4
0.6
0.8
1
1.2
1.4
1.6
1.8
2
0.5
1.5

Fig 10b

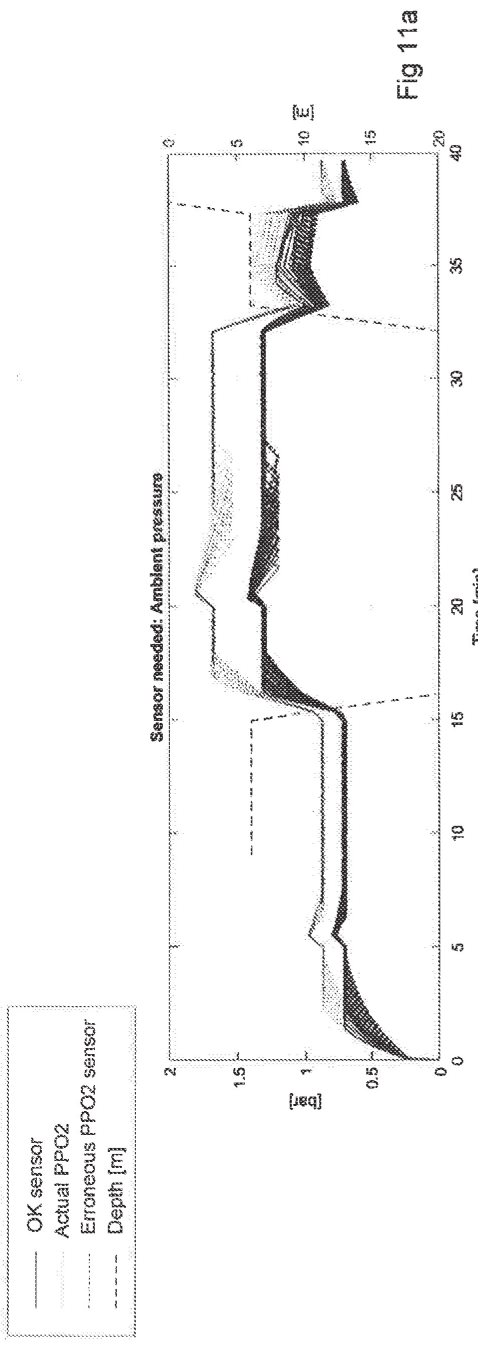

Fig 11a

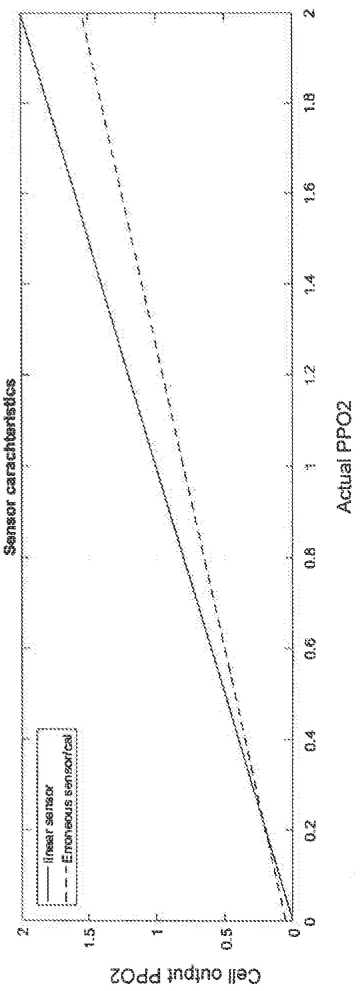

Fig 11b

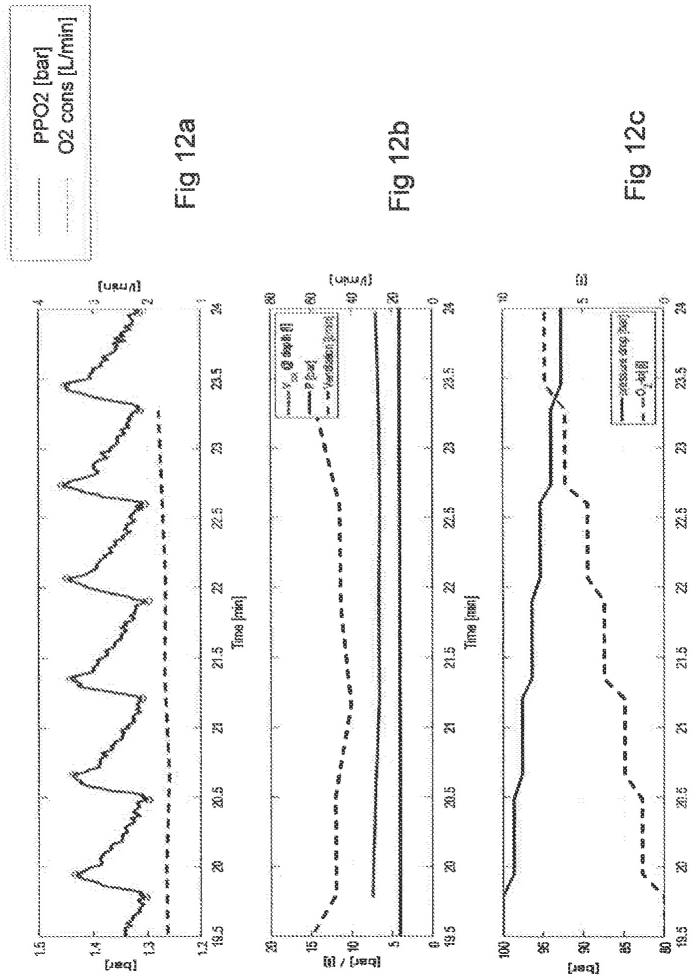

Fig 12a

Fig 12b

Fig 12c

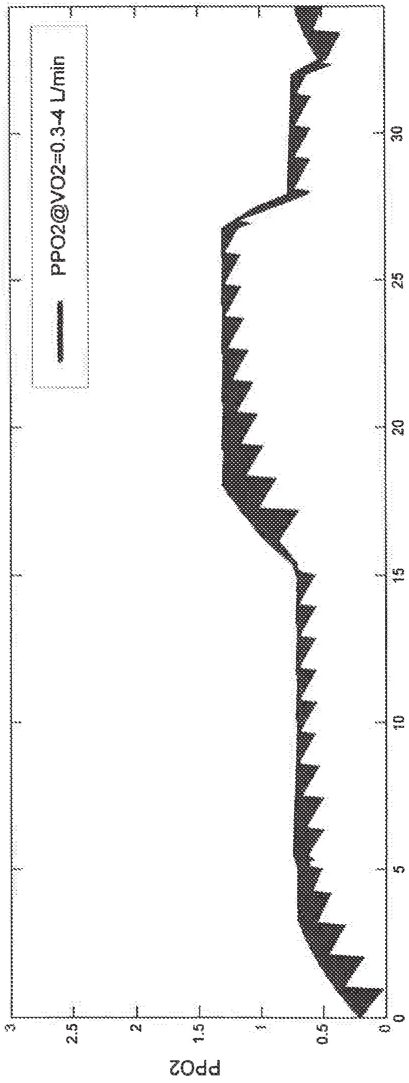

Fig 13

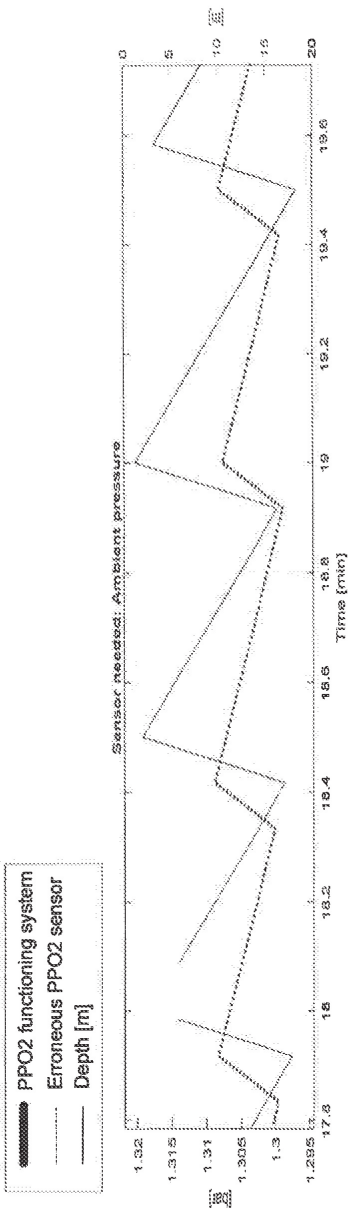
PPO2 functioning system
Erroneous PPO2 sensor
Depth [m]
Sensor heated: Ambient pressure
Time [min]
Depth [m]
1.32
1.315
1.31
1.305
1.3
1.295
17.8
18
18.2
18.4
18.6
18.8
19
19.2
19.4
19.6
20
0
5
10
15

Fig 14

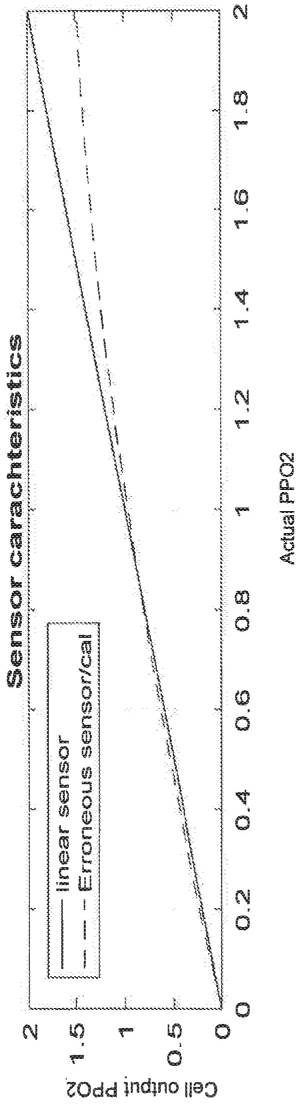
Sensor carachteristics
linear sensor
Erroneous sensor/cal
Cell output PPO2
Actual PPO2
0
0.5
1
1.5
2
0.2
0.4
0.6
0.8
1.2
1.4
1.6
1.8

Fig 15

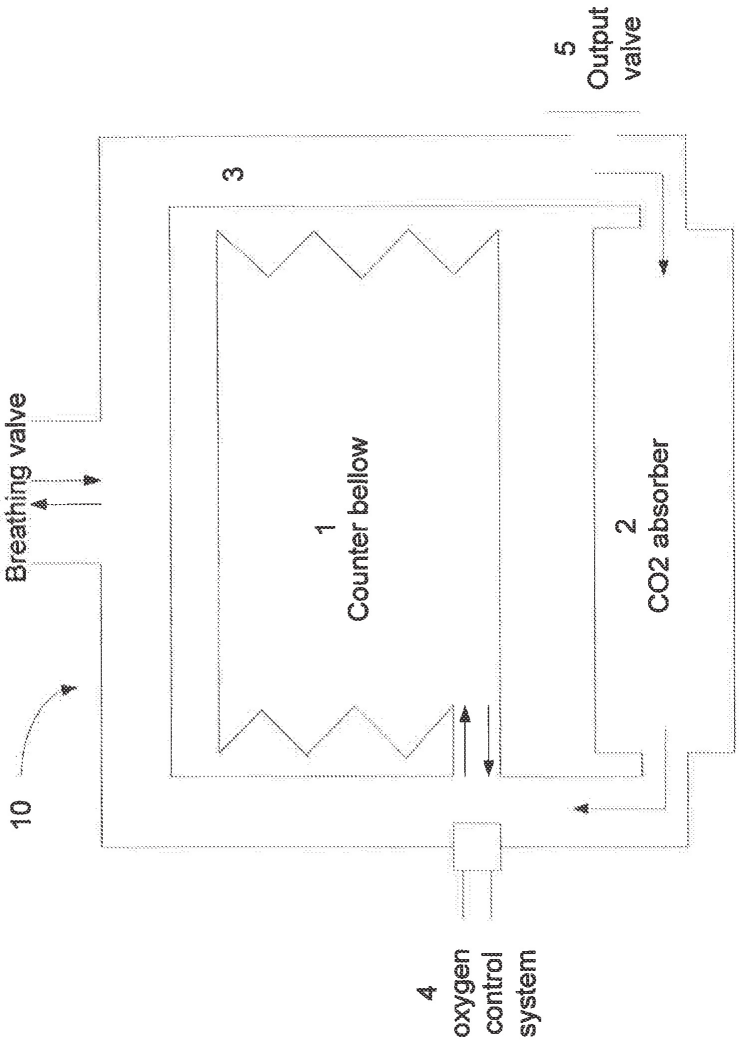
5
Output
valve
3
6
Breathing valve
1
Counter bellow
2
CO2 absorber
10
4
oxygen
control
system

Fig 16

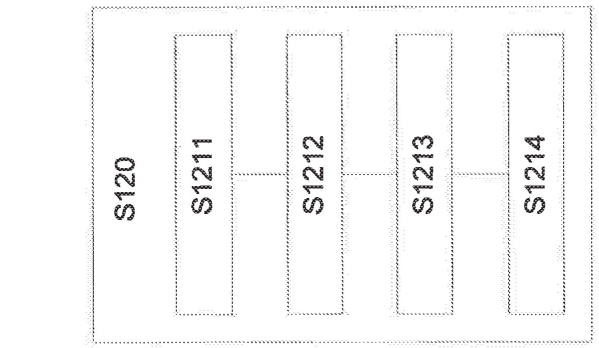

Fig 18

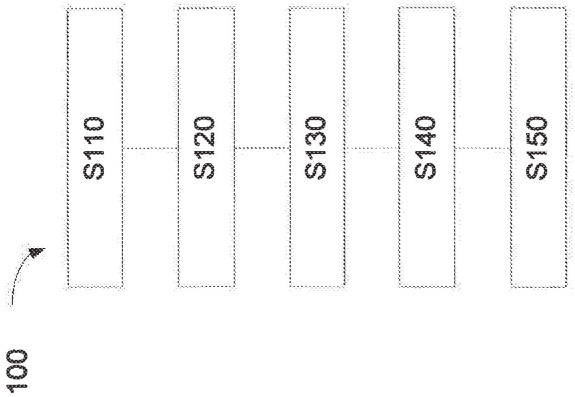

Fig 17

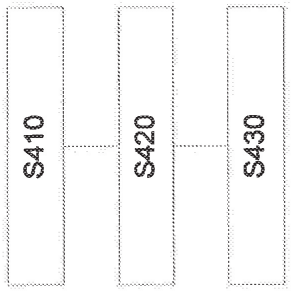

Fig 21

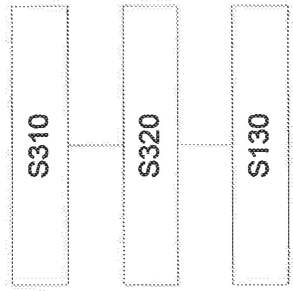

Fig 20

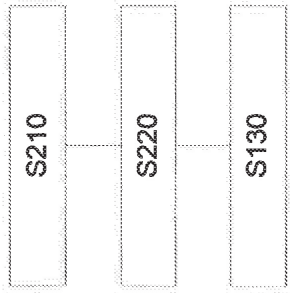

Fig 19

INTERNATIONAL SEARCH REPORT

International application No.
PCT/IB2017/054822

A. CLASSIFICATION OF SUBJECT MATTER

IPC: see extra sheet

According to International Patent Classification (IPC) or to both national classification and IPC

B. FIELDS SEARCHED

Minimum documentation searched (classification system followed by classification symbols)

IPC: A62B, B63C

Documentation searched other than minimum documentation to the extent that such documents are included in the fields searched

SE, DK, FI, NO classes as above

Electronic data base consulted during the international search (name of data base and, where practicable, search terms used)

EPO-Internal, PAJ, WPI data

C. DOCUMENTS CONSIDERED TO BE RELEVANT

Category*	Citation of document, with indication, where appropriate, of the relevant passages	Relevant to claim No.
X	US 20110041848 A1 (STONE WILLIAM C ET AL), 24 February 2011 (2011-02-24); paragraphs [0005]-[0006], [0033], [0146]	1, 3, 5, 10, 12, 14
X	US 6712071 B1 (PARKER MARTIN JOHN), 30 March 2004 (2004-03-30); column 9, line 5 - column 9, line 23	1
X	US 20070215157 A1 (STRAW PHILIP E), 20 September 2007 (2007-09-20); paragraph [0017]	1
X	WO 2015145106 A2 (AVON POLYMER PROD LTD), 1 October 2015 (2015-10-01); page 7, line 17 - page 7, line 25	1

☒ Further documents are listed in the continuation of Box C. ☒ See patent family annex.

* Special categories of cited documents:
"A" document defining the general state of the art which is not considered to be of particular relevance
"E" earlier application or patent but published on or after the international filing date
"L" document which may throw doubts on priority claim(s) or which is cited to establish the publication date of another citation or other special reason (as specified)
"O" document referring to an oral disclosure, use, exhibition or other means
"P" document published prior to the international filing date but later than the priority date claimed
"T" later document published after the international filing date or priority date and not in conflict with the application but cited to understand the principle or theory underlying the invention
"X" document of particular relevance; the claimed invention cannot be considered novel or cannot be considered to involve an inventive step when the document is taken alone
"Y" document of particular relevance; the claimed invention cannot be considered to involve an inventive step when the document is combined with one or more other such documents, such combination being obvious to a person skilled in the art
"&" document member of the same patent family

Date of the actual completion of the international search	Date of mailing of the international search report
27-11-2017	28-11-2017

Name and mailing address of the ISA/SE	Authorized officer
Patent- och registreringsverket Box 5055 S-102 42 STOCKHOLM Facsimile No. + 46 8 666 02 86	Ann Börjeson Telephone No. + 46 8 782 28 00

INTERNATIONAL SEARCH REPORT

International application No.
PCT/IB2017/054822

C (Continuation). DOCUMENTS CONSIDERED TO BE RELEVANT

Category*	Citation of document, with indication, where appropriate, of the relevant passages	Relevant to claim No.
A	US 20100313887 A1 (SIEBER ARNE), 16 December 2010 (2010-12-16); abstract -- --------	1

INTERNATIONAL SEARCH REPORT

International application No.
PCT/IB2017/054822

Box No. II Observations where certain claims were found unsearchable (Continuation of item 2 of first sheet)

This international search report has not been established in respect of certain claims under Article 17(2)(a) for the following reasons:

1. ☐ Claims Nos.:
because they relate to subject matter not required to be searched by this Authority, namely:

2. ☐ Claims Nos.:
because they relate to parts of the international application that do not comply with the prescribed requirements to such an extent that no meaningful international search can be carried out, specifically:

3. ☐ Claims Nos.:
because they are dependent claims and are not drafted in accordance with the second and third sentences of Rule 6.4(a).

Box No. III Observations where unity of invention is lacking (Continuation of item 3 of first sheet)

This International Searching Authority found multiple inventions in this international application, as follows:

The following separate inventions were identified:

1: Claims 1, 3, 5, 6, 10, 12, 14 and 15 directed to a method comprising the step of comparing the sensor signal amplitude with an expected amplitude, received by measuring at least one of the detected oxygen injection rate, oxygen injection volume, oxygen injection flow, breathing volume and oxygen consumption of the breathing apparatus.

.../...

1. ☐ As all required additional search fees were timely paid by the applicant, this international search report covers all searchable claims.

2. ☐ As all searchable claims could be searched without effort justifying additional fees, this Authority did not invite payment of additional fees.

3. ☐ As only some of the required additional search fees were timely paid by the applicant, this international search report covers only those claims for which fees were paid, specifically claims Nos.:

4. ☐ No required additional search fees were timely paid by the applicant. Consequently, this international search report is restricted to the invention first mentioned in the claims; it is covered by claims Nos.:

Remark on Protest

☐ The additional search fees were accompanied by the applicant's protest and, where applicable, the payment of a protest fee.

☐ The additional search fees were accompanied by the applicant's protest but the applicable protest fee was not paid within the time limit specified in the invitation.

☐ No protest accompanied the payment of additional search fees.

Continuation of: Box No. III

2: Claims 2, 4, 11, and 13 directed to a method comprising the step of measuring the time interval to reach a determined set point of the PP02 signal.

3: Claims 7-9 and 16-18 directed to a method comprising the step of calculating characteristics of the PP02 signal, both previous and actual, during the dive performed by the diver.

All inventions have been searched.

The present application has been considered to contain 3 inventions which are not linked such that they form a single general inventive concept, as required by Rule 13 PCT for the following reasons:

The single general concept of the present application is the technical features defined in claim 1. Document D1 discloses all these features (see comments in Written Opinion of the International Searching Authority, BOX V). Thus, the single general concept is known and cannot be considered as a single general inventive concept in the sense of Rule 13.1 PCT. No other features can be distinguished which can be considered as the same or corresponding special technical features in the sense of Rule 13.2 PCT. Thus, the application lacks unity of invention.

International application No.
PCT/IB2017/054822

Continuation of: second sheet
International Patent Classification (IPC)
B63C 11/24 (2006.01)

US	20110041848	A1	24/02/2011	EP	2205322	A1	14/07/2010
				EP	2205323	A4	06/03/2013
				US	20110114094	A1	19/05/2011
				US	8820135	B2	02/09/2014
				US	8800344	B2	12/08/2014
				WO	2009058083	A1	07/05/2009
				WO	2009058081	A1	07/05/2009
US	6712071	B1	30/03/2004	AU	9090698	A	05/04/1999
				DE	69813257	D1	15/05/2003
				EP	1015077	A1	05/07/2000
				GB	2329343	A	24/03/1999
				WO	9913944	A1	25/03/1999
US	20070215157	A1	20/09/2007	CA	2564999	A1	17/11/2005
				GB	2441117	B	15/04/2009
				US	20120132207	A1	31/05/2012
				WO	2005107390	A3	14/06/2007
WO	2015145106	A2	01/10/2015	GB	2525973	B	13/07/2016
				US	20170100610	A1	13/04/2017
US	20100313887	A1	16/12/2010	AT	9946	U1	15/06/2008
				AT	486005	T	15/11/2010
				DE	502007005494	D1	09/12/2010
				EP	2097312	B1	27/10/2010
				US	8424522	B2	23/04/2013
				WO	2008080948	A3	16/10/2008

Paper I

Technical report

The performance of 'temperature stick' carbon dioxide absorbent monitors in diving rebreathers

Mårten Silvanius[1,4], Simon J Mitchell[2], Neal W Pollock[3], Oskar Frånberg[4], Mikael Gennser[5], Jerry Lindén[1], Peter Mesley[6], Nicholas Gant[7]

[1] *Swedish Armed Forces Diving and Naval Medicine Centre, Karlskrona, Sweden*
[2] *Department of Anaesthesiology, University of Auckland, Auckland, New Zealand*
[3] *Department of Kinesiology, Université Laval Québec, QC, Canada*
[4] *Blekinge Institute of Technology, Karlskrona, Sweden*
[5] *School of Technology and Health, KTH Royal Institute of Technology, Stockholm, Sweden*
[6] *Lust for Rust Diving Expeditions, Auckland*
[7] *Department of Exercise Sciences, University of Auckland*

Corresponding author: *Nicholas Gant, Department of Exercise Sciences, Centre for Brain Research, University of Auckland, Auckland 1142, New Zealand*
n.gant@auckland.ac.nz

Key words
Hypercapnia; Monitoring; Technical diving; Soda lime; Equipment

Abstract
(Silvanius M, Mitchell SJ, Pollock NW, Frånberg O, Gennser M, Lindén J, Mesley P, Gant N. The performance of 'temperature stick' carbon dioxide absorbent monitors in diving rebreathers. Diving and Hyperbaric Medicine. 2019 March 31;49(1):48–56. doi: 10.28920/dhm49.1.48-56. PMID: 30856667.)
Introduction: Diving rebreathers use canisters containing soda lime to remove carbon dioxide (CO_2) from expired gas. Soda lime has a finite ability to absorb CO_2. Temperature sticks monitor the exothermic reaction between CO_2 and soda lime to predict remaining absorptive capacity. The accuracy of these predictions was investigated in two rebreathers that utilise temperature sticks.
Methods: Inspiration and rEvo rebreathers filled with new soda lime were immersed in water at 19°C and operated on mechanical circuits whose ventilation and CO_2-addition parameters simulated dives involving either moderate exercise (6 MET) throughout (mod-ex), or 90 minutes of 6 MET exercise followed by 2 MET exercise (low-ex) until breakthrough (inspired PCO_2 [P_iCO_2] = 1 kPa). Simulated dives were conducted at surface pressure (sea-level) (low-ex: Inspiration, n = 5; rEvo, n = 5; mod-ex: Inspiration, n = 7, rEvo, n = 5) and at 3–6 metres' sea water (msw) depth (mod-ex protocol only: Inspiration, n = 8; rEvo, n = 5).
Results: Operated at surface pressure, both rebreathers warned appropriately in four o five low-ex tests but failed to do so in the 12 mod-ex tests. At 3–6 msw depth, warnings preceded breakthrough in 11 of 13 mod-ex tests. The rEvo warned conservatively in all five tests (approximately 60 minutes prior). Inspiration warnings immediately preceded breakthrough in six of eight tests, but were marginally late in one test and 13 minutes late in another.
Conclusion: When operated at even shallow depth, temperature sticks provided timely warning of significant CO_2 breakthrough in the scenarios examined. They are much less accurate during simulated exercise at surface pressure.

Introduction

A closed circuit rebreather is a type of underwater breathing apparatus that recycles expired gas through a carbon dioxide (CO_2) absorbent and incorporates a gas addition system designed to maintain both a safe inspired pressure of oxygen (P_iO_2) and an appropriate mix of diluent gases. They are popular with so-called 'technical divers' and scientific divers performing deep and/or long dives because the recycling of expired breath markedly reduces use of expensive gases such as helium, and maintenance of a constant optimal P_iO_2 increases decompression efficiency.[1]

There are several forms of CO_2 absorbent, but the most commonly used is soda lime; a granular compound containing calcium hydroxide, water and sodium hydroxide. This is packed in a canister (often referred to as a 'scrubber') through which the exhaled gas is passed. Soda lime has a finite capacity for absorbing CO_2 and, if this capacity is exceeded, CO_2 will 'break through' the scrubber and its re-inhalation by the diver may lead to dangerous hypercapnia. Therefore, the soda lime must be replaced in a timely fashion. Rebreather manufacturers provide guidelines on scrubber canister duration, based on tests conducted under demanding conditions with high simulated CO_2 production

and low water temperature, which divers may consider to be conservative. Anecdotally, this often results in divers using soda lime for longer than recommended based on their previous experience and best guesses on expected duration.

In an attempt to bring some objectivity to determining safe duration of use of soda lime, several manufacturers have incorporated so-called 'temperature sticks' into the scrubber canister to monitor the exothermic reaction between CO_2 and soda lime. These devices are comprised of an array of thermistors that pass through the soda lime bed, and they apply proprietary algorithms to interpret the distal movement of the reaction as it progresses through the canister while proximal exhausted soda lime cools. Proximal in this context refers to the end of the scrubber canister where the exhaled gas enters. Two very popular rebreathers utilising temperature sticks are the Inspiration™ rebreather (Ambient Pressure Diving, Helston, Cornwall, UK), and the rEvo™ rebreather (rEvo Rebreathers, Brussels, Belgium).

The Inspiration rebreather control display notionally depicts the temperature profile in the soda lime bed as a bar that turns from clear to black as the scrubber heats up early in the dive, and then progressively (in six steps from proximal to distal) turns from black to clear as the reaction decreases. When the display has only one black step left, which has been designed to occur prior to a P_iCO_2 of 0.5 kPa, the diver receives a warning. The display bar is designed to become completely clear prior to a P_iCO_2 of 1 kPa, at which point the diver is advised to 'bail-out' off the rebreather and onto an open-circuit gas supply.

Soda lime in the rEvo is divided into two smaller separate canisters connected in series by a short conduit. Each canister has its own temperature stick. This configuration facilitates a cycling regimen between shorter dives whereby the proximal heavily used canister is discarded, the less consumed distal canister is moved into the proximal position and a new canister is placed in the distal position. The idea is to avoid discarding an entire canister containing a lot of unconsumed soda lime after a short dive. The temperature stick algorithm counts down a time (in minutes) to the point beyond which cycling (as above) is no longer considered appropriate. If the dive duration exceeds this cycling time threshold, then the two scrubbers are treated as one and the algorithm counts down a "*remaining scrubber time*" in minutes.

This presentation of information that is analogous to a CO_2 scrubber 'fuel gauge' inevitably invites the diver to interpret the data literally, and to base important decisions about conduct of the dive on the temperature stick. This requires that the temperature stick predictions of remaining scrubber life are reasonably accurate in the majority of plausible scenarios. Other than a reference to "*experimentally determined calibration*" in the patent describing the rEvo temperature stick[2] and an abstract alleging successful development of the same device,[3] no data could be found in the public domain describing the accuracy of these devices. Therefore, the ability of these rebreathers to predict CO_2 breakthrough was tested. The question in respect of both the Inspiration and rEvo devices was: would the temperature stick warn the diver prior to significant CO_2 breakthrough during simulated dives?

Methods

Those aspects of the protocol requiring human participation were approved by the University of Auckland Human Participation Ethics Committee (Reference 015280). This was a laboratory study in which an Evolution Plus™ (a rebreather model in the Inspiration range, henceforth referred to simply as the Inspiration) and a rEvo (standard model) rebreather were operated in a test circuit designed to simulate resting and exercising dives. Thus, in a preliminary phase of this study (described in more detail previously[4]) indicative values for respiratory minute ventilation (V_E), tidal volume (T_V), respiratory rate (RR), oxygen consumption (VO_2), and CO_2 production (VCO_2) were established in a working subject at the chosen exercise intensity.

A recent consensus on functional capacity for diving activity identified continuous exercise at 6 MET as a desirable and plausible target for sustained exercise output in a diver.[5] One MET [the approximate metabolic rate of an individual at rest] equals an assumed oxygen consumption of 3.5 mL·kg^{-1} body weight·minute^{-1} (min). Therefore, to establish the ventilation and CO_2 addition parameters for the benchtop tests our human participant exercised at 6 MET on an electronically braked cycle ergometer whilst breathing on the Inspiration rebreather in dry conditions. At steady state V_E was 44 L·min^{-1} (T_V = 2.0L, RR = 22 breaths·min^{-1}) and VCO_2 was 2.0 L·min^{-1}, actual temperature and pressure dry (ATPD).

SURFACE PRESSURE MECHANICAL TEST CIRCUIT

The initial studies were conducted at the University of Auckland, New Zealand. The ambient pressure for all New Zealand trials was at sea level (surface pressure), chosen of necessity because no pressure testing facility was available. In these studies, the inspiratory and expiratory hoses of the rebreather were attached to a test circuit (Figure 1). The test circuit was composed of 35 mm (internal diameter) smooth-bore respiratory tubing (MLA1015, AD Instruments, Dunedin, New Zealand) connected to a one-way respiratory valve (5710, Hans Rudolph, Shawnee, KS, USA) which simulated the rebreather mouthpiece. A port in the valve allowed continuous sampling of the inspired and expired gas for infrared analysis of inspired and end-tidal PCO_2 (ML206 Gas Analyser, AD Instruments, Dunedin, New Zealand). A clinical heater-humidifier (Fisher and Paykell Medical, Auckland, New Zealand) was incorporated into the exhale hose of the circuit to reproduce the heating and humidification of expired gas that would occur with a human breathing on the loop. The heating function was set to 34°C for all experiments.

Figure 1
Schematic layout of the test circuit and monitoring equipment; (see text for explanation)

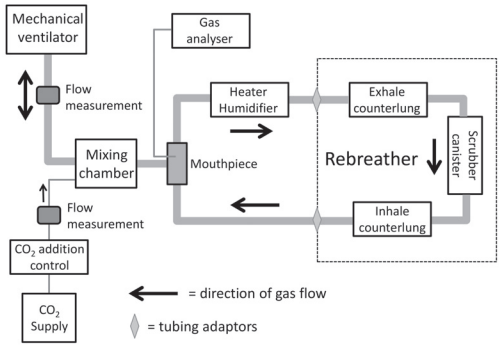

Breathing was simulated using a sinusoidal mechanical ventilator (17050-2 Lung Simulator, VacuMed, Ventura, CA, USA) with an inspiratory-expiratory ratio of 1:1. The T_V was set at 1.5 L and the RR at 30 breaths·min^{-1} for the 6 MET experiments. These parameters differed slightly from the derived human values described above (T_V 2.0 L, RR 22 breaths·min^{-1}) because the ventilator struggled with the work of moving gas around this circuit with a T_V of 2.0 L. Accurate ventilation was ensured through independent monitoring with a pneumotachograph (800 L, Hans Rudolph, Shawnee, KS, USA).

The ventilator was connected to the circuit one-way valve via a 4 L mixing chamber where the inspired and expired gas mixed with instrument grade CO_2 introduced at 2 L·min^{-1} ATPD using a precision flow pump (R-2 Flow Controller, AEI Technologies, Pittsburgh PA, USA) drawing from a Douglas bag reservoir. The CO_2 flow was also independently monitored to ensure accuracy using a flow transducer (MLT10L, AD Instruments, Dunedin, New Zealand).

Sofnolime 797™ (Molecular Products, Essex, UK) was used in both rebreathers for all experiments. All Sofnolime was newly purchased, in date, and stored in the manufacturer-supplied sealed containers before use. The Sofnolime was precisely weighed (2.64 kg for the Inspiration scrubber, and 1.35 kg for each of the two rEvo canisters) (GM-11, Wedderburn Scales, Auckland, New Zealand) prior to canister packing. Each new scrubber canister was packed approximately 15 min before the start of an experiment.

In all tests the rebreathers were immersed in water at room temperature (19°C), chosen as a matter of convenience. Although water temperature is known to affect scrubber duration, there are no data on how it may affect temperature stick performance, and any water temperature within the range frequented by divers is operationally relevant.

SURFACE PRESSURE TEST PROTOCOL

The circuit was tested for leaks by holding a positive pressure. The rebreather was switched on and the default surface PO_2 set point of 0.7 atmospheres (atm) was chosen for the Inspiration. The rEvo was operated with the oxygen addition system switched off because this unit has a constant mass flow oxygen addition system and with no actual oxygen consumption occurring this resulted in gas accumulation and over-pressure of the circuit. An easily exceeded surface PO_2 set point of 0.19 atm (19 kPa) was used to avoid constant hypoxia alarms. The diluent gas was air for all experiments. Ventilation of the circuit was initiated and, after appropriate operation was confirmed, a timed trial started with the continuous addition of CO_2 at 2.0 L·min^{-1} ATPD. Every 30 min the ventilation and CO_2 addition were briefly paused (approximately one min) to recalibrate the CO_2 flow and infrared sensors and to remove any excess moisture from the circuit hoses. These pauses did not elicit any alarms or obvious changes in the temperature stick display (Inspiration) or remaining scrubber time (rEvo).

For each rebreather we ran tests on two protocols. The first was designed to emulate the exercise and ventilation pattern of typical long dives where there would usually be moderate exercise initially followed by a long period of low exercise during decompression. Thus, the rebreathers (n = 5 for each model), each containing a newly packed soda lime scrubber, were run on 6 MET parameters (described above) for 90 min (half the Inspiration's expected scrubber life before breakthrough when operated at 6 MET),[4] followed by 2 MET parameters (ventilation 16.5 L·min^{-1} [Tv 1.5 L;, RR = 11 breasths·min^{-1}], VCO_2 = 0.67 L·min^{-1}) until the P_iCO_2 rose to 1 kPa; a P_iCO_2 that is considered dangerous,[6] and after which the rise in CO_2 is generally extremely rapid.

The second protocol was designed to emulate the less plausible scenario of continuous moderate exercise throughout a dive. Thus the rebreathers (n = 6 for the Inspiration and n = 5 for the rEvo) were run on the 6 MET parameters continuously until the P_iCO_2 rose to 1 kPa. Throughout the tests, the decay was noted of the six segments on the Inspiration temperature stick display and recorded the remaining scrubber time (at 10 min intervals) displayed by the rEvo. The primary endpoint in each test was whether the rebreather warned the diver (decay to one segment on the Inspiration and counting down to zero time remaining on the rEvo) prior to reaching breakthrough at 1 kPa.

HYPERBARIC TEST CIRCUIT

After some results of the surface pressure tests were found to be discordant with manufacturer tests conducted under pressure (Martin Parker, personal communication, December 2016), we elected to repeat the continuous moderate exercise tests in both rebreathers at elevated ambient pressure at the

Figure 2
The ANSTI underwater breathing apparatus test system. The pressure vessel is in the centre. The pressure control, ventilation and heater/cooler systems are on the right of the pressure vessel, and the monitoring system is on the left

Figure 3
Schematic layout of the ANSTI breathing test circuit and monitoring equipment; (see text for explanation)

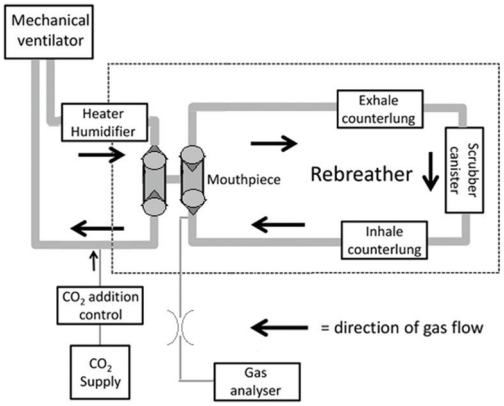

Swedish Armed Forces Diving and Naval Medicine Centre at Karlskrona. The same scrubber and temperature stick units used in the surface pressure experiments (both rebreathers) were employed here. In these studies, the rebreather was connected to an ANSTI machine test circuit.[7] The ANSTI machine is a purpose-built underwater breathing apparatus test station (Figure 2) that allows mechanical ventilation with heated and humidified gas, and precise CO_2 addition to an immersed rebreather under pressure.

The laboratory environment was maintained at 20°C and 35–45% relative humidity. As in the surface pressure circuit, CO_2 was precisely introduced to the ANSTI machine ventilation system at 1.86 L·min^{-1} standard temperature and pressure dry (STPD) giving a volume of 2 L·min^{-1} at ATPD via a mass flow controller (Brooks Instrument 0-5 L·min^{-1} CO_2, Hatfield PA, USA) such that it entered the exhale hose of the rebreather loop as it would during use by a diver (Figure 3). Gas from the rebreather inhale hose was sampled at 250 mL·min^{-1} for continuous analysis in an infrared CO_2 analyser (Servomex 1440 D, Crowborough, UK). This sampled gas was replaced, and rebreather loop volume preserved during compression to elevated pressures, by allowing the rebreathers' automatic diluent addition valves to add air into the rebreather circuit.

The experiments were identical to the surface pressure tests with respect to rebreather configuration, ventilation parameters, expired gas heating and humidification, water temperature and soda lime management (see above). As in the surface pressure experiments throughout each test there was periodic two-point calibration of the inspired CO_2 analyser using reference gases, and independent calibration of the CO_2 inflow rate (DryCal Definer 220, Butler NJ, USA).

HYPERBARIC TEST PROTOCOL

The set up and oxygen management in each rebreather was as described for the surface pressure studies, except that the rEvo would not accept a PO_2 set point of 0.19 atm at depth and the 0.7 atm (71 kPa) set point for the Inspiration was unacceptably high for safe operation of the ANSTI circuit. Therefore, a set point of 0.5 atm (50.6 kPa) was used for both rebreathers. The rEvo was run with the oxygen addition system switched off so that the constant oxygen flow would not disturb the measurements, and the hypoxia alarm was cancelled when it was active.

For each experiment the rebreather was secured in the ANSTI test chamber and immersed while being ventilated to check for leaks. The test chamber lid was then closed and the chamber pressurised to the chosen depth. Because the hyperbaric studies were being performed in response to the finding of suboptimal temperature stick performance at the surface (Figures 5 and 6), we ran the hyperbaric experiments at the shallowest depths that are nevertheless of undisputed relevance to divers during decompression (3 or 6 metres' sea water (msw)). Similarly, because the temperature sticks had performed well on the low exercise protocol but failed on the moderate exercise protocol at surface pressure, we only performed the hyperbaric studies in Sweden on the moderate exercise protocol.

Two Inspiration scrubber canisters were available (thus two different temperature sticks: stick A that had been used in the surface pressure experiments, and stick B, not previously used in our work). Two tests were run using each stick at 3 and 6 msw; a total of eight Inspiration tests. Five tests were run with the rEvo; three at 3 msw and two at 6 msw. Finally, in order to corroborate our previous finding of temperature stick failure during moderate exercise at surface pressure (sea level) one test was run with the Inspiration (stick A as previously used at surface pressure) immersed in the ANSTI machine but without pressurising the test chamber.

Table 1

The remaining scrubber time (RST) (minutes) displayed by the rEvo rebreather at the point of CO_2 breakthrough to a P_iCO_2 of 1 kPa in the low and high exercise tests conducted at surface pressure; a negative offset is the time elapsed between zero time remaining on the scrubber monitor and the actual time of breakthrough to P_iCO_2 = 1 kPa, and represents early warning; a positive offset is the time remaining on the scrubber monitor at the actual time of breakthrough to P_iCO_2 = 1 kPa, and represents a late warning; zero offset means that the remaining time on the scrubber monitor at exactly the same time as breakthrough to P_iCO_2 = 1 kPa

Condition	Low exercise tests						Moderate exercise tests				
Test number	1	2	3	4	5		1	2	3	4	5
RST at P_iCO_2 = 1 kPa	0	15	0	0	0		15	75	4	0	25
Offset (minutes)	-45	15	-57	-18	-63		15	75	4	0	25

Figure 4

Changes in the Inspiration temperature stick display over the course of each low exercise test conducted at surface pressure. Each bar represents a separate test; the top of the bar represents the time (y axis) of breakthrough to a P_iCO_2 of 1 kPa; the coloured shading represents the appearance of the temperature stick display according to the key. Note that the dark green segment at the base of each bar represents both the time taken for the stick display to become completely black signifying heat throughout the soda lime bed, and the time it remained completely black. The timing of both alarm conditions is shown (initial warning = dotted line occurring when one black segment remains, and bailout warning = solid line occurring when no black segments remain)

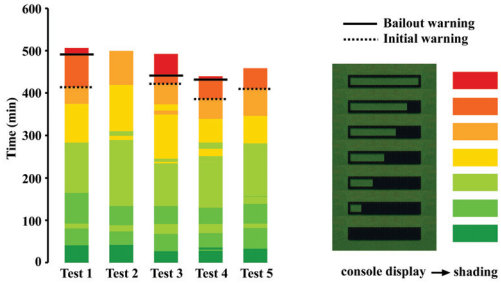

Temperature stick data from both rebreathers were recorded as described for the surface pressure studies.

THERMISTOR EVALUATION

After small but consistent differences were found in the performance of the two Inspiration temperature sticks (Figure 7), the readings obtained from the nine thermistors arrayed in each temperature stick were compared under carefully controlled temperature conditions. The two sticks were placed in a climate chamber (T-70/1000, CTS GmbH Hechingen, Germany), and the temperature reading of each thermistor noted after 30 minutes' stabilisation at 5ºC and 50ºC. Similarly, each stick was placed in a heated water bath and stabilised at a fixed temperature measured with a digital thermometer (Fluke 51, Fluke Corporation Everett, USA). The temperature reading of each thermistor was noted after five minutes' stabilisation.

Results

SURFACE PRESSURE TESTS

Both rebreather temperature sticks warned prior to significant breakthrough (P_iCO_2 = 1 kPa) in four of the five low-exercise tests conducted at surface pressure. The changes in the Inspiration temperature stick display over the course of each test are depicted in Figure 4. The time remaining on the rEvo scrubber monitor at the point of CO_2 breakthrough in each test is shown in Table 1.

In contrast, both rebreathers' temperature sticks failed to warn prior to significant CO_2 breakthrough in the moderate exercise tests conducted at surface pressure (Table 1 for the rEvo and Figure 5 for the Inspiration results, respectively). In testing of the rEvo, a lack of linearity was noted in the remaining scrubber time estimation which was over-estimated early in the test, then declined faster than real time later (Figure 6).

HYPERBARIC TESTS

Both rebreather temperature sticks performed substantially better on the constant moderate-exercise protocol when operated at pressure. There was no discernible difference in performance between 3 and 6 msw. The changes in the Inspiration temperature stick display over the course of eight tests are depicted in Figure 7.

Whereas the Inspiration temperature stick had failed to warn before breakthrough to P_iCO_2 = 1 kPa on any of six continuous moderate-exercise tests at atmospheric pressure, it warned before or soon after breakthrough in all the tests under pressure. However, there was a difference between the two sticks tested. The accuracy of Stick A in precisely predicting and defining breakthrough was remarkable. The P_iCO_2 data are not presented here, but in every test Stick A initially warned just prior to breakthrough to P_iCO_2

Figure 5
Changes in the Inspiration temperature stick display over the course of each moderate exercise test conducted at surface pressure; note the much shorter duration of each test in comparison with the low exercise tests in Figure 4; interpretation of the figure is otherwise as described as for Figure 4; none of the runs reached the alarm condition (1 black segment remaining) prior to P_iCO_2 = 1 kPa

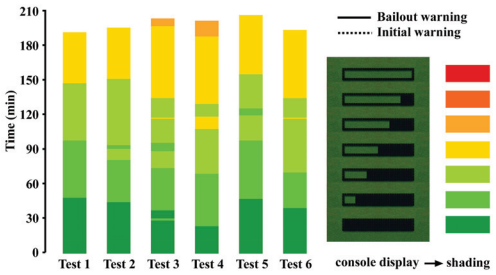

Figure 7
Changes in two Inspiration temperature stick displays (designated A and B) over the course of eight moderate exercise tests conducted at 3 and 6 msw as indicated; interpretation of the figure is otherwise as described for Figure 4

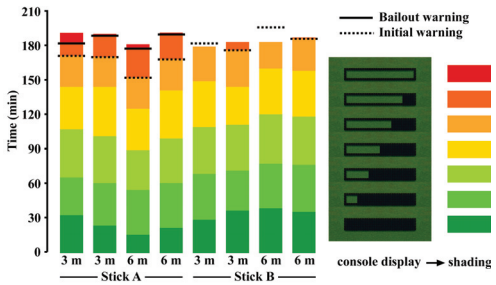

= 0.5 kPa, and then recommended bailout just prior to breakthrough to P_iCO_2 = 1 kPa. In contrast, Stick B gave warnings just prior to breakthrough to P_iCO_2 = 1 kPa in two tests, and 3 min after in one. The warning came 13 min after breakthrough in a fourth test (Figure 7). In contrast to the above results, in the single test performed using the Inspiration rebreather and Stick A in the ANSTI machine at surface pressure (data not shown) we recorded exactly the same failure to provide any warning prior to breakthrough to P_iCO_2 = 1 kPa as seen in the previous moderate-exercise tests at surface pressure.

The time remaining on the rEvo scrubber monitor at the point of CO_2 breakthrough in each test is shown in Table 2. Toward the end of several rEvo tests problems with moisture from the rebreather circuit entering the gas sampling line were experienced, and it was not possible to run every test through to a breakthrough of P_iCO_2 = 1 kPa. We did, however, get

Figure 6
Remaining scrubber time (blue lines) and $PiCO_2$ over the course of the five moderate exercise tests at surface pressure using the rEvo rebreather; time remaining predictions are non-linear

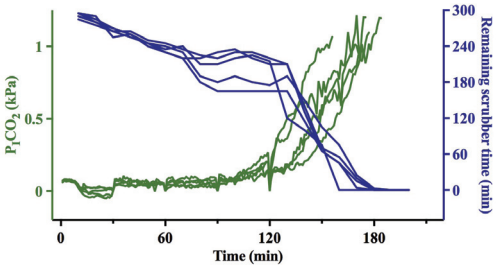

to P_iCO_2 = 0.5 kPa in all tests. We thus report 0.5 kPa as an alternative endpoint. In fact, our primary question was answered in the absence of continuing to a breakthrough of P_iCO_2 = 1 kPa because the remaining scrubber time had declined to zero prior to P_iCO_2 = 0.5 kPa in every test (see Table 2). As with the Inspiration, this result contrasted markedly with the rEvo temperature stick's failure to warn of breakthrough in four of five moderate-exercise tests conducted at surface pressure. We also noted that although there remained a minor tendency for the rEvo to report overly-optimistic remaining scrubber time estimations early in the dive, the decline in estimated time to zero was much more linear in the tests conducted under pressure (Figure 8).

The comparison of the temperature readings obtained from the nine thermistors on each of the two Inspiration temperature sticks (designated A and B respectively) in both the climate chamber and water bath evaluations are shown in Tables 3 and 4.

Discussion

Hypercapnia in diving may arise from either failure by the diver to ventilate adequately or from rebreathing of CO_2, or a combination of both.[8] The potential to rebreathe CO_2 is important in the use of rebreathers which rely on soda lime to remove CO_2 from the expired gas. Soda lime has a finite life and must be replaced in a timely fashion or expired CO_2 will break through the soda lime canister and be rebreathed. Temperature sticks represent an attempt to indirectly confirm CO_2 removal by measuring reactivity in the soda lime canister during a dive. This study evaluated the reliability of these devices in warning the diver prior to significant CO_2 breakthrough as soda lime became exhausted under two test conditions. The first simulated the work rate and respiratory parameters of a notional long decompression dive with moderate exercise early in the dive, followed by less activity during a long decompression when the soda lime would often be nearing the limits of its absorptive capacity. The second protocol involved moderate exercise throughout

Table 2
The remaining scrubber time (RST) (minutes) displayed by the rEvo rebreather at the point of CO_2 breakthrough in the moderate exercise tests conducted at 3 and 6 msw; a negative offset is the time elapsed between zero time remaining on the scrubber monitor and the actual time of breakthrough to P_iCO_2 specified and represents early warning

Depth (msw)	3				6	
Test number	1	2	3		4	5
RST at P_iCO_2 = 0.5 kPa	0	0	0		0	0
Offset (minutes)	-46	-36	-22		-40	-22
RST at P_iCO_2 = 1 kPa	–	0	–		0	–
Offset (minutes)	–	-60	–		-61	–

Table 3
Temperature readings from the nine individual thermistors (designated T0 – T8) on two Inspiration temperature sticks (designated A and B) recorded at 5 and 50ºC in a climate chamber

Thermistor number	T0	T1	T2	T3	T4	T5	T6	T7	T8
Stick A @ 5°C	4.5	6.6	5.0	5.5	5.5	5.0	5.5	6.0	6.0
Stick B @ 5°C	4.5	4.8	4.5	4.5	4.5	4.0	4.5	5.0	5.0
Stick A @ 50°C	49.0	50.9	49.0	49.0	49.0	48.0	48.5	48.5	48.0
Stick B @ 50°C	49.0	49.3	49.0	49.0	49.0	48.5	48.5	48.5	48.5

Table 4
Temperature readings from the nine individual thermistors (designated T0–T8) on two Inspiration temperature sticks (designated A and B) recorded at fixed temperatures in a water bath

Thermistor number	T0	T1	T2	T3	T4	T5	T6	T7	T8
Stick A @ 32.5°C	32.5	34.4	32.5	33.0	33.0	32.5	33.0	33.0	32.5
Stick B @ 33.1°C	31.5	31.9	31.5	31.5	31.5	31.0	31.5	31.5	29.5

the life of the scrubber. It should be made clear that the latter is a less plausible real-world scenario than the former, but it was purposely chosen as a relevant scenario thought likely to provoke failure in temperature stick predictions. Based on these results, the following observations about temperature sticks are offered.

Firstly, there was a substantial improvement in accuracy when tests were conducted at even shallow depths compared to surface pressure. It is notable that, in the process of following up on the results of the surface pressure tests, the manufacturer of the Inspiration rebreather also found less accuracy when conducting an ANSTI machine test on the moderate-exercise protocol at surface pressure (Martin Parker, personal communication, July 2017). It seems clear that even small elevations of ambient pressure are an important requirement for accurate function of temperature sticks. The basis for this effect of depth was not established. An explanation is both beyond the scope of this work and inconsequential to answering the current research question. It could, however, form the basis for further research.

Secondly, based on the reasonably good performance of both rebreathers' temperature sticks during the low-exercise protocol even at surface pressure (appropriate warnings occurred prior to significant breakthrough in four of five tests in both rebreathers) together with the finding of markedly improved accuracy at shallow depths compared to surface pressure, it is predicted that both rebreathers tested will reliably provide warnings prior to significant CO_2 breakthrough in typical long decompression dives where the diver is at rest in shallow, temperate water toward the end of scrubber life. One can feel confident in this prediction for conditions conforming to those of the study tests, but it must be acknowledged that the scrubbers had not been exposed to typical dive depths early in each test and that variations

Figure 8
Remaining scrubber time (blue lines) and P_iCO_2 over the course of the five moderate exercise tests conducted under pressure using the rEvo rebreather; time remaining predictions are more linear than when the rebreather was operated at surface pressure (Figure 6)

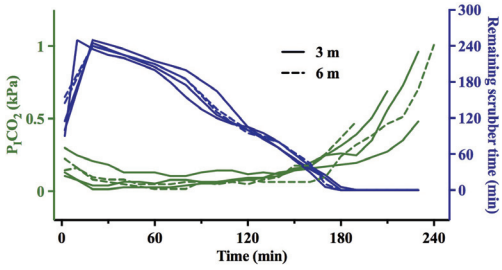

in other conditions such as water temperature could affect temperature stick performance.

Thirdly, both rebreathers performed surprisingly well in the much more provocative continuous moderate-exercise protocol when tests were conducted at depth, though both exhibited different vulnerabilities.

There was a difference in performance between the two Inspiration temperature sticks with one (Stick A) providing precisely timed and accurate warnings before significant breakthrough on all four tests, and the other (Stick B) providing appropriate warnings on two occasions, a marginally late warning on one occasion, and a warning 13 min late on another (Figure 7). The comparison of temperature measurements in the thermistor arrays of the two sticks did reveal some subtle differences in accuracy (Tables 3 and 4) which might explain their different behaviour, but one cannot be certain about this. More detailed investigation, which would include consideration of the dynamic nature of the responses, is beyond the scope of this study.

The rEvo temperature stick provided warnings prior to significant breakthrough on all the moderate exercise tests, but these warnings came an hour before our experimental end-point of 1 kPa of inspired CO_2, and could perhaps be interpreted as too conservative. On the other hand, if the goal is to warn before a lower pressure of inspired CO_2 (such as 0.5 kPa)[6] then the decline in "*remaining scrubber time*" to zero seems substantially less premature (Figure 8) with negative offsets between 22 and 46 min (Table 2). There was also a small degree of non-linearity in the time remaining predictions, with optimistic predictions early in the simulated dive and a subsequent decline that was faster than real time. These observations on both temperature sticks must be interpreted within the context of the experiment in which they were made; that is, a sustained exercise test scenario that was considered likely to provoke failure and which is relatively less plausible in real-world technical decompression diving.

Fourthly, the failure of both temperature sticks during the moderate exercise protocol tests conducted at surface pressure is potentially relevant to surface swimming at the end of a dive while breathing on the rebreather loop. Although the consequences of a hypercapnic event at the surface are likely to be much less serious than one occurring at depth, divers should nevertheless be aware that a temperature stick may not provide accurate data during a vigorous surface swim conducted near the end of scrubber life.

An obvious limitation of this study is the relatively small number of tests with the various temperature sticks in the different conditions, and the limited range of conditions tested. There are other scenarios such as deeper depths, colder and warmer water temperatures, use of different gases, and different patterns of exercise and rest in which temperature stick performance could be evaluated and might be different. This work was challenging and time consuming, and the effect of any variation in conditions requires multiple confirmatory repetitions. Thirty-five tests are reported in this paper; and each test took four to eight hours to complete depending on whether it addressed moderate or lower exercise, respectively.

It is germane to state that temperature sticks do not actually measure CO_2 and are not capable of detecting or predicting CO_2 rebreathing that occurs as a result of exhaled gas bypassing the scrubber bed, or abnormally channelling through it for some reason. Therefore, divers should adopt a holistic approach to appraisal of scrubber performance during diving and not consider temperature stick predictions to be immutably correct, especially in the face of symptoms that might suggest hypercapnia.

Conclusions

These data represent the first publicly reported demonstration that temperature sticks can reliably warn indirectly of CO_2 breakthrough before it occurs during simulation of a common rebreather diving scenario (resting decompression in 19°C temperate water). This was usually also true even during moderate exercise at shallow depths; conditions which, based on our tests at surface pressure, we incorrectly predicted would significantly confound temperature stick accuracy. However, despite this positive result, one cannot draw confident conclusions about temperature stick performance in conditions beyond those tested in this study. The possibility cannot be excluded that factors such as colder or warmer water, greater levels of exercise, greater pressures and different gases may change their accuracy.

References

1 Mitchell SJ, Doolette DJ. Recreational technical diving part 1: an introduction to technical diving methods and activities. Diving Hyperb Med. 2013;43:86–93. PMID: 23813462.
2 Warkander DE. Temperature based estimation of remaining absorptive capacity of a gas absorber. United States Patent No.

US 6,618,687 B2. September 09 2003. [cited 2018 October 12]. Available from: https://patentimages.storage.googleapis.com/fc/63/e6/b5df0bd127bd3c/US6618687.pdf.

3 Warkander DE. Development of a scrubber gauge for closed circuit diving. Undersea Hyperb Med. 2007;24:251. Available from: http://archive.rubicon-foundation.org/5110. [cited 2018 February 14].

4 Harvey D, Pollock NW, Gant N, Hart J, Mesley P, Mitchell SJ. The duration of two carbon dioxide absorbents in a closed-circuit rebreather diving system. Diving Hyperb Med. 2016;46:92–7. PMID: 27334997.

5 Mitchell SJ, Bove AA. Medical screening of recreational divers for cardiovascular disease: Consensus discussion at the Divers Alert Network Fatality Workshop. Undersea Hyperb Med. 2011;38:289–96. PMID: 21877558.

6 Shykoff BE, Warkander DE. Exercise carbon dioxide (CO_2) retention with inhaled CO_2 and breathing resistance. Undersea Hyperb Med. 2012;39:815–28. PMID: 22908838.

7 Life Support Equipment Test Facility. ANSTI Test Systems Ltd. [cited 2018 February 10]. Available from: http://www.ansti.com/.

8 Doolette DJ, Mitchell SJ. Hyperbaric conditions. Compr Physiol. 2011;1:163–201. PMID: 23737169.

Acknowledgements

We thank Eng. Ingmar Franzén and Lt(N) Roine Bystedt at the Swedish Armed Forces Diving and Naval Medicine Centre without whose technical expertise and diligence this work could not have been completed. We sincerely thank Martin Parker, Ambient Pressure Diving, UK for the loan of an Evolution Plus rebreather and several scrubber canisters, and Mr Bruce Partridge of Shearwater Research, Vancouver, Canada for the loan of a personal rEvo rebreather and his technical assistance with the experiments.

Funding

This work was supported by grants from Shearwater Research, Vancouver Canada, and the Eurotek Advanced Diving Conference Research Fund, Birmingham, UK.

Conflicts of interest

Simon Mitchell and Neal Pollock are members of the Editorial Board of *Diving and Hyperbaric Medicine*, but had no input into the peer review or decision-to-publish processes.

Submitted: 22 July 2018; revised 19 October 2018
Accepted: 09 December 2018

Paper II

Received: 24 July 2020 | Revised: 27 October 2020 | Accepted: 15 November 2020

DOI: 10.1002/app.50335

ARTICLE

Applied Polymer SCIENCE WILEY

Permeability properties of a pressure induced compacted polymer liner in gas cylinder

Mårten Silvanius | **Oskar Frånberg**

Department of Mathematics and Natural Sciences, Blekinge Institute of Technology, Karlskrona, Sweden

Correspondence
Mårten Silvanius, Blekinge Institute of Technology, Valhallavägen 1, 371 41 Karlskrona, Sweden.
Email: mzs@bth.se

Abstract

The permeability properties of composite gas cylinders for breathing gas with polymer inner-liner are investigated. The cylinder wall can be described as a composite membrane consisting of two layers. The permeability properties of the cylinder are presented as permeability coefficient and permselectivity. Deviation from the expected gas components might lead to incidents and potentially harmful situations when breathing gas from a compressed gas cylinder. Hence, gas permeability and potential changes in gas composition, must be considered when choosing cylinder materials. Cases of decompression sickness initiated this study. Experimental data show that pressure and oxygen fraction in the gas cylinder drops and that the permeability coefficient varies depending on the inner pressure. Permeability coefficients of 0.62–0.90 Barrer for oxygen and 0.44–0.56 Barrer for nitrogen are measured. Cracks in the inner-liner have caused an accentuated drop in of oxygen fraction and pressure.

KEYWORDS

composites, copolymers, theory and modeling, thermoplastics

1 | INTRODUCTION

Breathing gas cylinders are traditionally made from metal, regardless of what type of breathing apparatus is used. Composite gas cylinders are lighter, which simplifies handling and transport. The absence of corrosion and low maintenance are also considered beneficial. In mine-clearance diving, a low magnetic cylinder is advantageous to avoid sensor detection. For this purpose, a composite gas cylinder with carbon/glass fiber and epoxy resin outer shell and polymer inner-liner has been developed for the semi-closed mine-clearance diving rebreather ISMIX™ (Interspiro AB, Täby Sweden) to withstand cyclic pressures of 300 bars of nitrox (nitrogen/oxygen blend). Similar cylinders are also used within firefighting and traditional open circuit diving. The purpose of the inner-liner is to prevent gas leakage whereas the outer-liner withstands the pressure and is considered porous. The inner-liner is a 3.7–3.8 mm (volume weighted average) bellow made from Arnitel™ EB460 (DSM, Delft The Netherlands) a blend of soft-block polytetramethylene oxide PTMO and hard-block, polybutylene terephthalate PBT. The whole cylinder wall can be described as a composite with a dense top layer and a porous sublayer.[1]

This study aims to parameterize the inner-liner and describe a general model for the diffusion and permeability properties in a diving application. These predictions

can be used to identify an expected storage time for the composite gas cylinders before undesirable oxygen levels are reached. The composition of the gas is vital as it is related to breathing gas, where hypoxia or decompression sickness could be the result if breathing a gas with less than the expected oxygen fraction.

1.1 | The composite gas cylinder properties

The processes of gas diffusion through rubbery polymer materials, such as, the inner-liner, are well known and can be explained using the common solution-diffusion mechanisms while at room temperature.[2] In the late 19th century, the basics where described by Wroblewski.[3] The process was further described in 1920 by Daynes with experiments on hydrogen and other gasses in relationship to problems with leaking air-ship balloons.[4] *Fick's linear diffusion law*, describing that the diffusive flux is proportional to the concentration gradient (i.e. in this application meaning the difference in ambient partial pressure $pp_{i_{amb}}$ and upstream/inner partial pressure pp_i of the gas i), was used during these early experiments and is still applicable.[5] Investigations on gas permeability on composite containers without inner-liner have also been performed using the same basic principles.[6]

Composite gas cylinders are also used in other applications, such as, liquid petrol gas LPG and hydrogen for vehicle propulsion. The fibre reinforced plastic FRP used for LPG is normally designed without an inner-liner, but reveals some important characteristics, such as, higher reliability and safety since they start to leak instead of explode if exposed to fire or impact.[7] As hydrogen is a highly diffusive gas, effort is being put into decreasing the permeability properties but preserving the benefits of polymer liners, such as, low cost, lightweight, and durability.[8]

The composite gas cylinder is considered to be a justifiable way of containing gas under pressure. The disadvantages, which have been observed here and by others, are the poorer ability to hold pressure and fraction of the contained gas mix over time, compared with an equivalent metal cylinder, due to the permeability properties.[9,10] The outer-liner is considered porous and has much greater permeability than the polymer inner-liner. It will not influence the overall rate of depressurization and its permeability properties can therefore be ignored.[11]

The upper bound is a limitation for polymers described by Robeson, which shows how the permeability coefficient decreases as the permselectivity, in favor of oxygen, increases.[12] For many gas separation applications this is desired.[13] However, for gas cylinders that contain breathing gas, especially when storing for longer periods, this separation is highly undesirable. The optimal permselectivity for a gas storage cylinder with two gasses would be 1, as this would mean that the gas flux through the cylinder wall would be similar for both gasses.

The gas discharge, or the flux $J_{i,j}$,of the gasses i and j depend on the material properties of the cylinder wall, that is, permeability coefficient K_i, K_j and permselectivity α_{ij}, but also the design of the gas cylinder, such as, the area A and thickness L of the inner-liner, as well as total cylinder pressure p, ambient pressure p_{amb}, and storage temperature T.

1.2 | Transport mechanism of gas through polymers

There are two main ways for gas molecules to escape from a gas container, such as, the composite gas cylinder. Either there is effusion or permeation.[14] Effusion is described as a passage of gas through a small hole or a leak. The effusion rate is correlated to the molecular mass of the gas according to *Graham's law of diffusion*. For a gas cylinder this could, for example, occur at a bad seal at the valve.

The other main transport mechanism is permeation through the material where the gas molecules sorbs at the surface upstream and diffuses through the material toward the lower partial pressure. Permeation and diffusion are, among many factors, dependent on the gas molecule size and weight, shape, and phase.[15] Findings from other authors also describe that the roughness of the liner surface can reduce the liner surface resistance and affect the permeability properties.[16,17] in this study we have focused on the diffusion of nitrogen $N_2$and oxygenO_2. Water vapor and carbon dioxide are dried and scrubbed in the filling process by the compressor and are therefore not considered here. Out of these two, oxygen has the smallest kinetic diameter, 3.46 Å and nitrogen the largest 3.64 Å. However, the molar mass is greater for oxygen 32 g/mol whereas that of nitrogen is 28 g/mol.

We present here a model to predict the gas flux and oxygen/nitrogen separation in these types of composite gas cylinders, making it possible to predict the gas pressure drop and fraction alteration over time avoiding potential harmful compositions of breathing gas. The results reveal permeability property changes due to compaction of the polymer inner-liner, induced by the increased pressure.

2 | EXPERIMENTAL

By examining the gas cylinders in this study under water we decided whether there were any leaks from effusion

or permeation. Any bubble streaks from valves or sealing would be regarded as an effusion, whereas a bubble formation on the cylinder wall suggests permeation. This study revealed one cylinder with an obvious leakage/effusion, which was excluded, whereas the other cylinders only indicate permeation.

21 composite gas cylinders were stored in a controlled laboratory environment (20 ± 1°C, RH 30–60%) for up to 1257 days. The ambient pressure and fraction of oxygen was approximated to an average of 1013 mbar and 20.9% respectively. The gas cylinders have two different sizes and volumes, with identical inner-liner specifications. Type 1 is a double cylinder with 2 interconnected 5 liter cylinders and type 2 is a single cylinder with a volume of 5 liter. The cylinder surface area was determined by the cylinders volume V, lateral surface area A_l and base area A_b, with measured inner-liner thickness of L_l at the lateral surface and L_b at the base. One of each cylinder type was cut in half to be able to inspect liner thickness and potential anomalies. Type 2a (max 300 bar) showed significant cracks in the liner, however not completely penetrating the inner line and thus avoiding effusion. Type 2b (max 200 bar) showed small cracks in the liner. These cylinders where manufactured from the same specifications, in the same period and under the same conditions; however, the type 2a was allowed an increase in maximum pressure, from 200 to 300 bar after 10 years of duty, which could have caused these cracks to be more significant. The cracks originate from a crease in the bottom of the liner. Figure 1 shows an overall picture of the gas cylinders and the inner-liners, an illustration with denotations and the overall permeation process.

- Type 1: V = 2 × 5 liter glass/carbon fiber composite epoxy outer shell with inner-liner Arnitel™ EB460, L_l =0.37 ± 0.05 cm, L_b =0.5 ± 0.05 cm, A_l =2971 cm^2, A_b =285 cm^2, volume weighted average L_{vw}=0.38 cm;
- Type 2: 5 liter glass/carbon fiber composite epoxy outer shell with Arnitel™ EB460 inner-liner, L_l =0.37 ± 0.05 cm, L_b =0.5 ± 0.05 cm, A_l =1464 cm^2, A_b =147 cm^2, volume weighted average L_{vw}=0.37 cm;

The gas cylinders where in this study filled to pressures of 8 to 270 Barg with oxygen in nitrogen mixes (Nitrox) from 12.2% to 45.6% of oxygen.

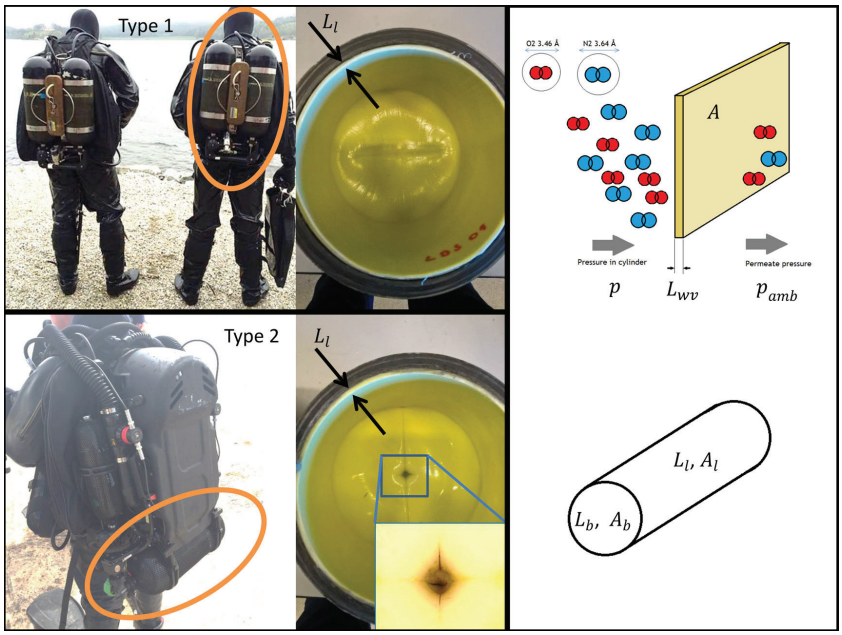

FIGURE 1 Top-left shows the type 1 gas cylinder in use on an open circuit diver, top-middle shows type 1 cylinder cut in half with visible inner-liner yellow and glass-/carbon fibre outer liner green. Bottom-left shows the type 2 gas cylinder in use on a semi-closed rebreather and bottom-middle shows the type 2 cylinder cut in half with visible crease and cracks (enlarged). To the right an illustrative picture shows the used parameters in the permeability calculations [Color figure can be viewed at wileyonlinelibrary.com]

To avoid any doubts regarding the outer-shell porosity a test was performed by sealing a cone without inner-liner and pressurizing it. This setup could not withstand any pressure and the leakage was visible to the eye when submerged and no pressure increase could be obtained. It was thereby determined to be porous.

For pressure measurements a temperature compensated digital manometer (Keller Eco 1 0–300 bar, Winterthur Switzerland) accuracy ±1% of FS was used and for oxygen measurements a galvanic oxygen sensor analyzer (Servomex Analox ATA™, Stokesley U.K.) accuracy ±1% of reading was used. The oxygen analyzer was calibrated in ambient air before each measure and the prescribed compensation chart (correcting for temperature and humidity) was used. Valves, hoses and gages internal volume was measured by pressurizing the complete measuring device and then measuring the total volume of gas that flows out while depressurizing using a flow meter (Hans Rudolph Pneumotach 3813, Shawnee Kansas) accuracy ±3% of reading. The total volume was approximately 0.027 liter, which later was used to compensate the calculations in pressure loss during storage.

During storage, the gas cylinders pressures and oxygen-fractions where measured intermittently not continuously, that is, pressure sensors, hoses, and gages where mounted and dismantled at each measurement. Typical interval for measuring was each week in the beginning of the study whereas at the end we measured every 2 months. The measuring was considered stable and recorded when oxygen-levels reached a steady state during 1 min. Thereafter, the gas cylinders where restored in the storage environment until the next occasion of measurement. The intervals between measurements were successively longer toward the end of the study.

2.1 | Calculating permeability coefficient K and flux J

Permeation or transport of gas i through polymer membranes are described as a combination of solubility or sorption S_i, according to *Henry's law* related to the partial pressure difference, and diffusion D_i described by *Fick's law*, according to equation 1.[14]

$$K_i = D_i \cdot S_i \tag{1}$$

The studied polymer liner is described by using the solution-diffusion model and assumes a uniform pressure drop through the polymer. The solution-diffusion model was further developed and suggested by Lundstrom as the DK_1K_2-model, which is described as a more mathematical correct version of describing the permeability and making it more consistent when using two gasses. Lundstrom however suggests that the *DS*-model, used in this study, is adequate if the thickness scaling parameter B is large. B increases with thicker liner and is assumed to be large in this study, which justifies the use of the *DS*-model. [18]

The flux J_i of the gas i passing through the cylinder inner-liner polymer can be determined from material specifications; however, these are not always specified by manufacturers. No confident permeability properties for oxygen or nitrogen through Arnitel™ EB460 could be found from material data sheets or handbooks.

To determine the area independent permeability coefficient K_i of the gas i, certain parameters need to be known, such as, the partial pressure difference between upstream and downstream of the gas i $\left(pp_i - pp_{i_{amb}}\right)$, the volume weighted liner thickness L_{vw}, the membrane wall area $A = A_l + A_b$ and the flux, see equation 2.[14]

$$K_i = D_i \cdot S_i = \frac{J_i \cdot L_{vw}}{A \cdot \left(pp_i - pp_{i_{amb}}\right)} \tag{2}$$

The permeability coefficient K_i can be expressed in the unit of $\left[10^{-10}\frac{\mathrm{cm^3(STP)\,cm}}{\mathrm{cm^2\,s\,cmHg}}\right]$, which is designated as the unit Barrer. Expressing Barrer in SI-units using mol instead of volume give $\left[3.35 \cdot 10^{-16}\frac{mol \cdot m}{m^2 \cdot s \cdot Pa}\right]$. Calculating with mol instead of volume (STP) we use *the real gas equation* in Equation 3, to describe the correlation.[19]

$$pV = Z(p)nRT \rightarrow n = \frac{pV}{Z(p)RT} \tag{3}$$

where n is mol, $Z(p)$ is the pressure dependent compressibility, R is the gas constant equal to 0.083143 $\frac{L\,bar}{K\,mol}$, and V is the cylinder volume in liter. The measured decrease of mol Δn_i, reveals the molar flux J_i in mol s^{-1}, of that particular gas according to Equation 4.

$$J_i = \frac{\Delta n_i}{\Delta t} = \frac{\left(\frac{pp_i(t_n)}{Z_i(t_n,p)} - \frac{pp_i(t_{n+1})}{Z_i(t_{n+1},p)}\right)}{t_{n+1} - t_n}\left(\frac{V}{RT}\right) \tag{4}$$

2.2 | Permselectivity α

The selectivity of gasses occur by differences in the solubility of gasses and the rate at which those gasses diffuse through the liner.[15]

In this study it is the permeability coefficients K_{O_2} for oxygen and K_{N_2} nitrogen are being described from empirical tests. This simplifies the calculations as the sorption and diffusion are not determined separately, rather the

specific permeability coefficient for each condition. The variability of the specimens includes upstream pressure p, oxygen fraction F_{O_2}, gas cylinder volume V, and liner area A.

The permselectivity α_{ij} is described as the materials ability to select gasses in favor of another. In this case permselectivity is described as the prioritization of oxygen relative to nitrogen in the permeation process.

The calculation to determine permselectivity is done by dividing the permeability coefficient for the two gasses i and j, that is, oxygen and nitrogen according to Equation 5.

$$\alpha_{ij} = \frac{K_i}{K_j} \tag{5}$$

2.3 | Inner-liner properties

The inner-liner thermoplastic co-polyester elastomer from DSM sold under the name Arnitel® EB460, now discontinued and replaced by EB463, is a heat resistive plastic material for multi-purpose usage. Other relevant properties for Arnitel® EB460 applicable to a gas cylinder are high tensile, compressive, and tear strength, good hydrolytic stability and resistance to fungus attacks.[20] The components of Arnitel® EB460 are soft-block polytetramethylene oxide PTMO and hard-block, polybutylene terephthalate PBT.[21] The fraction of each component is not known. The gas cylinders are manufactured between the years 2000 and 2004 and are still in operational use. No aging difference between the cylinders is anticipated, but cannot be excluded.

2.4 | Summary of findings from measurements

We measured changes in the gas composition and pressure in the gas cylinders over time, where a decreasing oxygen fraction, as well as a general pressure drop during the storage period could be observed. The total cylinder gas pressure also changes the permeability properties in an exponential way reaching a plateau where the inner-liner is fully compacted. Further a model is created to predict the pressure and fraction after storage of gas in these types of composite gas cylinders.

3 | RESULTS AND DISCUSSIONS

From a series of experimental data studies, in a laboratory controlled environment of actual operative gas-cylinders, it is shown that oxygen diffuses faster than nitrogen. Various sizes and volumes of cylinders with similar design were used in the study. We present experimental data over a period of minimum 136 to maximum of 1240 days.

The purpose of this long-term study was to determine the permeability properties of composite gas-cylinders used for storage of breathing gas up to 300 bars. The results will be used to calculate the time for which the gas-cylinders can be stored without risk of undesired fractions of gas. The final results will be presented as permeability of oxygen K_{O_2}, permeability of nitrogen K_{N_2}, and permselectivity of oxygen vs. nitrogen $\alpha_{O2/N2}$.

We measured the fraction of oxygen F_{O_2} and pressure p over time. The collected data show an obvious decrease in total pressure as well as a drop in fraction of oxygen. The rate of decrease is depending on the ambient and gas-cylinder pressure and fraction of oxygen, as well as the gas-cylinder properties.

According to Shangguan a rubbery polymer changes its permeability properties while it is compacted due to high pressure, this is expected to occur for Arnitel™ EB460.[22] Further Fujiwara et al examines hydrogen storage tanks with high-density polyethylene inner-liner and highlights that hydrogen permeability deteriorates with the increase of gas pressure.[23] These tests were performed up to 900 bar and reveals similar findings as we have found.

Since permeability properties are different depending on gas, each permeability coefficient must be treated separately. The experimental data for the different types of cylinders are presented in Table 1, which shows a general decrease of pressure and oxygen fraction over time.

3.1 | Data analysis

Our general analysis of the permeability coefficient includes a curve fitting of the data. We considered that a rubbery polymer like Arnitel™ EB460 experiences compacting when exposed to increased pressure and that the porous structure withstands any stretch or strain of the material.[22] Previous studies have recognized the difficulties and complexities in determining the permeability parameters when they go beyond the phenomenological coefficients.[24,25] From literature it is known that the permeability can be sufficiently expressed with the well-known sorption/diffusion approach and behaves exponentially.[14]

Our experimental data shows that there is still diffusion through the material even at high pressures where the material is highly compacted. Hence we anticipate that $p \to 300\, underline \lim K_{O_2} > K_{N_2} > 0$. This gives a choice for a general expression for an exponential curve fit according to Equation 6.

TABLE 1 Experimental data collected during storage of type 1 gas cylinders. Type indicates the type of cylinder examined with its serial number, Avg. p indicates the average cylinder pressure during the storage time, Avg. FO_2 indicates the average cylinder fraction of oxygen over the storage time, Δp indicates the cylinder pressure drop during the storage time and ΔFO_2 indicates the oxygen fraction drop during the storage time. The storage time presents how many days the cylinder was engaged in the experiments

Type 1 cyl. (snr)	**4018**	**4170**	**4793**	**4145**	**4307**	**4370**	**4306**	**4199**	**4234**	**4200**	**4183**	**4382**	**4482**
Avg. p [bar]	6.9	10.0	44.5	48.9	59.9	86.5	94.0	240.7	243.2	252.3	194.7	198.3	204.1
Avg. F_{O2} [%]	30.2	27.2	20.4	20.5	12.1	16.4	12.7	43.7	43.9	19.3	18.4	20.6	20.5
Δp [bar][a]	1.4	1.9	4.7	5.8	3.4	3.7	3.8	9.9	6.4	9.1	17.2	19.0	35.4
ΔF_{O2} [%]	1.2	1.3	0.7	0.8	0.2	0.0	0.3	0.4	0.3	0.4	1.0	0.5	0.6
Storage Time [days]	694	694	872	872	681	681	630	694	694	1080	1080	872	872
Type 2 cyl (snr)		**40459[b]**	**40483[b]**	**40548[b]**		**40840[b]**	**40796[b]**	**40450[c]**			**40617[c]**	**40665[c]**	
Δp [bar][a]		10.6	17.7	10.1		10.6	17.5	31.6			3.9	4.2	
ΔF_{O2} [%]		0.6	1.3	0.5		1.0	1.0	2.6			0.5	1.1	
Avg. p [bar]		200.9	197.1	202.1		198.4	196.1	179.1			73.6	50.2	
Avg. F_{O2} [%]		27.5	27.3	27.6		45.1	45.1	26.4			28.3	36.8	
Storage Time [days]		136	300	136		136	136	1257			184	281	

[a]excluding sample gas pressure loss.
[b]type 2 (max 300 bar).
[c]type 2 (max 200 bar).

$$K_{O_{2_{model}}} \approx a \cdot e^{-b \cdot p} + c \tag{6}$$

where a is a constant determining the intercept in Barrer
b is the constant determining the slope in bar^{-1}.
c is the constant determining the offset and the intercept in Barrer.

Using a least square curve fit method to Equation 6 gives an R-square of 0.96 for K_{O_2} when a = 0.679 Barrer, b = 0.0284 bar^{-1}, and c = 0.110 Barrer. For K_{N_2} R-square is 0.99 when a = 0.486 Barrer, b = 0.0235 bar^{-1}, and c = 0.025 Barrer, see Figure 2 (top-left). The curve fit suggests that there is a large compaction of the inner-liner between 0 and 150 bar. At higher pressures the compaction is reduced and above 200 bar the polymer is near fully plasticized and any increase in pressure will not change the structure or permeability parameters.

The fitted curve for Type 1 has an R-square of 0.96 for oxygen and 0.99 for nitrogen and is transferrable to the real experimental data. However, three data points deviate which could be explained by unrevealed effusion, larger inner-liner thickness variations or cracks. Upon splitting the cylinders and measuring the liner thickness revealed a liner no less than 0.22 cm. The overall weight of the liner should according to drawings be 755 ± 20 g. Using the inner area of the liner and the density of the liner 1.14 g/cm^3 this gives a volume weighted average thickness of the liner = 0.37–0.38 cm, which is used in the calculations.[20] Figure 2 (low-left) shows the permselectivity calculated according to Equation 5.

3.2 | Comparison with other TPE permeability properties

Permeability properties or PTMO fraction in Arnitel™ EB460 are not published. This could otherwise be helpful comparing it with other materials and results. Other TPE polymer properties can be found in literature and data sheets. [21] Most of the published data reveals the permeability properties for very thin sheets <0.1 cm. The permeability properties change with thickness; however, conclusions whether the permeability coefficient increase or decrease are debated, which of course depends on the test set-up, material properties, pressure, temperature, and gas. [26] Results from tests with a thinner PEBAX™ 1074 film indicate permselectivity $\alpha_{O2/N2} \approx 2$, increasing under the influence of higher pressure and permeability coefficients $K_{O2} \approx 4$ barrer and $K_{N2} \approx 2$ barrer decreasing with higher pressure, for a thin membrane in the order of μm.[22] This indicates that a thinner film is also affected by pressure, but not in the same magnitude as our thicker liner.

3.3 | Adjusting for anomalies in Type 2 cylinders

When splitting and examining the type 2 cylinders we found cracks in the inner-liner. These cracks where located near a crease in the bottom of the cylinder on the

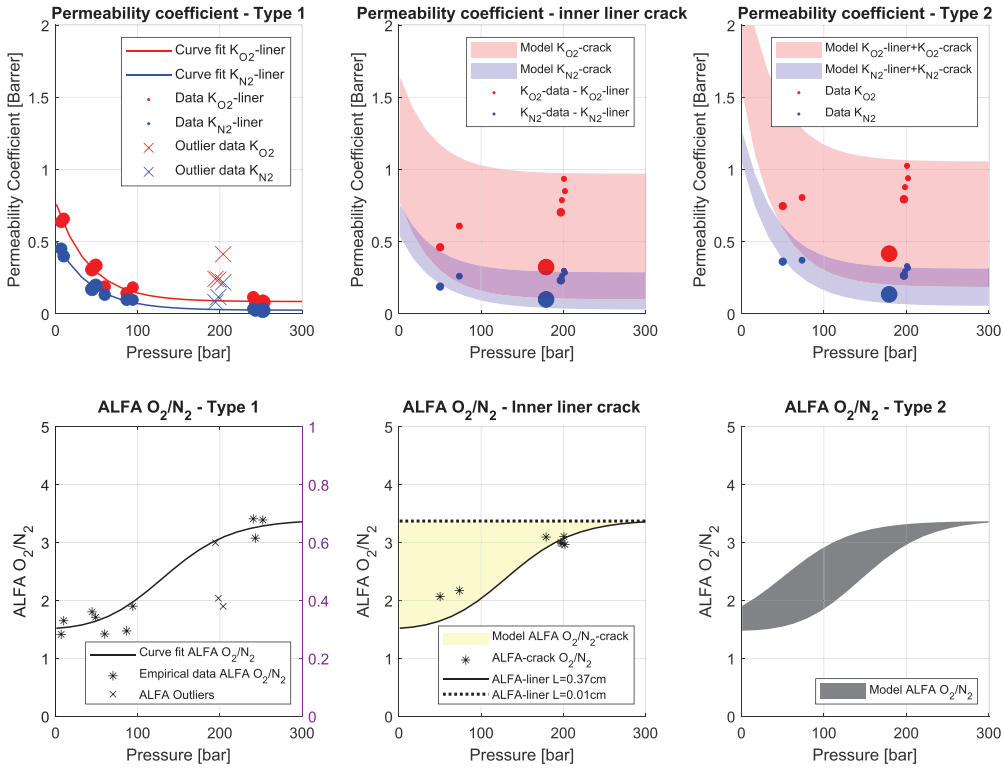

FIGURE 2 Top-left shows the measured permeability coefficient for oxygen and nitrogen related to pressure for type 1 gas cylinder, and low-left shows the calculated permselectivity. Outliers are either determined or suggested to have anomalies in the liner or leaks. Top-mid shows the suggested permeability properties for an inner-liner crack as present in type 2 gas cylinders, low-mid shows the calculated permselectivity for such a crack. Variations are represented by the drawn area. Top-right shows the measured permeability coefficient for type 2 cylinder, where the area represents the suggested permeability properties when combining type 1 and the crack. Low-right shows the suggested permselectivity calculated from the general permeability properties for type 2 [Color figure can be viewed at wileyonlinelibrary.com]

type 2 cylinders. These cracks where not observed in the type 1 cylinders as they lack the crease, hence an observable design difference.

This could explain why the measurements reveal that type 2 cylinder leak faster than type 1. To consider this, when modeling the diffusion, we used the approach of adding a parallel flux with thinner liner to the calculations according to Equation 7.

$$J_{i_{tot}} = J_{i_{liner}} + J_{i_{crack}} \tag{7}$$

The permeability coefficient K_i for the gas i through the cylinder wall is calculated separately in order to determine this. The general expression for calculating the total permeability coefficient K_{tot} of the parallel permeable membranes is as follows.[27]

$$K_{tot} = \frac{\sum_{j=1}^{n} K_j \cdot A_j}{\sum_{j=1} A_j} \tag{8}$$

For this application we then have the following expression for the gas i

$$K_{i_{tot}} = \frac{K_{i_{liner}} \cdot A_{liner} + K_{i_{crack}} \cdot A_{crack}}{A_{liner} + A_{crack}} = \frac{K_{i_{liner}} \cdot A_{liner} + K_{i_{crack}} \cdot A_{crack}}{A_{tot}} \tag{9}$$

With the approach that A_{crack} is $<<$ A_{liner} gives us

$$A_{tot} \approx A_{liner}$$

$$K_{i_{tot}} = K_{i_{liner}} + \frac{K_{i_{crack}} \cdot A_{crack}}{A_{liner}} \rightarrow \quad (10a)$$

$$K_{i_{tot}} - K_{i_{liner}} = \frac{K_{i_{crack}} \cdot A_{crack}}{A_{liner}} \quad (10b)$$

The general expression in 10b cannot be solved as $K_{i_{crack}}$ and A_{crack} is unknown; however, from experimental data $K_{i_{tot}}$, represented as $K_{i_{data}}$, and $K_{i_{liner}}$ is known. Letting $\frac{K_{i_{crack}} \cdot A_{crack}}{A_{liner}}$ be a variable called k_{icrack}, representing the permeability coefficient for the crack including A_{crack} proportional to A_{liner}, still in the unit *barrer* according to a dimensional analysis we get the expression.

$$k_{icrack} = K_{i_{data}} - K_{i_{liner}} \quad (11)$$

The permeability coefficient for the crack is depending on cylinder pressure, liner thickness at the crack, crack area, and flux in correlation to Equation 2, $k_{icrack}(p, A_{liner}, L_{liner}, J_{i_{liner}})$ represents any combination of these parameters that correlate with $K_{i_{tot}} - K_{i_{liner}}$. From type 1 cylinder data we learned the pressure dependency on the permeability properties of the liner and thus we let the variable k_{icrack} to vary exponential with p as seen in Figure 2 top-left, but with an offset to match the experimental data, $K_{i_{data}}$. The suggested permeability coefficient contribution from the cracks are shown in Figure 2 top-mid and presented as $K_{O2_{data}} - K_{O2_{liner}}$ and $K_{N2_{data}} - K_{N2_{liner}}$. The red and blue area in the same picture represents plausible variations of crack areas and liner thickness.

As we have so few parameters known for the crack and its properties we must consider that the permeability coefficients for oxygen and nitrogen can vary with thickness. This will be presented as a variation in permselectivity shown in Figure 2 low-mid. For a thick crack it will behave similar to the normal liner and the lower bound is therefore same as for the thick liner. The upper bound represents a thin liner and is constant with pressure and represented by the highest possible permselectivity registered for the material, shown at high pressures in Figure 2 bottom-left. This is shown by Shangguan 2011 to be valid for thin liners of other polymers, like PEBAX™.[22] The result is a variable permselectivity depending on crack thickness and cylinder pressure. A variation in permselectivity also verifies that

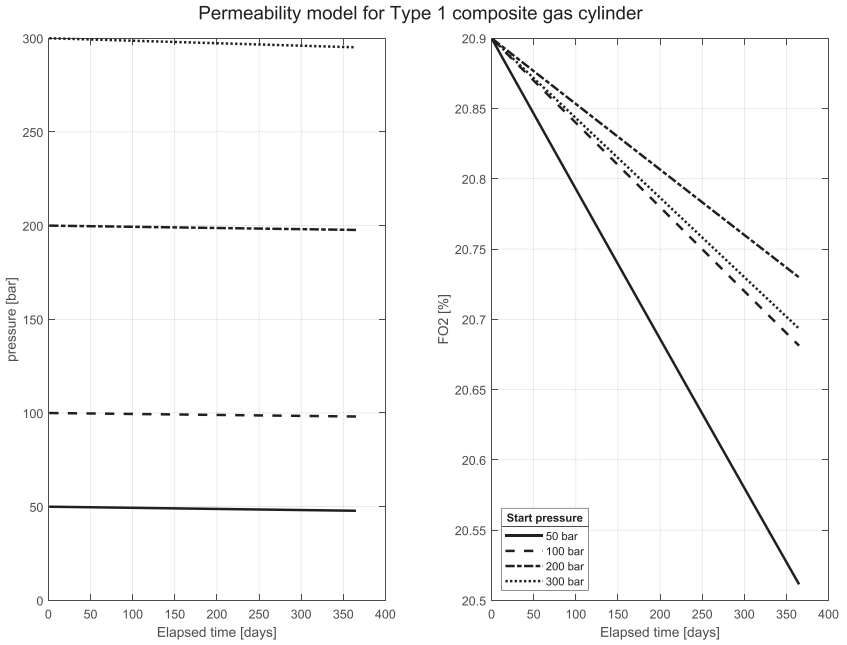

FIGURE 3 The pressure loss and oxygen fraction drop for type 1 gas cylinders presented for four start pressures, gas mix is air, over a period of 1 year. The pressure drop is hardly noticeable and this reveals that the process is very slow for type 1 cylinders

the crack cannot have a linear behavior related to increased pressure, similar to the general liner behavior.

The total permeability coefficient for the type 2 cylinder with cracks are shown in Figure 2 top-right, where the crack and general liner permeability properties from Figure 2 top-left and mid-left are added according to Equation 8. The results for parameters used to describe the highest permeability coefficient for type 2 are for oxygen described with parameters a = 1.382 Barrer, b = 0.0247 bar^{-1}, c = 1.055 Barrer, and for nitrogen a = 0.970 Barrer, b = 0.0239 bar^{-1}, c = 0.313 Barrer utilized in Equation 6. The lowest permeability coefficient for oxygen are described with parameters a = 1.382 Barrer, b = 0.0247 bar^{-1}, c = 0.185 Barrer, and for nitrogen a = 0.995 Barrer, b = 0.0223 bar^{-1}, c = 0.0546 Barrer utilized in Equation 6.

3.4 | Creating a general model

One of the purposes of this study was to determine the allowable storage time for this type of gas cylinder. The general model is produced with approximations and assumptions and must be used with caution. For type 1, the general expression for pressure and fraction loss are described according to Equation 6 with parameters already determined. For type 2, we choose to use the parameters for the highest permeability as these describe the worst case. A numerical approach of gas loss is used to calculate storage time, where it is calculated with time increments of 1 day. Figure 3–5 shows the actual gas loss for some gasses and pressures normally used with these gas cylinders over a period of 1 year. The purpose of these figures is to get an overview of the oxygen fraction and pressure decline over time for the end user.

The suggested model for predicting oxygen fraction during storage shows that a

- 10 liter composite gas cylinder of type 1 can store air for more than one year,
- 5 liter composite gas cylinder of type 2 with worst observed cracks in inner-liner can store
  - 28% Nitrox for approximately 60 days at start pressure 50 bar and 80 days at start pressure 300 bar,

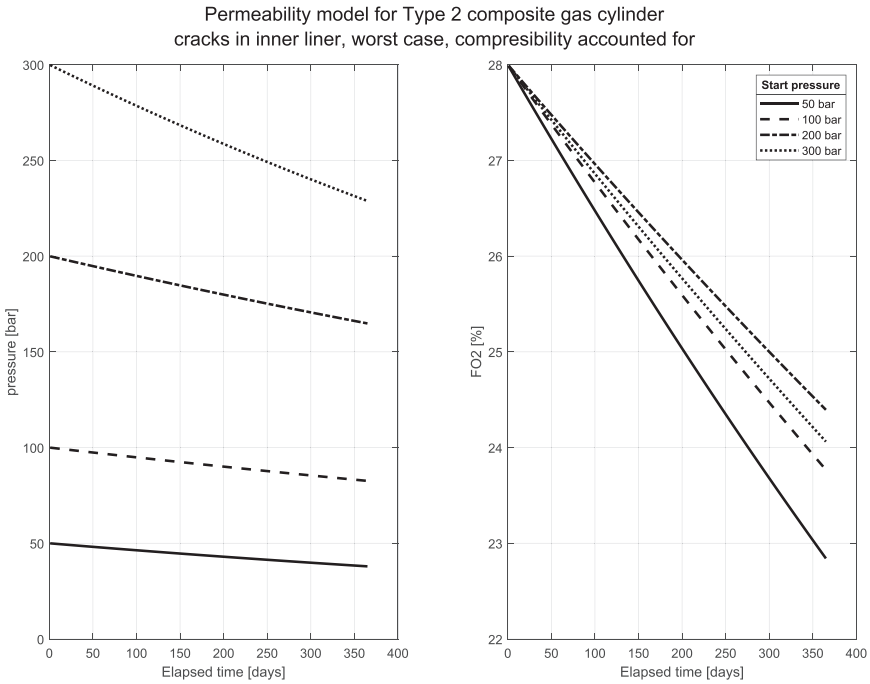

FIGURE 4 The worst case pressure loss and oxygen fraction drop for type 2 gas cylinders presented for four start pressures, gas mix is 28% Nitrox, over a period of 1 year

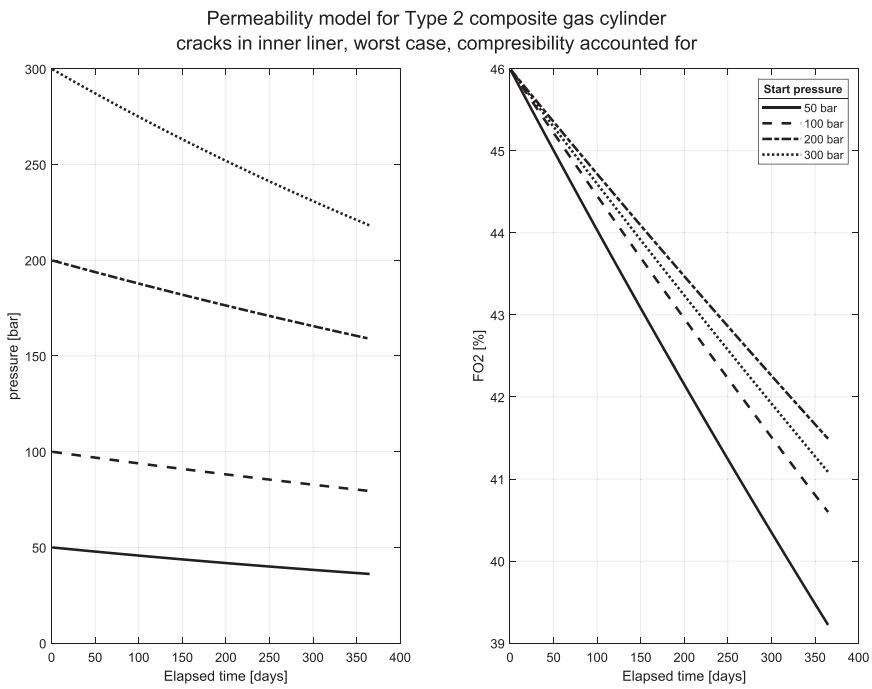

FIGURE 5 The worst case pressure loss and oxygen fraction drop for type 2 gas cylinders presented for four start pressures, gas mix is 46% Nitrox, over a period of 1 year

- 46% Nitrox for approximately 50 days at start pressure 50 bar and 70 days at start pressure 300 bar,

based on a maximum allowed drop in oxygen fraction of 1%-unit in storage temperature of 20°C.

In this study, the complexities have consisted of undesired effusion and anomalies in the inner-liner such as cracks. The permeability behavior of the rubbery polymer Arnitel™ EB460 indicates that the liner thickness also adds a complexity as it changes with thickness and pressure and the compaction of the material makes the torturous path for the molecules of oxygen and nitrogen more difficult.[28] This is indicated by the permselectivity increasing with pressure. This means that the permeability properties for Arnitel™ EB460 vary through-out the whole spectrum of pressure and thicknesses. Interaction between molecules and a potential change in permeability properties due to high or low FO_2 Nitrox where not seen. The fraction of oxygen; however, affects the differential pressure between upstream and downstream as this is related to the partial pressures.

A liner made from rubbery polymer quickly becomes less permeable as the pressure increases due to compaction.[28,29] The flexibility of the rubbery material could be affected negatively by age and temperature fluctuations from adiabatic compression during pressurization. Possible reasons for the upcoming of cracks or increased sizes of cracks are the increased maximum allowed pressure implemented at a modification of the diving system. Another theory could be that a rapid decrease of pressure could cause gas entrapment in the inner-liner and crack it when discharging this stored gas into the less pressurized cylinder. A sudden pressure drop can occur if using the discouraged method of opening the cylinder valve and let it free flow into ambient pressure. These thoughts are derived from findings of blisters in EPDM O-ring being depressurized from 100 bar.[30]

4 | CONCLUSIONS

The permeability properties of composite gas cylinders with a two-layered cylinder wall containing nitrox up to 300 bar were examined. The pressure and oxygen fraction of two types of composite gas cylinders were measured over a period of up to 3 years. By determining the

thickness of the inner-liner, made from Arnitel™ EB460, we were able to define the inner-liner permeability coefficient and selectivity for oxygen and nitrogen for that specific thickness L=0.37–0.38 cm. The carbon−/glass fibre resin outer shell were from experiments determined to be porous and unable to detain any gas pressure. From the measurements in the study we were also able to suggest a general model for oxygen diffusion for each type of gas cylinder and correlate it with the collected experimental data.

The permeability coefficient for the rubbery polymer Arnitel™ EB460 is varying with gas cylinder pressure, where an increase in pressure decreases the permeability coefficients, further affecting the permselectivity.

Curve fitting of experimental data from this study reveals a permeability coefficient for 0.37–0.38 cm Arnitel™ EB460 of 0.62–0.90 Barrer for oxygen and 0.44–0.56 barrer for nitrogen (95% confidence interval) at 1 barg. The compaction due to increased cylinder pressure causes an exponential decrease of the permeability coefficient and reaches a plateau at 250–300 bar where the permeability coefficients are 0.04–0.13 Barrer for oxygen and 0.01–0.05 Barrer for nitrogen (95% confidence interval). Permselectivity of oxygen/nitrogen increases from 1.5 at low pressures to 3.3 at maximum cylinder pressure. These results are directly applicable on type 1 cylinders, which do not have cracks in the inner-liner. Type 2 cylinders, which have cracks in the inner-liner, reveal a dominant flux from the cracks. The measured permeability is a combination of the full liner with 0.37 cm thickness and the cracks.

ACKNOWLEDGMENTS

We thank Eng. Ingmar Franzén, Lt(N) Roine Bystedt and Eng. Patrik Brånhede at the Swedish Armed Forces Diving and Naval Medicine Centre whose assistance during measurements and examinations where significant and vital for the success of this study.

ORCID

Mårten Silvanius https://orcid.org/0000-0002-4629-6324
Oskar Frånberg https://orcid.org/0000-0001-7051-3256

REFERENCES

[1] M. Mulder, *Basic Principles of Membrane Technology*, 2nd ed., Kluwer Academic Publishers, Dordrecht, The Netherlands **1996**, p. 81.
[2] R. W. Baker, in *Advanced Membrane Technology and Applications* (Eds: N. N. Li, A. G. Fane, W. S. Ho, T. Matsuura), John Wiley & Sons, Inc, Hoboken, NJ **2008**; Chapter 21, p. 559.
[3] S. Wroblewski, *Annalen der Physik* **1879**, *244*, 29.
[4] H. A. Daynes, *Proc. R. Soc.* **1920**, *97*, 286.
[5] A. Fick, *Annalen der Physik* **1855**, *170*, 59.
[6] V. Defauchy, H. Le Corre, X. Colin, *J. Compos. Sci.* **2018**, *2*, 21.
[7] A. Tripathi, A. Kumar, M. K. Chandrakar, *Int. J. Sci. Res. Dev.* **2017**, *5*, 871.
[8] Y. Sun, H. Lv, W. Zhou, C. Zhang, *Int. J. Hydrogen Energy* **2020**, *45*(46), 24980.
[9] L. M. Robeson, Q. Liu, B. D. Freeman, D. R. Paul, *J. Membr. Sci.* **2015**, *476*, 421.
[10] S. Armstrong, B. Freeman, A. Hiltner, E. Baer, *Polymer* **2012**, *53*, 1383.
[11] S.-B. Shim, J. C. Seferis, *J. Appl. Polym. Sci.* **1998**, *65*, 5.
[12] L. M. Robeson, *J. Membr. Sci.* **2008**, *320*, 390.
[13] A. Brunetti, F. Scura, G. Barbier, E. Drioli, *J. Membr. Sci.* **2010**, *359*, 115.
[14] L. W. McKeen, W. Andrew, *Permeability Properties of Plastics and Elastomers*, 4th ed., Elsevier, Oxford, UK **2017**; Chapter 1, p. 2.
[15] M. Hanna, T. Sabu, in *Transport Properties of Polymeric Membranes* (Eds: T. Sabu, R. Wilson, K. S. Anil, G. C. Soney), Elsevier, Amsterdam, The Netherlands **2017**; Chapter 2, p. 18.
[16] G. Firpo, E. Angeli, P. Guida, R. L. Savio, L. Repetto, U. Valbusa, *Sci. Rep.* **2018**, *8*, 6345.
[17] G. Firpo, E. Angeli, P. Guida, D. Pezzuoli, D. Repetto, L. Repetto, U. Valbusa, *Polymer* **2019**, *11*, 910.
[18] J. Lundstrom, *J. Memb. Sci.* **2015**, *486*, 138.
[19] E. J. Hoffman, *Membrane Separations Technology*, Elsevier, Burlington **2003**; Chapter 2, p. 52.
[20] DSM Datasheet Arnitel EB460. (accessed May 22, 2020)
[21] L. W. McKeen, W. Andrew, *Permeability Properties of Plastics and Elastomers*, 4th ed., Elsevier, UK **2017**; Chapter 10.3, p. 216.
[22] Shangguan Y. Intrinsic Properties of Poly(Ether-B-Amide) (Pebax®1074) for Gas Permeation and Pervaporation. Master Thesis, University of Waterloo, Waterloo, Ontario, Canada, 2011
[23] H. Fujiwara, H. Ono, K. Onouea, S. Nishimura, *Int. J. Hydrogen Energy* **2020**, *45*, 29082.
[24] C. E. Rogers, J. R. Semancik, S. Kapur, *Polym. Sci. Technol.* **1973**, *1*, 297.
[25] H. Yasuda, *J. Polym. Sci.* **1967**, *5*, 2952.
[26] Permeability Properties of Plastics and Elastomers. in *A Guide to Packaging and Barrier Materials*, 2nd ed., Cambridge University Press, Massey L.K. **2003**, p. 436.
[27] A. Tarek, *Reservoir Engineering Handbook*, 2nd ed., Butterworth-Heinemann, Woburn MA **2001**; Chapter 4, p. 238.
[28] K. W. Lawson, M. S. Hall, D. R. Lloyd, *J. Membr. Sci.* **1994**, *101*, 99.
[29] V. E. Reinsch, A. R. Greenberg, S. S. Kelley, R. Peterson, L. J. Bond, *J. Membr. Sci.* **2000**, *171*, 217.
[30] A. Koga, T. Yamabe, H. Sato, K. Uchida, J. Nakayama, J. Yamabe, S. Nishimura, *Tribol. Online* **2013**, *8*, 68.

How to cite this article: Silvanius M, Frånberg O. Permeability properties of a pressure induced compacted polymer liner in gas cylinder. *J Appl Polym Sci*. 2020;e50335. https://doi.org/10.1002/app.50335

Paper III

UNDERSEA & HYPERBARIC MEDICINE

Proposed Thalmann algorithm air diving decompression table for the Swedish Armed Forces

Mårten Silvanius, MSc [1,2]; Hans Rullgård, PhD [1]; Magnus Ekström, MD, PhD [3]; Oskar Frånberg, PhD [1,3]

[1] Department of Mathematics and Natural Sciences, Blekinge Institute of Technology, Karlskrona Sweden
[2] Swedish Armed Forces Diving and Naval Medicine Centre, Karlskrona Sweden
[3] Department of Respiratory Medicine and Allergology, Institution for Clinical Sciences, Lund University, Lund, Sweden

CORRESPONDING AUTHOR: Mårten Silvanius – *mzs@bth.se*

ABSTRACT

Silvanius M, Rullgård H, Ekström M, Frånberg O. Proposed Thalmann algorithm air diving decompression table for the Swedish Armed Forces. Undersea Hyperb Med. 2023 Second Quarter; 50(2):67-83.

The Swedish Armed Forces (SwAF) air dive tables are under revision. Currently, the air dive table from the U.S. Navy (USN) Diving Manual (DM) Rev. 6 is used with an msw-to-fsw conversion. Since 2017, the USN has been diving according to USN DM rev. 7, which incorporates updated air dive tables derived from the Thalmann Exponential Linear Decompression Algorithm (EL-DCM) with VVAL79 parameters. The SwAF decided to replicate and analyze the USN table development methodology before revising their current tables. The ambition was to potentially find a table that correlates with the desired risk of decompression sickness.

New compartmental parameters for the EL-DCM algorithm, called SWEN21B, were developed by applying maximum likelihood methods on 2,953 scientifically controlled direct ascent air dives with known outcomes of decompression sickness (DCS). The targeted probability of DCS for direct ascent air dives was ≤1% overall and ≤1‰ for neurological DCS (CNS-DCS).

One hundred fifty-four wet validation dives were performed with air between 18 to 57 msw. Both direct ascent and decompression stop dives were conducted, resulting in incidences of two joint pain DCS (18 msw/59 minutes), one leg numbness CNS-DCS (51 msw/10 minutes with deco-stop), and nine marginal DCS cases, such as rashes and itching.

A total of three DCS incidences, including one CNS-DCS, yield a predicted risk level (95% confidence interval) of 0.4-5.6% for DCS and 0.0-3.6% for CNS-DCS. Two out of three divers with DCS had patent foramen ovale. The SWEN21 table is recommended for the SwAF for air diving as it, after results from validation dives, suggests being within the desired risk levels for DCS and CNS-DCS. ∎

KEYWORDS: decompression sickness; decompression tables; deterministic modeling; diving research; military diving; probabilistic modeling

INTRODUCTION

Diving with air as breathing gas comprises decompression strategies, as the nitrogen that resides in the body can cause decompression sickness (DCS) during decompression [1]. The Swedish Armed Forces (SwAF) has traditionally adopted the U.S. Navy (USN) dive tables [2-4]. As of 2017, the USN discontinued the air decompression table that the SwAF still uses [5]. SwAF needs to determine whether to stay with the old, adopt the new, or choose another solution. The SwAF requires air

decompression tables that comprise flexibility, interoperability, operational demands, and acceptable risk of DCS.

This study aims to use existing probabilistic methods and deterministic models and combine them to produce dive tables with ≤1% iso-risk of DCS and ≤1‰ for neurological decompression sickness (CNS-DCS) within the limits of direct ascent, meaning dives with no required decompression stops. The novelties in the study are: first, a new probabilistic model estimating the risk for DCS and CNS-DCS after a direct ascent air dive; and second, an algorithm assigning maximum permissible tissue tension (MPTT) parameters based on the probabilistic model. Compared to most other published probabilistic models [6-8], our model has a limited scope, as it applies only to direct ascent dives. However, these other models were found to be unsuitable to our needs since limiting the DCS risk to 1% gives unacceptably short bottom times, presumably because these models overestimate the risk of anticipated safe direct-ascent dives.

We will compare our probabilistic model to three previously published models: LEM from [7], StandAir from [8], and the logistic model from Table 6 in Southerland [9]. These three models were chosen because the publications describe the models in detail, and also present data, allowing our replication of the models to be validated. LEM represents a class of models studied in other publications [10,11], while StandAir and Southerland are of a fundamentally different type.

We choose to implement and replicate the decompression algorithm EL-DCM, the Thalmann (Exponential Linear Decompression Model) for table calculations. Once a new set of MPTT parameters, called SWEN21B, are provided, these control the replicated algorithm to produce all desired profiles for a new set of air dive tables, including decompression stops and decompression using oxygen. After successful validation dives in a controlled wet chamber environment, tables are suggested to the SwAF. This study was approved by the Swedish Ethical Review Authority (Dnr: 2020-06865). Individual, informed, written consent was obtained from all participants. Vascular bubble data from the validation dives, presented herein, are to be published by C. Hjelte, MD, and O. Plogmark, MD. The validation dive data set is called ValTKLHN2021.

METHODS

Our method consists of the following steps:

1) assembling a database of results from previous dive trials;
2) fitting the parameters of probabilistic models for the risk of DCS and CNS-DCS after direct ascent dives;
3) using the probabilistic models and maximum prescribed risks to determine the MPTT parameters of the replicated EL-DCM algorithm;
4) using the EL-DCM algorithm to compute dive tables; and
5) performing validation dives for a selection of dive profiles from the tables.

Data set

We assembled a database called DB-SWEN21v1 comprising data from 2,953 well-documented direct ascent air dives from various sources. The data for each dive included dive depth, dive bottom time, whether DCS occurred, and whether any DCS was categorized as CNS-DCS. Categorization of the type of DCS was taken strictly from the source unless otherwise stated. Marginal DCS cases were categorized as no-DCS. We use the conversion convention *1 fsw = 0.30643 msw = 0.030643 bar,* and all pressures are given in gauge (g) terms.

More than half of the database – 1,629 dives – was obtained directly from [12], which based most of its data from [13]. Another 374 dives in our database are taken from [13], specifically from the data sets EDU557, ASATARE, ASATNSM, ASATNMR, NMR9209, EDUAS45, ASATDC, ASATFR85, EDU849S2, which are not included in [12]. For these dives, we assessed the DCS type by analyzing the symptoms described in the source, where joint pain was categorized as DCS, and any neurological impact was categorized as CNS-DCS. The remaining

950 dives in DB-SWEN21v1 are taken from various other sources, summarized in Table 3, printed later herein.

Logistic probabilistic models were fit to this dataset to generate a new air diving decompression table as described below. After validation diving on this new table had commenced, errors were discovered in the DB-SWEN21v1 dataset which were remedied to produce a corrected dataset, DB-SWEN21v2, where 12 dives were excluded. The logistic probabilistic models were refit to this corrected dataset and found to provide risk estimates that did not differ sufficiently from those obtained with the models fit to DB-SWEN21v1 to warrant replacement of the first version of the dive table, which we consequently retained. Datasets, models and other names labeled v1 are used for the SWEN21 table. Those labeled v2 are presented only for comparison.

Probabilistic modeling

The probabilistic model we use is a logistic model, similar to the models studied in [9]. Doolette 2009 also uses a similar model for CNS-DCS risk after a direct ascent dive. (12) These models express the risk for DCS or CNS-DCS as a logistic equation in terms of dive depth D and bottom time T,

$$P_{CNS\text{-}DCS} = \frac{1}{(1+\exp(-L))} \qquad 1.$$

where

$$L = \beta_0 + \beta_1 \bullet ln(D) + \beta_2 \bullet ln(T) + \beta_3 \bullet ln(T)^2$$

Our choice of model uses a slightly modified expression to increase flexibility/accuracy over a broader range of depth/time combinations,

$$L = \beta_0 + \beta_1 \bullet ln(D) + F(ln(T)) \qquad 2.$$

where $F(x)$ is a piecewise quadratic polynomial function. More precisely, we chose a number of node points $T_1 < T_2 < \ldots < T_n$ and let $F(x)$ satisfy the conditions:

1. $F(x)$ is a quadratic polynomial in x on each of the intervals $\ln(T_k) < x < \ln(T_{k+1})$.
2. $F(x)$ is continuous and has a continuous derivative at each $x = \ln(T_k)$.
3. $F(x) = 0$ for $x > \ln(T_n)$. This reflects that after some time at a constant depth, tissues will be saturated so longer exposure does not increase DCS risk further.
4. $F(x)$ is linear for $x < \ln(T_1)$.

Any $F(x)$ satisfying these conditions can be written as a linear combination,

$$F(ln(T)) = \sum_{(k=1)}^{(n-1)} \beta_{T,k} \bullet F_k(ln(T)) \qquad 3.$$

Where

$$F_k(\ln(T)) = 0 \qquad \text{if } T_{k+1} \le T$$

$$F_k(\ln(T)) = \frac{(\ln_{(Tk+1)} - \ln(T))^2}{2(\ln_{(Tk+1)} - ln(T_k))} \qquad \text{if } T_k \le T \le T_{k+1}$$

$$F_k(\ln(T)) = \frac{\ln_{(Tk)} + \ln_{(Tk+1)}}{2} - \ln(T) \qquad \text{if } T \le T_k$$

Deterministic modeling

An implementation of the EL-DCM Thalmann algorithm in Matlab replicated the published profiles in USN Diving manual rev. 7 for verification. Once our script was verified, we could safely implement any desired parameters, expecting that the calculations would be according to the intended method.

The mathematics are described thoroughly by other authors but originates from theories of Boycott/Haldane and the approach of Workman, simplified by Braithwaite and later computerized by Thalmann with linear/exponential washout to determine decompression strategies for oxygen partial pressure controlled diving apparatuses with the use of dive computers [14-16]. We replicated the description of these calculations from [15].

The EL-DCM is based on a computation of the inert gas tissue load P_{T_j} in a number of different tissues indexed by a variable j. Each P_{T_j} is a function of time during the dive which is given as the solution of a differential equation in,

$$\frac{dP_{T_j}}{dt} = \frac{(P_{T_{aj}} - K_{exp/in}) \bullet SDR \bullet log\,(2)}{T_{1/2}} \qquad 4.$$

where

P_{T_j}	tissue/compartment inert gas load
$P_{T_{aj}}$	arterial inert gas load (related to ambient pressure)
SDR	Saturation desaturation ratio (SDR) is a parameter to control the inert gas transportation in tissues normally set to 1,

indicating that there is no difference between saturation or desaturation in compartments. In USN Tables Rev. 6, Rev. 7 and our implementation set to 0.7 if inspired oxygen fraction $F_{iO_2} > 0.8$. The convention of SDR is further explained in [17].

$T_{1/2}$ half-time of compartment j

$K_{exp/lin}$ depends on whether exponential or linear kinetics are applied. If $P_{iTj} > P_{amb} + P_{XO} - P_{fvg}$ then linear kinetics are applied and $K_{exp/lin} = P_{amb} + P_{XO} - P_{fvg}$, else exponential kinetics are applied and $K_{exp/lin} = P_{Tj}$

P_{amb} is the ambient pressure

P_{XO} is the crossover tissue tension where the gas kinetics switches from linear to exponential, set to 10 fsw according to [17].

P_{fvg} is the fixed venous gas pressure set to 4.3 fsw according to [17] by combining venous pressures of carbon dioxide, oxygen and water vapor.

Ascent can proceed if the inert gas in all tissue compartments is less than the maximum permissible tissue tension (*MPTT*): $P_{Tj} \leq MPTT_j$. The *MPTT* is computed as $MPTT_j = M_{0j} + \Delta M \bullet D$ where D is the current depth. Here M_0 is the surface *MPTT*. The EL-DCM Thalmann algorithm sets $\Delta M = 1$ in all tissues.

Descent and ascent rates of 23 msw/minute and 9 msw/minute, respectively, were assumed. Other Thalmann Algorithm pressure and gas tension parameters originally given in units of fsw according to (17) were converted appropriately into the units used in our Thalmann Algorithm implementation.

Transferring from risk to maximum permissible tissue tension

Once we have obtained models estimating the probability of DCS, P_{DCS} and the probability of CNS-DCS, $P_{CNS\text{-}DCS}$ after a direct ascent dive, we use these models to determine *MPTT* parameters for the EL-DCM algorithm with the goal of keeping P_{DCS} and $P_{CNS\text{-}DCS}$ within specified limits. The algorithm used consists of the following steps:

1. Select a list of dive depths of interest, D_1, $D_2 \ldots D_n$. For each depth D_i, determine the maximum bottom time T_i such that $P_{DCS}(D_i,T_i) \leq 1\%$ and $P_{CNS\text{-}DCS}(D_i,T_i) \leq 1‰$. At this stage we do not require T_i to be an integer number of minutes. On the contrary, each T_i is rounded up to the closest minute and then decreased by a few seconds. In the end, when generating a dive table using the EL-DCM algorithm, the bottom times will be rounded back down to the closest minute, ensuring that the estimated risks are within the prescribed limits.

2. For each tissue j and each depth-time pair (D_i,T_i) determine the inert gas load $P_{Tj}(D_i,T_i)$ when surfacing after a dive to depth D_i with bottom time T_i. Note that, although our probabilistic model does not consider the descent and ascent rates, the tissue loads in the EL-DCM algorithm do depend on the descent and ascent rates. For this step we therefore need to assume those rates. For our calculations, we used a descent rate of 23 msw/minute and an ascent rate of 10.5 msw/minute, which is close to the average in the calibration data used for the probabilistic models.

Note that the calculated risks for a table subsequently generated by the EL-DCM algorithm are guaranteed to be strictly within the prescribed limits only if the same descent and ascent rates are used in the EL-DCM algorithm. In practice, the calculated risks will be close to the limits even if other descent and ascent rates are used. This explains why some of the risks computed in Table 2B exceed desired limit of $P_{CNS\text{-}DCS} = 0.1\%$, as the table is computed with ascent speed 9msw/minute compared to the statistical analysis, calculated with 10.5 msw/minute.

3. The final step is to choose the surface *MPTT*, M_0, such that for each (D_i,T_i) there is at least one tissue j with $M_{0j} \leq P_{Tj}(D_i,T_i)$ this tissue will then enforce that a direct ascent dive to depth D_i does not exceed time T_i. This problem admits multiple different solutions (including solutions with obviously undesirable properties – for example, assigning an excessively low value to a single M_0). We arrive at a solution which is, in a certain sense, optimal by the following method.

Assign a preliminary value to each parameter:

$$M_{0j} = \max_i P_{Tj}(D_i, T_i) \quad 5.$$

The preliminary parameters will typically allow slightly too long bottom times at certain depths and must therefore be adjusted downward. This is done by repeating steps b and c.

b. For each (D_i, T_i) compute the quantity

$$A_i = \min_j \frac{M_{0j} - P_{Tj}(D_i, T_i)}{M_{0j} - P_{surf}} \quad 6.$$

where P_{surf} denotes the ambient pressure at the surface. If $A_i \leq 0$ for all i, we are done. Otherwise, continue with step c.

c. Choose the index i_{max} with the maximum value of A_i and the index j_{min} for which the minimum in the definition of $A_{i_{max}}$ is achieved. Then change the value of $M_{0j_{min}}$ according to

$$M_{0j_{min}} = P_{Tj_{min}}(D_{i_{max}}, T_{i_{max}}) \quad 7.$$

Note that since $A_{i_{max}} > 0$, the value of $M_{0j_{min}}$ will be decreased.

Repeat steps b and c until $A_i \leq 0$ for all i.

Validation dives

The validation dives were performed in a pressure chamber at the SwAF Diving and Naval Medicine Centre, with horizontal cylindrical wet volume separated by a lock adjoining air and water volumes. The wet volume in the chamber was 2.6 meters in diameter, and pressure was set so that the desired ambient pressure was present at 0.3 meters from the chamber floor. Divers were directed to that depth level but could deviate and descend 0.3 meters below or 2.3 meters above the intended depth since they could swim freely. Pressure chamber operators informed the divers if they deviated from the intended depth.

Divers wore regular Swedish military diving equipment – i.e., drysuit (shell), undergarment, wetsuit gloves, and open-circuit breathing apparatus Interspiro MKIII (Interspiro AB, Täby). Breathing gas was air. The use of either a full face mask or mouthpiece was a free choice. The water temperature was 10 ± 1°C, and the divers were asked to do light work.

Divers were equipped with an optical heart rate monitor (Polar OH1, Polar Electro Oy, Kempele). Descent speed was 23 msw/minute, and ascent speed was 9 msw/minute. For dive profiles with oxygen decompression, the oxygen was supplied from a BIBS-mask with the diver standing submerged, with head out of water in the lock.

In a series of 150 dives (the estimated number of dives to be conducted during validation), with an assumed risk of DCS = 1% and risk of CNS-DCS = 1‰, the incidence of DCS should be at most four and the incidence of CNS-DCS at most one with 95% confidence based on a binomial distribution. Therefore, safety criteria for terminating the study were set at more than four events of DCS or more than one event of CNS-DCS.

Selection of profiles for validation

The direct ascent profiles to validate were selected based on the direct ascent threshold limits from the probabilistic approach followed by the MPTT for compartments with halftimes (HT) of 5, 10, 20, 40, 80, 120, 160, 200 and 240 minutes. Direct ascent profiles, with bottom-time limits governed by compartments with HT>40 minutes, were considered too time-consuming to validate at this stage of the table development. However, profiles with decompression stops were needed for validation. We selected profiles that were known from previous dive trials within the SwAF, being 39 msw/20 minutes, 51 msw/10 minutes and 57 msw/15 minutes.

Definition of DCS

The divers were informed to be observant on any DCS-related symptoms that might occur and be linked to the validation dives. They were closely observed by medical staff for two hours from surfacing. When they were sent home, they received an informational letter asking them to be observant of any DCS-related symptoms during the following 24 hours. We defined DCS as any symptom that was treated with hyperbaric oxygen (HBO_2) therapy and could be linked to the test dive.

Table 1A: Parameters for probabilistic models calibrated against DB-SWEN21 databases v1 and v2

	P_{DCS}-SWEN21v1	P_{DCS}-SWEN21v2	$P_{CNS-DCS}$-SWEN21v1	$P_{CNS-DCS}$-SWEN21v2
β_0	-18.949	-18.728	-21.268	-21.210
β_D	8.187	8.115	7.909	7.909
$\beta_{T,1}$	2.254	2.280	0.245	0.312
$\beta_{T,2}$	-2.715	-2.746	-1.142	-1.190
$\beta_{T,3}$	-0.723	-0.613	-1.427	-1.341
$\beta_{T,4}$	-1.999	-2.051	-1.406	-1.462
LL	-287.72	-287.97	-101.59	-101.47
AIC	587.43	587.95	215.18	214.94

Table 1B: Shows the parameters β_0, β_D and $\beta_{T,1}$ for the resulting models with reduced set of knots

	P_{DCS}-SWEN21v1-red	P_{DCS}-SWEN21v2-red	$P_{CNS-DCS}$-SWEN21v1-red	$P_{CNS-DCS}$-SWEN21v2-red
β_0	-18.038	-17.831	-20.724	-20.656
β_D	7.644	7.560	7.597	7.571
$\beta_{T,1}$	-4.507	-4.470	-3.883	-3.872
LL	-289.43	-289.88	-101.68	-101.57
AIC	584.86	585.76	209.35	209.15

The responsible dive supervisor and dive physician on duty decided whether HBO_2 should be initiated. Symptoms such as itching and rashes were considered marginal DCS and were not treated with HBO_2.

RESULTS

The results are separated into four parts:

1) parameters for the probabilistic model:
2) the MPTTs derived from the probabilistic method;
3) the tables generated from those parameters using the replicated EL-DCM Thalmann Decompression Algorithm; and
4) results from the validation dives.

Parameters for probabilistic models

Using $T_1 = 8$ minutes, $T_2 = 40$ minutes, $T_3 = 200$ minutes, T4 = 1,000 minutes and T5 = 5,000 minutes, we estimate the parameters β_0, β_D and $\beta_{T,k}$ using the method of maximum likelihood to the set of data assembled. For each version of the database DB-SWEN21v1 and DB-SWEN21v2, we obtain one set of parameters estimating the risk of DCS and another set of parameters estimating the risk of CNS-DCS, including the Akaike information criterion (AIC) (Table 1A).

Retrospectively, we also decided to investigate if the five knot points are statistically warranted by the data. This was done by successively removing knot points and applying the AIC. In all the models this resulted in just two knot points, T_1 = 40 minutes and T_2 = 5,000 minutes remaining. Parameters for the resulting models with reduced set of knots are presented in Table 1B.

The risks computed by these reduced models (Px-SWEN21vX-red) are compared to the five knot models (PX-SWEN21vX) in Tables 2A and 2B.

It can be noted that the majority of the direct ascent times presented in column 2 of Tables 2A and 2B are controlled by the criteria $P_{CNS-DCS} <$ 0.1%. This occurs since both $P_{DCS} <$ 1% and $P_{CNS-DCS}$

Table 2A: Comparison of risk (%) for DCS computed by different versions of our probabilistic model

depth (msw)	time (min)	P_{DCS}-SWEN21v1	P_{DCS}-SWEN21v1-red	P_{DCS}-SWEN21v2	P_{DCS}-SWEN21v2-red
7	1017	1.00 (0.55-1.83)	1.28 (0.77-2.11)	1.04 (0.58-1.88)	1.35 (0.82-2.21)
8	563	0.85 (0.40-1.81)	1.25 (0.77-2.02)	0.86 (0.41-1.82)	1.31 (0.82-2.11)
9	356	0.76 (0.35-1.65)	1.10 (0.68-1.77)	0.76 (0.35-1.65)	1.15 (0.72-1.84)
10	242	0.67 (0.31-1.44)	0.89 (0.54-1.44)	0.68 (0.32-1.44)	0.93 (0.57-1.50)
12	151	0.78 (0.36-1.67)	0.85 (0.53-1.36)	0.80 (0.37-1.70)	0.89 (0.56-1.41)
14	100	0.64 (0.29-1.43)	0.66 (0.41-1.08)	0.66 (0.30-1.46)	0.69 (0.43-1.12)
16	74	0.55 (0.25-1.20)	0.59 (0.36-0.97)	0.57 (0.26-1.23)	0.61 (0.38-1.00)
18	59	0.51 (0.24-1.06)	0.58 (0.35-0.95)	0.53 (0.25-1.09)	0.60 (0.37-0.98)
20	49	0.48 (0.24-0.97)	0.59 (0.36-0.96)	0.50 (0.25-0.99)	0.61 (0.38-0.99)
22	39	0.32 (0.15-0.66)	0.45 (0.26-0.76)	0.33 (0.16-0.67)	0.46 (0.28-0.78)
24	33	0.27 (0.12-0.58)	0.41 (0.24-0.71)	0.27 (0.13-0.59)	0.42 (0.25-0.72)
26	28	0.22 (0.10-0.51)	0.36 (0.21-0.63)	0.23 (0.10-0.52)	0.37 (0.21-0.65)
28	25	0.24 (0.11-0.53)	0.38 (0.22-0.67)	0.24 (0.11-0.54)	0.39 (0.23-0.68)
30	22	0.23 (0.10-0.51)	0.36 (0.21-0.64)	0.24 (0.11-0.52)	0.37 (0.21-0.66)
33	17	0.16 (0.07-0.36)	0.24 (0.12-0.44)	0.17 (0.07-0.37)	0.24 (0.13-0.46)
36	15	0.19 (0.09-0.41)	0.26 (0.14-0.49)	0.20 (0.09-0.42)	0.27 (0.14-0.50)
39	12	0.16 (0.07-0.33)	0.18 (0.09-0.35)	0.16 (0.08-0.33)	0.18 (0.09-0.36)
42	10	0.15 (0.07-0.31)	0.14 (0.07-0.28)	0.15 (0.07-0.32)	0.14 (0.07-0.29)
45	8	0.12 (0.05-0.30)	0.08 (0.04-0.19)	0.13 (0.05-0.31)	0.09 (0.04-0.19)
48	7	0.14 (0.05-0.37)	0.08 (0.03-0.17)	0.14 (0.05-0.39)	0.08 (0.03-0.18)
51	6	0.14 (0.04-0.45)	0.06 (0.03-0.14)	0.15 (0.04-0.48)	0.06 (0.03-0.15)
54	6	0.22 (0.07-0.71)	0.09 (0.04-0.21)	0.23 (0.07-0.75)	0.10 (0.04-0.21)
57	5	0.19 (0.05-0.81)	0.06 (0.03-0.15)	0.20 (0.05-0.86)	0.06 (0.03-0.15)
60	5	0.29 (0.07-1.22)	0.09 (0.04-0.21)	0.31 (0.07-1.29)	0.09 (0.04-0.21)

The time presented in Column 2 are the direct ascent time in the SWEN21 table further explained later (see Table 6). The ranges in brackets are 95% confidence intervals computed from the Fisher information matrix.

<0.1% must be fulfilled and the statistical analysis apparently gives shorter times for $P_{CNS\text{-}DCS}$. Note also that a few profiles in Table 2B with depths of 20, 22, 28, 30, and 36 msw have an estimated $P_{CNS\text{-}DCS}$-SWEN21v1, slightly exceeding the prescribed limit of 0.1%. This is due to a discrepancy between the employed probabilistic model and the subsequently used Thalmann algorithm, where the direct ascent limits prescribed depend on the descent and ascent rates, while the risk computed by our probabilistic model does not take those rates into account. When the ascent rate is decreased from 10.5 msw/minute, as used in the statistical analysis, to 9 msw/minute, some depths get a slightly longer bottom time, resulting in a somewhat elevated risk according to the probabilistic model.

Goodness of fit analysis

We perform two analyses to check how well the probabilistic models (PX-SWEN21v1) explain the statistics in the database used for calibration.

First, we use the probabilistic models to compute the predicted number of DCS and CNS-DCS cases in each dataset in the database. These values are compared to the observed outcomes by computing squared Pearson residuals (PR^2). The results are shown in Table 3. The sum G of all squared PR^2 is used to compute a global χ^2 statistic. A few of the Pearson residuals for individual datasets are rather high, while the global χ^2 statistic is $P(\chi^2 > G) = 0.186$ for PDCS ($G = 43.373$, $df = 36$) and $P(\chi^2 > G) = 0.100$ for $P_{CNS\text{-}DCS}$ ($G = 47.241$, $df = 36$). These P-values exceed a model rejection criterion of $P<0.05$, motivat-

Table 2B: Comparison of risk (%) for CNS-DCS computed by different versions of our probabilistic model

depth (msw)	time (min)	P_{DCS}-SWEN21v1	P_{DCS}-SWEN21v1-red	P_{DCS}-SWEN21v2	P_{DCS}-SWEN21v2-red
7	1017	0.09 (0.02-0.38)	0.09 (0.02-0.37)	0.09 (0.02-0.38)	0.10 (0.02-0.37)
8	563	0.10 (0.02-0.57)	0.11 (0.03-0.38)	0.10 (0.02-0.56)	0.11 (0.03-0.39)
9	356	0.10 (0.02-0.61)	0.11 (0.03-0.36)	0.09 (0.01-0.60)	0.11 (0.03-0.37)
10	242	0.08 (0.01-0.51)	0.10 (0.03-0.33)	0.08 (0.01-0.51)	0.10 (0.03-0.33)
12	151	0.09 (0.02-0.54)	0.11 (0.04-0.35)	0.09 (0.02-0.54)	0.12 (0.04-0.35)
14	100	0.08 (0.01-0.53)	0.11 (0.04-0.32)	0.09 (0.01-0.53)	0.11 (0.04-0.32)
16	74	0.09 (0.01-0.51)	0.11 (0.04-0.32)	0.09 (0.01-0.51)	0.11 (0.04-0.32)
18	59	0.10 (0.02-0.51)	0.12 (0.05-0.34)	0.10 (0.02-0.51)	0.13 (0.05-0.34)
20	49	0.11 (0.02-0.51)	0.14 (0.05-0.37)	0.11 (0.02-0.51)	0.14 (0.05-0.37)
22	39	0.10 (0.02-0.43)	0.12 (0.04-0.33)	0.10 (0.02-0.43)	0.12 (0.05-0.33)
24	33	0.10 (0.02-0.43)	0.12 (0.05-0.33)	0.10 (0.02-0.43)	0.12 (0.05-0.34)
26	28	0.10 (0.02-0.43)	0.12 (0.04-0.33)	0.10 (0.02-0.42)	0.12 (0.04-0.33)
28	25	0.11 (0.03-0.47)	0.13 (0.05-0.36)	0.11 (0.03-0.46)	0.14 (0.05-0.36)
30	22	0.12 (0.03-0.48)	0.14 (0.05-0.37)	0.12 (0.03-0.47)	0.14 (0.05-0.37)
33	17	0.09 (0.02-0.37)	0.10 (0.04-0.31)	0.09 (0.02-0.37)	0.11 (0.04-0.31)
36	15	0.11 (0.03-0.40)	0.12 (0.04-0.35)	0.11 (0.03-0.40)	0.13 (0.04-0.36)
39	12	0.09 (0.03-0.31)	0.10 (0.03-0.30)	0.09 (0.03-0.31)	0.10 (0.03-0.30)
42	10	0.08 (0.02-0.28)	0.08 (0.03-0.28)	0.08 (0.03-0.28)	0.08 (0.03-0.28)
45	8	0.06 (0.02-0.25)	0.06 (0.02-0.22)	0.06 (0.02-0.26)	0.06 (0.02-0.22)
48	7	0.06 (0.01-0.31)	0.06 (0.01-0.22)	0.06 (0.01-0.32)	0.06 (0.02-0.23)
51	6	0.06 (0.01-0.37)	0.05 (0.01-0.21)	0.06 (0.01-0.39)	0.05 (0.01-0.21)
54	6	0.09 (0.01-0.57)	0.08 (0.02-0.29)	0.09 (0.01-0.59)	0.08 (0.02-0.29)
57	5	0.07 (0.01-0.67)	0.06 (0.01-0.24)	0.07 (0.01-0.70)	0.06 (0.01-0.24)
60	5	0.10 (0.01-0.99)	0.08 (0.02-0.32)	0.11 (0.01-1.04)	0.09 (0.02-0.32)

The time presented in column 2 are the direct ascent time in the SWEN21 table further explained later (see Table 6). The ranges in brackets are 95% confidence intervals computed from the Fisher information matrix.

ing acceptance of the models as able to accurately reproduce the observed DCS and CNS-DCS incidences

Second, we split the database into a number of subsets according to dive depth and computed risk. Again, the predicted number of DCS or CNS-DCS cases in each subset is computed and compared to the observed outcome. Results are shown in Table 4A for DCS and Table 4B for CNS-DCS. The global χ^2 statistic is $P(\chi^2 > G) = 0.256$ ($G = 14.732$, $df = 12$) for DCS and $P(\chi^2 > G) = 0.256$ ($G = 15.872$, $df = 13$) for CNS-DCS, again providing no reason to reject any of the models.

Figure 1 shows the increased risk with increased bottom time for direct ascent and air as breathing gas. Three of the depths were validated during these tests; the other two (12 msw and 60 msw) are of general interest to the SwAF.

MPTT parameters for deterministic model

The *MPTT* parameters that correlate with our desired risk levels for DCS and CNS-DCS are presented in Table 5, named SWEN21B. As a comparison, we also present the VVAL79 parameters, which are used to produce the air decompression table in USN DM rev. 7. The VVAL18M parameters were used in USN DM rev. 6, except for some profiles with manual adjustments (see details in [35]). The parameters are presented in unit of bar and represent the surfacing *MPTT*, also referred to as M_0. The slope, also referred to as ΔM, for determining *MPTT* at other depths such as decompression stops is 1.

Table 3, the statistical database DB-SWEN21v1 with values from the goodness to fit analysis and predicted outcome of DCS and CNS-DCS according to PX-SWEN21v1

reference	dataset name	#dives	#DCS	#DCS pred	$(PR)^2$	#CNS -DCS	#CNS -DCS pred	$(PR)^2$
[Doolette] (12)	DC4D	257	1	2.004	0.507	0	0.874	0.877
	EDU885A	112	4	1.624	3.527	0	0.664	0.668
	DC4W	69	3	1.150	3.028	1	0.510	0.474
	EDU1351NL	143	2	2.968	0.323	0	0.937	0.943
	EDU849LT2	140	26	29.701	0.585	9	9.743	0.061
	NMR97NOD	103	3	2.246	0.259	2	0.263	11.510
	NMRNSW2	48	5	2.545	2.500	1	0.335	1.332
	PASA	5	1	0.073	11.878	0	0.028	0.028
	NSM6HR	57	3	2.584	0.070	0	0.320	0.322
	RNPLX50	6	0	0.160	0.164	0	0.019	0.020
	NEDU2008	689	7	7.246	0.008	6	3.785	1.303
[Temple] (13)	EDU557	104	0	1.398	1.417	0	0.680	0.684
	ASATARE	30	2	0.865	1.533	0	0.054	0.054
	ASATNSM	34	4	5.709	0.615	0	0.404	0.409
	ASATNMR	50	1	1.873	0.422	0	0.111	0.111
	NMR9209	48	2	1.194	0.559	0	0.070	0.070
	EDUAS45	12	2	4.337	1.971	0	0.409	0.424
	ASATDC	23	8	3.383	7.387	3	0.301	24.503
	ASATFR85	13	0	0.988	1.069	0	0.068	0.069
	EDU849S2	60	13	14.476	0.198	0	1.848	1.906
[Bennett] [a] (18)	-	24	0	0.023	0.023	0	0.011	0.011
[Brett] (19)	-	20	0	0.114	0.115	0	0.021	0.021
[Cameron] (20)	-	138	0	0.278	0.278	0	0.027	0.027
[Eckenhoff-1990] (21)	-	111	0	0.823	0.830	0	0.051	0.051
[Eckenhoff-1991] (22)	-	34	0	0.583	0.593	0	0.036	0.036
[Eftedal] (23)	-	30	0	0.052	0.052	0	0.012	0.012
[Gawthrope] (24)	-	24	0	0.013	0.013	0	0.007	0.007
[Hamilton] (25)	-	76	0	0.059	0.059	0	0.028	0.028
[Ikeda] (26)	-	29	4	1.852	2.662	0	0.113	0.114
[Jones] (27)	-	4	1	0.712	0.142	0	0.060	0.060
[Ljubkovic] (28)	-	34	0	0.098	0.098	0	0.026	0.026
[Madden] (29)	-	20	0	0.017	0.017	0	0.005	0.005
[Monney in Eckenhoff] [b] (30)	-	251	0	0.536	0.537	0	0.042	0.042
[Papadopoulou] (31) -		17	0	0.056	0.057	0	0.029	0.029
[Theunissen] (32)	-	42	0	0.139	0.140	0	0.073	0.073
[Thom] (33)	-	64	0	0.110	0.110	0	0.026	0.026
[Silvanius] (34)	-	20	0	0.014	0.014	0	0.007	0.007
Total		**2941**	**92**	**92.001**	**43.760**	**22**	**21.997**	**46.343**
$P(\chi^2 > G)$ df = 35					**0.147**			**0.095**

[a] email conversation with Prof. Balestra to clarify the outcome of DCS. One marginal DCS occurred, skin rash.

[b] email conversation with Prof. Eckenhoff to verify Dr. Monney statement. It was established that the stated dives were performed in Jules Undersea Lodge, Key Largo, Florida, by paying guests and could be considered reliable.

Table 4A, a comparison of observed DCS cases with prediction from P_{DCS}-SWEN21v1 model.

	5-15 msw				15-30 msw				30-60 msw			
pred risk	# dives	# DCS obs	# DCS pred	PR^2	# dives	# DCS obs	# DCS pred	PR^2	# dives	# DCS obs	# DCS pred	PR^2
0-1%	412	0	0.8 (0-3)	0.817	345	0	0.8 (0-3)	0.798	707	2	1.9 (0-5)	0.006
1-2%	152	0	2.5 (0-6)	2.504	53	0	0.7 (0-3)	0.678	393	10	5.7 (2-11)	3.290
2-5%	191	5	5.1 (1-10)	0.003	34	1	1.0 (0-3)	0.002	135	1	3.9 (1-8)	2.183
5-10%	100	8	7.8 (3-13)	0.007	38	5	2.4 (0-6)	3.029	45	2	2.8 (0-6)	0.252
>10%	102	30	26.6 (18-35)	0.577	-	-	-	-	106	25	27.6 (19-36)	0.329

Table 4B, Comparison of observed CNS-DCS cases with prediction from $P_{CNS\text{-}DCS}$-SWEN21v1 model.

	5-15 msw				15-30 msw				30-60 msw			
pred risk	# dives	# CNS-DCS obs	# CNS-DCS pred	PR^2	# dives	# CNS-DCS obs	# CNS-DCS pred	PR^2	# dives	# CNS-DCS obs	# CNS-DCS pred	PR^2
0-0.1%	437	0	0.1 (0-1)	0.088	284	0	0.1 (0-1)	0.116	452	0	0.2 (0-1)	0.206
0.1-0.2%	157	0	0.2 (0-1)	0.182	79	0	0.1 (0-1)	0.115	71	0	0.1 (0-1)	0.120
0.2-0.5%	198	3	0.6 (0-2)	9.617	53	1	0.2 (0-1)	3.051	196	1	0.7 (0-3)	0.144
0.5-1%	57	0	0.4 (0-2)	0.414	47	0	0.3 (0-2)	0.326	377	4	2.8 (0-6)	0.524
>1%	108	2	2.9 (0-7)	0.311	7	0	0.1 (0-1)	0.106	290	10	12.0 (6-19)	0.362

Direct ascent air table generated with *MPTT* parameters SWEN21B and EL-DCM

Direct ascent times computed with EL-DCM, preceded with analysis from the maximum likelihood analysis and *MPTT* parameters SWEN21B are presented in Table 6 as bottom time with a predicted risk of 1% for DCS or 1‰ for CNS-DCS, whichever has the shortest time of the controlling requirement.

Depths between 7 and 60 msw were considered relevant, as ≤6 msw are considered as safe direct ascents from saturation on air [37]. Depths deeper than 60 msw are considered irrelevant for air diving due to the narcotic effect and oxygen toxicity.

Using the PX-SWEN21v1 risk-model we compared the estimated risk for direct ascent times in VVAL79 metric from [36], RMS-Dyk 2013 from [4] and SWEN21 presented in Table 7.

Validation dives

From Table 6 we chose direct ascent profiles to be validated that could represent each controlling compartment from five- to 40-minute HTs. We specifically included 45 msw/8 minutes, as it increased the bottom time extensively compared to previous SwAF air dive tables [4]. Table 8 summarizes all the profiles validated, number

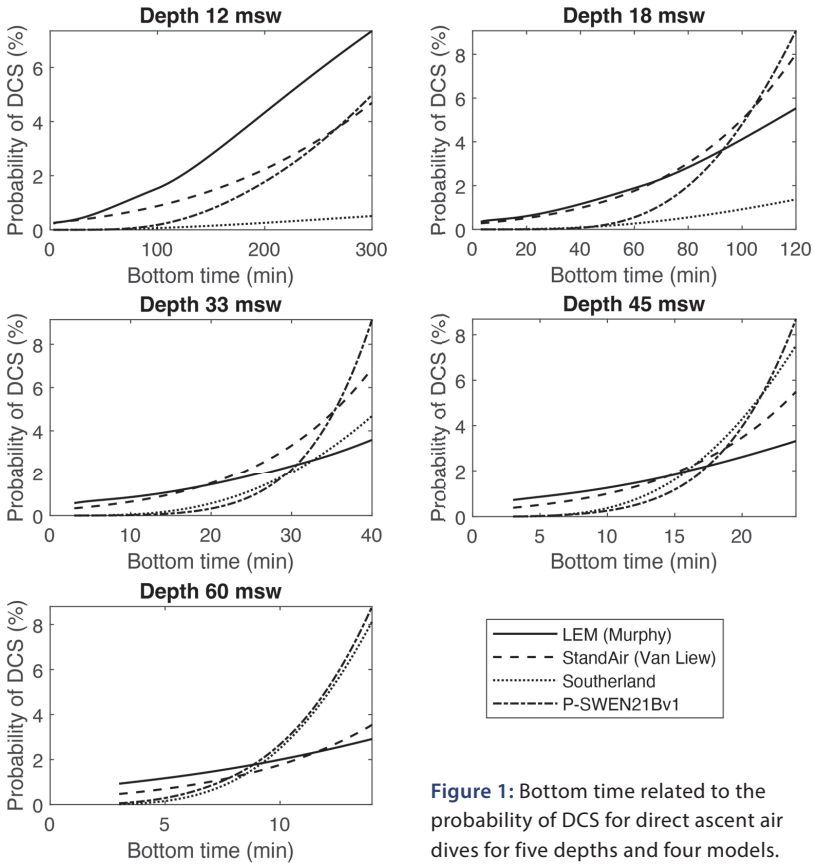

Figure 1: Bottom time related to the probability of DCS for direct ascent air dives for five depths and four models.

Table 5: Some relevant surfacing MPTT-parameters for exponential linear decompression theory

Compartmental	Half-time [min]								
M0-value	5	10	20	40	80	120	160	200	240
VVAL18M	3.6772	3.0031	2.3905	1.716	1.4862	1.3943	1.3636	1.3483	1.3330
VVAL79	3.0428	2.6874	2.3902	1.716	1.4862	1.3943	1.3636	1.3483	1.3330
SWEN21B	3.0086	2.5354	2.0311	1.6636	1.4461	1.3729	1.3299	1.3013	1.2766

SWEN21B is our suggested parameter setting; VVAL79 is used to produce the tables in USN Diving manual rev. 7 and VVAL18M partially for air tables in USN DM rev. 6. *MPTT* parameters are given in the unit bar.

Table 6: Direct ascent bottom times

USN		Rev 6	Rev 7	RMS-DYK 2013		SWEN21		VVAL-79	
depth [msw] [a]	depth [fsw]	time [min]	time [min]	depth [msw]	time [min]	depth [msw]	time [min]	depth [msw]	time [min]
						7	1017		
7.7	25	595	1102	7.5	595	8	563		
9.2	30	371	371	9	371	9	356	9	394
10.7	35	232	232	10.5	232	10	242		
12.3	40	163	163	12	163	12	151	12	169
13.8	45	125	125	13.5	125	14	100		
15.3	50	92	92	15	92			15	96
16.9	55	74	74	16.5	74	16	74		
18.4	60	60	63	18	60	18	59	18	65
				21	48	20	49	21	49
21.5	70	48	48			22	39		
24.5	80	39	39	24	39	24	33	24	40
						26	28		
27.6	90	30	33	27	30	28	25	27	34
30.6	100	25	25	30	25	30	22	30	27
33.7	110	20	20	33	20	33	17	33	21
36.8	120	15	15	36	15	36	15	36	15
39.8	130	10	12	39	10	39	12	39	12
42.9	140	10	10	42	10	42	10	42	10
46	150	5	8	45	5	45	8	45	8
49	160	5	7	48	5	48	7	48	7
52.1	170	5	6	51	5	51	6	51	7
55.2	180	5	6	54	5	54	6	54	6
58.2	190	5	5	57	5	57	5	57	5

[a] 1 msw = 3.26336 fsw.

Direct ascent bottom times for air diving according to EL-DCM with SWEN21B parameters. A comparison between USN DM rev6, rev7, RMS- Dyk 2013 and VVAL79 metric from [36] is also presented.

of dives, number of DCS, CNS-DCS and marginal DCS. From the outcome of DCS we also present the expected probability of DCS and CNS-DCS related to the number of dives conducted, with a 95% confidence interval.

The number of dives totaled 154, of which three DCS incidences occurred and were treated with HBO_2 USN Treatment Table 6. Nine marginal symptoms, such as rashes and itching, occurred. One hundred dives were conducted with direct ascent (two DCS, one marginal) and 54 were with decompression stop (one CNS-DCS, eight marginal).

DISCUSSION

Using a database of 2,953 direct ascent air dives, with known outcome of DCS, we use probabilistic modeling to set *MPTT* parameters for a deterministic model. We have developed an air dive table SWEN21 with a predicted risk of DCS level of ≤1% for DCS and ≤1‰ for CNS-DCS for direct ascent air dives.

The actual prescribed *MPTT* limit for SWEN21B parameters at desired risk level, derived from PX-SWEN21v1, could be questioned as there are still few validation dives performed. It can be noted that USN DM rev. 7 allows longer exposure for

Table 7: Risks according to P_{DCS}-SWEN21v1 and $P_{CNS-DCS}$-SWEN21v1, for three different direct ascent air tables

	BOTTOM TIME			DCS RISK %			CNS-DCS RISK %		
depth (msw)	VVal79 metric	SWEN21	RMS-Dyk 2013	VVal79 metric	SWEN21	RMS-Dyk 2013	VVal79 metric	SWEN21	RMS-Dyk 2013
9	394	356	371	0.97	0.76	0.84	0.12	0.10	0.11
12	169	151	163	1.10	0.78	0.99	0.13	0.09	0.12
15	96	85	92	0.96	0.59	0.81	0.13	0.08	0.11
18	65	59	60	0.80	0.51	0.55	0.14	0.10	0.10
21	49	43	48	0.72	0.37	0.65	0.16	0.10	0.15
24	40	33	39	0.74	0.27	0.64	0.21	0.10	0.19
27	34	26	30	0.81	0.21	0.43	0.28	0.10	0.17
30	27	22	25	0.60	0.23	0.42	0.26	0.12	0.19
33	21	17	20	0.40	0.16	0.32	0.21	0.09	0.17
36	15	15	15	0.19	0.19	0.19	0.11	0.11	0.11
39	12	12	10	0.16	0.16	0.08	0.09	0.09	0.05
42	10	10	10	0.15	0.15	0.15	0.08	0.08	0.08
45	8	8	5	0.12	0.12	0.03	0.06	0.06	0.01
48	7	7	5	0.14	0.14	0.05	0.06	0.06	0.02
51	7	6	5	0.23	0.14	0.08	0.10	0.06	0.03
54	6	6	5	0.22	0.22	0.12	0.09	0.09	0.05
57	5	5	5	0.19	0.19	0.19	0.07	0.07	0.07

direct ascent on 60 fsw and 90 fsw compared to Rev. 6. This is a result of Rev. 7 strictly following the calculated bottom times without manual adjustments, as was done in Rev. 6 for some depths [17,35]. For example, the 60-fsw no-deco dive in Rev. 6 was manually adjusted to 60 minutes but would allow 63 minutes according to the pre-calculated profile with VVAL18M-parameters, which is also found in Rev. 7. This reveals that VVAL18M and VVAL79 have the same *MPTT* for the leading tissue for a 60-msw no-deco profile. Comparing the VVAL79 metric and SWEN21, we recommend even shorter exposure for 18 msw (~60 fsw) and 27 msw (~90 fsw) [36].

The expected outcome of the validation dives, assuming 1% risk for DCS and 0.1% risk for CNS-DCS with 95% confidence interval is 0-3 cases of DCS and 0-1 cases of CNS-DCS. The confidence interval for the 54 dive profiles with decompression stop is 0-2 cases of DCS and 0-1 cases of CNS-DCS. We are within expected limits if marginal DCS incidences are classified as non-events, as recommended by Murphy et al. [7].

The two DCS cases on profile 18 msw/59 minutes were diffuse limb pain and might have been affected by each other since they performed the same dive and were in the same examination room at the same time. There are no indications that the profile, workload or temperature deviated from other dives performed on the same profile. Both divers were relieved of their pain during HBO_2. One of these divers was later confirmed to have a patent foramen ovale (PFO), which is recognized as a risk factor [38].

The single incidence CNS-DCS was discovered the morning after the dive. The diver described numbness in one leg and reported to the dive physician on duty. The diver was treated with HBO_2 and received relief. This diver was later confirmed as having a PFO.

Two out of three divers with DCS were screened for PFO and reported with presence thereof. None of the other divers were screened or had any previous report of having PFO. The DCS cases presented here were all mild and may not even have

Table 8. summary of the dives performed and the outcome

profile	deco stop	n	all DCS [a]	CNS-DCS	any symptom (marginal DCS + all DCS)
18msw/59min	-	20	2 ($P_{0.95}$=1.2-31.7%)	0 ($P_{0.95}$=0.0-16.8%)	2 ($P_{0.95}$=1.2-31.7%)
24msw/33min	-	20	0 ($P_{0.95}$=0.0-16.8%)	0 ($P_{0.95}$=0.0-16.8%)	0 ($P_{0.95}$=0.0-16.8%)
33msw/17min	-	24	0 ($P_{0.95}$=0.0-14.2%)	0 ($P_{0.95}$=0.0-14.2%)	1 ($P_{0.95}$=0.1-21.1%)
39msw/12min	-	20	0 ($P_{0.95}$=0.0-16.8%)	0 $P_{0.95}$=0.0-16.8%)	0 $P_{0.95}$=0.0-16.8%)
45msw/8min	-	16	0 ($P_{0.95}$=0.0-20.6%)	0 ($P_{0.95}$=0.0-20.6%)	0 ($P_{0.95}$=0.0-20.6%)
Total direct ascent dives		**100**	**2 ($P_{0.95}$=0.2-7.0%)**	**0 ($P_{0.95}$=0.0-3.6%)**	**3 ($P_{0.95}$=0.6-8.5%)**
39msw/20min	6msw/13min	22	0 ($P_{0.95}$=0.0-15.4%)	0 ($P_{0.95}$=0.0-15.4%)	1 ($P_{0.95}$=0.1-22.8%)
51msw/10min	6msw/2min, 3msw/4min	16	1 ($P_{0.95}$=0.2-30.2%)	1 ($P_{0.95}$=0.2-30.2%)	1 ($P_{0.95}$=0.2-30.2%)
57msw/15min	15msw/1min, 12msw/3min, 9msw/5min, 6msw/13min, 3msw/8min [b]	8	0 ($P_{0.95}$=0.0-36.9%)	0 ($P_{0.95}$=0.0-36.9%)	5 ($P_{0.95}$=25.5-91.5%)
57msw/15min	15msw/1min, 12msw/3min, *switch to* O_2 9msw/3min, 6msw/4min, 3msw/7min	8	0 ($P_{0.95}$=0.0-36.9%)	0 ($P_{0.95}$=0.0-36.9%)	2 ($P_{0.95}$=3.2-65.1%)
Total decompression stop dives		**54**	**1 ($P_{0.95}$=0.0-9.9%)**	**1 ($P_{0.95}$=0.0-9.9%)**	**9 ($P_{0.95}$=7.9-29.3%)**
TOTAL		**154**	**3 ($P_{0.95}$=0.4-5.6%)**	**1 ($P_{0.95}$=0.0-3.6%)**	**12 (P0.95=4.1-13.2%)**

Note that a CNS-DCS is also included as a DCS. $P_{0.95}$ represents the 95% confidence interval for probability of DCS.

[a] treated with HBO2, also include CNS-DCS

[b] this unconventional decompression profile, shorter at the last decompression depth, is one the optional features with SWEN21 where longer time is spent at deeper decompression stop to retrieve a shorter total decompression time. This can be explained with the design of the model and does not necessarily provide a more effective decompression strategy.

Table 9: Probability of DCS for our validated profiles related to different models

depth	time	TDT	DCS risk % P-SWEN21v1	DCS risk % LEM [7]	DCS risk % StandAir [8]	DCS risk % Southerland (9)	DCS-CNS risk % P-SWEN21v1	DCS-CNS risk % Doolette [12]
18	59	-	0.51	1.84	1.71	0.25	0.10	0.07
24	33	-	0.27	1.52	1.55	0.34	0.10	0.08
33	17	-	0.16	1.24	1.18	0.33	0.09	0.09
39	12	-	0.16	1.19	1.01	0.29	0.09	0.09
45	8	-	0.12	1.10	0.78	0.16	0.06	0.06
39	20	13	N/A	1.49	1.97	N/A	N/A	N/A
51	10	6	N/A	1.17	1.21	N/A	N/A	N/A
57	15	30	N/A	1.95	2.48	N/A	N/A	N/A

Models that cannot calculate decompression dives are denoted with N/A

been treated in other organizations or during other conditions. The divers with joint pain were uncertain if they would have discovered these symptoms during a regular diving operation, and this could be one of the reasons why chamber testing is more prone to produce DCS, as previously mentioned. The CNS-symptoms might have been ignored during other conditions, as the symptoms were diffuse, and the diver hesitated or delayed the reporting. We continue to encourage all test divers to report even the slightest symptom.

Probabilistic models for the risk of DCS or CNS-DCS are attractive since they allow conclusions to be drawn about the risk associated with many different dive profiles without the need to perform hundreds of test dives for each profile. However, it is essential to remember that any such model in its formulation encodes implicit assumptions about how the risks will vary with changing depth and time. Moreover, predictions of these models for low-risk dive profiles will depend to a large extent on extrapolation from higher-risk profiles under the model assumptions. Therefore, it is not surprising that different models can give diverging risk predictions, particularly for comparatively low-risk dive profiles. Compared to many previously published models, such as LEM [7] and StandAir [8], our model predicts a rapidly declining risk with decreasing bottom time at a fixed depth (Figure 1). This could be explained partially with our model being calibrated with direct ascent dives only, which tend to be generally lower risk according to previously published tables and risk analysis. We believe that our model could be overly optimistic in this regard. However, it follows the desired criteria P_{DCS}=0 if bottom time is zero. On the other hand, it seems likely that the LEM and StandAir models (along with many other similar models) tend to overestimate the risk associated with low-risk profiles. We do not believe that our model is generally more accurate than previously published models. Rather, where the results of different models diverge (see Table 9), we would argue that it is prudent to expect some uncertainties in all the models

CONCLUSION

We replicated the decompression algorithm EL-DCM Thalmann, and by using the VVAL79 parameters, we could reproduce the air dive table in U.S. Navy Diving Manual Rev. 7, verifying the accuracy of our replication. Our novel maximum permissible tissue tensions were derived from a statistical perspective, with dives from various conditions; however, only air dives with direct ascent were included. Risk levels of 1% decompression sickness and 0.1% neurological decompression sickness were considered acceptable. The predicted and acceptable outcome of decompression sickness that would meet these requirements during some 150 validation dives were ≤4 incidences, of which ≤1 were neurological. From our 154 dives, we had two cases of joint pain on profile 18 msw/59 minutes

and one case of leg numbness on profile 51 msw/10 minutes, treated with hyperbaric oxygen. All divers were relieved from symptoms during hyperbaric oxygen treatment. Two of the three divers with DCS had PFO. The SWEN21 air dive table is equally or more conservative in every profile compared to air dive tables in the U.S. Navy Diving Manual Rev. 7 and NEDU TR 16-05 (VVAL79 metric). We recommend that the Swedish Armed Forces implement SWEN21 as the new air dive table and continue evaluation, analysis, and development during implementation and beyond. The increased risk of DCS for divers with PFO ought to be considered.

Acknowledgments

We express our gratitude to all the divers who participated in this study, Cdr Jansson and Cdr Djurstedt-Holm for making it possible from a financial and resource perspective, employees at the Swedish Armed Forces Diving and Naval Medicine Centre, and Prof. Eckenhoff and Prof. Balestra for their help in clarifying the outcome of DCS in some of the published articles we refer to.

Funding

The Swedish Armed Forces supported this work through Swedish Defense Material Administration under Grant [430919-LB967593]; additional support from the Swedish Society of Medical Research and the Swedish Research Council under Grant [2019-02081].

REFERENCES

1. Vann RD, Butler FK, Mitchell SJ, Moon RE. Decompression illness. The Lancet. 2011 Jan 8;377(9760):153-164.

2. Hamilton RW, Muren A, Röckert H, Örnhagen H. Proposed new Swedish air decompression tables. In: Paper no 10. Aberdeen: EUBS; 1988.

3. Regler för militär sjöfart RMS-Dyk. Vol. 2010. Stockholm, Sweden: Högkvarteret; 2010.

4. Regler för militär sjöfart RMS-Dyk. Vol. 2013. Stockholm, Sweden: Högkvarteret; 2013.

5. US Navy Diving Manual. rev. 7. Washington DC, USA: Naval Sea Systems Command; 2017.

6. Gerth WA, Vann RD. Probabilistic gas and bubble dynamics models of decompression sickness occurrence in air and nitrogen-oxygen diving. Undersea Hyperb Med. 1997 Jan 1;24(4):275-292.

7. Murphy FG, Swingler AJ, Gerth WA, Howle LE. Iso-risk air no decompression limits after scoring marginal decompression sickness cases as non-events. Comput Biol Med. 2018 Jan 1;92:110-117.

8. Van Liew H, Flynn E. A simple probabilistic model for estimating the risk of standard 29 Air dives. Panama City, U.S.: NEDU; 2004 Dec. Report No. TR 04-41.

9. Southerland DG. Logistic regression and decompression sickness. Durham U.S. Graduate School of Duke University; 1992 Jun.

10. Thalmann ED, Parker EC, Survanshi SS, Weathersby PK. Improved probabilistic decompression model risk prediction using linear-exponential kinetics. Undersea Hyper Med. 1997; 24(4):255-274.

11. Parker EC, Survanshi SS, Massell PB, Weathersby PK. Probabilistic models of the role of oxygen in human decompression sickness. J Appl Physiol. 1998 Mar 1;84(3): 1096-1102.

12. Doolette D, Gerth WA, Gault KA. Risk of central nervous system decompression sickness in air diving to no-stop limits. Panama City, U.S.: NEDU; 2009 Jan. Report No. TR 09-03.

13. Temple D, Ball R, Weathersby P, Parker EC, Survanshi SS. The dive profiles and manifestations of decompression sickness cases after air and nitrogen oxygen dives. Washington DC, USA: NMRC; 1999 Jan. Report No. NMRC 99-02.

14. Braithwaite W. Systematic guide to decompression schedule calculations. Washington DC, USA: NEDU; 1972 Jul. Report No. 11-72.

15. Thalmann ED. Phase II - Testing of decompression algorithms for use in the U.S. Navy underwater decompression computer. Panama City, U.S.: NEDU; 1984 Jan. Report No. 1-84.

16. Howle LE, Weber PW, Vann RD. A computationally advantageous system for fitting probabilistic decompression models to empirical data. Comput Biol Med. 2009 Dec;39(12): 1117-1129.

17. Gerth WA, Doolette D. VVal-79 Maximum permissible tissue tension table for Thalmann algorithm support of air diving. Panama City, U.S.: NEDU; 2012 Mar. Report No. TR 12-01.

18. Bennett P, Marroni A, Cronjé F, et al. Effect of varying deep stop times and shallow stop times on precordial bubbles after dives to 25 msw (82 fsw). Undersea Hyperb Med. 2007 Nov 1;34:399-406.

19. Brett K, Nugent N, Fraser N, Bhopale V, Yang M, Thom S. Microparticle and interleukin-1β production with human simulated compressed air diving. Sci Rep. 2019 Sep 16;9(1): 13320.

20. Cameron B, Olstad C, Clark J, Gelfand R, Ochroch E, Eckenhoff R. Risk factors for venous gas emboli after decompression from prolonged hyperbaric exposures. Aviat Space Environ Med. 2007 Jun 1;78:493-499.

21. Eckenhoff RG, Olstad CS, Carrod G. Human dose-response relationship for decompression and endogenous bubble formation. J Appl Physiol Bethesda Md 1985. 1990 Sep;69(3):914-918.

22. Eckenhoff RG, Olstad CS. Ethanol and venous bubbles after decompression in humans. Undersea Biomed Res. 1991 Jan;18(1):47-51.

23. Eftedal I, Ljubkovic M, Flatberg A, Jørgensen A, Brubakk AO, Dujic Z. Acute and potentially persistent effects of scuba diving on the blood transcriptome of experienced divers. Physiol Genomics. 2013 Oct 16;45(20):965-972.

24. Gawthrope IC, Summers M, Macey DJ, Playford DA. An observation of venous gas emboli in divers and susceptibility to decompression sickness. Diving Hyperb Med. 2015 Mar;45(1):25-29.

25. Hamilton RW, Rogers RE, Powell MR. Development and validation of no-stop decompression procedures for recreational diving: The DSAT recreational dive planner. Santa Ana, CA: Diving Science and Technology; 1994.

26. Ikeda T, Okamoto Y, Hashimoto A. Bubble formation and decompression sickness on direct ascent from shallow air saturation diving. Aviat Space Environ Med. 1993 Feb; 64(2):121-125.

27. Jones R, Owens G, Crawford P. Exercise "Sea Snail." Malta: Royal Military Academy Sandhurst; 1966.

28. Ljubkovic M, Dujic Z, Møllerløkken A, Bakovic D, Obad A, Breskovic T, et al. Venous and arterial bubbles at rest after no-decompression air dives. Med Sci Sports Exerc. 2011 Jun;43(6):990-995.

29. Madden D, Thom SR, Yang M, Bhopale VM, Ljubkovic M, Dujic Z. High intensity cycling before SCUBA diving reduces post-decompression microparticle production and neutrophil activation. Eur J Appl Physiol. 2014 Sep;114(9):1955-1961.

30. Eckenhoff RG, Osborne SF, Parker JW, Bondi KR. Direct ascent from shallow air saturation exposures. Undersea Biomed Res. 1986 Sep;13(3):305-316.

31. Papadopoulou V, Germonpré P, Cosgrove D, Eckersley RJ, Dayton PA, Obeid G, et al. Variability in circulating gas emboli after a same scuba diving exposure. Eur J Appl Physiol. 2018 Jun;118(6):1255-1264.

32. Theunissen S, Balestra C, Boutros A, De Bels D, Guerrero F, Germonpré P. The effect of pre-dive ingestion of dark chocolate on endothelial function after a scuba dive. Diving Hyperb Med. 2015 Mar;45(1):4-9.

33. Thom SR, Milovanova TN, Bogush M, et al. Microparticle production, neutrophil activation, and intravascular bubbles following open-water SCUBA diving. J Appl Physiol Bethesda Md 1985. 2012 Apr;112(8):1268-1278.

34. Silvanius M, Gennser M. Rapport efter utredning av incidenter med dykapparat OMD-10. Karlskrona: FM DNC; 2016. Report No. FM2016 4114:13.

35. Gerth WA, Doolette DJ. Schedules in the Integrated Air Decompression Table of U.S. Navy Diving Manual, Revision 6: Computation and Estimated Risks of Decompression Sickness: [Internet]. Fort Belvoir, VA: Defense Technical Information Center; 2009 Jun.

36. Gerth WA, Doolette DJ. VVAL-79 Thalmann algorithm metric and imperial air decompression tables. Panama City, U.S.: 2016 Nov. Report No. NEDU TR 16-05.

37. Van Liew HD, Flynn ET. Direct ascent from air and N_2-O_2 saturation dives in humans: DCS risk and evidence of a threshold. Undersea Hyperb Med J Undersea Hyperb Med Soc Inc. 2005 Dec;32(6):409-419.

38. Honěk J, Šrámek M, Šefc L, et al. High-grade patent foramen ovale is a risk factor of unprovoked decompression sickness in recreational divers. J Cardiol. 2019 Dec 1; 74(6):519-523.

Paper IV

Diving and Hyperbaric Medicine

Manuscript:	DHM-0-0 - (981)
Title:	Early nitrogen wash-out for inside attendants during hyperbaric oxygen therapy – a novel oxygen distribution regimen
Authors(s):	Mårten Silvanius (Corresponding Author), Oscar Tom Viktor Plogmark (Co-author), Oskar Frånberg (Co-author)
Keywords:	Decompression sickness, Decompression tables, Hyperbaric oxygen treatment, Hyperbaric research, Pressure chambers
Type:	Original Article

Early nitrogen wash-out for inside attendants during hyperbaric oxygen therapy – a novel oxygen distribution regimen

Abstract

INTRODUCTION

Hyperbaric oxygen therapy HBOT is widely used as treatment of decompression sickness, DCS. The patient breaths oxygen at an elevated oxygen partial pressure of up to 280 kpa, whereas any inside attendant IA normally breaths air. This gives the IA a nitrogen supersaturation which must be considered during decompression. The US Navy treatment table 6, TT6 suggests periods of oxygen at depth and during ascend to surface to avoid DCS for the IA, however this is distributed at the end of the HBOT and disallows any rapid decompression in the event of an emergency earlier.

METHOD

We suggest rescheduling the distribution of oxygen for the IA to an earlier stage of the HBOT, which would allow emergency decompression during a greater period of time than the traditional TT6 oxygen regimen. To verify the amount of oxygen periods and when it would be appropriate, we use the exponential linear Thalmann decompression algorithm with SWEN21B parameters to analyze compartmental gas load and perform a comparison between the original and our newly proposed.

RESULTS

We were able to find an alternative oxygen regimen for the IA without violating the decompression algorithm demands but providing the ability to do emergency decompression over a longer time span.

CONCLUSIONS

According to the decompression model used herein we can conclude that it is possible to give more flexibility when it comes to emergency decompression if the oxygen regimen for the IA is moved to an earlier stage of the therapy session.

Introduction

Hyperbaric Oxygen Therapy (HBOT) is widely recognized as the gold standard for treating decompression illness. This treatment has been known for over a century and has shown good results in mitigating symptoms resulting from rapid decompression or arterial gas emboli.[1] HBOT is typically performed at hospitals, military facilities, offshore facilities, ships, or private facilities. There are two types of chambers used in HBOT: monoplace chambers, where the patient is attended from outside the chamber, and multiplace chambers, which have one or more attendants inside the chamber.

The typical pressure used in HBOT ranges from 240-280 kPa, which corresponds to a depth of 14-18 meters of seawater (msw). The pressurizing gas is typically air, although some monoplace chambers may be filled with pure oxygen, eliminating the need for a built-in breathing system (BIBS). In multiplace chambers, the oxygen is normally distributed through a BIBS or a hood. The inside attendants (IA) breathe the chamber atmosphere, which normally is air at depth, and therefore absorb nitrogen into their tissues in the same way as they would during a dive, but without any submersion, thermal, or workload-related issues. [2,3,4]

In the Swedish Armed Forces, the standard treatment protocol for decompression sickness is the US Navy Treatment Table 6 (TT6).[5] The TT6 consists of three 20-minute oxygen periods followed by a 5-minute air-break at 18 msw, and a 30-minute oxygen decompression to 9 msw. At 9 msw, an additional six oxygen periods are performed, with a final 30-minute oxygen decompression to the surface. To reduce the risk of decompression sickness, the IA breathes oxygen during the last period at 9 msw and throughout the decompression to the surface. If the IA was previously exposed, three oxygen periods are mandatory at 9 msw before surfacing on oxygen, however no further details on the previous exposure is provided.[4]

If full recovery of the patient is achieved after 10 minutes at 18 msw it is recommended to switch to the shorter Treatment Table 5 (TT5) which comprise two periods at 18 msw and one period at 9 msw, which also simplifies for the IA decompression.[4] The patient may be directly decompressed depending on the seriousness of purpose being treated, whereas the tender must be considered to have a diluent load that potentially could cause decompression sickness.[3] Shorter tables such as TT5 have been evaluated and shown good results and alternative treatment protocols, similar to TT5, have been proposed for the treatment of decompression sickness and have shown promising outcomes.[6,7,8] Alternative gases such as nitrox with fractions of oxygen (F_{O2}) 50% and 60.5% have been suggested for the IA to provide the

possibility to decompress at any time during regular treatment or if the time at depth was prolonged.[9,10] This might be an attractive alternative if gas logistics can be settled and the IA can breathe from a BIBS regularly.

The maximum depth of a TT6 is 18 msw, with suggested direct ascent time varying between 50-60 minutes, depending on the decompression table used. For instance, the no-decompression time for SWEN21-table is 59 minutes.[11]

Emergencies can arise in situations where the patient's condition deteriorates significantly, the chamber facility is on fire, or in the case of a ship-based chamber, the ship is sinking, among other scenarios. We can also hypothesize scenarios where the IA needs to leave quickly due to physical or psychological reasons or attending urgent military tasks, if required. The safety for IA must always be remembered regardless of situation.[12]

In most scenarios, especially in the military, chamber operators have limited support and flexibility apart from standard decompression tables, even though there are strategies described in US Navy Diving Manual such as “Recompression treatment abort procedures”, however the IA is more or less confined or locked in until the completion of the therapy session.[4]

According to multiple studies, the risk of DCS for IAs during HBOT is considered low and acceptable, with reported levels below 1%.[13,14] Severe cases of central nervous system (CNS) bends have though occurred, even if they are within limits of compartmental gas load.[2,15,16]

The primary aim in this study is related to the oxygen distribution regimen for the IA and the possibilities for an emergency decompression during a longer period of time of the HBOT session. The secondary aim is to describe a comparison of the IA gas load for different HBOTs by introducing a ratio of supersaturation (ROS) for the compartments.

Method

We hypothesize that it is possible to optimize the distribution of oxygen periods to reduce the proportion of time during which the chamber attendant is restricted to ascend immediately. The objective of the proposed new oxygen regimen is to start administering oxygen earlier in order to maintain the nitrogen load below the maximum permissible tissue tension MPTT defined by SWEN21B parameters.[11] Additionally, it is desirable to keep the number of oxygen periods equal to or less than the current regimen when possible. However, it is important to note that breathing oxygen at depths greater than 50 fsw (~15 msw) can result in the risk of oxygen seizures.[4]

Previous studies from University of California San Diego (UCSD) with three different HBOTs[3] and Haukeland with two different HBOTs[17] are herein used as reference to indicate the acceptable compartmental nitrogen gas load. To be able to perform any comparison of the nitrogen gas load between the different HBOT we used the method of calculating compartmental gas load using the deterministic exponential-linear algorithm described by Thalmann and the SWEN21B parameters[11] and introduce the term of ROS, ratio of supersaturation. The ROS will be determined as the percentage of MPTT rather than actual compartmental gas load, as described by Short and Flahan[18] and utilized by Witucki et al.[3] The advantage is that different compartments with different MPTT can be compared. ROS equal to 0% represent atmospheric partial pressure of nitrogen in the compartment. A positive ROS denotes a supersaturation and 100% represents the compartmental gas load being equal to the MPTT. A subsaturation of nitrogen in the compartment is denoted with a negative ROS and can be as low as -100% if all nitrogen is flushed out, for example after a long oxygen breathing. However, ours and the US Navy implementation of the Thalmann algorithm involves a deliberate limitation: it does not account for F_{O2} greater than 80%. As a result, when faced with F_{O2} greater than 80%, the lowest possible value of ROS is -80%.[11,19]

Results

The results from our gas load analysis for standard, extended, previously exposed IA and extended TT6 with previously exposed IA are shown in figures 1 to 4 and presents the leading compartment/tissue supersaturation over time, dive profile and inhaled F_{O2}.

FIGURE 1a & 1b

FIGURE 2a & 2b

FIGURE 3a & 3b

FIGURE 4a & 4b

If any leading tissue is saturated above the acceptable level for direct ascent this is shown in the figures 1-4 with a plotted area which increases during on-gassing when the partial pressure of nitrogen in the tissue $P_{N2tissue}$ is lower than the partial pressure of nitrogen in the lung P_{N2lung} and decreases during the off-gassing if $P_{N2tissue} > P_{N2lung}$. The oxygen distribution for our proposed regimen can clearly be seen to suppress the nitrogen gas load for leading compartments.

The overall benefits of less lock in time together will desired periods of oxygen is compared and presented in table 1.

TABLE 1

The ROS when surfacing together with previously observed DCS outcome and oxygen seizures from UCSD and Haukeland, are presented in table 2.

TABLE 2

Figure 5 shows the ROS when surfacing for TT6 compared to our proposal. “UCSD 1”, “Haukeland new” and the direct ascent profile 18msw 59 min are presented as comparison for the standard protocols.

FIGURE 5

In figure 5 it is apparent that the 40 min compartment is the leading tissue for the 18msw/59min profile as it has reached its MPTT revealing a ROS of 100%. It can also be observed that the ROS when surfacing is higher in the slower compartments with half-time HT ≥120min for TT6 and our proposal compared to “UCSD 1”, “Haukeland new” and 18msw/59min.

In figure 6 the average ROS when surfacing is presented as a comparison between all analyzed HBOT and the 18msw/59min dive profile.

FIGURE 6

Our analysis indicates that the average ROS when surfacing is lower with our proposal than for the UCSD, Haukeland and the 18msw/59min dive profile however higher than the original USN TT6, with or without extension or previous exposure.

A further analysis is made of the distribution of the ROS between the different HBOTs and the dive profile 18msw/59min and presented in figure 7.

FIGURE 7

The distributional analysis from figure 7 indicates that our proposal and the TT6 has a lower maximum and minimum ROS when surfacing than for the “UCSD 1”, “Haukeland old” and the 18msw/59min profile. The median and the 75^{th} percentile is in one case of our proposal (previous exposed) higher than the HBOTs but comparable to the 18msw/59min.

Discussion

In high-risk situations or environments such as on a warship in a conflict zone, or any situation where the treatment may need to be abruptly terminated, it can be more appropriate to adopt this alternative oxygen regimen for the attendant during hyperbaric oxygen therapy. Moreover, in the event of an unexpected decline in the patient's condition, it may be imperative to promptly evacuate them to the surface while avoiding any potential decompression illness in the attendant. This may also be an important property if chamber is small and transportable.

While this alternative oxygen regimen reduces the amount of time the chamber attendant must undergo a decompression stop, it is important to consider some potential criticisms. Firstly, there are rare instances of emergencies during this type of treatment. Secondly, the attendant could instead undergo recompression using a surface decompression strategy if considered plausible. Thirdly, the increased partial pressure of oxygen (P_{O2}) during the initial oxygen period (15 msw to 9 msw transport) could pose a risk for oxygen convulsions. Fourthly, the attendant must sometimes assist the patient and equipment during decompression, potentially compromising their ability to administer oxygen to themselves. Fifthly, the oxygen regimen for the chamber attendant outlined in TT6 has been widely recognized as effective in reducing instances of decompression sickness. Lastly, an alternative solution to achieve the desired availability to decompress the IA at any time, could be to have several IAs alternating prior to the no-decompression time has ended.

To address the potential drawbacks previously described, we recommend separating a traditional hospital setting from a military environment, where this new oxygen regimen may be more appropriate in the latter. In an emergency, there may not be access to a pressure chamber for surface decompression for any desire to recompress the tender. It is uncommon for convulsions to occur with pure oxygen breathing at depths shallower than 50 fsw (~15 msw), especially if there has been no prior oxygen exposure or if the workload is low.[4] Any concern of oxygen convulsions during transport between 15-9 msw can be mitigated by allowing the chamber attendant to hold the oxygen mask rather than having it securely fastened, as this will avoid continued breathing from the mask if unexpected convulsions occur. This certain period still poses a low risk, as the time and ascent are favorable to avoid convulsions and referring to experiences from UCSD and Haukeland, no cases of oxygen convulsions have been reported during > 20,000 of treatments with up to 30 minutes of oxygen exposure at a depth of 14 meters.[2,3] During ascent, there may be multiple tasks to attend to, which is similar to the

situation during transport from 9 msw to the surface. According to the decompression algorithm used, there are similarly low ROS with this oxygen decompression regimen compared to the TT6 regimen. Lastly, it may not always be possible to have multiple available and unexposed IAs.

When deciding the best treatment option for the patient, it is relevant to highlight the advantages of shorter treatment tables, such as the USN Treatment Table 5 or the Freemantle Hospital Hyperbaric Medicine Unit FH01, figure 8.[4,8]

FIGURE 8

The TT5 and FH01 HBOT have demonstrated equal or better resolution than the longer Treatment Table 6 for a range of conditions, including mild neurological symptoms, pain, lymphatic/skin and constitutional/non-specific symptoms resolved within 10 minutes at bottom.[6,7,8] By using a shorter treatment table it may lower the threshold for initiating HBOT, especially in the case where only a smaller (transportable) hyperbaric chamber is available. For these HBOTs it is also possible to decompress the inside attendant at any time, according to our mathematical analysis, which can be beneficial referring to previous discussion.

The studies that are used herein, as reference of CNS DCS in IA, shows one case where no patent foramen ovale (PFO) was present[15] whereas another describes a large PFO being present[16] and the third no knowledge of this is presented.[2] PFO is described as a risk factor for DCS, and CNS DCS to an even higher extent, and might introduce a general bias for outcome of DCS.[21-25] An extended review on the subject is found in.[26] Additionally, it has been determined that there is no increased risk for the IA if the chamber is located at high altitude, as demonstrated by.[27]

Conclusion

Our main finding is that an alternative oxygen regimen for the inside attendant (IA), compared to the US Navy Diving Manual Treatment Table 6 (USN TT6) with extensions and previously exposure, is feasible and allows for emergency decompression to be conducted over a greater period. This analysis is based on the compartmental gas load according to the exponential linear Thalmann algorithm with SWEN21B parameters. We also found that the average ratio of supersaturation (ROS) when surfacing is slightly higher for our proposed regimen compared to

the standard USN TT6, however lower compared to other uneventful hyperbaric oxygen therapies (HBOTs) and the diving profile 18msw/59min. The slower compartments half-time ≥120min has a higher ROS when surfacing for USN TT6 and our proposal compared to reference dive profile and HBOTs.

Our proposed oxygen regimen for IA during USN TT6 is believed to be particularly beneficial for handling unforeseen situations such as emergency decompressions. The traditional oxygen regimen, however, has been extensively verified and does not pose any increased risk of oxygen convulsions due to high partial pressures of oxygen or substantial risk for decompression sickness. After human evaluations it can be warranted to switch to this new regimen as the standard method for the IA oxygen distribution.

Conflicts of interest

The authors declare no conflicts of interest.

References

1. Moon RE, Mitchell SJ. Hyperbaric oxygen for decompression sickness: 2021 update. Undersea Hyperb Med. 2021;48(2):195–203.

2. Risberg J, Englund M, Aanderud L, Eftedal O, Flook V, Thorsen E. Venous gas embolism in chamber attendants after hyperbaric exposure. Undersea Hyperb Med. 2004;31(4):417–29.

3. Witucki P, Duchnick J, Neuman T, Grover I. Incidence of DCS and oxygen toxicity in chamber attendants: a 28-year experience. Undersea Hyperb Med. 2013;40(4):345–50.

4. US Navy Diving Manual Revision 7. United States: US Naval Sea Systems Command; 2016.

5. Regler för militär sjöfart RMS-Dyk. Vol. 2013. Stockholm, Sweden: Högkvarteret; 2013.

6. Goodman MW, Workman RD. Minimal-recompression, oxygen-breathing approach to treatment of decompression sickness in divers and aviators. Res Rep 5-65. Rep US Navy Exp Diving Unit. 1965:1–40. PMID: 5295232.

7. Green JW, Tichenor J, Curley MD. Treatment of type I decompression sickness using the U.S. Navy treatment algorithm. Undersea Biomed Res. 1989;16:465–70. PMID: 2603243.

8. Banham N, Hawkings P, Gawthrope I. A prospective single-blind randomised clinical trial comparing two treatment tables for the initial management of mild decompression sickness. Diving Hyperb Med. 2022;52(2):85–91.

9. Larsson A, Uusijärvi J, Frånberg O, Eksborg S, Lindholm P. Nitrox permits direct exit for attendants during extended hyperbaric oxygen treatment. Undersea Hyperb Med. vol 39, 2012(1):605–12.

10. Hansen MB, Jansen T, Sifakis MB, Hyldegaard O, Jansen EC. Chamber personell's use of Nitrox 50 during hyperbaric oxygen treatment: A quality study. Undersea Hyperb Med. Vol.40, 2013(5):395–402.

11. Silvanius M, Rullgård H, Ekström M, Frånberg O. Proposed Thalmann Algorithm Air Diving Decompression Table for the Swedish Armed Forces Based on Logistic Probabilistic Modeling of No-Stop Air Diving Data. Undersea and Hyperb Med. Vol. 51, 2023(2):

12. UHM 2017, Vol. 44, No. 6 Undersea & Hyperbaric Medical Society, Inc. - Health care worker decompression sickness: incidence, risk and mitigation - Richard Clarke, CHT

13. Sheffield PJ, Pirone CJ. Decompression sickness in inside attendants. In: Hyperbaric Facility Safety - A practical guide. Flagstaff, AZ: Best Publishing Company; p. 643–63.

14. Uzun G, Mutluoglu M, Ay H, Yildiz S. Decompression sickness in hyperbaric nurses: Retrospective analysis of 4500 treatments. Journal of clinical nursing. 2011 Jun 1;20:1784–7.

15. Kot J, Lenkiewicz E, Lizak E, Góralczyk P, Chreptowicz U. Spinal cord decompression sickness in an inside attendant after a standard hyperbaric oxygen treatment session. Diving Hyperb Med. 2021 Mar 31;51(1):103–6.

16. Johnson-Arbor K. Type II decompression sickness in a hyperbaric inside attendant. Undersea Hyperb Med. 2012;39:915–9.

17. Brattebo G, Aanderud L, Risberg J, Thorsen E, Forland M. Incidence of decompression illness among HBO2 nurses [Abstract]. Zdrav Vestn 97;66:17A.

18. Short DR, Flahan CM. Reconstructing the Navy Tables. Proceedings of dive computer workshop AAUS. September 26-28, 1988: 181-7.

19. Gerth WA, Doolette D. VVal-79 Maximum Permissible Tissue Tension Table for Thalmann Algorithm Support of Air Diving. Panama City, U.S.: NEDU; 2012 Mar. Report No.: TR 12-01.

20. Murphy FG, Swingler AJ, Gerth WA, Howle LE. Iso-risk air no decompression limits after scoring marginal decompression sickness cases as non-events. Comput Biol Med. 2018 Jan 1;92:110–7.

21. Bove AA. Risk of decompression sickness with patent foramen ovale. Undersea Hyperb Med.;Vol. 25, 1998(3).

22. Moon R.E, Camporesi E.M, Kisslo J.A. Patent foramen ovale and decompression sickness in divers. The Lancet. 1989 Mar 11;333(8637):513–4.

23. Torti SR, Billinger M, Schwerzmann M, Vogel R, Zbinden R, Windecker S, et al. Risk of decompression illness among 230 divers in relation to the presence and size of patent foramen ovale. European Heart Journal. 2004 Jun 1;25(12):1014–20.

24. Honěk J, Šrámek M, Šefc L, Januška J, Fiedler J, Horváth M, et al. High-grade patent foramen ovale is a risk factor of unprovoked decompression sickness in recreational divers. Journal of Cardiology. 2019 Dec 1;74(6):519–23.

25. 1. Germonpre P, Lafère P, Portier W, Germonpré FL, Marroni A, Balestra C. Increased Risk of Decompression Sickness When Diving With a Right-to-Left Shunt: Results of a Prospective Single-Blinded Observational Study (The "Carotid Doppler" Study). Frontiers in Physiology. 2021 Oct 1;12:763408.

26. Saary M, Gray G. The Possible Relationship Between Patent Foramen Ovale and Decompression Sickness: 1999 Jan p. 36. Report No.: DCIEM TR 1999-001.

27. Bell J, Thombs PA, Davison WJ, Weaver LK. Decompression tables for inside chamber attendants working at altitude. Undersea Hyperb Med.; Vol. 41, 2014(6): 505-13

Figure 1, leading tissue supersaturation for an original USN TT6 compared to our proposed oxygen regimen for the IA.

Figure 2, leading tissue supersaturation for an original USN TT6 compared to our proposed oxygen regimen for the IA with previous exposure from a 18msw, 59 min dive.

Figure 3, leading tissue supersaturation for an original extended USN TT6 compared to our proposed oxygen regimen for the IA. Observe the necessity for total additional oxygen periods in this case.

Figure 4, leading tissue supersaturation for an original extended USN TT6 compared to our proposed oxygen regimen for the IA with previous exposure from a 18msw, 59 min dive. Observe the necessity for additional oxygen periods in this case

Table 1, the "lock in time" describes start and stop time for where the IA cannot be directly taken to surface without decompression stop.

Table 2, comparison of some detailed studies of number of exposures (n) related to DCS and oxygen seizure outcome and their fractional gas load of maximum permissible tissue tension (color coded as red representing high ROS and green representing low ROS) when surfacing.

Figure 5, a comparison of ratio of supersaturation ROS when surfacing for USN TT6 and our proposal. "UCSD 1", "Haukeland new" and the direct ascent profile 18msw 59 min are shown as comparison with the standard protocols.

Figure 6, the average ROS when surfacing in comparison of the analyzed HBOT's and 18msw/59min dive profile.

Figure 7, distribution of the ROS when surfacing presented as comparisons with all HBOT and dive profile that we have analyzed. The box plot shows max/min value (dashed line), median (horizontal line in box) and 25th-75th percentile (box) for all nine analyzed compartments.

Figure 8, USN Treatment Table 5 and the Freemantle Hospital Hyperbaric Medicine Unit FH01 shows that there are no mandatory decompression stops for the IA as the leading tissue supersaturation doesn't pass the ceiling adjusted to be represented by atmospheric pressure.

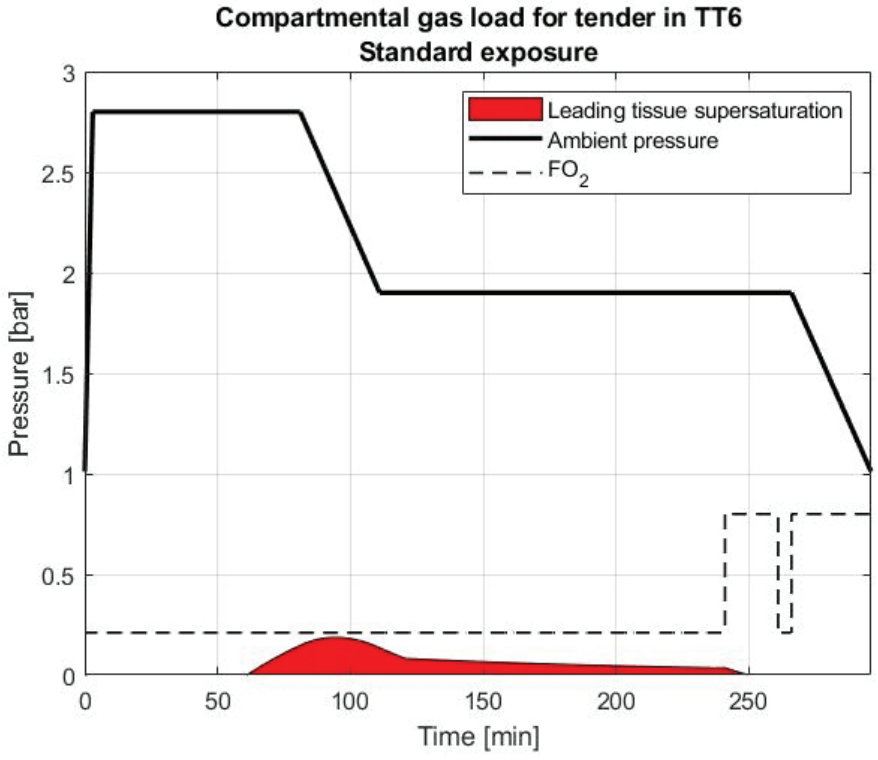
Compartmental gas load for tender in TT6
Standard exposure
Leading tissue supersaturation
Ambient pressure
FO2
Pressure [bar]
Time [min]
0
0.5
1
1.5
2
2.5
3
0
50
100
150
200
250

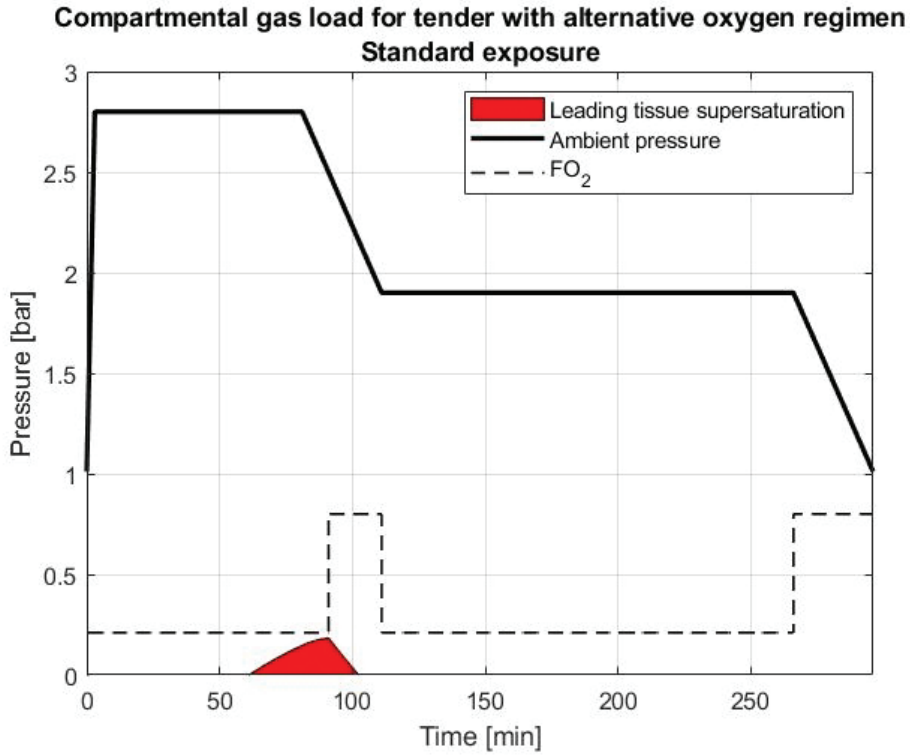
Compartmental gas load for tender with alternative oxygen regimen
Standard exposure
Leading tissue supersaturation
Ambient pressure
FO2
Pressure [bar]
Time [min]
0
0.5
1
1.5
2
2.5
3
0
50
100
150
200
250

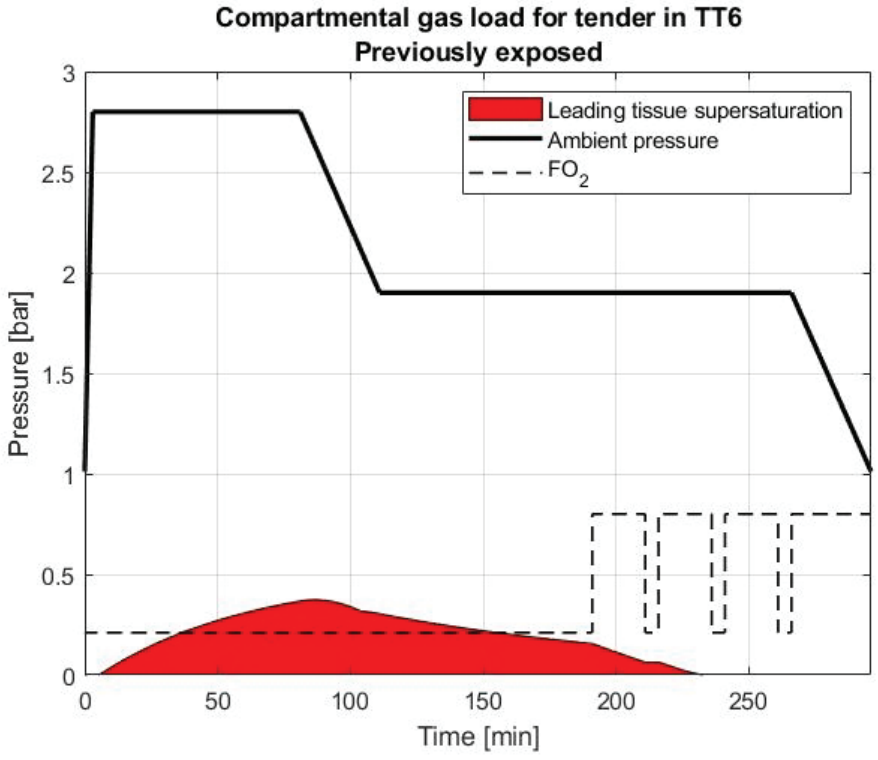
Compartmental gas load for tender in TT6
Previously exposed
Leading tissue supersaturation
Ambient pressure
FO2
Pressure [bar]
Time [min]
0
0.5
1
1.5
2
2.5
3
0
50
100
150
200
250

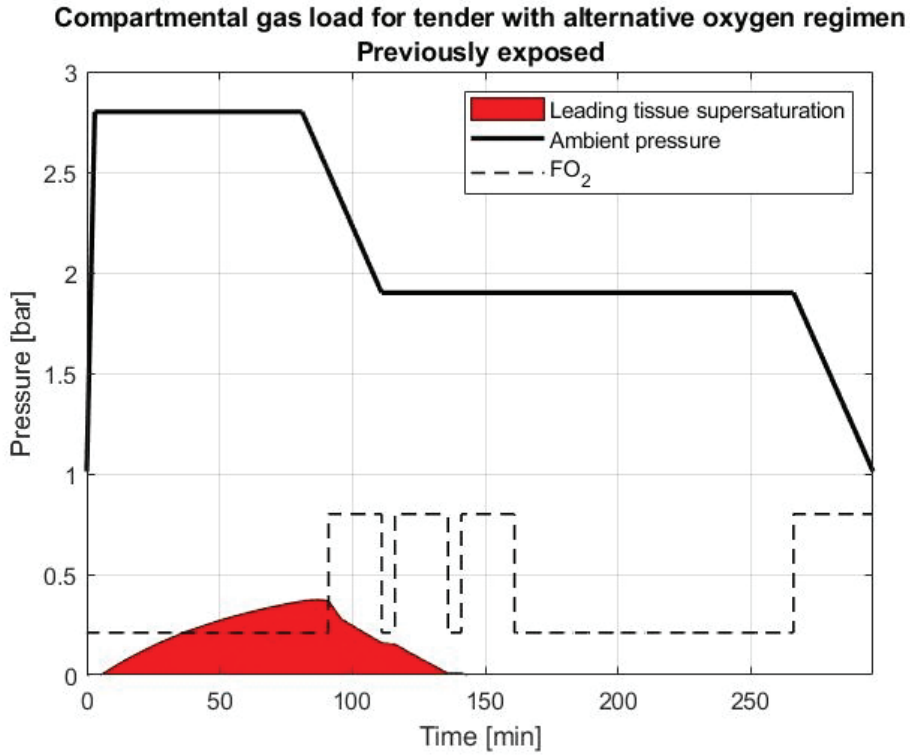
Compartmental gas load for tender with alternative oxygen regimen
Previously exposed
Leading tissue supersaturation
Ambient pressure
FO2
Pressure [bar]
Time [min]
0
0.5
1
1.5
2
2.5
3
0
50
100
150
200
250

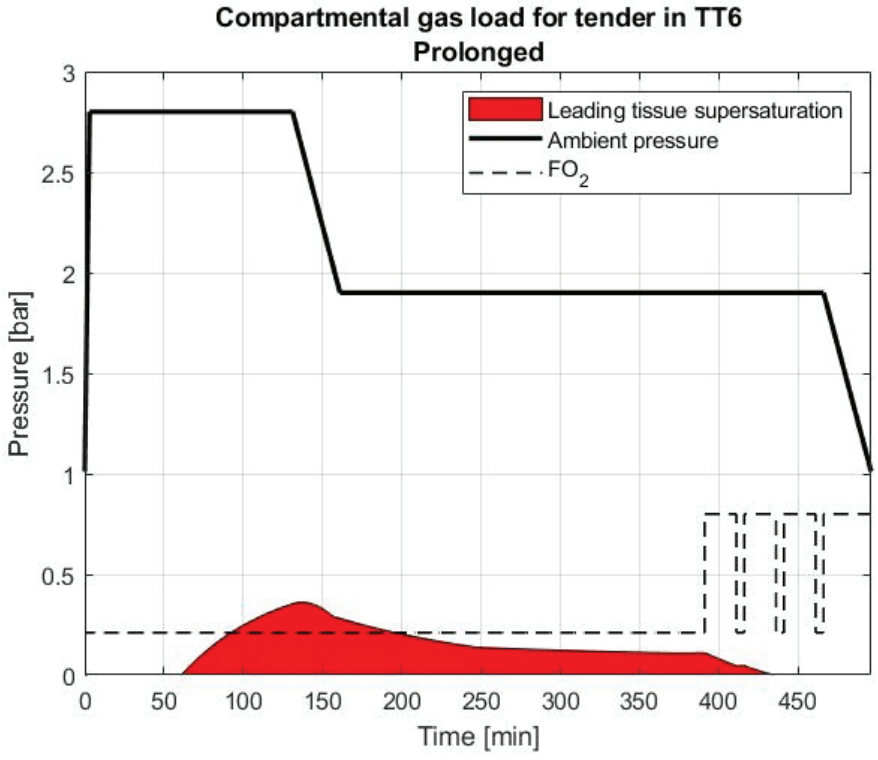
Compartmental gas load for tender in TT6
Prolonged
Leading tissue supersaturation
Ambient pressure
FO2
Pressure [bar]
Time [min]
0
0.5
1
1.5
2
2.5
3
0
50
100
150
200
250
300
350
400
450

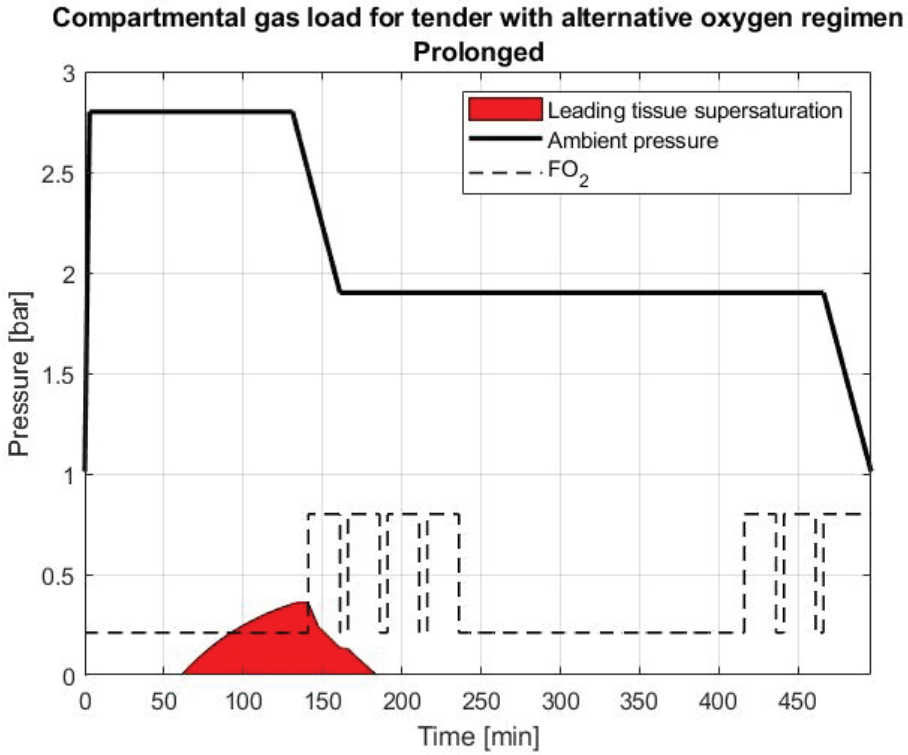
Compartmental gas load for tender with alternative oxygen regimen
Prolonged
Leading tissue supersaturation
Ambient pressure
FO2
Pressure [bar]
Time [min]
0
0.5
1
1.5
2
2.5
3
0
50
100
150
200
250
300
350
400
450

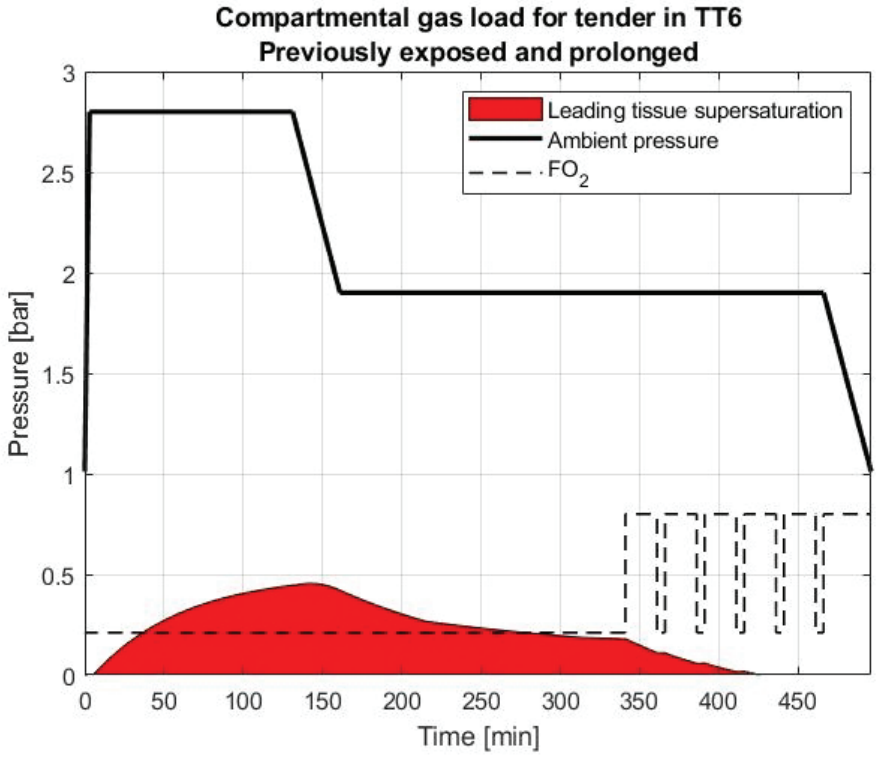
Compartmental gas load for tender in TT6
Previously exposed and prolonged
Leading tissue supersaturation
Ambient pressure
FO2
Pressure [bar]
Time [min]
0
0.5
1
1.5
2
2.5
3
0
50
100
150
200
250
300
350
400
450

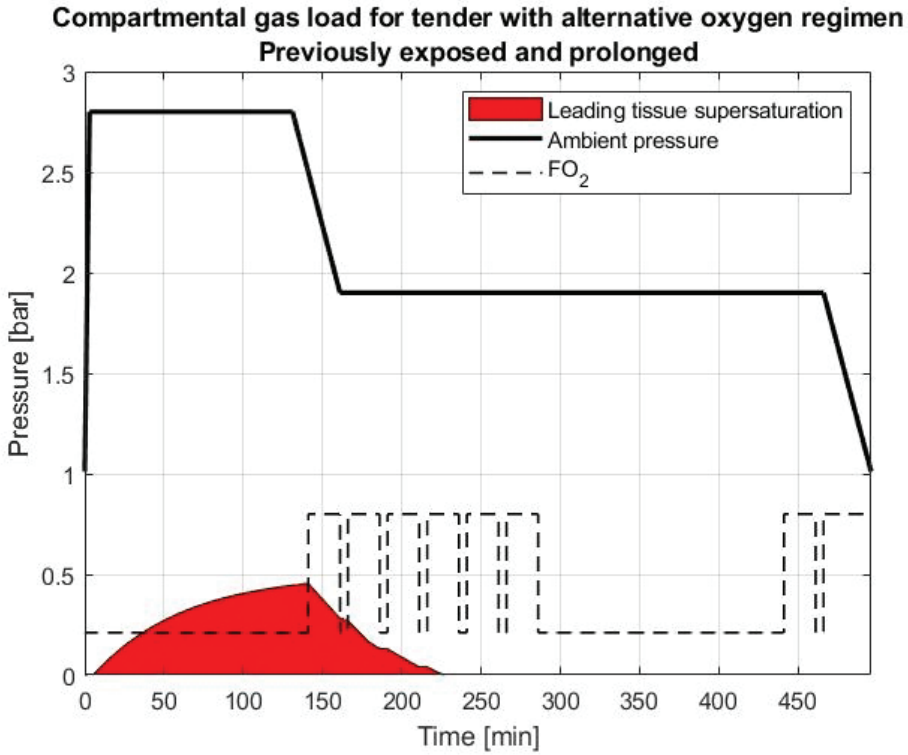
Compartmental gas load for tender with alternative oxygen regimen
Previously exposed and prolonged
Leading tissue supersaturation
Ambient pressure
FO2
Pressure [bar]
Time [min]
0
0.5
1
1.5
2
2.5
3
0
50
100
150
200
250
300
350
400
450

	Protocol	Depth	Bottom-time	O2	Start lock in [min]	Stop lock in [min]	Percentual lock in time
US Navy[4]	TT6	18 --> 9	253	20min @ 9msw, 30min @ ascent	59	249	75%
	TT6 - prev. exp. [o]	18 --> 9	253	3x20min @ 9msw, 30min @ ascent	5	230	89%
	TT6 - extended	18 --> 9	463	3x20min @ 9msw, 30min @ ascent	59	433	81%
	TT6 - extended & prev. exp. [o]	18 --> 9	463	5x20min @ 9msw, 30min @ ascent	5	425	91%
	TT5	*18 --> 9*	*103*	*20min @ 15-9msw, 30min @ ascent*	-	-	*0%*
New Proposal	TT6 mod	18 --> 9	250 + compression	20min @ 15-9msw, 30min @ ascent	59	102	17%
	TT6 mod – prev. exp. [o]	18 --> 9	250 + compression	20min @ 15-9msw, 2x20min @ 9 msw, 30min @ ascent	5	143	55%
	TT6 mod - extended	18 --> 9	460 + compression	20min @ 15-9msw, 2x20min @ 9 msw, 30min @ ascent	59	184	27%
	TT6 mod - extended & prev. exp. [o]	18 --> 9	460 + compression	20min @ 15-9msw, 6x20min @ 9 msw, 30min @ ascent	5	227	48%

[o] Previous exposure is represented by a dive to 18 msw 59 min with direct ascent and no surface interval

					Half time of compartment [min] and ROS [%]												
	Protocol	Depth	Exposure	O2	**5**	**10**	**20**	**40**	**80**	**120**	**160**	**200**	**240**	**Mean (SD)**	***n***	**DCS**	**O2 seizures**	**$P_{0.95}$ [%]**
UCSD[3]	1	14	<80min	no	37	54	76	88	79	66	56	49	44	**61 (16)**	228	0	0	0-1.6
	2	14	80-119 min	15 min @ 14msw, Air during ascent	11	23	49	77	82	72	64	57	51	**54 (23)**	23679	0	0	0-0.15
	3	14	120-139 min	30 min @ 14msw, Air during ascent	5	9	30	60	73	68	61	55	50	**46 (24)**	709	0	0	0-0.52
Haukeland[17]	New	14	100 min + compression	5-10min O2 @ 14msw, 7min @ ascent	2	24	54	79	79	68	60	53	47	**52 (24)**	1139	0*	0	0-0.32
	Old	14	100 min + compression	7 min @ ascent	14	37	65	88	86	74	64	56	51	**59 (22)**	395	0 *(3)***	0	0-0.93 *(0.16-2.20)*

* this schedule was later reported with a serious case of CNS DCS, however no data on how many exposures in relation to occurance could be found **(2)**

** described as skin manifestations which in statistical analysis are suggested as non-events **(20)**

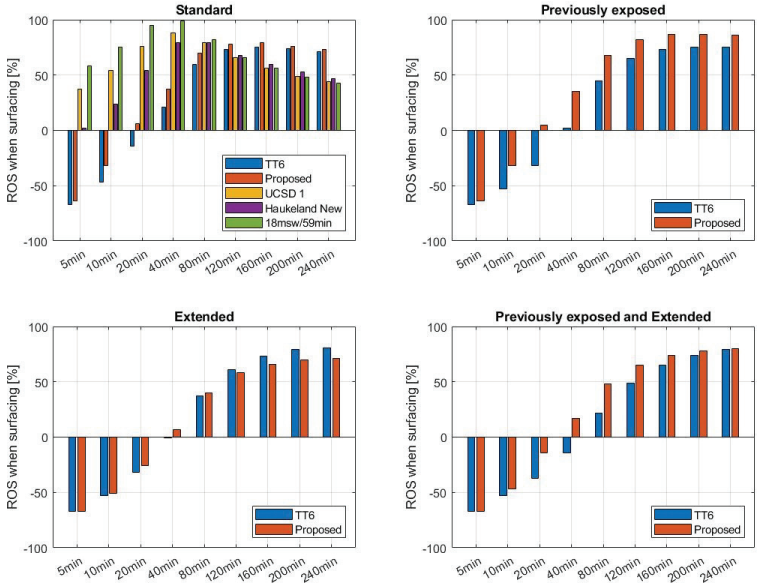
Standard
Previously exposed
Extended
Previously exposed and Extended
ROS when surfacing [%]
100
50
0
-50
-100
5min
10min
20min
40min
80min
120min
160min
200min
240min
TT6
Proposed
UCSD 1
Haukeland New
18msw/59min

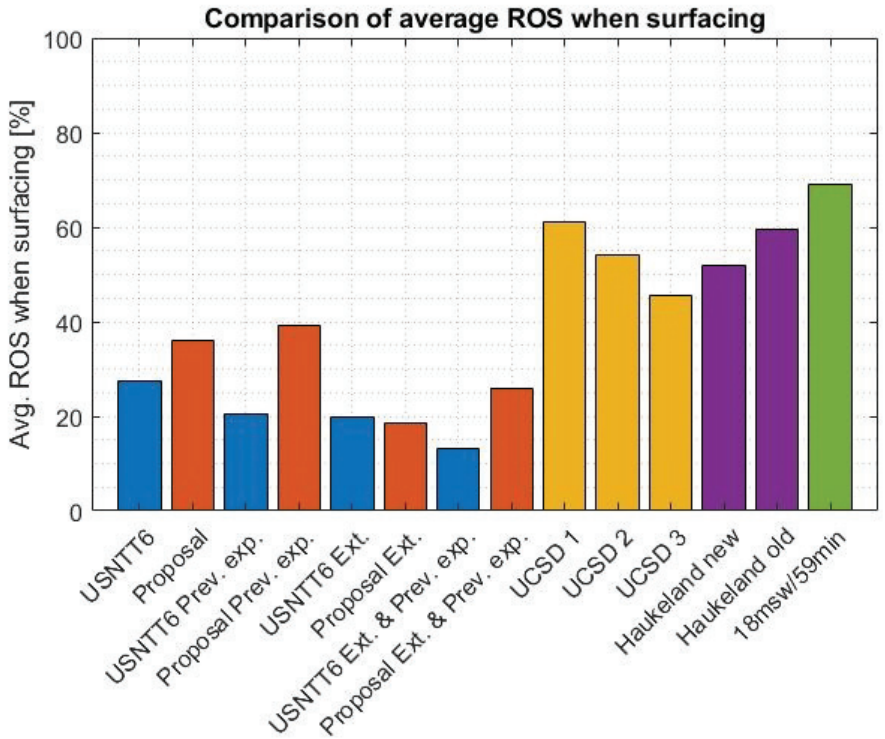
Comparison of average ROS when surfacing
Avg. ROS when surfacing [%]
0
20
40
60
80
100
USNTT6
Proposal
USNTT6 Prev. exp.
Proposal Prev. exp.
USNTT6 Ext.
Proposal Ext.
USNTT6 Ext. & Prev. exp.
Proposal Ext. & Prev. exp.
UCSD 1
UCSD 2
UCSD 3
Haukeland new
Haukeland old
18msw/59min

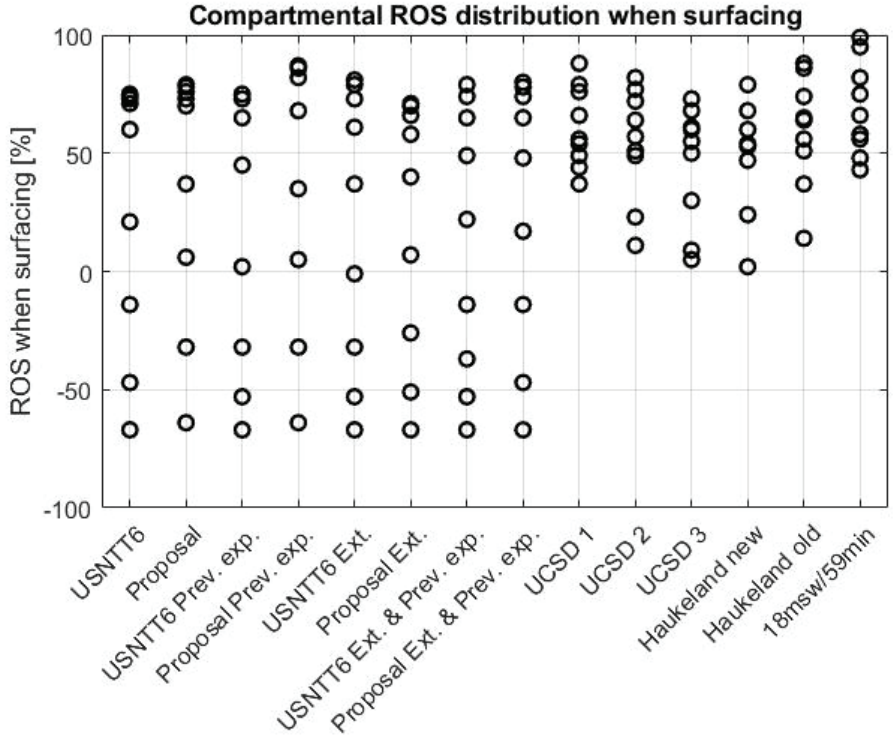
Compartmental ROS distribution when surfacing
ROS when surfacing [%]
100
50
0
-50
-100
USNTT6
Proposal
USNTT6 Prev. exp.
Proposal Prev. exp.
USNTT6 Ext.
Proposal Ext.
USNTT6 Ext. & Prev. exp.
Proposal Ext. & Prev. exp.
UCSD 1
UCSD 2
UCSD 3
Haukeland new
Haukeland old
18msw/59min

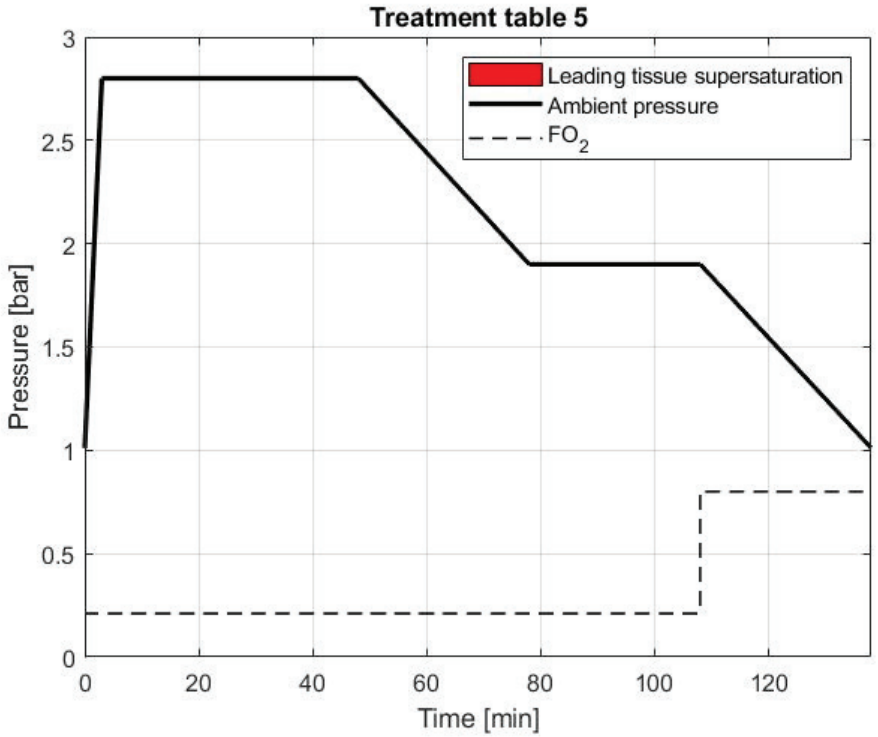
Treatment table 5
Leading tissue supersaturation
Ambient pressure
FO2
Pressure [bar]
Time [min]
0
0.5
1
1.5
2
2.5
3
0
20
40
60
80
100
120

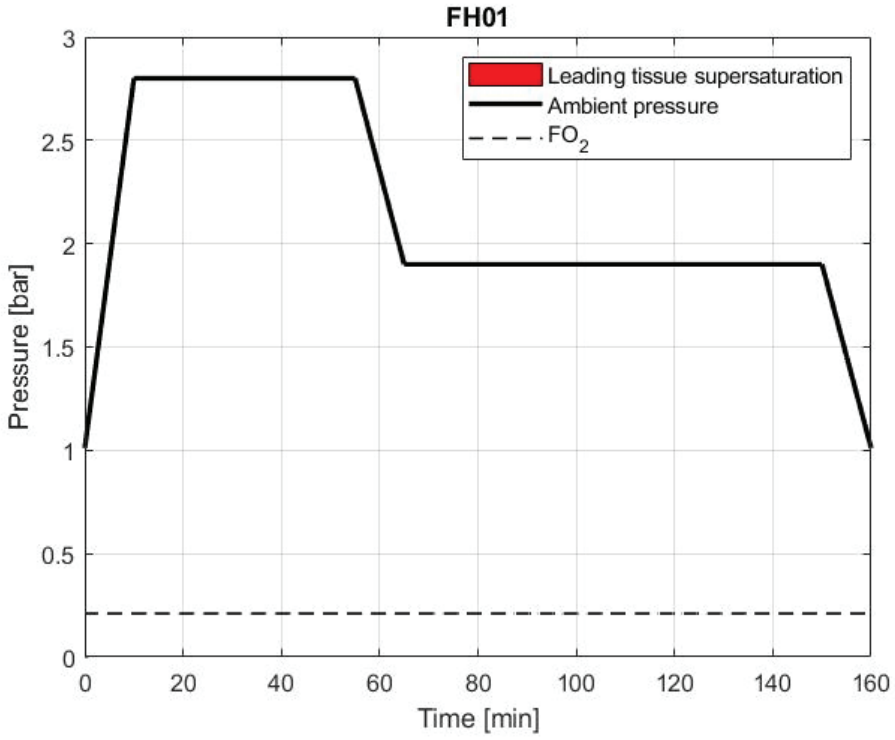
FH01
Leading tissue supersaturation
Ambient pressure
FO2
Pressure [bar]
Time [min]
0
0.5
1
1.5
2
2.5
3
0
20
40
60
80
100
120
140
160

Appendix A

1 No-stop table

	SWEN21B	
Depth (MSW)	Bottom time (min)	(Leading tissue)
7	1017	(240)
8	563	(160)
9	356	(120)
10	242	(80)
12	151	(80)
14	100	(40)
16	74	(40)
18	59	(40)
20	49	(20)
22	39	(20)
24	33	(20)
26	28	(20)
28	25	(20)
30	22	(10)
33	17	(10)
36	15	(10)
39	12	(5)
42	10	(5)
45	8	(5)
48	7	(5)
51	6	(5)
54	6	(5)
57	5	(5)
60	5	(5)

2 Decompression tables

Decompression times in **bold face** indicate decompression on oxygen.

N/A indicates that total decompression time would be longer than 60 minutes.

	SWEN21B; 9 MSW			
Bottom time (min)	Deco stop (MSW) 6	3	TDT	Rep. group	O2-per
360	3		4:00	Z	
	1		2:00		0.5
		1	2:00	Z	
420	39		40:00	-	
	7		8:00		0.5
		13	14:00	-	
480	N/A				
	14		15:00		1
		29	30:00	-	
540	N/A				
	21		22:00		1
		46	47:00	-	

	SWEN21B; 10 MSW				
Bottom	Deco stop (MSW)		TDT	Rep.	O2-
time (min)	6	3		group	per
270	11		12:07	Z	
	3		4:07		0.5
		5	6:07	Z	
300	33		34:07	Z	
	7		8:07		0.5
		13	14:07	Z	
330	54		55:07	Z	
	12		13:07		0.5
		22	23:07	Z	
360	N/A				
	16		17:07		1
		30	31:07	-	
420	N/A				
	26		27:07		1
		52	53:07	-	

	SWEN21B; 12 MSW			
Bottom time (min)	Deco stop (MSW) 6	3	TDT	Rep. group	O2-per
160	9		10:20	O	
	3		4:20		0.5
		5	6:20	N	
170	18		19:20	O	
	6		7:20		0.5
		9	10:20	O	
180	26		27:20	O	
	8		9:20		0.5
		13	14:20	O	
190	33		34:20	Z	
	10		11:20		0.5
		17	18:20	O	
200	39		40:20	Z	
	12		13:20		0.5
		21	22:20	O	
210	48		49:20	Z	
	14		15:20		1
		24	25:20	Z	
220	N/A				
	16		17:20		1
		27	28:20	Z	
230	N/A				
	17		18:20		1
		32	33:20	Z	
240	N/A				
	20		21:20		1
		37	38:20	Z	
270	N/A				
	28		29:20		1.5
		50	51:20	Z	

	SWEN21B; 14 MSW				
Bottom	Deco stop (MSW)		TDT	Rep.	O2-
time (min)	6	3		group	per
110	4		5:33	M	
	2		3:33		0.5
		3	4:33	M	
120	11		12:33	N	
	4		5:33		0.5
		6	7:33	N	
130	26		27:33	O	
	8		9:33		0.5
		13	14:33	N	
140	38		39:33	O	
	12		13:33		0.5
		20	21:33	O	
150	48		49:33	O	
	15		16:33		1
		26	27:33	O	
160	56		57:33	Z	
	19		20:33		1
		32	33:33	O	
170	N/A				
	21		22:33		1
		37	38:33	Z	
180	N/A				
	24		25:33		1
		42	43:33	Z	
190	N/A				
	26		27:33		1
		47	48:33	Z	
200	N/A				
	30		31:33		1.5
		53	54:33	Z	

	SWEN21B; 16 MSW			
Bottom time (min)	Deco stop (MSW) 6	3	TDT	Rep. group	O2-per
80	5		6:47	L	
	2		3:47		0.5
		4	5:47	L	
90	11		12:47	M	
	5		6:47		0.5
		10	11:47	M	
100	19		20:47	N	
	8		9:47		0.5
		15	16:47	N	
110	38		39:47	O	
	12		13:47		0.5
		20	21:47	N	
120	52		53:47	O	
	17		18:47		1
		29	30:47	O	
130	N/A				
	22		23:47		1
		38	39:47	O	
140	N/A				
	26		27:47		1
		46	47:47	O	
150	N/A				
	29		30:47		1.5
		53	54:47	O	

	SWEN21B; 18 MSW				
Bottom	Deco stop (MSW)		TDT	Rep.	O2-
time (min)	6	3		group	per
60	1		3:00	K	
	1		3:00		0.5
		1	3:00	K	
70	11		13:00	L	
	5		7:00		0.5
		10	12:00	L	
80	18		20:00	M	
	9		11:00		0.5
		18	20:00	M	
90	35		37:00	N	
	12		14:00		0.5
		24	26:00	N	
100	54		56:00	O	
	18		20:00		1
		31	33:00	N	
110	N/A				
	24		26:00		1
		42	44:00	O	
120	N/A				
	29		31:00		1.5
	3	51	55:40	O	

	SWEN21B; 20 MSW				
Bottom time (min)	Deco stop (MSW) 6	3	TDT	Rep. group	O2-per
50	1		3:13	J	
	1		3:13		0.5
		1	3:13	J	
55	8		10:13	K	
	4		6:13		0.5
		7	9:13	K	
60	13		15:13	L	
	7		9:13		0.5
		13	15:13	K	
70	22		24:13	M	
	11		13:13		0.5
		23	25:13	M	
80	43		45:13	N	
	15		17:13		1
		31	33:13	N	
90	N/A				
	22		24:13		1
	4	36	41:53	N	
100	N/A				
	29		31:13		1.5
	9	45	55:53	O	

	SWEN21B; 22 MSW				
Bottom time (min)	Deco stop (MSW) 6	3	TDT	Rep. group	O2-per
40	1		3:27	I	
	1		3:27		0.5
		1	3:27	I	
45	4		6:27	J	
	3		5:27		0.5
		4	6:27	J	
50	12		14:27	K	
	6		8:27		0.5
		11	13:27	K	
55	18		20:27	L	
	9		11:27		0.5
		18	20:27	L	
60	24		26:27	M	
	12		14:27		0.5
		24	26:27	L	
70	43		45:27	N	
	17		19:27		1
	1	35	38:07	M	
80	N/A				
	24		26:27		1
	9	35	46:07	N	

	SWEN21B; 24 MSW				
Bottom	Deco stop (MSW)		TDT	Rep.	O2-
time (min)	6	3		group	per
35	2		4:40	I	
	1		3:40		0.5
		2	4:40	I	
40	7		9:40	J	
	4		6:40		0.5
		7	9:40	J	
45	14		16:40	K	
	7		9:40		0.5
		13	15:40	K	
50	21		23:40	L	
	11		13:40		0.5
		22	24:40	K	
55	28		30:40	M	
	14		16:40		1
	1	28	31:20	L	
60	35		37:40	N	
	18		20:40		1
	3	33	38:20	M	
70	N/A				
	23		25:40		1
	12	35	49:20	N	

	SWEN21B; 26 MSW				
Bottom	Deco stop (MSW)		TDT	Rep.	O2-
time (min)	6	3		group	per
30	2		4:53	H	
	1		3:53		0.5
		2	4:53	H	
35	8		10:53	J	
	4		6:53		0.5
		8	10:53	J	
40	14		16:53	K	
	7		9:53		0.5
		14	16:53	K	
45	23		25:53	L	
	12		14:53		0.5
	1	22	25:33	K	
50	30		32:53	M	
	16		18:53		1
	5	27	34:33	L	
55	40		42:53	N	
	20		22:53		1
	8	32	42:33	M	
60	N/A				
	23		25:53		1
	12	34	48:33	N	

	SWEN21B; 28 MSW					
Bottom	Deco stop (MSW)			TDT	Rep.	O2-
time (min)	9	6	3		group	per
30		7		10:07	I	
		4		7:07		0.5
			8	11:07	I	
35		13		16:07	K	
		7		10:07		0.5
			15	18:07	J	
40		22		25:07	L	
		11		14:07		0.5
		3	20	25:47	K	
45		31		34:07	M	
		16		19:07		1
		7	25	34:47	L	
50		40		43:07	N	
		21		24:07		1
		11	31	44:47	M	
55		N/A				
		25		28:07		1
		15	35	52:47	N	
60		N/A				
	1	**28**		31:47		1.5
	2	20	35	59:27	N	

	SWEN21B; 30 MSW					
Bottom	Deco stop (MSW)			TDT	Rep.	O2-
time (min)	9	6	3		group	per
25		5		8:20	H	
		3		6:20		0.5
			5	8:20	H	
30		12		15:20	J	
		7		10:20		0.5
			14	17:20	I	
35		19		22:20	K	
		10		13:20		0.5
		3	18	24:00	K	
40		30		33:20	M	
		16		19:20		1
		9	22	34:00	L	
45		40		43:20	N	
		21		24:20		1
		14	27	44:00	M	
50		N/A				
	1	**25**		29:00		1
	2	16	33	53:40	N	

	SWEN21B; 33 MSW					
Bottom	Deco stop (MSW)			TDT	Rep.	O2-
time (min)	9	6	3		group	per
20		3		6:40	H	
		2		5:40		0.5
			3	6:40	G	
25		11		14:40	I	
		6		9:40		0.5
			13	16:40	I	
30		20		23:40	K	
		11		14:40		0.5
		5	17	25:20	J	
35		31		34:40	L	
		16		19:40		1
		12	19	34:20	L	
40	2	41		46:20	N	
	1	**21**		25:20		1
	2	16	26	47:00	M	
45		N/A				
	4	**23**		30:20		1
	7	15	33	58:00	N	

	SWEN21B; 36 MSW					
Bottom	Deco stop (MSW)			TDT	Rep.	O2-
time (min)	9	6	3		group	per
20		7		11:00	H	
		4		8:00		0.5
			8	12:00	H	
25		18		22:00	J	
		10		14:00		0.5
		4	16	23:40	J	
30		28		32:00	L	
		15		19:00		1
		12	17	32:40	K	
35	4	38		45:40	M	
	2	**20**		25:40		1
	4	16	23	46:20	M	
40		N/A				
	5	**23**		31:40		1.5
	10	16	29	58:20	N	

	SWEN21B; 39 MSW						
Bottom	Deco stop (MSW)				TDT	Rep.	O2-
time (min)	12	9	6	3		group	per
15			4		8:20	G	
			2		6:20		0.5
				4	8:20	G	
20			13		17:20	I	
			7		11:20		0.5
			3	12	19:00	I	
25		1	24		29:00	K	
		1	**13**		18:00		1
		1	9	17	30:40	K	
30		5	33		42:00	M	
		3	**17**		24:00		1
		5	14	20	42:40	L	
35			N/A				
	1	**6**	**20**		31:00		1
	1	11	15	27	57:20	N	

	SWEN21B; 42 MSW						
Bottom	Deco stop (MSW)				TDT	Rep.	O2-
time (min)	12	9	6	3		group	per
15			7		11:40	H	
			4		8:40		0.5
			1	7	12:20	G	
20			19		23:40	J	
			11		15:40		0.5
			8	13	25:20	J	
25		5	27		36:20	L	
		3	**14**		21:20		1
		5	11	18	38:00	K	
30	2	9	38		53:00	N	
	2	**5**	**19**		30:20		1
	2	9	16	22	52:40	M	

	SWEN21B; 45 MSW						
Bottom	Deco stop (MSW)				TDT	Rep.	O2-
time (min)	12	9	6	3		group	per
10			2		7:00	F	
			1		6:00		0.5
				2	7:00	F	
15			11		16:00	H	
			6		11:00		0.5
			3	9	16:40	H	
20		4	21		29:40	K	
		2	**12**		18:40		1
		4	8	15	31:20	J	
25	3	6	32		45:20	M	
	3	**3**	**16**		26:40		1
	3	6	14	19	46:00	L	

	SWEN21B; 48 MSW						
Bottom	Deco stop (MSW)				TDT	Rep.	O2-
time (min)	12	9	6	3		group	per
10			4		9:20	F	
			2		7:20		0.5
				4	9:20	F	
15		1	14		20:00	I	
		1	**7**		13:00		0.5
		1	6	9	20:40	I	
20	1	7	23		35:40	L	
	1	**4**	**12**		22:00		1
	1	7	8	17	37:20	K	
25	6	7	37		54:40	N	
	6	**4**	**18**		33:00		1
	6	7	16	22	55:20	M	

	SWEN21B; 51 MSW						
Bottom	Deco stop (MSW)				TDT	Rep.	O2-
time (min)	12	9	6	3		group	per
10			6		11:40	G	
			3		8:40		0.5
			2	4	11:20	G	
15		3	17		25:20	J	
		2	**9**		16:20		0.5
		3	8	10	26:00	I	
20	4	7	27		43:00	L	
	4	**4**	**13**		26:20		1
	4	7	10	17	42:40	L	

	SWEN21B; 54 MSW							
Bottom	Deco stop (MSW)					TDT	Rep.	O2-
time (min)	15	12	9	6	3		group	per
10				8		14:00	G	
				5		11:00		0.5
				4	5	14:40	G	
15		2	4	19		30:20	J	
		2	**2**	**10**		19:40		0.5
		2	4	8	12	31:00	J	
20	2	6	7	32		52:00	M	
	2	6	**3**	**16**		32:20		1
	2	6	7	11	21	51:40	M	

	SWEN21B; 57 MSW							
Bottom	Deco stop (MSW)					TDT	Rep.	O2-
time (min)	15	12	9	6	3		group	per
10			2	9		17:00	H	
			1	**5**		12:00		0.5
			2	3	7	17:40	H	
15	1	3	5	21		35:20	K	
	1	3	**3**	**10**		22:40		0.5
	1	3	5	8	14	36:00	K	

	SWEN21B; 60 MSW							
Bottom	Deco stop (MSW)					TDT	Rep.	O2-
time (min)	15	12	9	6	3		group	per
10			3	11		20:20	H	
			2	**6**		14:20		0.5
			3	4	8	21:00	H	
15	2	4	6	22		39:40	L	
	2	4	**3**	**12**		27:00		1
	2	4	6	8	16	41:20	K	

3 Repetitive group designators

Depth (MSW)	A	B	C	D	E	F	G	H	I	J	K	L	M	N	O	Z
3	59	104	164	257	472	*										
4	42	71	106	150	209	298	494	*								
5	33	54	79	108	142	185	242	329	509	*						
6	27	44	63	84	109	137	171	213	269	353	520	*				
7	23	37	52	69	88	109	133	162	195	237	291	372	528	1017		
8	19	32	45	59	74	91	110	131	155	182	216	256	310	388	535	563
9	17	28	39	51	64	78	93	110	129	150	173	201	233	274	326	356
10	15	25	35	45	56	68	81	95	111	127	146	166	190	217	242	
12	12	20	28	37	45	55	65	75	86	98	111	125	140	151		
14	10	17	24	31	38	46	54	62	71	80	90	100				
16	9	14	20	26	33	39	46	53	60	68	74					
18	8	13	18	23	28	34	40	46	52	58	59					
20	7	11	16	20	25	30	35	40	46	49						
22	6	10	14	18	23	27	32	36	39							
24	5	9	13	16	20	24	28	33								
26	5	8	11	15	19	22	26	28								
28	4	7	10	14	17	20	24	25								
30	4	7	10	13	16	19	22									
33	3	6	8	11	14	17										
36	3	5	7	10	12	15										
39	2	4	7	9	11	12										
42	2	4	6	8	10											
45		3	5	7	8											
48		3	5	7												
51		3	4	6												
54			4	5	6											
57			3	5												
60			3	4	5											

4 Residual nitrogen time

Depth (MSW)	Z	O	N	M	L	K	J	I	H	G	F	E	D	C	B	A
3												473	258	165	104	60
4										495	299	209	151	107	72	43
5								510	330	243	186	143	108	80	55	34
6						521	354	270	214	172	138	110	85	64	45	28
7				529	373	292	238	196	162	134	110	89	70	53	38	24
8	687	535	389	311	257	217	183	156	132	111	92	75	60	46	33	20
9	356	327	275	234	202	174	151	130	111	94	79	65	52	40	29	18
10	266	250	218	191	167	147	128	112	96	82	69	57	46	36	26	16
12	184	176	157	141	126	112	99	87	76	66	56	47	38	29	21	14
14	143	137	124	113	101	91	81	72	63	55	47	39	32	25	18	12
16	117	113	103	94	85	77	69	61	54	47	40	34	28	22	16	10
18	100	96	88	81	73	66	60	53	47	41	35	30	24	19	14	9
20	87	84	77	71	65	59	53	47	42	37	32	27	22	17	13	8
22	77	74	69	63	58	52	47	42	38	33	29	24	20	16	11	7
24	69	67	62	57	52	47	43	39	34	30	26	22	18	14	11	7
26	63	61	56	52	48	43	39	35	31	28	24	20	17	13	10	6
28	57	56	52	48	44	40	36	33	29	26	22	19	15	12	9	6
30	53	51	48	44	40	37	34	30	27	24	21	17	14	11	8	6
33	48	46	43	40	36	33	30	27	24	22	19	16	13	10	8	5
36	43	42	39	36	33	30	28	25	22	20	17	15	12	10	7	5
39	39	38	36	33	30	28	25	23	20	18	16	13	11	9	7	4
42	36	35	33	30	28	26	23	21	19	17	15	12	10	8	6	4
45	34	33	30	28	26	24	22	20	18	16	14	12	10	8	6	4
48	31	30	28	26	24	22	20	18	17	15	13	11	9	7	5	4
51	29	29	27	25	23	21	19	17	16	14	12	10	9	7	5	3
54	28	27	25	23	22	20	18	16	15	13	11	10	8	6	5	3
57	26	25	24	22	20	19	17	16	14	12	11	9	8	6	5	3
60	25	24	22	21	19	18	16	15	13	12	10	9	7	6	4	3